ISSN 0021-9673

VOL. 623 NO. 1 OCTOBER 9, 1992

JOURNAL OF CHROMATOGRAPHY

INCLUDING ELECTROPHORESIS AND OTHER SEPARATION METHODS

ELSEVIER

JOURNAL OF CHROMATOGRAPHY

INCLUDING ELECTROPHORESIS AND OTHER SEPARATION METHODS

Scope. The *Journal of Chromatography* publishes papers on all aspects of **chromatography, electrophoresis** and related methods. Contributions consist mainly of research papers dealing with chromatographic theory, instrumental developments and their applications. The section *Biomedical Applications*, which is under separate editorship, deals with the following aspects: developments in and applications of chromatographic and electrophoretic techniques related to clinical diagnosis or alterations during medical treatment; screening and profiling of body fluids or tissues related to the analysis of active substances and to metabolic disorders; drug level monitoring and pharmacokinetic studies; clinical toxicology; forensic medicine; veterinary medicine; occupational medicine; results from basic medical research with direct consequences in clinical practice. In *Symposium volumes*, which are under separate editorship, proceedings of symposia on chromatography, electrophoresis and related methods are published.

Submission of Papers. The preferred medium of submission is on disk with accompanying manuscript (see *Electronic manuscripts* in the Instructions to Authors, which can be obtained from the publisher, Elsevier Science Publishers B.V., P.O. Box 330, 1000 AH Amsterdam, Netherlands). Manuscripts (in English; *four* copies are required) should be submitted to: Editorial Office of *Journal of Chromatography*, P.O. Box 681, 1000 AR Amsterdam, Netherlands, Telefax (+31-20) 5862 304, or to: The Editor of *Journal of Chromatography, Biomedical Applications*, P.O. Box 681, 1000 AR Amsterdam, Netherlands. Review articles are invited or proposed in writing to the Editors who welcome suggestions for subjects. An outline of the proposed review should first be forwarded to the Editors for preliminary discussion prior to preparation. Submission of an article is understood to imply that the article is original and unpublished and is not being considered for publication elsewhere. For copyright regulations, see below.

Publication. The *Journal of Chromatography* (incl. *Biomedical Applications*) has 40 volumes in 1993. The subscription prices for 1993 are:

J. Chromatogr. (incl. *Cum. Indexes*, Vols. 601–650) + *Biomed. Appl.* (Vols. 612–651):
Dfl. 8520.00 plus Dfl. 1320.00 (p.p.h.) (total *ca.* US$ 5927.75)

J. Chromatogr. (incl. *Cum. Indexes*, Vols. 601–650) only (Vols. 623–651):
Dfl. 7047.00 plus Dfl. 957.00 (p.p.h.) (total *ca.* US$ 4821.75)

Biomed. Appl. only (Vols. 612–622):
Dfl. 2783.00 plus Dfl. 363.00 (p.p.h.) (total *ca.* US$ 1895.25).

Subscription Orders. The Dutch guilder price is definitive. The US$ price is subject to exchange-rate fluctuations and is given as a guide. Subscriptions are accepted on a prepaid basis only, unless different terms have been previously agreed upon. Subscriptions orders can be entered only by calender year (Jan.–Dec.) and should be sent to Elsevier Science Publishers, Journal Department, P.O. Box 211, 1000 AE Amsterdam, Netherlands, Tel. (+31-20) 5803 642, Telefax (+31-20) 5803 598, or to your usual subscription agent. Postage and handling charges include surface delivery except to the following countries where air delivery via SAL (Surface Air Lift) mail is ensured: Argentina, Australia, Brazil, Canada, China, Hong Kong, India, Israel, Japan*, Malaysia, Mexico, New Zealand, Pakistan, Singapore, South Africa, South Korea, Taiwan, Thailand, USA. *For Japan air delivery (SAL) requires 25% additional charge of the normal postage and handling charge. For all other countries airmail rates are available upon request. Claims for missing issues must be made within three months of our publication (mailing) date, otherwise such claims cannot be honoured free of charge. Back volumes of the *Journal of Chromatography* (Vols. 1–611) are available at Dfl. 217.00 (plus postage). Customers in the USA and Canada wishing information on this and other Elsevier journals, please contact Journal Information Center, Elsevier Science Publishing Co. Inc., 655 Avenue of the Americas, New York, NY 10010, USA, Tel. (+1-212) 633 3750, Telefax (+1-212) 633 3764.

Abstracts/Contents Lists published in Analytical Abstracts, Biochemical Abstracts, Biological Abstracts, Chemical Abstracts, Chemical Titles, Chromatography Abstracts, Clinical Chemistry Lookout, Current Awareness in Biological Sciences (CABS). Current Contents/Life Sciences, Current Contents/Physical, Chemical & Earth Sciences, Deep-Sea Research/Part B: Oceanographic Literature Review, Excerpta Medica, Index Medicus, Mass Spectrometry Bulletin, PASCAL-CNRS, Pharmaceutical Abstracts, Referativnyi Zhurnal, Research Alert, Science Citation Index and Trends in Biotechnology.

US Mailing Notice. *Journal of Chromatography* (main section ISSN 0021-9673, *Biomedical Applications* section ISSN 0378-4347) is published (78 issues/year) by Elsevier Science Publishers (Sara Burgerhartstraat 25, P.O. Box 211, 1000 AE Amsterdam, Netherlands). Annual subscription price in the USA US$ 5927.75 (subject to change), including air speed delivery. Application to mail at second class postage rate is pending at Jamaica, NY 11431. **USA POSTMASTERS:** Send address changes to *Journal of Chromatography*, Publications Expediting, Inc., 200 Meacham Avenue, Elmont, NY 11003. Airfreight and mailing in the USA by Publication Expediting.

See inside back cover for Publication Schedule, Information for Authors and information on Advertisements.

0021-9673/92/$05.00

CONTENTS

(Abstracts/Contents Lists published in Analytical Abstracts, Biochemical Abstracts, Biological Abstracts, Chemical Abstracts, Chemical Titles, Chromatography Abstracts, Current Awareness In Biological Sciences (CABS), Current Contents/Life Sciences, Current Contents/Physical, Chemical & Earth Sciences, Deep-Sea Research/Part B: Oceanographic Literature Review, Excerpta Medica, Index Medicus, Mass Spectrometry Bulletin, PASCAL-CNRS, Referativnyi Zhurnal, Research Alert and Science Citation Index)

REGULAR PAPERS

Column Liquid Chromatography

Gas Chromatography

(Continued overleaf)

FOR ADVERTISING INFORMATION PLEASE CONTACT OUR ADVERTISING REPRESENTATIVES

USA/CANADA

Weston Media Associates
Mr. Daniel S. Lipner
P.O. Box 1110, GREENS FARMS, CT 06436-1110
Tel: (203) 261-2500, Fax: (203) 261-0101

GREAT BRITAIN

T.G. Scott & Son Ltd.
Tim Blake
Portland House, 21 Narborough Road
COSBY, Leicestershire LE9 5TA
Tel: (0533) 753-333, Fax: (0533) 750-522
Mr. M. White or Mrs. A. Curtis
30-32 Southampton Street, LONDON WC2E 7HR
Tel: (071) 240 2032, Fax: (071) 379 7155,
Telex: 299181 adsale/g

JAPAN

ESP - Tokyo Branch
Mr. S. Onoda
20-12 Yushima, 3 chome, Bunkyo-Ku
TOKYO 113
Tel: (03) 3836 0810, Fax: (03) 3839-4344
Telex: 02657617

REST OF WORLD

ELSEVIER SCIENCE PUBLISHERS
Ms. W. van Cattenburch
P.O. Box 211, 1000 AE AMSTERDAM,
The Netherlands
Tel: (20) 515.3220/21/22, Telex: 16479 els vi nl
Fax: (20) 683.3041

Capillary Electrophoresis

Principles, Practice and Applications

by **S.F.Y. Li**, *National University of Singapore, Singapore*

Journal of Chromatography Library Volume 52

Capillary Electrophoresis (CE) has had a very significant impact on the field of analytical chemistry in recent years as the technique is capable of very high resolution separations, requiring only small amounts of samples and reagents. Furthermore, it can be readily adapted to automatic sample handling and real time data processing. Many new methodologies based on CE have been reported. Rapid, reproducible separations of extremely small amounts of chemicals and biochemicals, including peptides, proteins, nucleotides, DNA, enantiomers, carbohydrates, vitamins, inorganic ions, pharmaceuticals and environmental pollutants have been demonstrated. A wide range of applications have been developed in greatly diverse fields, such as chemical, biotechnological, environmental and pharmaceutical analysis.

This book covers all aspects of CE, from the principles and technical aspects to the most important applications. It is intended to meet the growing need for a thorough and balanced treatment of CE. The book will serve as a comprehensive reference work and can also be used as a textbook for advanced undergraduate and graduate courses. Both the experienced analyst and the newcomer will find the text useful.

Contents:

1992 xxvi + 586 pages
Price: US$ 225.50 / Dfl. 395.00
ISBN 0-444-89433-0

TO ORDER

Contact your regular supplier or:

ELSEVIER SCIENCE PUBLISHERS
P.O. Box 211
1000 AE Amsterdam
The Netherlands

Customers in the USA & Canada:

ELSEVIER SCIENCE PUBLISHERS
Attn. Judy Weislogel
P.O. Box 945
Madison Square Station
New York, NY 10160-0757, USA

No postage will be added to prepaid book orders. US $ book prices are valid only in the USA and Canada. In all other countries the Dutch guilder (Dfl.) price is definitive. Customers in The Netherlands please add 6% BTW. In New York State please add applicable sales tax. All prices are subject to change without prior notice.

ELSEVIER
SCIENCE PUBLISHERS

JOURNAL OF CHROMATOGRAPHY

VOL. 623 (1992)

JOURNAL of CHROMATOGRAPHY

INCLUDING ELECTROPHORESIS AND OTHER SEPARATION METHODS

ELSEVIER

AMSTERDAM — LONDON — NEW YORK — TOKYO

0021-9673/92/$05.00

Printed in the Netherlands

Journal of Chromatography, 623 (1992) 1–14
Elsevier Science Publishers B.V., Amsterdam

CHROM. 24 486

Development of an enzyme-linked immunosorbent assay for C.I. Reactive Blue 2 and its application to a comparison of the stability and performance of a perfluorocarbon support with other immobilised C.I. Reactive Blue 2 affinity adsorbents

David J. Stewart, Duncan R. Purvis, Jennifer M. Pitts and Christopher R. Lowe

Institute of Biotechnology, University of Cambridge, Tennis Court Road, Cambridge CB2 1QT (UK)

(First received March 13th, 1992; revised manuscript received July 3rd, 1992)

ABSTRACT

An indirect competitive enzyme-linked immunosorbent assay capable of detecting the reactive triazine dye C.I. Reactive Blue 2 at concentrations down to 300 p*M* was developed, and representing a 3000-fold higher sensitivity over direct spectrophotometric analysis. An investigation of the cross-reactivity of the polyclonal antibody against various compounds structurally related to C.I. Reactive Blue 2 revealed that the immunoassay appeared to be specific for anthraquinone-containing dyes and was largely unaffected by substitutions at the triazine ring. These characteristics suggest that the immunoassay may be exploited to analyse the leaching of the ligand C.I. Reactive Blue 2 from dye-affinity adsorbents. The performance of a novel perfluoropolymer affinity support containing C.I. Reactive Blue 2 was compared with eight other commercially available dyed affinity adsorbents by three separate criteria: pressure–flow-rate characteristics, protein binding capacities and dye leakage under selected conditions. All the affinity adsorbents were subjected to six purification cycles of albumin from human plasma prior to comparison. In the pressure–flow-rate comparison, the perfluoropolymer support, in contrast to the other adsorbents, showed a non-linear relationship between pressure and flow-rate. Human serum albumin dynamic load capacities were determined by frontal analysis and were found to be in the range 10.1–48.5 mg/ml. The perfluoropolymer support displayed the lowest capacity, probably because of its lack of porosity and, consequently, low surface area. In the dye leakage analysis, the perfluoropolymer support exhibited the lowest leakage of immobilised dye under all conditions tested including exposure to sodium isothiocyanate (5 *M*), hydrochloric acid (1 *M*) and sodium hydroxide (1 *M*). This study suggests that although the novel C.I. Reactive Blue 2–perfluoropolymer support displays low protein binding capacity, it otherwise compares very favourably with a range of commercially available dye-affinity adsorbents.

INTRODUCTION

Immobilised textile dyes are being used increasingly as affinity adsorbents for the purification of biological macromolecules [1-7]. The triazine dyes are robust molecules possessing a mixture of aromatic and charged moieties that bind relatively selectively to proteins at sites where natural substrates, inhibitors, cofactors and nucleotides interact. The reactive chlorotriazine ring enables facile coupling of the dye to hydroxyl-containing chromatographic matrices, thereby allowing the preparation of versatile affinity adsorbents. Thus, not suprisingly, immobilised triazine dyes are increasingly replacing natural biological ligands as adsorbents for affinity chromatography since their low cost and broad applicability coupled with their ease of immobilisation and resistance to chemical and biological degrada-

Correspondence to: Dr. C. R. Lowe, Institute of Biotechnology, University of Cambridge, Tennis Court Road, Cambridge CB2 1QT, UK.

0021-9673/92/$05.00

tion is particularly advantageous at process scale [7,8]. However, the wider acceptance of triazine dyes as affinity ligands, particularly for the purification of high value therapeutic proteins, has been beset by concerns over dye leakage and resultant product contamination either through matrix breakdown or solvolysis of the matrix–ligand bond [1]. There still remains a requirement for the development of novel chromatographic matrices and coupling chemistries that are able to withstand not only the high pressures used in high performance affinity chromatography, but also treatment with extremes of acid and alkali used for *in situ* column clean-up, chemical sanitisation and depyrogenation [9].

Perfluorocarbons are chemically and biologically inert, high density (1.8–2.1 g/ml), thermally stable synthetic materials that are totally insoluble in aqueous and organic solvents. They are extremely hydrophobic and do not immediately appear to be materials suitable for biochromatography. However, effective affinity adsorbents can be synthesised by wetting the surfaces of solid or liquid perfluoropolymers with perfluoroalkylated dyes. Thus, the preparation of several bis-perfluoroalkylated dichlorotriazinyl dyes and their subsequent adsorption to a perfluoropolymer matrix and application to the purification of lactate dehydrogenase from a crude rabbit muscle extract by affinity chromatography has been reported [10]. These materials, however, were still prone to ligand leakage on exposure to organic solvents or harsh aqueous conditions. Since the extent of leakage appeared to depend on the number and length of perfluorocarbon anchoring groups, attachment of the triazine dye to an inert hydrophilic polymer containing a number of pendant perfluorinated anchoring groups should provide a highly stable adsorbed polymeric coating on the perfluoropolymer matrix. The synthesis of perfluoroalkylated polyvinyl alcohol, its immobilisation onto a perfluoropolymer matrix and subsequent derivatisation with C.I. Reactive Blue 2 and its application to the purification of rabbit muscle lactate dehydrogenase and human serum albumin by affinity chromatography has recently been reported [11]. The adsorbent exhibited negligible non-specific adsorption and similar capacities and degrees of purification as previously reported for dyed silica [12]. Furthermore, a long-term study lasting more than nine months was unable to detect dye leakage spectrophotometrically on exposure of the perfluoropolymer adsorbents to water, sodium hydroxide (1 *M*), hydrochloric acid (1 *M*), urea (1 *M*) or acetone, suggesting that this novel affinity adsorbent might compare very favourably with commercially available dyed affinity adsorbents.

Although the textile dyes are intensely coloured, spectrophotometric analysis is limited to a detection limit of 10^{-6} *M* if no prior concentration of the leachate is carried out; in practice, sample turbidity may reduce the sensitivity even further. Consequently, the development of a sensitive assay to detect the leakage of ligands, particularly the widely used triazine dye C.I. Reactive Blue 2, from affinity adsorbents, is now long overdue. The development of an enzyme-linked immunosorbent assay (ELISA) [13] for C.I. Reactive Blue 2 would not only greatly facilitate the assessment of adsorbent stability under operational conditions, but also permit the level of contamination of injectable therapeutic products by leachates to be quantitatively determined.

This paper describes the development and application of an enzyme-linked immunoassay for C.I. Reactive Blue 2 to compare the leakage of dye from the perfluoropolymer support with a number of commercially available C.I. Reactive Blue 2-containing affinity adsorbents. Adsorbent stability was analysed under a variety of conditions and care was taken to treat the materials identically by pre-treating all media with six human serum albumin purification cycles prior to the leakage study. In order to offer a comprehensive assessment of the performance of the materials, two further comparisons were undertaken: flow-rate was measured as a function of pressure for all the materials, which included inorganic, organic and several agarose-based materials, together with the coated perfluoropolymer adsorbent. In addition, the dynamic load capacity of these adsorbents for human serum albumin was measured by frontal analysis to evaluate the performance of the perfluoropolymer support compared to other adsorbents. A similar comparative study of commercially available Protein A affinity adsorbents has recently been reported [14].

MATERIALS AND METHODS

Materials

C.I. Reactive Blue 2, ovalbumin, bovine serum albumin (fraction V, 96–99%), goat anti-rabbit immunoglobulin G(IgG)–peroxidase conjugate were all purchased from Sigma (Poole, UK). *ortho*-Phenylenediamine was purchased from Dakopatts (High Wycombe, UK) while Falcon 3912 Micro test III flexible microtitre plates were obtained from Beckton Dickinson Labware (Oxnard, CA, USA). Sephadex LH-20, Sephadex G-25 (disposable PD-10 columns) and Mono Q (HR5/5) were obtained from Pharmacia (Milton Keynes, UK). Bromaminic acid was from Sandoz (Basle, Switzerland) and other compounds used in cross-reactivity studies were a kind gift from Dr Steven Burton of the University of Cambridge. The following affinity adsorbents were purchased either from manufacturers or suppliers: Mimetic Blue 1 A6XL [Affinity Chromatography, (ACL), Isle of Man, UK], Affigel Blue gel (Bio-Rad, UK), Blue-Trisacryl M (IBF, France), Fractogel TSK AF-Blue (Merck, Germany), Blue Sepharose CL-6B (Pharmacia, UK), immobilised Cibacron Blue F3GA (Pierce, UK), Cibacron Blue F3GA = Si500 (Serva, GDR) and C.I. Reactive Blue 2 Sepharose CL-6B (Sigma, Poole, UK). The particulate perfluoropolymer matrix (6–8m^2/g) was kindly provided by DuPont (Wilmington, DE, USA). Polyvinyl alcohol (average M_r 14 000, 100% hydrolyzed) was purchased from Sigma, perfluorooctanoyl chloride was bought from Fluorochem (Old Glossop, UK) and the triazine dye C.I. Reactive Blue 2 and acetone (SLR) were from BDH (Poole, UK). Human plasma was obtained from a known donor at the National Blood Transfusion Centre (Nottingham, UK) and tested HIV III$^-$, HBS antigen$^-$ and syphilis$^-$. All other chemicals/biochemicals were of analytical grade and were obtained from Sigma. All chromatography was carried out using a Pharmacia FPLC system fitted with two P-500 pumps, twin MV-8 and single MV-7 valves, 50-ml superloop, UV-1 monitor and LCC 500 controller.

Preparation of dye-protein conjugates for immunoassay

Conjugates of C.I. Reactive Blue 2 with ovalbumin and bovine serum albumin were both prepared as follows. Crude C.I. Reactive Blue 2 was purified on Sephadex LH-20 equilibrated with methanol–water (50:50, v/v) according to the method of Pearson *et al.* [15]. Solid purified dye (200 mg) was added to a solution of protein (100 mg) in 0.2 *M* sodium bicarbonate solution, pH 9.0, (5 ml) and the mixture stirred for 15 h at 36°C, after which unreacted dye was removed by gel filtration on PD-10 columns equilibrated with distilled water. The coloured fraction appearing in the void volume was freeze-dried and stored at −20°C. The molar ratio of dye to protein in the conjugate was calculated from the absorbance at 620 nm of a solution containing a known weight of conjugate, assuming a molar extinction coefficient of 12 700 M^{-1} cm^{-1} for C.I. Reactive Blue 2 and molecular masses of 840, 44 000 and 68 800 for C.I. Reactive Blue 2, ovalbumin and bovine serum albumin, respectively.

Preparation of rabbit anti-C.I. Reactive Blue 2 antibody

Rabbits (New Zealand White, 2.5 kg) were immunised with C.I. Reactive Blue 2–bovine serum albumin conjugate (11.8 mol dye / mol protein). Primary immunisation was by subcutaneous injections of conjugate made 2 mg/ml in sodium chloride (0.85%, w/v) and emulsified in an equal volume of Freund's Complete adjuvant (100 μg conjugate, total of 2 injections per rabbit). Subcutaneous booster injections of conjugate prepared as before in Freund's Incomplete adjuvant (200 μg conjugate, 2 injections per rabbit) were given six weeks later, followed by subcutaneous booster injections of conjugate made 1 mg/ml in sodium chloride solution (0.85%, w/v)(200 μg conjugate, 2 injections per rabbit) every six weeks. Blood was collected from the marginal ear vein two weeks after booster injections and prepared sera were kept frozen at −20°C.

Purification of rabbit IgG by ion-exchange chromatography

Buffers A (20 m*M* Tris–HCl, pH 9.0) and B (20 m*M* Tris–HCl, 1 *M* NaCl, pH 7.7) were filtered through 0.2-μm filters and degassed. Rabbit sera from two immunised rabbits were transferred into buffer A using disposable PD-10 columns according to the manufacturer's instructions, filtered through 0.2-μm filters and then samples (1 ml) loaded on to a Mono Q anion-exchange column installed in a

comprehensive Pharmacia fast protein liquid chromatography (FPLC) system. The salt gradient was applied over a total volume of 18 ml and fractions (1 ml) were collected, assayed for antibody titre using a standard ELISA, aliquotted where appropriate and kept frozen at −20°C.

Determination of antibody titre and appropriate antiserum dilution for indirect competitive ELISA

Measurement of antibody titres and determination of appropriate antibody concentration for the indirect competitive enzyme immunoassay were carried out simultaneously. In summary, plates precoated with dye–ovalbumin conjugate (4.5 mol dye/mol protein: 10 μg/ml) were incubated with serial dilutions of purified IgG fractions of rabbit antiserum to C.I. Reactive Blue 2, and following exhaustive washing, with excess anti-rabbit IgG-peroxidase conjugate. Maximal binding of anti-dye antibody to the dye hapten was observed for dilutions above 800-fold. The antibody dilution for use in the competitive assay was chosen as the dilution at which approximately 70% of maximal antibody binding occurs, thereby providing non-saturated conditions in which added dye competes directly with bound dye for antibody binding.

To identify both the fraction containing the highest titre of specific antibody and the appropriate dilution of this fraction for subsequent assays, antigen-coated microtitre plates were prepared by incubating wells with a solution of C.I. Reactive Blue 2–ovalbumin conjugate (10 μg/ml) in 50 m*M* carbonate, pH 9.6, overnight at 4°C (100 μl/well). Plates were blocked with Marvel (3%, w/v) in phosphate-buffered saline (PBS) containing 0.1% (w/v) Tween 20 (PBST) at 37°C for 2 h (blocking buffer, BB)(200 μl/well) and then thoroughly washed six times (with two 3-min soaks) with 0.9% (w/v) NaCl containing 0.05% (w/v) Tween 20 (washing buffer, WB). Dilutions (1/50) of crude sera and purified fractions from both rabbits were prepared in PBST containing 0.1% (w/v) gelatin (PBST/G) and serially diluted (1:2) across the microtitre plates. After 1 h incubation at 37°C, plates were washed as before with WB after which goat anti-rabbit IgG–horse radish peroxidase conjugate diluted 1/1000 in PBST/G was added to the plates (50 μl per well), followed by a further incubation step of 1 h at 37°C. *ortho*-Phenylenediamine was made 1 m*M* in 0.1 *M* citric acid–phosphate buffer, pH 5.0 (substrate buffer, SB) and the plates were washed three times with WB followed by distilled water. Hydrogen peroxide (30%)(5 μl) was added just prior to addition of the freshly prepared substrate (50 μl/well). After 30 min incubation in the dark at room temperature, 1 *M* H_2SO_4 (50 μl/well) was added to stop the reaction and the absorbances of the wells read at 492 nm using a Titertek ELISA plate reader.

Indirect competitive enzyme-linked immunoassay

An indirect competitive assay was used in order to detect free dye. In this procedure, free antigen was serially diluted (1:2) across the plate. Standard curves were obtained using a series of C.I. Reactive Blue 2 standards (10 μ*M* to 1 n*M*) serially diluted (50 μl/well) across the plate to which was added a standard aliquot of appropriately diluted antibody (50 μl/well) in 2 × PBST/G. Plates were agitated at room temperature for 15 min and then incubated at 37°C for 1 h as before. Bound antibody was detected as previously described. Unknown samples were similarly diluted and the curves generated compared with standard curves to yield values of the concentration of C.I. Reactive Blue 2 in the unknown samples. Assays were typically carried out in triplicate.

The effect on assay sensitivity of antigen coating concentration was studied by incubating microtitre plates with dilutions of antigen ranging from 0.01–10 μg/ml using a lower-substituted dye–ovalbumin conjugate (1.14 mol dye/mol protein). Standard dye solutions were used to assess the sensitivity of the assay depending on the extent of antigen coating.

Cross-reactivity of anti-C.I. Reactive Blue 2 antibody with various analogues and structural fragments of C.I. Reactive Blue 2

All compounds were made 5 m*M* in water and serial dilutions were prepared as for standard C.I. Reactive Blue 2 after which the appropriate dilution of antibody was added in 2 × PBST/G. The concentration of compound required to yield an absorbance of 1.0 at 492 nm was estimated from the linear region of the antibody binding curves. Comparison with the C.I. Reactive Blue 2 concentration yielded the relative cross-reactivity of the compound for anti-C.I. Reactive Blue 2 antiserum. Assays were performed in triplicate.

Synthesis of C.I. Reactive Blue 2 polyvinyl alcohol-coated perfluoropolymer support. Modification of the perfluorocarbon matrix

C.I. Reactive Blue 2 was immobilised to the polyvinyl alcohol-coated perfluoropolymer support according to the procedure described in ref. 11. Immobilised ligand content was estimated according to a previously described procedure [11].

Preparation of affinity adsorbents

Commercial adsorbents were initially prepared as recommended by the manufacturers. Where no recommendations were available, gels were mixed/swollen with approximately 50 volumes distilled water, washed with 50 volumes 50 m*M* phosphate buffer, pH 7.0 and then packed in Pharmacia HR5/10 columns (2 ml). Thereafter, experiments were conducted on each 2 ml packed sample in a sequential manner: (i) pretreatment; (ii) determination of albumin capacity by frontal analysis; (iii) leakage of dye in buffer; and (iv) leakage of dye in rigorous conditions. Flow-rate *versus* pressure analyses were carried out in packed Pharmacia HR5/10 columns using prepared but untreated gels which were discarded after use.

Flow-rate versus pressure analysis

Prior to adsorbent packing, all end-frits were sonicated in 1 *M* hydrochloric acid. After packing, adsorbent flow-rates were generated using Pharmacia's FPLC system with a safety cut-off at 4.5 MPa. Values for flow-rate (ml/min) were made independent of column geometry by dividing by the cross-sectional area of the HR5/10 columns.

Pretreatment of affinity adsorbents

Adsorbents were pre-equilibrated in 20 m*M* acetate buffer, pH 5.5. Human plasma was diluted 1/4 in this buffer, filtered through 0.2-μm filter, the pH adjusted to 5.5 with 0.1 *M* hydrochloric acid and 1 ml samples ($\approx$20 mg protein) loaded onto each column. Bound protein was eluted with 1 *M* potassium chloride in 20 m*M* phosphate, pH 8.0 in a total volume of 5 ml. Each column was then re-equilibrated with 20 m*M* acetate buffer, pH 5.5 and diluted plasma loaded once more. In all, each column underwent six plasma load–wash–elute–re-equilibration cycles. Columns were run at 1 ml/min, with the exception of Bio-Rad's Affi-Gel Blue matrix which was run at 0.25 ml/min.

Dynamic load capacity for human serum albumin

Dynamic load capacities of the adsorbents were determined according to the method described in ref. 16. Human serum albumin-binding capacity was measured by pumping 10 mg/ml pure albumin in 20 m*M* acetate buffer, pH 5.5, until the absorbance at 280 nm of the output and input streams were identical. Protein loading was halted, the column washed with buffer until the eluent contained negligible protein by absorbance at 280 nm and bound albumin was then eluted with potassium chloride (1 *M*) in 20 m*M* phosphate buffer, pH 8.0; the recovery of bound protein was determined by absorbance at 280 nm. Protein concentrations were determined by absorbance at 280 nm assuming an extinction coefficient for pure human serum albumin of 0.53 ml mg^{-1} cm^{-1} [17].

Dye leakage: detection by enzyme immunoassay

In order to detect free dye, the indirect competitive ELISA was used. A standard curve was obtained using a known solution of C.I. Reactive Blue 2 (5 μM) serially diluted across the microtitre plate. Unknown samples were serially diluted six-fold across identically coated microtitre plates and curves generated were fitted to the standard curve to yield values of the concentration of C.I. Reactive Blue 2 in each sample. For this study conditions were adjusted to detect unknown dye concentrations from the limits of spectrophotometric detection (1 μM) down to 3 n*M* in order to maximise the possible range of detection. Where dye was visible in the initial sample, the sample was diluted ten-fold before being serially diluted across the microtitre plate. Acidic and basic samples were neutralised with small aliquots of strong base or acid. High chaotrope concentrations which interfered with the immunoassay could not be easily removed by techniques such as gel filtration without affecting the dye concentration. After thorough investigation, it was concluded that antibody binding in serial dilutions containing below 320 m*M* NaSCN was identical to controls in the absence of chaotrope. Therefore, samples containing 5 *M* NaSCN were initially diluted 1:1 with antibody in the first well, yielding a chaotrope concentration of 2.5 *M* NaSCN, and were then serially diluted six-fold across the plate; only the final three wells, containing 313, 157 and 79 m*M* NaSCN, respectively, were used for the analysis of those samples.

Dye leakage in buffer

Packed gels (2 ml bed volume) were thoroughly washed with 50 m*M* phosphate buffer, pH 7.0 (50 column volumes) and left to stand in this buffer at room temperature (72 h). Buffer (10 ml) was run through the columns, collected and assayed for leakage of dye by competitive ELISA. Leakage data were corrected to give values for the average daily loss of dye from the affinity adsorbents.

Dye leakage in rigorous conditions

Affinity adsorbents were sequentially exposed to three increasing concentrations of chaotrope (NaSCN), acid and base; after each exposure, the gel was immediately washed with an equal volume of distilled water, and then left while the next adsorbent was challenged. Each gel was thus exposed to 10 ml volumes of 0.5 *M* NaSCN, 0.1 *M* HCl, 0.1 *M* NaOH, 1.25 *M* NaSCN, 0.25 *M* HCl, 0.25 *M* NaOH, 5 *M* NaSCN, 1 *M* HCl and 1 *M* NaOH, each exposure followed immediately by a 10 ml water wash and a pause of 140 min before the next challenge. All fractions were collected, neutralised where necessary and assayed for C.I. Reactive Blue 2 by competitive ELISA.

RESULTS AND DISCUSSION

ELISA development

Purification and characterisation of rabbit IgG to C.I. Reactive Blue 2. The fraction containing the highest antibody titre against C. I. Reactive Blue 2 was purified from the crude antiserum of one New Zealand White rabbit by anion-exchange chromatography and assayed by standard ELISA. Fig. 1A shows the standard dilution curve for this fraction incubated with bound C.I. Reactive Blue 2–ovalbumin conjugate (10 μg/ml; 4.5 mol dye/mol protein) and shows that a 1/3200 dilution gives approximately 70% maximal binding of antibody. Therefore all competitive assays were carried out using a 1/3200 dilution of the highest titre fraction. Fig. 1B

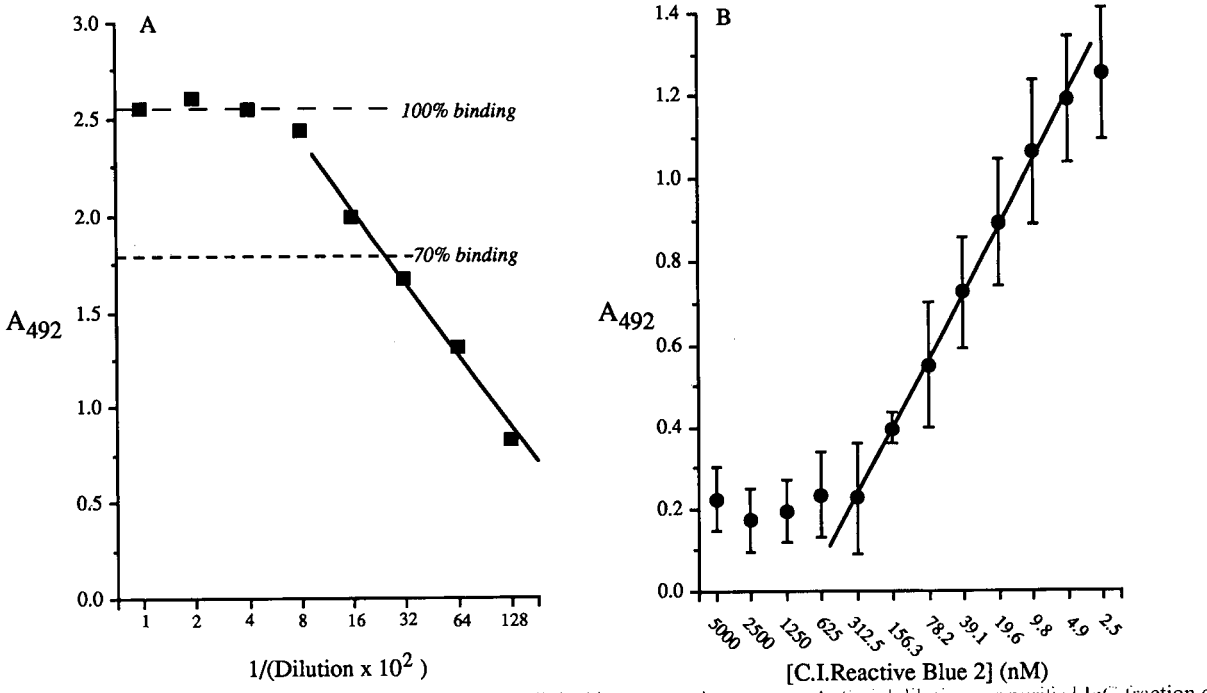

Fig. 1. Calibration curves for indirect competitive enzyme-linked immunosorbent assay. (A) Serial dilutions of purified IgG fraction of rabbit antiserum to C.I. Reactive Blue 2 incubated on plates pre-coated with dye–ovalbumin conjugate (4.5 mol dye/mol protein; 10 μg/ml). Values shown represent actual measurements. (B) Serial dilutions of C.I. Reactive Blue 2 incubated together with 1/3200 dilution of purified IgG fraction on identical plates to (A). Values shown represent means and standard deviations of triplicate samples.

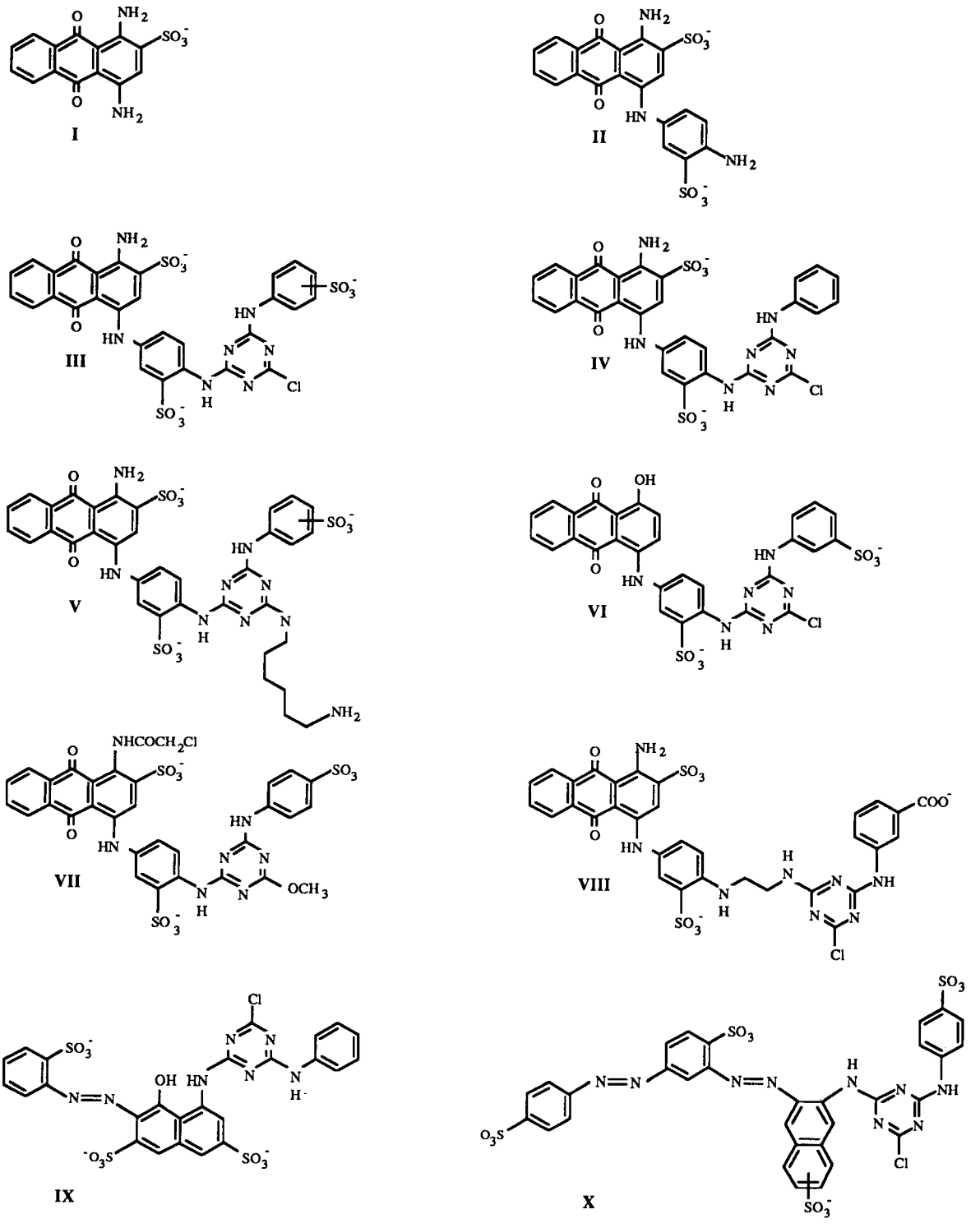

Fig. 2. Structures of fragments and analogues of C.I. Reactive Blue 2: (**I**) = 1,4-diaminoanthraquinone; **II** = Blue base; **III** C.I. Reactive Blue 2; **IV** = *anilino*-C.I. Reactive Blue 2; **V** = 1,6- diaminohexane-*m*-C.I. Reactive Blue 2; **VI** = 1-hydroxy-2-desulpho-*m*-C.I. Reactive Blue 2; **VII** = acryloyl anthraquinone-methoxy-*p*-C.I. Reactive Blue 2; **IX** = Procion red H-3B, **VIII** = *m*-benzoic-*s*-triazino-1,2-ethylenediamine-blue base; **X** = Procion brown H-2G. All compounds purified by Sepharose LH-20 chromatography according to Lowe and Pearson [2].

shows the mean standard curve and deviation for C.I. Reactive Blue 2 using the indirect competitive assay across a broad range of dye concentrations (2.4 n*M*–5 μ*M*). The assay is linear between 5 and 300 n*M* C.I. Reactive Blue 2 under the conditions used.

Sensitivity of the competitive ELISA for C.I. Reactive Blue 2. Analysis of the potential sensitivity of the indirect competitive ELISA was performed using a lighter substituted dye–protein conjugate (1.14 mol dye/mol protein) and a range of coating concentrations down to 10 ng conjugate/ml. The sensitivity of the assay increased as the amount of bound antigen decreased and under certain conditions the assay could detect dye concentrations down to 300 p*M*. The amount of bound antibody did, however, decrease with lower antigen coating concentrations, producing a lower absorbance value against a fixed background (the plate itself) and thereby more potential for error. Amplification systems such as those based on the biotin–avidin system [18] may be expected to increase the sensitivity further. This aspect was not investigated since, for our purposes, the assay was required to measure a broad range of dye concentrations up to spectrophotometric detection limits (1 μ*M*) and this necessitated choosing a higher concentration of coating antigen (10 μg/ml) with concomitant loss of sensitivity (>3 n*M*; ≈3 ng/ml).

Specificity of the competitive ELISA for C.I. Reactive Blue 2. The specificity of the immunoassay was studied by measuring the ability of structural fragments and analogues of C.I. Reactive Blue 2 and other reactive dyes to block antibody binding of C.I. Reactive Blue 2-coated microtitre plates. Fig. 2 shows the structures of some compounds tested for their cross-reactivity with antibody to the parent dye . Structures **I** and **II** are intermediates in the synthesis of C.I. Reactive Blue 2 (**III**), while **IV** is an unsubstituted terminal ring isomer of the dye [19]. Compound **V** represents the parent dye substituted at the triazine ring with 1,6-diaminohexane, a bridging or spacer group commonly used in affinity chromatography to separate the affinity ligand from the matrix backbone. Compounds **VI** and **VII** each possess substituted anthraquinone moieties, though the latter retains the charged anthraquinone sulphonate group. **VIII** is essentially an analogue of C.I. Reactive Blue 2 possessing an 1,2-ethylenediamine spacer group between the blue base moiety (**II**) and the triazine ring. Compounds **IX** and **X** represent two azo triazine dyes, Procion Red H-3B and Procion Brown H-2G respectively, that do not contain the anthraquinone group.

TABLE I

CROSS-REACTIVITY OF CERTAIN FRAGMENTS AND STRUCTURAL ANALOGUES OF C.I. REACTIVE BLUE 2 IN ELISA

Microtitre plates were presented with dye–ovalbumin conjugate (4.5 μmol dye/μmol protein; 10 μg/ml). Plates were incubated with serial dilutions of 5 μ*M* stocks of analogues together with a 1/3200th dilution of purified IgG factor of rabbit antiserum to C.I. Reactive Blue 2. Values shown represent the means of triplicate samples.

Compound	No.	Concentration[a] (n*M*)	Relative cross-reactivity (%)
1,4-Diaminoanthraquinone	**I**	360	3.6
Blue base	**II**	32	40.6
C.I. Reactive Blue 2	**III**	13	100
anilino-C.I. Reactive Blue 2	**IV**	24	54.2
1,6-Diaminohexane-*m*-C.I. Reactive Blue	**V**	14	92.9
1-Hydroxy-2-desulpho-*m*-C.I. Reactive Blue 2	**VI**	180	7.2
Acryloyl anthraquinone-methoxy-*p*-C.I. Reactive Blue 2	**VII**	180	7.2
m-Benzoic-*s*-triazino-1,2-ethylenediamine-blue base	**VIII**	17	76.5
Procion red H-3B	**IX**	5000	0.3
Procion brown H-2	**X**	3300	0.4

[a] These values represent that concentration of each compound yielding an absorbance at 492 nm of 1.0 in the indirect competitive ELISA.

The extent of cross-reactivity of a compound with C.I. Reactive Blue 2 was estimated by comparing the concentration of competing dye analogue necessary to produce an absorbance of 1.0 at 492 nm relative to the required concentration of parent dye. The concentration was estimated from the linear region of the mean antibody binding curve for each compound. Table I shows that dye analogues (**II**, **IV**, **V** and **VIII**) containing the structural motif comprising a 1,4-diaminoanthraquinone ring coupled to a *p*-diaminobenzene sulphonate such as C.I. Reactive Blue 2 itself (**III**) are potent inhibitors of the immune binding reaction. Modification of this structural motif either by removal of the *p*-diaminobenzene sulphonate ring (**I**) or by alteration of the anthraquinone ring itself (**VI** and **VII**) reduce the potency of the competitive binding analogue by at least an order of magnitude. Moreover, dyes altogether lacking an anthraquinone group (**IX** and **X**) showed reduced binding by over two orders of magnitude. That these dyes cross-react to some extent with antibodies raised to C.I. Reactive Blue 2 suggests that some weak antigenic determinancy resides in the triazine and terminal sulphonated rings. This is supported by the lowered immune response exhibited by compound **IV** that lacks a terminal sulphonate negatively-charged groups are thought to play an important role in antigenic determinancy [20].

The observation that the predominant antigenic determinant of C.I. Reactive Blue 2 appears to be the structural motif comprising anthraquinone and *p*-diaminobenzene sulphonate rings may depend in large part on the manner of synthesis of the dye–protein conjugate used for immunisation. C.I. Reactive Blue 2 is coupled to the carrier protein by nucleophilic substitution, through, for example, the ε-amino group of a surface lysine residue of bovine serum albumin, at the triazine ring and, therefore, this region of the hapten is least accessible for recognition by the immune system. Availability of the anthraquinone and *p*-diaminobenzene sulphonate rings for interaction with antibody has thus conferred the desired specificity on the polyclonal antibody. Substitution at the triazine ring, whether by 1,6-diaminohexane or a larger molecule such as degraded fragments of the agarose matrix, should thus have little effect on the recognition of C.I. Reactive Blue 2 by the antibody. Therefore, the rabbit antibody may be fruitfully used to detect low concentrations of both free C.I. Reactive Blue 2 and derivatives in which the leached dye is attached to matrix fragments via the triazine ring without concentration of the eluent or any other prior treatment of the sample.

Evaluation of the adsorbents

Evaluation of the overall performance of an affinity adsorbent for any particular application must include parameters such as mechanical rigidity, capacity for protein binding, and stability under selected conditions. These operational parameters determine the maximum permissible flow-rate through the adsorbent, the protein throughput and the degradation of the adsorbent during use and regeneration.

Flow-rate versus pressure analysis. The two immobilised dye adsorbents based on silica and cross-linked polyvinyl alcohol, Cibacron Blue F3GA Si = 500 and Fractogel TSK AF-Blue, respectively, display a linear relationship between flow-rate and

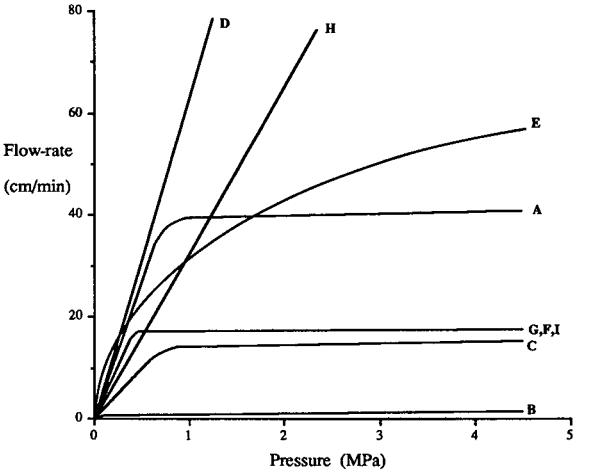

Fig. 3. Flow-rate *versus* pressure curves for C.I. Reactive Blue 2-containing affinity adsorbents. Adsorbents were packed in Pharmacia HR 5/10 columns (2 ml) and flow-rates measured as a function of applied pressure and divided by the column cross-sectional area. Adsorbents are as follows: A = Mimetic Blue A6XL (ACL); B = Affi-Gel Blue (Bio-Rad); C = Blue Tris-acryl-M (IBF); D = Fractogel TSK AF-Blue (Merck); E = C.I. Reactive Blue 2 polyvinyl alcohol-coated perfluorocarbon matrix; F = Blue Sepharose CL-6CB; G = Immobilized Cibacron Blue F3GA (Pierce); H = Cibacron Blue F3GA = Si 500 (Serva); and I = Reactive Blue 2-Sepharose CL-6B (Sigma).

pressure that is characteristic of "hard" chromatography gels and suggests that both materials are suitable for use as high performance media (Fig. 3). In contrast, agarose-based and acrylate-based materials only exhibit this proportionality at low pressures, with further increases in pressure beyond a characteristic point producing no further increase in flow-rate; this observation suggests that compression of the gel is occurring, with flow through the column actually decreasing in some cases if further pressure is applied. Maximal flow-rates through the agarose-based materials varied from less than 2 cm/min for Affi-Gel Blue to almost 40 cm/min for MIMETIC Blue 1 A6XL and appeared to depend on the extent of cross-linking of the matrix. Affi-Gel Blue probably represents native agarose, with Blue Sepharose CL-6B, Immobilised Cibacron Blue F3GA and Reactive Blue 2-Sepharose CL-6B being examples of mildly cross-linked materials, while the rigidity of MIMETIC Blue 1 A6XL must be attributable to a substantial degree of cross-linking. In contradistinction to these affinity adsorbents, the coated perfluoropolymer adsorbent exhibits a non-linear relationship between flow-rate and pressure with an extrapolated working maximum of approximately 80 cm/min. This suggests that the perfluoropolymer matrix undergoes slow compression as the pressure is increased. Furthermore, it has been observed that the amount of adsorbed polymer coating per unit weight of base matrix also appears to play a part in the pressure-flow-rate performance of the perfluoropolymer adsorbent support. Thinner polymeric coatings permit the application of higher flow-rates, although there remains a requirement for sufficient adsorbed polymer to enable immobilisation of the affinity ligand to the matrix and to prevent nonspecific adsorption of protein.

Dynamic load capacity for human serum albumin. Table II displays the suppliers' figures, where available, for immobilised ligand concentrations per ml of affinity adsorbent together with their measured dynamic load capacities for human serum albumin per ml of each affinity adsorbent. Dynamic load capacities do not appear to correlate with ligand densities, since ligand usage (μmol albumin/μmol dye) ranging from 7.8% for the C.I. Reactive Blue 2 polyvinyl alcohol-coated perfluoropolymer to 31.1% exhibited by Immobilised Cibacron Blue F3GA. This difference may result from the fact that while both these gels have comparable ligand densities per unit wet weight (1.9 and 2.0 μmol/g, respectively), the ligand density per unit surface area of the perfluoropolymer adsorbent is much higher because of its low total surface area, and consequently, less protein may be bound per unit volume of adsorbent. Use of alternative perfluoropolymer matrices with higher total surface areas would be expected to offer greater protein binding capacities without a requirement for increasing the ligand concentration per unit wet weight of matrix.

A further point of interest arising from the capacity data given in Table II is the considerable difference in albumin binding capacities exhibited by the 6% cross-linked agaroses, immobilised Cibacron Blue F3GA, Blue Sepharose CL-6B and Reactive Blue 2-Sepharose CL-6B; these gels exhibited near-identical flow-pressure curves and contained equivalent concentrations of immobilised C.I. Reactive Blue 2. This observation may reflect the use of an alternative coupling chemistry in the preparation of immobilised Cibacron Blue F3GA. Similarly, the substantial albumin-binding capacity of MIMETIC Blue 1 A6XL even over the less cross-linked Affi-Gel Blue may result from the manufacturer's acknowledged use of a spacer-arm to separate the ligand from the matrix and facilitate interaction with the complementary protein [21].

Dye leakage in buffer. The dye leakage figures (pmol/day) of the adsorbents shown in Table II were determined after six successive human serum albumin purification cycles, each of which included equilibration, albumin challenge, buffer wash, elution with 1 *M* potassium chloride and re-equilibration. These conditions would be expected to displace any unbound dye remaining after implementation of the manufacturers' washing procedures. Thus, the leakage of dye from Affi-Gel Blue, Blue Trisacryl-M and Immobilised Cibacron Blue F3GA must represent a realistic daily loss arising either through hydrolysis of the dye–matrix bond or the matrix itself. In context, however, this means that even Affi-Gel Blue, the adsorbent displaying the highest rate of ligand loss at 0.0009%/day, would lose less than 0.33% of its immobilised dye per year when standing at room temperature in 50 m*M* phosphate buffer at pH 7.0. No leakage of dye was detectable from the coated perfluoropolymer adsorbent under these conditions.

TABLE II

LIGAND CONCENTRATION, HUMAN SERUM ALBUMIN CAPACITY AND STABILITY IN BUFFER OF C.I. REACTIVE BLUE 2-CONTAINING AFFINITY ADSORBENTS

Adsorbent[a]	Manufacturer/supplier	Ligand content[b] (μmol/ml)	Human serum albumin capacity[e] (mg/ml)	Dye leakage (pmol/day)	Immobilised dye loss (%loss/day)
Mimetic Blue 1 A6XL	ACL	2.5 ± 0.2	48.9	U[f]	–
Affi-Gel Blue	Bio-Rad	>2.3[c]	45.5	43	<0.0009
Immobilised Cibacron Blue F3GA	Pierce	≈2.0	42.3	17	0.0004
Fractogel TSK AF-Blue	Merck	–[d]	40.6	U	–
Cibacron Blue F3GA-silica	Serva	–[d]	33.4	U	–
Blue Trisacryl-M	IBF	≈4.0	29.7	27	0.0003
Blue Sepharose CL-6B	Pharmacia	≈2.0	25.4	U	–
Reactive Blue 2-Sepharose CL-6B	Sigma	≈2.0	23.2	U	–
Blue polyvinyl alcohol-coated perfluorocarbon adsorbent	–	1.9 ± 0.2	10.1	U	–

[a] Packed adsorbents (2 ml) were washed with 50 m*M* phosphate buffer, pH 7.0 (50 column volumes) and then allowed to stand for 72 h in this buffer. Further buffer (10 ml) was then added, collected and assayed for C.I. Reactive Blue 2 by competitive ELISA.
[b] Manufacturer/suppliers' figures.
[c] Calculated assuming formule weight for C.I. Reactive Blue 2 = 840.
[d] Figures not supplied.
[e] Albumin capacities were measured by frontal analysis of 10 mg/ml human serum albumin in 50 m*M* sodium acetate, pH 5.5.
[f] Undetectable (< pmol/day).

Dye leakage in rigorous conditions. Leakage of immobilised ligand from affinity adsorbents may be attributable to cleavage of the dye–matrix bond, hydrolysis or dissolution of the matrix backbone or displacement of tightly adsorbed but non-covalently bound ligand remaining after adsorbent synthesis. Fig. 4 displays the results of exposing a number of affinity adsorbents to increasing concentrations of chaotrope, acid and base. The effect of high chaotrope concentrations on the immunoassay illustrates how serial dilutions rather than single well samples are required to analyse dye loss under these conditions. Leakage of ligand was undetectable from most adsorbents in 0.5 *M* NaSCN and, even in 1.25 *M* NaSCN, the coated perfluoropolymer and MIMETIC Blue 1 A6XL displayed no leakage. Under all other conditions, the immunoassay detected loss of dye from all the adsorbents. However, the extent of ligand loss varied widely for any given condition: for example, in 1 *M* sodium hydroxide solution, loss of only 0.1% of the total dye content of the perfluoropolymer adsorbent was observed, whilst under the same conditions, approximately 13.5% of total ligand content of the silica-based Cibacron Blue F3GA = Si500, assuming an initial dye content of 2 μmol/ml silica, was lost. It is well known that silica is labile in alkali and dissolution occurs at pH values above 8.0 [22]. In contrast, silica is stable at low pH and, therefore, the leakage exhibited in acidic conditions probably arises from hydrolysis of the siloxane bonds between ligand and the support. Pellicular coatings for silica comprising polymers such as dextran have been developed which coat the surface and facilitate ligand immobilisation [23]. However, coating imperfections will still allow solvent attack on the base matrix and will inevitably lead to ligand loss.

The 1,4-ether bond between the D-galactose and 3,6-anhydro-L-galactose moieties of agarose is known to hydrolyse in acidic conditions, resulting in breakdown of the matrix [24]. Furthermore, uncrosslinked polymer chains of agarose are aggregated by hydrogen bonds which may be disrupted by chaotropic agents as well as by acid and base. The stabilities of the agarose-based materials follow a heirarchy: A ≫ F,G,I > B. This order mirrors the results of the flow-rate *versus* pressure analysis and is explicable in terms of the extent of chemical cross-linking introduced within the agarose polymer chains. The notable stability of A (MIMETIC

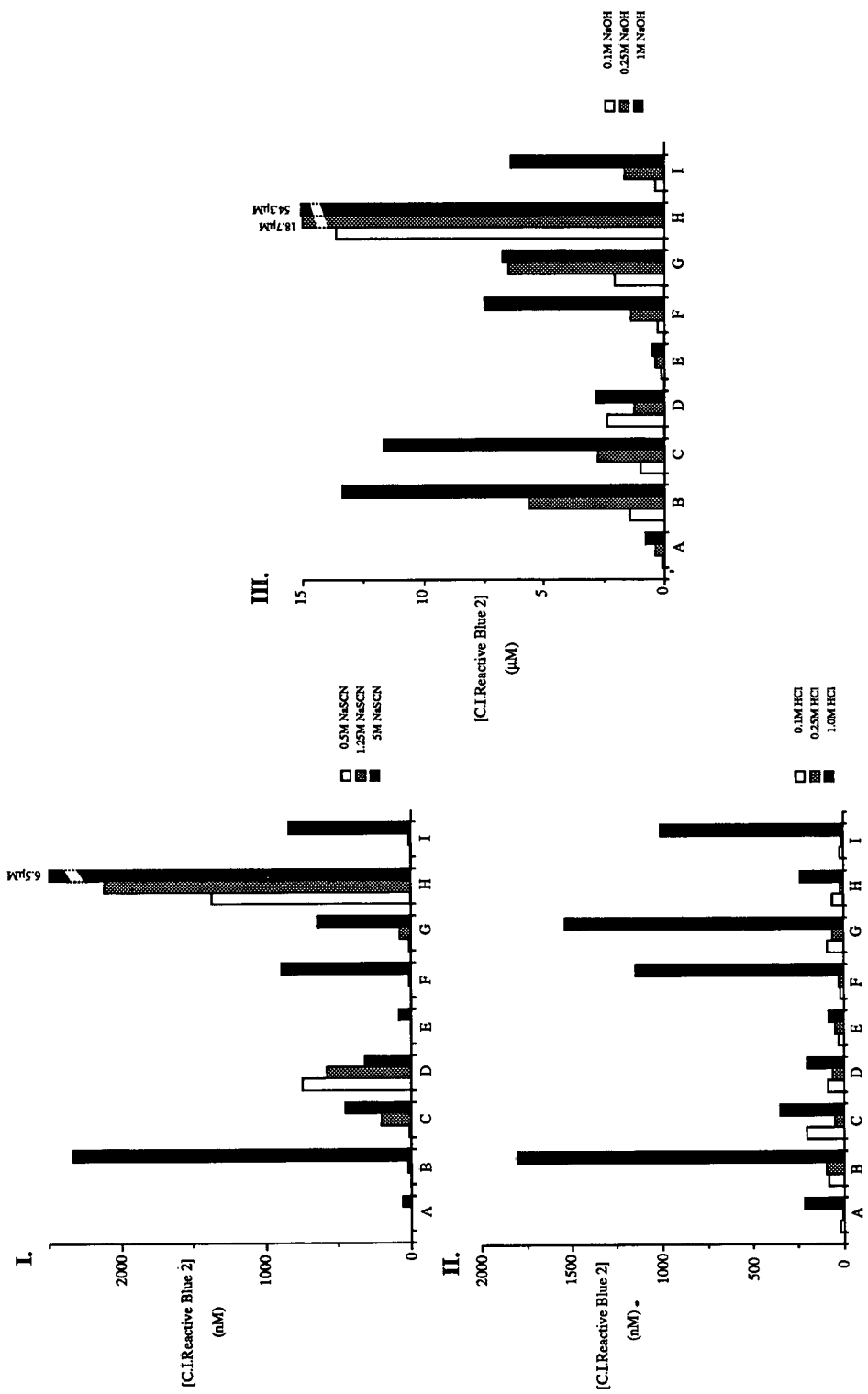

Fig. 4. Leakage data for nine C.I. Reactive Blue 2-containing affinity adsorbents on exposure to conditions of (I) high chaotropic, (II) acidic and (III) basic conditions. Packed columns were washed with challenging solution (10 ml) followed by a water wash (10 ml); dye leakage was measured by competitive ELISA and challenging solution and water wash results summed. Adsorbents are as follows: A = Mimetic Blue A6XL (ACL); B = Affi-Gel Blue (Bio-Rad); C = Blue Trisacryl-M (IBF); D = Fractogel TSK AF-Blue (Merck); E = C.I. Reactive Blue 2 polyvinyl alcohol-coated perfluorocarbon matrix; F = Blue Sepharose CL-6B; G = Immobilised Cibacron Blue F3GA (Pierce); H = Cibacron Blue F3GA = Si500 (Serva); and I = Reactive Blue 2-Sepharose CL-6B (Sigma).

Blue 1 A6XL) in basic, as well as acidic and chaotropic, conditions may also depend on the unique spacer arm chemistry used to link the dye to the matrix. In contrast, direct coupling of the triazine dye to the matrix yields a triazinyl ether bond that may be hydrolysed by extremes of pH [1]. The acrylic polymer, Trisacryl Blue-M (C), offers superior stability to the agaroses (F,G,I) in acidic and chaotropic conditions but is less able to withstand alkali. Fractogel TSK AF-Blue (D) performs moderately well under all conditions, but it is particularly noticeable that this adsorbent does not withstand lower chaotropic, acidic or basic conditions well; this material may benefit from a pre-treatment that includes exhaustive washing in these conditions prior to use.

The C.I. Reactive Blue 2 polyvinyl alcohol-coated perfluoropolymer displays the lowest leakage under all conditions although slight leakage in both acidic and basic conditions is observed. This may be attributable either to hydrolysis of the triazinyl ether bond between the adsorbed polyvinyl alcohol and the triazine dye or to desorption of the entire perfluoroalkylated dyed polymer from the perfluoropolymer surface. The use of cross-linking agents to strengthen further the stability of the coating layer may circumvent the latter problem.

CONCLUSIONS

The enzyme-linked immunoassay developed for the detection of the triazine dye C.I. Reactive Blue 2 exhibits a considerable increase in the senstivity of detection over spectrophotometric methods. The assay appears to be specific for the anthraquinone moiety of the dye and therefore offers the possibility of monitoring the leakage of immobilised dye from affinity adsorbents irrespective of whether fragments of the matrix remain attached to the dye. In applying this immunoassay to a comparison of eight commercial affinity adsorbents and one novel dyed perfluoropolymer support, leakage of ligand from adsorbents in buffer at pH 7.0 was undetectable from most of the adsorbents, although, on exposure to more rigorous conditions that might be applied during the lifetime of a working column, leakage was evident from all the dyed adsorbents. The C.I. Reactive Blue 2 polyvinyl alcohol-coated perfluoropolymer exhibited the lowest loss of ligand in both acidic and basic conditions by a substantial margin, and offered reasonable pressure/flow-rate characteristics with potential maximal flow-rates in the region of 80 cm/min. Of the commercial adsorbents, Fractogel TSK-AF Blue would appear to offer advantages for high performance liquid affinity chromatography although careful monitoring of leakage is advisable. Overall, MIMETIC Blue 1 offers the best capacity and stability of all commercial adsorbents and its increased rigidity suggests that it is suitable both for low and medium pressure applications. Unfortunately, the low binding capacity of the perfluoropolymer for proteins, attributable to its lack of porosity and low surface area, limits its current usefulness. Nevertheless, work is underway to remedy these shortcomings by the use of more porous perfluoropolymer matrices. The remarkable stability of the perfluoropolymer adsorbents should make them attractive propositions for the purification of therapeutic proteins where harsh conditions could be employed to effect *in situ* depyrogenation, sterilisation and cleaning.

ACKNOWLEDGEMENTS

We would like to thank E.I. du Pont de Nemours & Co. Inc. for their financial support of this work.

REFERENCES

1 C. R. Lowe, *Topics in Enzyme and Fermentation Biotechnology*, Ellis Horwood, Chichester, 1984, p. 78, Vol. 9.
2 C. R. Lowe and J. C. Pearson, *Methods Enzymol.*, 104 (1984) 97.
3 F. Qadri, *Trends Biotechnol.*, 3 (1985) 7.
4 G. Birkenmeier, G. Kopperschlager and G. Johansson, *Biomed. Chromatogr.*, 165 (1986) 301.
5. R. K. Scopes, *J. Chromatogr.*, 376 (1986) 131.
6 Y. D. Clonis, *Reactive Dyes in Protein and Enzyme Technology*, Macmillan, Basingstoke, 1987, Ch. 3, p. 33.
7 J. E. More, A. G. Hitchcock, S. Price, J. Rott and M. J. Harvey in M. A. Vijayalakshmi and O. Bertrand (Editors), *Protein–Dye Interactions: Developments and Applications*, Elsevier, Barking, 1989, p. 265.
8 Y. Clonis, in M. T. W. Hearn (Editor), *HPLC of Proteins, Peptides and Polynucleotides*, VCH, New York, 1991, p. 453.
9 P. Knight, *Bio/technology*, 7 (1989) 243.
10 D. J. Stewart, P. Hughes and C.R Lowe., *J. Biotechnol.*, 11 (1989) 253.
11 D. J. Stewart, D. R. Purvis and C. R. Lowe, *J. Chromatogr.*, 510 (1990) 177.
12 D. A. P. Small, T. Atkinson and C. R. Lowe, *J. Chromatogr.*, 266 (1983) 151.

13 E. Engvall and P. Perlmann *Immunochemistry*, 8 (1971) 874.
14 P. Fuglistaller, *J. Immunol. Method.*, 124 (1989) 171.
15 J. C. Pearson, S. J. Burton and C. R. Lowe, *Anal Biochem.*, 158 (1986) 328.
16 J. Jacobson, J. Frenz and Cs. Horváth, *J. Chromatogr.*, 316 (1984) 53.
17 T. Peters, Jr., *The Plasma Proteins* Vol. I, Academic Press, New York, 1975, p.133.
18 J. Guesdon, T. Ternyck and S. Avarmeas, *J. Histochem. Cytochem.*, 27 (1979) 1131.
19 S. J. Burton, C. V. Stead and C. R. Lowe, *J. Chromatogr.*, 455 (1988) 201.
20 J.W. Goodman, *The Antigens*, Vol. 3, Academic Press, London, 1975, p.187.
21 Affinity Chromatography, Isle of Man, *ACL Technical Data Sheet*, 1989.
22 Y. D. Clonis and D. A. P. Small, *Reactive Dyes in Protein and Enzyme Technology*, Macmillan, Basingstoke, UK, 1987, Ch. 5, p. 87.
23 X. Santarelli, D. Muller and J. Jozefonvicz, *J. Chromatogr.*, 443 (1988) 55.
24 C. R. Lowe and P. D. G. Dean, *Affinity Chromatography*, Wiley, London, 1974, Ch. V, p. 200.

Journal of Chromatography, 623 (1992) 15–21
Elsevier Science Publishers B.V., Amsterdam

CHROM. 24 391

Comparison of adsorption properties of Florisil and silica in high-performance liquid chromatography

II. Retention behaviour of bi- and trifunctional model solutes

Monika Waksmundzka-Hajnos

Department of Inorganic and Analytical Chemistry, Medical Academy, Staszica 6, 20-081 Lublin (Poland)

(First received April 16th, 1992; revised manuscript received June 1st, 1992)

ABSTRACT

The retention of several bi- and trifunctional model solutes using different adsorbents, Florisil and silica, and different binary eluent systems containing isopropanol, dioxane or tetrahydrofuran as modifiers in *n*-heptane was investigated by high-performance liquid chromatography. The retention parameters are presented as log k'–log k' relationships obtained for solutes in different chromatographic systems. The selectivity of the systems investigated and the influence of modifiers on the adsorptive properties of the adsorbents are discussed.

INTRODUCTION

In previous papers, the special properties of Florisil in comparison with silica were demonstrated using various model solutes such as aromatic hydrocarbons, phenols, anilines and nitroarenes [1] and aromatic acids and aldehydes [2] using continuous thin-layer chromatography (TLC) (quasi-column conditions). In a recent paper [3], the results obtained for monofunctional aromatic model solutes in high-performance liquid chromatography (HPLC) were reported. Although some analogies between adsorption on Florisil and silica for derivatives of anilines and phenols (solutes of class AB according to the Pimentel–McClellan classification [4]) were found, a better capability for the separation of isomers on Florisil was observed.

Correspondence to: Dr. M. Waksmundzka-Hajnos, Department of Inorganic and Analytical Chemistry, Medical Academy, Staszica 6, 20-081, Lublin, Poland.

The investigations revealed distinct differences in the acidity of adsorption centres and their distribution on Florisil and silica surfaces. Quinoline bases (class B) were more strongly adsorbed and better separated on Florisil in all eluent systems investigated [3].

The influence of modifiers on the adsorptive properties of Florisil was also examined. It was found that dioxane modified both Florisil and silica surfaces [3,5,6] in such a way that solutes interacted with the ether oxygens of the solvent film on the surface (co-adsorption effect) or displaced the solvent molecules from the adsorbent surface (displacement effect). On the other hand, the molecules of tetrahydrofuran deactivate and shield the surface of Florisil. For this reason, separation on Florisil in the latter system is poorer [3].

It was considered of interest to examine these effects using compounds with more complex molecular structures. In this work, the retention behaviour of several bi- and trifunctional aromatic com-

0021-9673/92/$05.00

pounds was examined by HPLC in chromatographic systems using Florisil as an adsorbent and isopropanol, dioxane or tetrahydrofuran in *n*-heptane as mobile phases. The chromatographic data were compared with those obtained earlier by HPLC on silica [7,8].

The analysis of steric and mesomeric effects of solutes also permits a better recognition of the distribution and chemical properties of active centres on the Florisil surface.

EXPERIMENTAL

The chromatographic experiments with Florisil were performed at 19 ± 1°C using a Type 302 liquid chromatograph (Institute of Physical Chemistry, Polish Academy of Sciences), equipped with a syringe pump (at a flow-rate of 1.2 ml/min) and a UV detector (254 nm). Single solutes dissolved in the eluent were injected with the help of a 5-μl injection valve.

HPLC-grade 10-μm Florisil was prepared in the Institute of Inorganic Chemistry (Gliwice, Poland). Florisil (Fluka, Buchs, Switzerland) for TLC was milled in a Model 100 AFG counterflow-fluid mill produced by Alpine (Augsburg, Germany). Particle segregation of ground Florisil was carried out in a Model 100 MZR pneumatic separator (Alpine). The column (150 × 4 mm I.D.) was packed with 10-μm Florisil [specific surface area (BET) 340 m^2/g, total porosity 46.2%] by the slurry method. The experimental results represent the averages of three runs. As mobile phases *n*-heptane solutions of isopropanol (for HPLC, E. Merck, Darmstadt, Germany), 1,4-dioxane (for HPLC, Romil Chemicals, Shepshed, UK) or tetrahydrofuran (for chromatography, redistilled, International Enzymes, Windsor, UK) were used. For further details, see ref. 3.

The chromatographic experiments with silica were performed using a Perkin-Elmer (Norwalk, CT, USA) Model 1210 liquid chromatograph with dual syringe pumps and UV detector. The column (125 × 4 mm I.D.) was packed with 10-μm LiChrosorb Si 60 (E. Merck). For further details, see refs. 7 and 8.

TABLE I

COMPOUNDS INVESTIGATED

Solute	Abbreviation	Polar groups type
1,3-Dihydroxynaphthalene	13HN	AB–AB
1,3-Dihydroxy-5-methylbenzene (orcinol)	13H5MB	AB–AB
1,4-Dihydroxybenzene (hydroquinone)	14HB	AB–AB
4-Aminophenol	4AP	AB–AB
3-Aminophenol	3AP	AB–AB
4-Hydroxybenzaldehyde	4HBal	AB–B
2,6-Dichloro-4-nitroaniline	26C4NtAn	AB–B
2-Chloro-4-nitroaniline	2C4NtAn	AB–B
4-Chloro-3-nitroaniline	4C3NtAn	AB–B
4-Nitroaniline	4NtAn	AB–B
3-Nitroaniline	3NtAn	AB–B
2-Nitroaniline	2NtAn	AB–B
2,4-Dinitroaniline	24NtAn	AB–B–B
4-Nitrophenol	4NtP	AB–B
5-Aminoacridine	5AAcr	AB–B
1,2-Dinitrobenzene	12NtB	B–B
1,4-Dinitrobenzene	14NtB	B–B
4-Nitrobenzaldehyde	4NtBal	B–B
6-Nitroquinoline	6NtQ	B–B
2-Chloro-3-nitropyridine	2C3NtPy	B–B
2-Chloro-5-nitropyridine	2C5NtPy	B–B

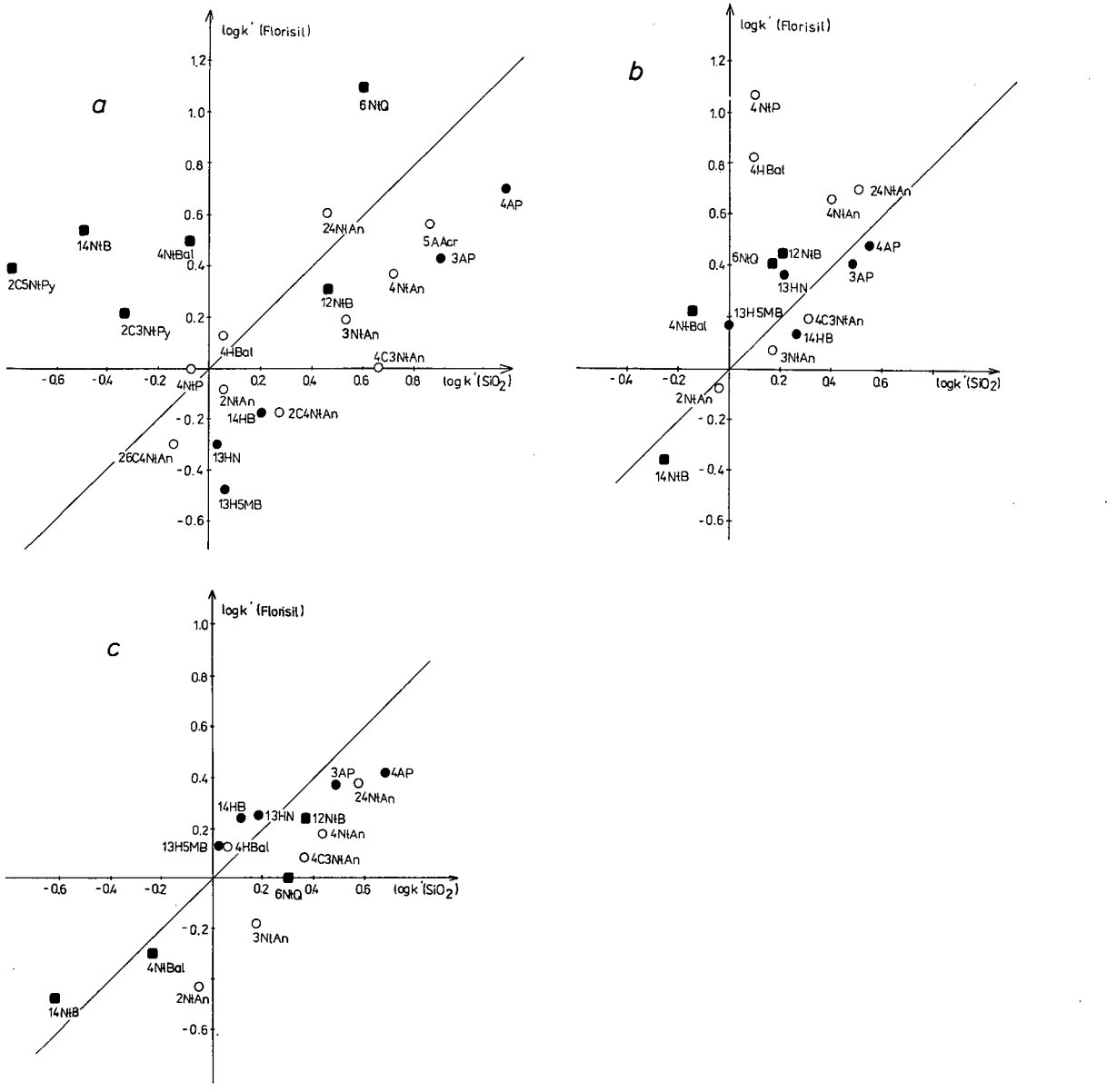

Fig. 1. Correlation between log k' values of bi- and trifunctional aromatic compounds on Florisil and silica. Solutes: ■ = compounds with B–B groups; ○ = compounds with AB–B groups; ● = compounds with AB–AB groups. For abbreviations of solutes, see Table I. Mobile phases: (a) isopropanol–*n*-heptane [30:70 (v/v) for Florisil and 12.5:87.5 (v/v) for silica]; (b) dioxane–*n*-heptane [50:50 (v/v) for Florisil and 40:60 (v/v) for silica]; (c) tetrahydrofuran–*n*-heptane [40:60 (v/v) for both adsorbents].

RESULTS AND DISCUSSION

The experimental results obtained for the bi- and trifunctional model solutes listed in Table I are given in Fig. 1 as the relationships of log k' values (k' = capacity factor) of the solutes adsorbed on Florisil against log k' values for the same solutes adsorbed on silica in different eluent systems.

Fig. 1a shows log k' (Florisil) *vs.* log k' (silica) relationships in the isopropanol–*n*-heptane system.

Molecular interactions in the isopropanol system are complex owing to its linear autoassociation [9,10], which leads to an apparent decrease in their solvent strength especially with respect to solutes possessing functional groups of class B. Such a difference in the solvation mechanism of the solutes belonging to class B or AB is a reason for the different retentions of compounds. Hydroxyl groups on the surface of either silica or Florisil interact competitively with isopropanol and solute molecules and adsorption of solutes can be considered as a result of displacement and solvation effects. Hence, it appears that solutes interact directly with active centres of adsorbents and differences in retention parameters depend largely on the adsorptive properties of the adsorbents. The analysis of chromatographic data and the structures of the solutes shows many dissimilarities in the type, distribution and properties of active centres of both adsorbents, as can be seen in Fig. 1a. The solutes with B–B groups (6-nitroquinoline, 4-nitrobenzaldehyde, 2-chloro-3-nitropyridine, 2-chloro-5-nitropyridine and 1,4-dinitrobenzene) are adsorbed more strongly on the active acidic centres of Florisil than on the silica surface. The solutes with AB–AB groups are adsorbed less strongly on Florisil than on the silica surface (*e.g.* 1,3-dihydroxy-5-methylbenzene, 1,3-dihydroxynaphthalene, 1,4-dihydroxybenzene, 3-aminophenol and 4-aminophenol); nevertheless, they are better separated on Florisil (see Fig. 1a). Bifunctional compounds with B- and AB-type groups (*e.g.*, nitro and amino or chloro, nitro and amino substituents) are similarly adsorbed on both adsorbents. Although the nitro group has a relatively weak adsorption energy, the introduction of a second nitro group into the solute molecule usually increases the adsorption affinity (compare 2-nitroaniline and 2,4-dinitroaniline, Fig. 1a), especially of *ortho* and *para* derivatives owing to the ability to create resonance forms. The weaker adsorption of 2,6-dichloro-4-nitroaniline, 4-nitroaniline and 2-chloro-4-nitroaniline is presumably due to the steric shielding effects of the halogen substituents.

In the dioxane–heptane system the dispersion of correlation points is less pronounced (Fig. 1b). For example, solutes with B–B groups are adsorbed less strongly than in the isopropanol–*n*-heptane system. This indicates that the strongly acidic centres of the Florisil surface are blocked with dioxane molecules [3], which consequently permits a co-adsorption effect comparable to that described for silica [5,6]. Nevertheless, compounds with B and AB groups, such as 4-nitrophenol, 4-hydroxybenzaldehyde, 4-nitroaniline and 2,4-dinitroaniline, are more strongly adsorbed on Florisil than on the silica surface. These compounds reveal a positive mesomeric effect ($+M$) of AB groups intensified by the negative mesomeric effect ($-M$) of the B groups (NO_2, CHO), so that the proton-donor effect of OH and NH_2 AB groups is intensified. This causes stronger adsorption on the Florisil surface covered with a bonded dioxane film (see Fig. 1b).

Fig. 1c presents the log k' (Florisil) *vs.* log k' (silica) correlations in the system tetrahydrofuran–*n*-heptane. The spread of points in this system is less pronounced and the slope of the correlation line is less than 1, indicating that silica in this instance is generally a more selective adsorbent. Moreover, all compounds except 1,4-dihydoxybenzene, 1,3-dihydroxynaphthalene, 1,3-dihydroxy-5-methylbenzene and 4-hydroxybenzaldehyde are more strongly adsorbed on the silica surface than on the Florisil surface in this system, including compounds with electron-donor B–B groups (Fig. 1c). Similarly to dioxane molecules, tetrahydrofuran modifier molecules cover the Florisil surface, blocking the adsorption centres. The oxygen atoms in tetrahydrofuran molecules interact strongly with the acidic centres of the Florisil surface, forming a film that deactivates the adsorbent surface.

To summarize these results, the spread of points in the correlations indicates the accumulation of several effects such as the chemical character of polar groups and internal hydrogen bonding; *ortho* and mesomeric effects also have an influence on the adsorption energy of solutes. The interaction of solutes with adsorbent sites also depends on the distance between two polar substituents, adjusting better or worse to the arrangement of surface hydroxyl groups on the adsorbent (localization and delocalization effects) [11].

The correlation of log k' for two different solvents is very useful in the search for optimum systems for the separation of the investigated compounds (Fig. 2). It allows the selectivities of modifiers to be compared and the composition of the mobile phase to be chosen for rechromatography of complex fractions not separated in one system. For

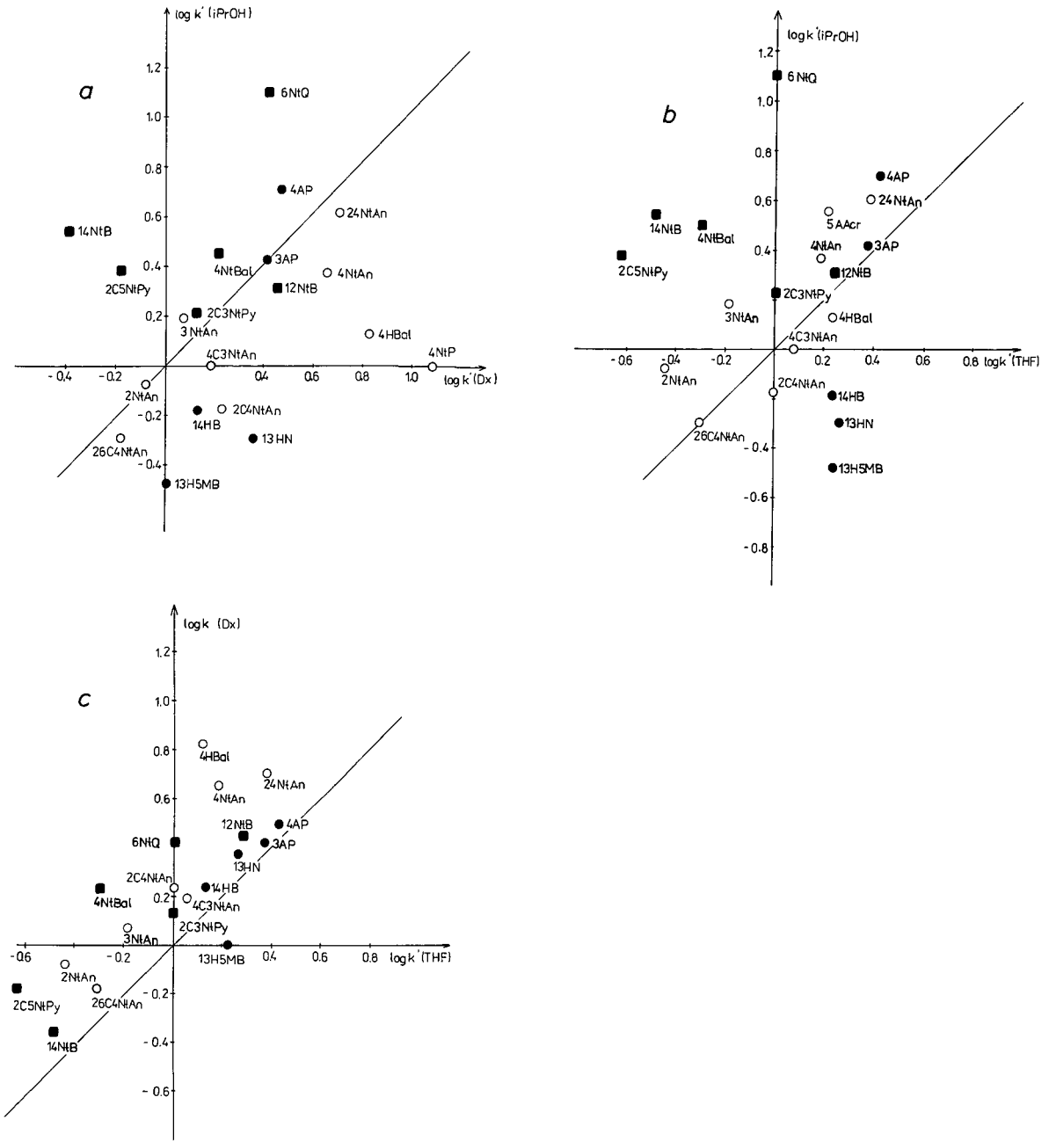

Fig. 2. (a) Correlation of log k' values for isopropanol–*n*-heptane [30:70 (v/v)] against log k' values for dioxane–*n*-heptane [50:50 (v/v)]. Adsorbent: Florisil. (b) Correlation of log k' values for isopropanol–*n*-heptane [30:70 (v/v)] against log k' values for tetrahydrofuran–*n*-heptane [40:60 (v/v)]. Adsorbent: Florisil. (c) Correlation of log k'values for dioxane–*n*-heptane [50:50 (v/v)] against log k' values for tetrahydrofuran–*n*-heptane [40:60 (v/v)]. Adsorbent: Florisil. Solutes as in Fig. 1.

example, 2,4-dinitroaniline and 4-nitroaniline, 4-chloro-3-nitroaniline and 2-chloro-4-nitroaniline, 4-aminophenol and 3-aminophenol and 2-nitroaniline and 2,6-dichloro-4-nitroaniline, which are not separated in the dioxane–*n*-heptane system, have a much greater resolution in the 2-propanol–*n*-heptane system (Fig. 2a); on the other hand 2-chloro-3-nitropyridine and 2-chloro-5-nitropyridine, 1,4-dihydroxybenzene and 1,3-dihydroxynaphthalene and 1,4-dinitrobenzene and 1,2-dinitrobenzene, which are not separated in the isopropanol–*n*-heptane system, are better separated using the dioxane–*n*-heptane system (Fig. 2a). Similarly, 1,4-dihydroxybenzene, 1,3-dihydroxynaphthalene and 1,3-dihydroxy-5-methylbenzene or 4-aminophenol and 3-aminophenol, 6-nitroquinoline and 2-chloro- 3-nitropyridine eluted together with the tetrahydrofuran–*n*-heptane system but can be separated when 2-propanol is used as a modifier (Fig. 2b). Some solutes from each group of compounds investigated have similar retentions in tetrahydrofuran–*n*-heptane. Most of the investigated compounds are less strongly retained in the tetrahydofuran–*n*-heptane system (Figs. 2b and 2c). This verifies the hypothesis that the molecules of tetrahydrofuran form a film that deactivates the surface of Florisil, so that its specific properties decrease.

Another method for comparing the investigated eluent systems is to plot the log k' "spectrum" obtained for a constant concentration of a modifier (comparable solvent strength) for bi- and trifunctional model solutes. This diagram (Fig. 3) gives a possibility of observing selectivity and sequence changes for the investigated solutes in three systems. The influence of the structural effects on the retention of the chromatographed compounds can be elucidated from this diagram.

Correlations of retention parameters (Figs. 1 and 2) are very useful in planning separations of complex mixtures. A hypothetical correlation diagram in two chromatographic systems is as follows:

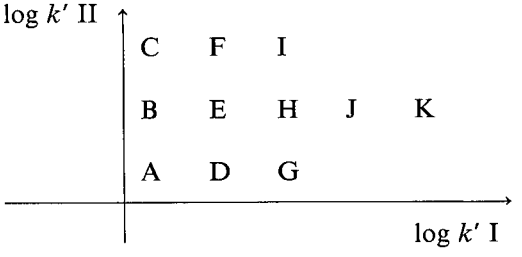

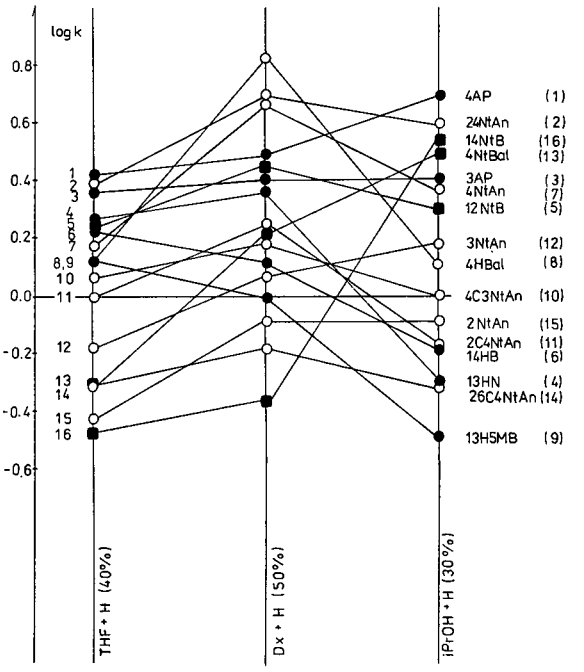

Fig. 3. Graphical comparison of log k' values obtained for Florisil. Mobile phases: tetrahydrofuran–*n*-heptane [40:60 (v/v)], dioxane–*n*-heptane [50:50 (v/v)] and isopropanol–*n*-heptane [50:50 (v/v)].

The diagram indicates that in system I group separation is possible (ABC) + (DEF) + (GHI) + J + K . In system II isolation of individual solutes from separated groups can be obtained:

(ABC) → A + B + C
(DEF) → D + E + F
(GHI) → G + H + I

This makes application of correlations for planning separations on the analytical and micropreparative scales possible.

CONCLUSIONS

Differences in selectivity of most popular adsorbents (*e.g.*, silica and Florisil) and eluent systems can be utilized in difficult separation problems with isomers or closely related compounds.

The specific properties of Florisil depend on modifiers being used as polar components of binary solvents. Dioxane molecules modify the surface of both Florisil and silica so that especially proton-donor solutes can interact with the oxygen atoms of the solvent film. It changes the specific surface prop-

erties of adsorbents. The film of tetrahydrofuran shields and deactivates especially acidic centres on the Florisil surface.

ACKNOWLEGEMENT

The author is obliged to Professor Edward Soczewiński for valuable discussions.

REFERENCES

1 M. Waksmundzka-Hajnos, *Chem. Anal. (Warsaw)*, 31 (1991) 289.
2 M. Waksmundzka-Hajnos, *J. Planar Chromatogr.*, 4 (1991) 127.
3 M. Waksmundzka-Hajnos, T. Wawrzynowicz and T. H. Dzido, *J. Chromatogr.*, 600 (1992) 51.
4 G. C. Pimentel and A. L. McClellan *The Hydrogen Bond*, Freeman, San Francisco, 1960.
5 E. Soczewinski, *J. Chromatogr.*, 388 (1987) 91.
6 T. Dzido and E. Soczewiński, *J. Chromatogr.*, 395 (1987) 489.
7 E. Soczewinski and T. Dzido, *Chromatographia*, 22 (1986) 25.
8 T. Dzido and E. Soczewiński, *J. Chromatogr.*, 388 (1987) 99.
9 A. B. Littlewood and F. W. Willmott, *Anal. Chem.*, 38 (1966) 1031.
10 E. Soczewiński and G. Matysik, *J. Chromatogr.*, 96 (1974) 155.
11 L. R. Snyder, *Principles of Adsorption Chromatography*, Marcel Dekker, New York, 1968, p. 270.

Journal of Chromatography, 623 (1992) 23–31
Elsevier Science Publishers B.V., Amsterdam

CHROM. 24 394

Thermal treatment of supports for chiral stationary phases and its influence on enantioselectivity

Rolf Straub* and Hans Arm

Institute of Organic Chemistry, University of Berne, Freiestrasse 3, CH-3012 Berne (Switzerland)

(First received March 1st, 1992; revised manuscript received June 1st, 1992)

ABSTRACT

Thermal treatment of silica at temperatures above 800°C leads to a significant decrease in the silanol surface concentration. Chiral modification of such thermally treated silicas gives derived stationary phases with lower specific surface areas and lower surface concentrations of ligands. The resolution of chiral amides was in some instances better with thermally treated π-donor chiral stationary phases based on (*R*)-1-(1-naphthyl)ethylamine in comparison with the corresponding untreated phases. Correlation experiments with two homologous series indicate that retention also depends on other hydrogen-bond acceptors such as secondary hydroxyl groups near the chiral selector.

INTRODUCTION

Pirkle and co-workers [1–3] synthesized π-donor chiral stationary phases (CSPs) for high-performance liquid chromatography (HPLC) with a lower surface loading of chiral ligands by using smaller amounts of reactants. These "diluted" CSPs were developed and tested with a view to clarifying chiral recognition mechanisms.

Däppen *et al.* [4] obtained CSPs with various surface coverages depending on the order of connection of the spacer, 3-glycidoxypropyltrimethoxysilane, with the chiral selector molecule and the surface silanol groups. A decrease in the number of active polar sites on the silica support can increase the enantioselectivity of the CSP for polar solutes.

When using ordinary "diluted" chiral stationary phases for the separation of enantiomers it is necessary to consider that residual silanol groups can cause disturbing polar adsorption (non-chiral interaction with polar functional groups of the solute) which lower the chiral recognition by peak broadening. A thermal treatment prior to a chemical modification deactivates these surfaces so much that such polar adsorptions are mostly suppressed. For this treatment, temperatures up to 1000°C for several hours have been applied. Thermal treatment reduces the surface area of the silica to an extent dependent on the temperature applied and the purity of the silica [5–9].

The aim of the first part of this study was to investigate whether a thermal treatment of silica prior to the chemical reaction decreases the surface density of chiral ligands. We also compared these thermally treated and lightly loaded chiral stationary phases (TCSPs) with the CSPs previously described [4,10,11]. The basic structure of the CSPs is given in Fig. 1. The only differences between slightly and heavily loaded CSPs are the surface density of the chiral ligands, the number of remaining silanol groups and the structure of the support.

EXPERIMENTAL

Two chiral stationary phases, one with an N-pivaloyl group, R_1, [CSP I (PIV)] and another with an

Correspondence to: Professor Dr. H. Arm, Institute of Organic Chemistry, University of Berne, Freiestrasse 3, CH-3012 Berne, Switzerland.

* This paper is part of the Dissertation of R. Straub [10].

0021-9673/92/$05.00

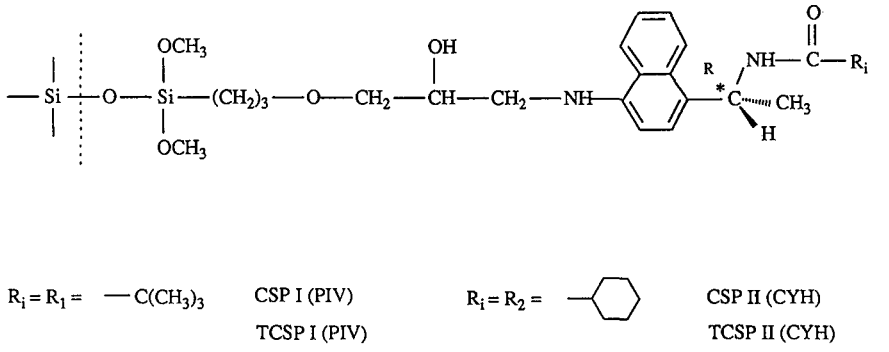

Fig. 1. Chiral stationary phases (CSPs and TCSPs) I and II. N-Acyl derivatives of (*R*)-4-(N-1-alkyloylamino-1-ethyl)-1-naphthylamine.

N-cyclohexylcarbonyl group, R_2, [CSP II (CYH)] were synthesized starting from (*R*)-1-(1-naphthyl) ethylamine according to a procedure described earlier [4,10,11]. Similar phases, TCSP I (PIV) and TCSP II (CYH), but from thermally treated supports were also made and are discussed below.

The elemental analyses were done with a routine analyser in the microanalytical department of Ciba-Geigy (Basle, Switzerland) and specific surface area (S_{BET}) measurements with a Carlo Erba Sorptomatic Series 1800 instrument. All samples used were synthesized according to common laboratory methods.

Materials

LiChrospher Si 100 (Merck, Darmstadt, Germany) with a particle size of 5 μm and a specific surface area S_{BET} = 264.4 ± 5.4 m^2/g was dried at 150°C and 0.01 mbar for 6 h prior to the bonding procedure. All chemicals were purchased from Merck or Fluka (Buchs, Switzerland). All solvents used for reactions or for washing were dried according to general laboratory procedures. For liquid chromatography, HPLC-grade solvents from Romil Chemicals (Shepshed, UK) were used.

Silylation of thermally treated silica

Thermal treatment. Three 0.55-g portions of silica in covered porcelaine crucibles were heated at 600, 800 and 1000°C for 4 h in a muffle furnace. A further portion of silica was heated for the same period in a Büchi GKR-51 Kugelrohr oven at 150°C and 0.01 mbar. The differently thermally treated solids were cooled in a desiccator containing phosphorus pentoxide and then moved into a dry-box; further preparations were carried out in a dry nitrogen atmosphere.

Silylation. Samples of 0.18–0.5 g of the thermally treated silica were refluxed with 0.1 ml of dry pyridine and 0.8 mmol of *n*-octadecyldimethylchlorosilane (ODCS) per gram of silica in 6 ml of dry toluene for 137 h. The derived silicas were filtered and washed successively with toluene, methanol, methanol–water (1:1), water, methanol and diethyl ether and dried for 6 h at 150°C and 0.01 mbar. No. 1 (150°C): weight increase 16.7%. Analysis: found, C 13.98, H 2.56, Cl <0.1%. No. 2 (600°C): weight increase 9.5%. Analysis: found, C 13.83, H 2.70, Cl <0.2%. No. 3 (800°C): weight increase 10.5%. Analysis: found, C 13.76, H 2.83, Cl <0.2%. No. 4 (1000°C): weight increase 6.08%. Analysis: found, C 10.42, H 1.89, Cl <0.1%. Data on surface coverages calculated from elemental analysis are given in Table I.

CSPs I and II

CSP I (PIV). Weight increase 9.0%. Analysis: found, C 6.99, H 1.51, N 0.69%. Calculated: 0.25 mmol of (*R*)-ligand/g stationary phase (based on N) and 0.23 mmol of (*R*)-ligand/g stationary phase (based on C).

CSP II (CYH). Weight increase 7.8%. Analysis: found, C 6.43, H 1.34, N 0.83%. Calculated: 0.22 mmol of (*R*)-ligand/g stationary phase (based on N) and 0.20 mmol of (*R*)-ligand/g stationary phase (based on C).

TCSPs I and II

Thermal treatment. In a covered porcelain crucible, 2.3–2.4 g of silica were heated at 1000°C for 6 h

in a muffle furnace, cooled in a desiccator over phosphorus pentoxide and moved for further treatment into a dry-box.

Coating. Samples of 1.9–2.0 g of thermally treated silica were reacted with 0.7 mmol of (*R*)-4-(N-1-pivaloylamino-1-ethyl)-1-naphthylamine or (*R*)-4-(N-1-cyclohexylcarboxamido-1-ethyl)-1-naphthylamine and an equimolar amount of 3-glycidoxypropyltrimethoxysilane in 15 ml of dry toluene according to the procedure reported previously [4,10,11].

All calculations are based on the thermally treated silica gel.

TCSP I (PIV). Weight increase 5.1%. Analysis: found, C 4.71, H 0.67, N 0.3%. Calculated: 0.11 mmol of (*R*)-ligand/g stationary phase (based on N) and 0.16 mmol of (*R*)-ligand/g stationary phase (based on C).

TCSP II (CYH). Weight increase 4.9%. Analysis: found, C 4.91, H 0.73, N 0.3%. Calculated: 0.11 mmol of (*R*)-ligand/g stationary phase (based on N) and 0.15 mmol of (*R*)-ligand/g stationary phase (based on C).

Liquid chromatography

To eliminate fines, the CSPs and the TCSPs were sedimented five times in methanol. Stainless-steel tubes (25 cm × 3.2 mm I.D.) were used as columns. A slurry prepared from 1.9 g of the phase and 30 ml of dibromomethane–*n*-hexane (8:2) was packed into the columns with a Haskel (Burbank, CA, USA) Model 27486-4 airdriven fluid pump at a pressure of 680 bar. The columns were conditioned with methanol and *n*-hexane.

Chromatography was performed using an Altex (Berkeley, CA, USA) Model 110 solvent metering pump, a Hitachi Model 100-10 variable-wavelength UV detector (Kontron, Zürich, Switzerland) with detection at 254 nm, a Rheodyne (Berkeley, CA, USA) Model 7125 syringe-loading sample injector with a 20-μl loop, and a Tarkan W & W Model 600 recorder (Kontron) and an HP 3396 A integrator (Hewlett-Packard, Widen, Switzerland).

The mobile phases were *n*-hexane–tetrahydrofuran (3:1) and *n*-hexane–2-propanol (78:22) at a flow-rate of 1 ml/min. The columns and the mobile phase container were held at 20°C (Assistant WTE var 3185 thermostat; R. C. Kuhn, Berne, Switzerland). Toluene as a non-retained standard, dissolved in the appropriate mobile phase, was used to determine the dead time, t_0, and number of theoretical plates, N_0. The results are given in Table II.

RESULTS AND DISCUSSION

Thermal treatment

The number of silanol groups per unit area of porous glass or silica has been estimated or measured by numerous workers and values in the range 4–8/nm^2 were found [12–14]. The generally accepted value is 4.6/nm^2 for surface silanol groups of a properly dried silica. Davydov [15] has shown that the surface concentration of silanol groups dropped from 5.3/nm^2 at 100°C to 2.6/nm^2 at 400°C and < 1.0/nm^2 at about 850°C or higher temperatures of thermal treatment. The rehydration of the siloxane groups formed is usually slow and often the thermally treated silica or porous glass must be heated in hot acids [16].

In preliminary experiments with bonded chiral stationary phases we attempted to react thermally treated silica, from the same batch as the support used for chiral modification, with *n*-octadecyldimethylchlorosilane in dry toluene. Table I shows the results of the elemental analyses. A measurable decrease in the *n*-octadecyldimethylsilyl (ODS) surface concentration was obtained only after thermal treatment of the silica at above 800°C prior to chemical reaction. In contrast, a 4-h treatment at 1000°C diminished the active silanol groups very effectively so that a significant decrease to 0.47 mmol ODS/g was measured. The bulky ODS was used to obtain almost comparable conditions to the bonding procedure with chiral ligands.

TABLE I

SILYLATION OF THERMALLY TREATED SILICA: RESULTS FROM ELEMENTAL ANALYSES

T = Temperature of thermal treatment; O_M(C) = surface concentration of ODS, based on C, from elemental analysis data.

No.	T (°C)	O_M(C) (mmol/g)
1	150	0.74
2	600	0.71
3	800	0.66
4	1000	0.47

TABLE II

COLUMN PARAMETERS OF STATIONARY PHASES I AND II

O_M(C) = surface concentration based on C; O_M(N) surface concentration based on N; S_{BET} = specific surface area; t_0 = dead time; N_0 = number of theoretical plates; ε = total porosity; mobile phases, *n*-hexane–2-propanol (78:22) and *n*-hexane–tetrahydrofuran (3:1); flow-rate, 1 ml/min; column, 25 cm × 3.2 mm I.D., 5 μm. Mean results from ten measurements with each mobile phase.

Stationary phase	O_M(C) (mmol/g)	O_M(N) (mmol/g)	S_{BET} (m^2/g)	t_0[a] (min)	N_0[a]	ε[a]
CSP I	0.23	0.25	290	1.72	4300	0.85
TCSP I	0.16	0.11	60	1.51	7900	0.75
CSP II	0.20	0.22	290	1.71	2300	0.85
TCSP II	0.15	0.11	20	1.46	7900	0.73

[a] Toluene as non-retained standard.

For the "diluted" CSPs, silica was heated at 1000°C for 6 h in the muffle furnace, cooled and reacted with 3-glycidoxypropyltrimethoxysilane and one of the chiral selectors under dry atmospheric conditions. Both elemental analyses and weight difference measurements indicated a twofold lower coverage with organic molecules than the 0.25 mmol/g for heavily loaded CSPs. Table II shows relevant physical characteristics of the four tested stationary phases.

Heavely loaded silicas have specific surface areas (S_{BET}) that differ only slightly from that of the unmodified support. Thermal treatment of silica at 1000°C with a subsequent surface reaction causes a severe decrease in S_{BET} to below 60 m^2/g [8,17,18]. Therefore, it can be assumed that at 1000°C significant changes in the structure of silica occur.

The chromatographic data (dead time, t_0, number of theoretical plates, N_0, and total porosity, ε [19]) in Table II indicate a good packing quality of the columns made from these "diluted" phases.

TABLE III

PHENYL- AND NAPHTHYL-CONTAINING SAMPLES **1–6** USED IN CHROMATOGRAPHIC EXPERIMENTS

DNB = 3,5-Dinitrobenzoyl.

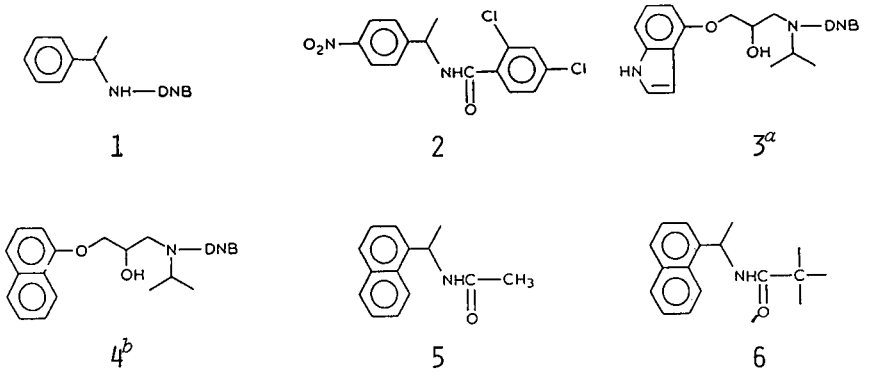

[a] **3** = DNB amide of pindolol.
[b] **4** = DNB amide of propranolol.

TABLE IV

RESOLUTION OF SAMPLES **1–6** ON STATIONARY PHASES I AND II

Conditions: mobile phase, *n*-hexane–tetrahydrofuran (3:1); flow-rate, 1 ml/min; column, 25 cm × 3.2 mm I.D., 5 μm; detection, UV at 254 nm. k'_1 = Capacity factor of the first-elute enantiomer; α = separation factor.

Stationary	Sample											
	1		**2**		**3**		**4**		**5**		**6**	
	k'_1	α	k'_1	α	k'_1	α	k'_1	α	k'_1	α	k'_1	α
CSP I	4.92	2.17	2.82	1.01	6.66	1.05	2.86	1.10	10.30	1.05	0.50	1.06
TCSP I	5.63	2.14	2.23	1.03	6.95	1.17	2.48	1.18	4.30	1.08	0.75	1.13
CSP II	4.14	2.15	3.56	n.r.[a]	6.19	1.12	3.24	1.09	8.18	1.04	0.51	n.r.[a]
TCSP II	7.11	2.26	3.01	1.08	8.44	1.16	2.33	1.10	5.28	1.07	0.75	1.25

[a] No resolution.

Samples

The phases were tested with aromatic amides derived with N-acyl groups of different π-acidity and bulkiness. Table III shows the structures and Table IV gives the chromatographic results for six samples.

The thermally treated chiral stationary phases separate virtually all test enantiomers better than the corresponding heavily loaded phases; the separation factors, α, are about 0.1 unit higher. The capacity factors, k'_1, follow no distinct tendency. In fact, for the amides 1, 3 and 6 longer retention times were measured on TCSPs I and II than on the corresponding CSPs without thermal treatment of the support. Mauss and Engelhardt [8] examined the influence of thermal treatment on chromatographic selectivity and reported similar effects for aromatic molecules which can act as hydrogen-bond acceptors. They also claimed that the retention of solutes with hydrogen-bond acceptors is not affected by the removal of vicinal silanols.

Correlation methods

To compare the phases and to obtain more information on the recognition mechanisms involved, two homologous series with different alkyl chain lenghts were used for chromatographic correlation experiments; the racemic 1-phenylalkyl amines **1a–l** and 1-phenylglycine derivatives **7a–j**, both derived as 3,5-dinitrobenzoyl (DNB) amides, were eluted with *n*-hexane–2-propanol (78:22). Fig. 2 shows the structures of the test homologues. The results are listed in Tables V and VI and in Figs. 3–6.

For the separation of **1a–l**, all four CSPs show similar selectivity depending on the chain length (Fig. 3). The separation factors, α, are without exception higher for the type II phases. TCSP I (PIV) has better separation properties than the heavily loaded CSP I and the type II phases show just the opposite behaviour. Apart from this difference in selectivity, all the tested phases point to the same chiral recognition mechanism, recently described for correlation experiments with heavily loaded phases [11].

The plots of k'_1 *versus* carbon number *n* in the Fig. 4 indicate differences in the retention behaviour. The thermally treated and lightly loaded TCSPs I and II show a large decrease in capacity factors with increasing hydrophobicity (solutes **1** with longer *n*-alkyl chains) than the CSPs I and II. Only after *n*-propyl (TCSP I) or *n*-pentyl (TCSP II)

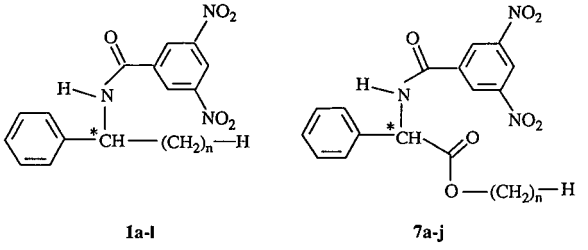

1a-l **7a-j**

Fig. 2. N-3,5-Dinitrobenzoyl (DNB)-derived homologous series **1a–l** and **7a–j**. For carbon numbers *n* see Tables V and VI and Figs. 3–6.

TABLE V

RESOLUTION OF N-3,5-DINITROBENZOYL-1-PHENYLALKYLAMINES **1a–l** ON STATIONARY PHASES I AND II

HPLC conditions: mobile phase, *n*-hexane–2-propanol (78:22); flow-rate, 1 ml/min; column, 25 cm × 3.2 mm I.D., 5 μm; detection, UV at 254 nm. n = Number of carbon atoms in the alkyl chain; k'_1 = capacity factor of the first-eluted enantiomer; α = separation factor; Conf. = configuration of last-eluted enantiomer.

n	CPS I (PIV)		TCSP I (PIV)		CSP II (CYH)		TCSP II (CYH)		Conf.
	k'_1	α	k'_1	α	k'_1	α	k'_1	α	
1	9.48	2.08	11.65	2.04	8.54	2.19	11.23	2.21	*R*
2	9.94	2.50	12.58	2.55	8.76	2.61	12.28	2.62	*R*
3	9.69	2.52	12.77	2.53	9.08	2.67	12.49	2.62	*R*
4	10.27	2.38	12.08	2.40	10.22	2.55	12.72	2.52	*R*
5	10.29	2.50	11.75	2.45	10.69	2.64	12.87	2.66	
7	9.29	2.47	10.49	2.57	9.62	2.77	11.62	2.72	
8	8.77	2.52	9.44	2.59	8.77	2.85	10.92	2.78	
9	8.43	2.57	9.17	2.62	8.61	2.94	8.98	2.86	
10	8.14	2.59	8.20	2.64	8.56	2.99	8.98	2.87	
13	7.57	2.67	5.52	2.73	7.75	3.08	7.97	2.93	
15	7.00	2.68	4.81	2.77	7.16	3.14	7.34	2.98	
17	5.53	2.70	4.42	2.79	6.96	3.19	6.96	3.01	

was a decrease in retention with increasing chain length of the DNB-amides **1d–l** observed.

For an interpretation of this behaviour it must also be considered that in addition to the remaining silanol groups on the silica surface, there are likewise polar secondary hydroxyl groups on the spacer (Fig. 1) formed in the amination step of the epoxide [4,11]. In the heavily loaded CSPs I and II the resid-

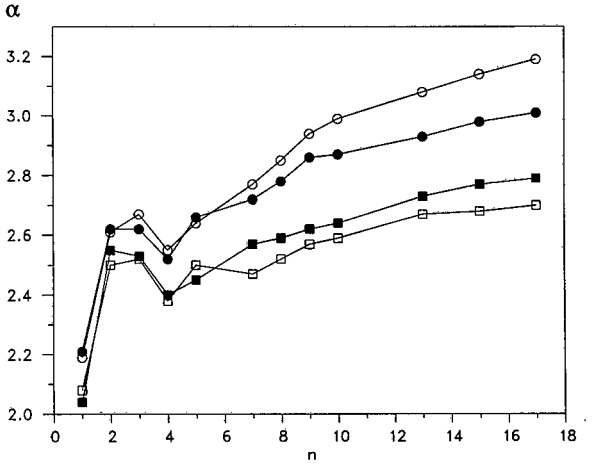

Fig. 3. Separation of phenylalkyl DNB derivatives **1a–l** on CSP and TCSP I and II using 2-propanol–*n*-hexane (22:78) as mobile phase. Separation factor α *versus* carbon number n. □ = CSP (PIV); ■ = TCSP I (IV); ○ = CSP II (CYH); ● = TCSP II (CYH).

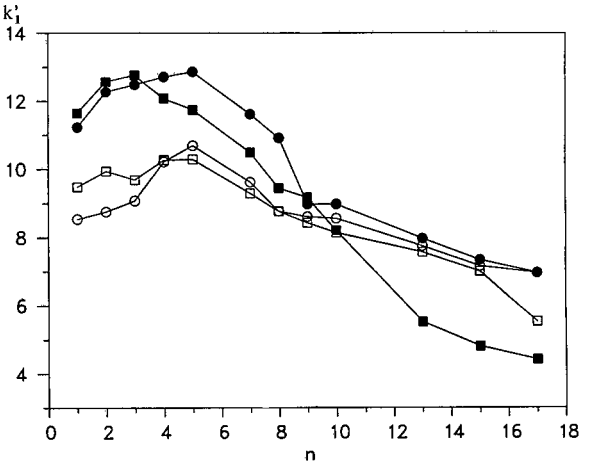

Fig. 4. Separation of phenylalkyl DNB derivatives **1a–l** on CSP and TCSP I and II using 2-propanol–*n*-hexane (22:78) as mobile phase. Capacity factor k'_1 *versus* carbon number n. ○ =CSP-I (PIV); ■ = TCSP I (PIV); ○ = CSP II (CYH); ● = TCSP II (CYH).

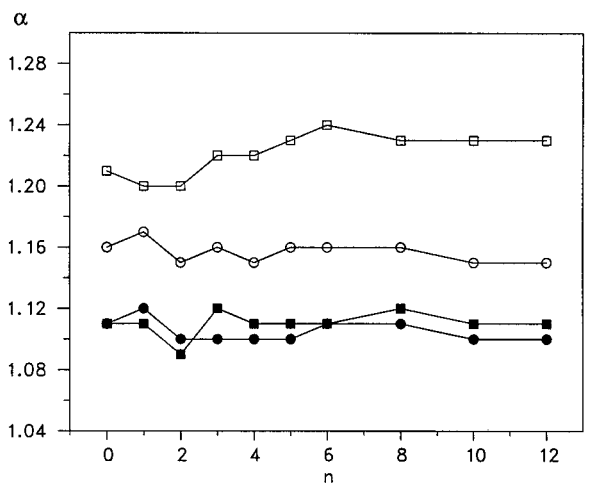

Fig. 5. Separation of phenylglycine DNB derivatives **7a–j** on CSP and TCSP I and II using 2-propanol–*n*-hexane (22:78) as mobile phase. Separation factor α *versus* carbon number *n*. □ = CSP I (PIV); ■ = TCSP I (PIV); ○ = CSP II (CYH); ● = TCSP II (CYH).

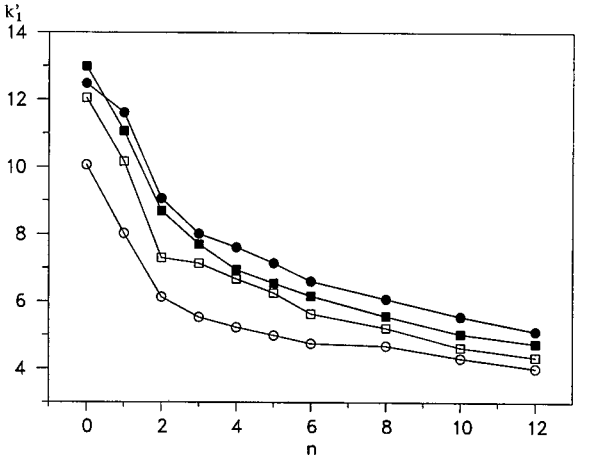

Fig. 6. Separation of phenylglycine DNB derivatives **7a–j** on CSP and TCSP I and II using 2-propanol–*n*-hexane (22:78) as mobile phase. Capacity factor k'_1 *versus* carbon number *n*. □ = CSP I (PIV); ■ = TCSP I (PIV); ○ = CSP II (CYH); ● = TCSP II (CYH).

ual silanol groups are very effectively screened by the bulky organic molecules. Hence, they excert a smaller contribution to the retention of polar DNB-amides. On the other hand, higher surface loadings with chiral ligands increase the number of secondary polar hydroxyl groups. The high k'_1 values of samples **1a–h** with TCSPs I and II support the assumption that polar adsorptive effects take place

TABLE VI

RESOLUTION OF *n*ALKYL ESTERS **7a–j** OF N-3,5-DINITROBENZOYL-1-PHENYLGLYCINE ON STATIONAY PHASES I AND II

HPLC conditions: mobile phase, *n*-hexane–2-propanol (78:22); flow-rate, 1 ml/min; column, 25 cm × 3.2 mm I.D., 5 μm; detection, UV at 254 nm. *n* = Number of carbon atoms in the alkoxy chain; k'_1 = capacity factor of the first-eluted enantiomer; α = separation factor; Conf. = configuration of last-eluted enantiomer.

n	CPS I (PIV)		TCSP I (PIV)		CSP II (CYH)		TCSP II (CYH)		Conf.
	k'_1	α	k'_1	α	k'_1	α	k'_1	α	
0	12.05	1.21	12.99	1.11	10.06	1.16	12.48	1.11	
1	10.16	1.20	11.06	1.11	8.02	1.17	11.61	1.12	*R*
2	7.29	1.20	8.69	1.09	6.13	1.15	9.06	1.10	*R*
3	7.13	1.22	7.70	1.12	5.53	1.16	8.01	1.10	*R*
4	6.67	1.22	6.94	1.11	5.23	1.15	7.61	1.10	
5	6.25	1.23	6.54	1.11	4.99	1.16	7.14	1.10	*R*
6	5.63	1.24	6.16	1.11	4.75	1.16	6.60	1.11	
8	5.21	1.23	5.56	1.12	4.68	1.16	6.07	1.11	
10	4.63	1.23	5.03	1.11	4.31	1.15	5.55	1.10	
12	4.34	1.23	4.75	1.11	4.01	1.15	5.11	1.10	

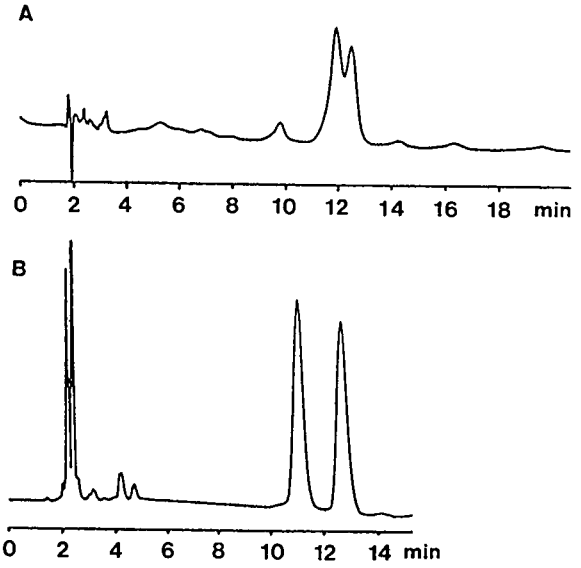

Fig. 7. Separation of DNB amide of (*R/S*)-pindolol (**3**) on (A) CSP I (PIV) and (B) TCSP II (PIV). Mobile phase, *n*-hexane–tetrahydrofuran (3:1); flow-rate, 1 ml/min; temperature, 20°C.

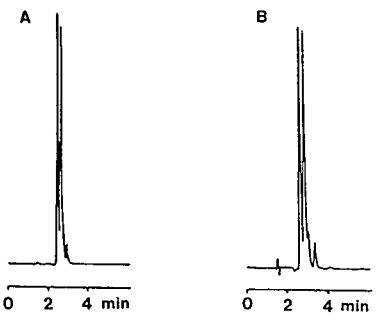

Fig. 8. Separation of (*R/S*)-1-(N-1-pivaloylamino-1-ethyl)naphthalene (**6**) on (A) TCSP I (PIV) and (B) TCSP II (CYH). Mobile phase, *n*-hexane–tetrahydrofuran (3:1); flow-rate, 1 ml/min; temperature, 20°C.

from residual silanol groups and also from secondary hydroxyl groups. For samples with long *n*-alkyl chains, where an intercalation between the strands of the chiral ligands is excluded for steric reasons, the role of the secondary hydroxyl group on the spacer is predominant. Remaining silanols on the silica matrix may not act as strong adsorption sites for such solutes. This leads to similar or even lower k'_1 values in comparison with CSPs I and II.

Samples with dominant hydrogen bonding such as the homologous 1-phenylglycine derivatives **7a–j** whose *n*-alkoxy chain does not intercalate between the strands are less resolved on TCSPs I and II than on the appropriate CSPs I and II, as shown in Fig. 5. The lower enantioselectivity of these phases is due to a smaller number of available chiral selectors. The retention times of the 1-phenylglycine derivatives **7a-j** are higher for both diluted phases than for the more highly loaded phases (Fig. 6).

Examples of the DNB-amide of (*R/S*)-pindolol (**3**) (Table III) separated on CSP I (PIV) and TCSP I (PIV) are given in Fig. 7. The diluted phase has a higher resolution for the racemate, shown in the baseline-separated peaks in chromatogram B. Similar observations with thermally treated silica were reported for various aromatic solutes by Mauss and Engelhardt [8]. The CSPs I and II resolved the naphthyl-containing sample **6** (Table III) only very incompletely ($1.0 \leqslant \alpha \leqslant 1.06$). In comparison with this lack of selectivity, TCSPs I and II resolved this sample better ($1.13 \leqslant \alpha \leqslant 1.25$), as can be seen in the chromatograms in Fig. 8.

CONCLUSIONS

Chromatographic selectivity with chiral stationary phases is not only a function of the chiral selector used to form diastereomeric solute–CSP complexes but also depends on non-enantioselective interactions of surface silanol groups or other polar sites on the phase.

The retention of solutes which are able to interfere directly by hydrogen bonding is strongly affected by thermal treatment of silica.

The observed retention of various samples suggests a more polar silica surface than would be expected after thermal treatment at 1000°C. This treatment lowers te specific surface area severely but in some instances increases the selectivity of the chiral stationary phase owing to the lower surface concentration of silanols. The reason is fewer polar interaction sites, which leads to additional peak broadening. In the tested phases, the polar secondary hydroxyl group near the chiral selector part can influence the retention of samples.

ACKNOWLEDGEMENTS

We thank Mr. B. Trusch for his help with specific

surface area measurements of silica, Dr. W. Padowetz of Ciba-Geigy, Basle, for elemental analysis data and Mrs. H. Murray for linguistic advice.

REFERENCES

1 W. H. Pirkle, M. H. Hyun and B. Bank, *J. Chromatogr.*, 316 (1984) 585.
2 W. H. Pirkle, M. H. Hyun, A. Tsipouras, B. C. Hamper and B. Bank, *J. Pharm. Biomed. Anal.*, 2 (1984) 173.
3 W. H. Pirkle and M. H. Hyun, *J. Chromatogr.*, 328 (1985) 1.
4 R. Däppen, V. R. Meyer and H. Arm, *J. Chromatogr.*, 361 (1986) 93.
5 L. R. Snyder and J. W. Ward, *J. Phys. Chem.*, 70 (1966) 3941.
6 R. K. Iler, *The Chemistry of Silica*, Wiley, Chichester, 1979.
7 K. K. Unger, *Porous Silica, (Journal of Chromatography Library,* Vol. 16), Elsevier, Amsterdam, 1979.
8 M. Mauss and H. Engelhardt, *J. Chromatogr.*, 371 (1986) 235.
9 C. H. Lochmüller and M. T. Kersey, *Langmuir*, 4 (1988) 572.
10 R. Straub, *Dissertation*, University of Berne, 1990.
11 R. Straub, M. Pfister and H. Arm. *J. Chromatogr.*, 585 (1991) 195.
12 M. L. Hair and I. D. Chapman, *J. Am. Ceram. Soc.*, 49 (1966) 651.
13 R. K. Iler, *Colloid Chemistry of Silica and Silicates*, Cornell University press, Ithaca, NY, 1955, p. 242.
14 J. A. Hockey, *Chem. Ind. (London)*, 1 (1965) 57.
15 V. Y. Davydov, *Trans Faraday Soc.*, 60 (1965) 1129.
16 D. L. Eaton, in D. E. Leyden and W. T. Collins (Editors), *Silylated Surfaces (Midland Macromolecular Series*, Vol. 7), Gordon and Breach, New York, 1978, p. 213.
17 E. A. Flood, *The Solid–Gas Interface*, Vols. 1 and 2, Marcel Dekker, New York, 1967.
18 K. D. Lork, K. K. Unger and J. N. Kinkel, *J. Chromatogr.*, 352 (1986) 199.
19 L. R. Snyder and J. J. Kirkland, *Introduction to Modern Liquid Chromatography*, Wiley, New York, 2nd ed., 1979, p. 220.

Journal of Chromatography, 623 (1992) 33–41
Elsevier Science Publishers B.V., Amsterdam

CHROM. 24 455

Efficient enantioselective separation and determination of trace impurities in secondary amino acids (*i.e.*, imino acids)

Janusz Zukowski, Maria Pawlowska and Daniel W. Armstrong

Department of Chemistry, University of Missouri-Rolla, Rolla, MO 65401 (USA)

(First received April 13th, 1992; revised manuscript received June 19th, 1992)

ABSTRACT

An *R*-(−)-1-(1-naphthyl)ethyl carbamoylated-β-cyclodextrin bonded phase in conjunction with a nonaqueous polar mobile phase was used for the highly selective enantioseparation of a number of secondary amino acids after their pre-column derivatization with 9-fluorenylmethyl chloroformate (FMOC). Under the conditions employed, the FMOC reagent served to "lock" the imino acid into their existing conformation thereby preventing the possibility of racemization. Furthermore, it served to increase the sensitivity to the point that trace level enantiomeric impurities were easily detected. Compared with separations that use traditional reversed-phase solvents, this method showed several advantages: higher selectivity towards the imino acid enantiomers investigated, shorter analysis times, faster equilibration of the column, more stable baseline and more sensitive fluorescence detection. The detection limits for FMOC derivatives of proline, *trans*-4-hydroxyproline, *cis*-4-hydroxyproline, pyroglutamic acid, 3,4-dehydroproline, thiaproline, penicillamine acetone adduct and pipecolic acid are in the low femtomole range. The method was used for evaluation of enantioselectivity of a number of "optically pure" commercial imino acid standards. Enantiomeric impurities as low as 0.0001% (1 ppm) can be determined in some cases. High precision determination of trace levels of D-imino acids in the presence of large amounts of corresponding (opposite) L enantiomer at 1, 0.1, 0.01% and below are demonstrated.

INTRODUCTION

Amino acids form a large group of compounds of pharmaceutical and biochemical interest. The stereoisomers of amino acids differ in biological activity, hence their configuration and optical purity are very important in many fields of peptide and polypeptide chemistry. Because D-amino acids are rare in nature compared with the L enantiomers, their determination in complex biological samples requires selective, efficient and highly sensitive screening techniques. As has been shown in recent years, the method of choice often is high-performance liquid chromatography (HPLC) with fluorimetric detection.

In the past two decades, a number of different HPLC procedures have been developed for enantiomeric separation of amino acids using both direct and indirect methods. The progress made in the field can be found in many original research papers and review articles and will not be discussed in detail here [1–3].

HPLC methods are often combined with pre- or post-column derivatization in order to achieve high-sensitivity fluorimetric or photometric detection. Many chromatographic procedures use derivatization reagents such as: 7-chloro-4-nitrobenzo-2-oxa-1,3-diazole (NBD-Cl) [4–6], dansyl chloride (DNS-Cl) [7–12], phenylisothiocyanate (PITC) [13–15], *ortho*-phthalaldehyde–mercaptoethanol (OPA–

Correspondence to: Dr. D. W. Armstrong, Department of Chemistry, University of Missouri-Rolla, Rolla, MO 65401, USA.

ME) [16–20], 9-fluorenylmethyl chloroformate (FMOC-Cl) [21–25] and naphthalenedialdehyde and analogues [26,27].

The above methods have been successfully used for chiral and achiral separation of a number of amino acids. However, each method has distinct advantages and disadvantages. It is especially difficult to conduct the DNS-Cl derivatization reaction adequately when the amino acids are present in low concentration in complex mixtures [28]. The OPA–ME derivatization is more rapid and sensitive, but its use is limited to primary amino acids. The PITC reagent requires an evaporation of the sample to remove excess of reagent prior to HPLC. In addition, all of these derivatives show only limited stability. The labeling with FMOC-Cl avoids the problems mentioned above and combines high sensitivity in fluorescence detection with favorable chromatographic properties and ease of derivatization for both primary and secondary amino acids.

This paper presents the results of enantioseparation of a number of secondary amino acids (imino acids) including naturally occurring proline, hydroxyprolines, pipecolic acid and pyroglutamic acid. Their physiological and pathological roles have received attention from numerous workers [29–31]. Several different HPLC techniques have been used for quantitative achiral determination of secondary amino acids in biological samples [5,22, 25,32–38], however a precise, accurate and sensitive method for chiral determination is still needed.

The enantiomeric separation of the FMOC–imino acids was obtained on a *R*-(−)-1-(-naphthyl)ethyl carbamoylated-β-cyclodextrin (RN-β-CD) column which has been previously used for successful resolution of a large variety of enantiomers in the normal-phase and reversed-phase mode [22,39,40]. In the present study the RN-β-CD column, operated with a nonaqueous polar mobile phase, was used for separation of secondary amino acids after their pre-column derivatization with FMOC-Cl. To our knowledge, it is the first enantioseparation of highly fluorescent FMOC derivatives of proline [22], pipecolic acid and their analogues. The method was used for determination of enantiomeric contamination of a number of "optically pure" commercial imino acid standards.

EXPERIMENTAL

Apparatus

The HPLC system consisted of three pumps (LC-6A, Shimadzu, Kyoto, Japan), a system controller (SCL-6B, Shimadzu), UV detector (SPD-6A, Shimadzu), fluorescence detector (RF-535, Shimadzu), switching valve (Rheodyne, Cotati, CA, USA) and 0.2-μl injector valve (Valco, Houston, TX, USA). The columns were 100 × 4.6 mm C_{18}, 250 × 4.6 mm acetylated-β-cyclodextrin (AC-β-CD) and RN-β-CD (Astec, Whippany, NJ, USA).

Chemicals

Amino acids were purchased from different sources listed in Table II. Acetonitrile, water, acetic acid and triethylamine were of HPLC grade and supplied from EM Science (Gibbstown, NJ, USA).

Procedure

Derivatizing agent FMOC-Cl was purchased from Sigma (St. Louis, MO, USA). Derivatization was performed according to ref. 21. D-Thiaproline was obtained by racemization of L-thiaproline in boiling 6 *M* HCl solution. *trans*-4-Hydroxy-D-proline was obtained by epimerization of *cis*-4-hydroxy-L-proline according to ref. 41. Isomerization degree of both racemization and epimerization reactions was checked using a C_{18}/RN-β-CD column switching method. After derivatization of post reaction mixtures with FMOC-Cl, 5 μl of the sample was injected onto the C_{18} column and chromatographed using acetonitrile–water–acetic acid (200:800:2, v/v/v) at 0.5 ml/min. A UV wavelength of 266 nm was used to monitor the effluent. The switching valve was turned for 2 s after the signal reached the maximum of the standard retention time. In this way a small portion of the eluting peak of *trans*-4-hydroxyproline or thiaproline was introduced into the chiral column.

RESULTS AND DISCUSSION

Optimization of mobile phase composition

Most FMOC-functionalized imino acids can be resolved in either a conventional reversed-phase mode (hydro-organic solvents) or with a mobile phase consisting almost entirely of acetonitrile (containing small amount of glacial acetic acid and triethylamine modifiers). The latter of these will be

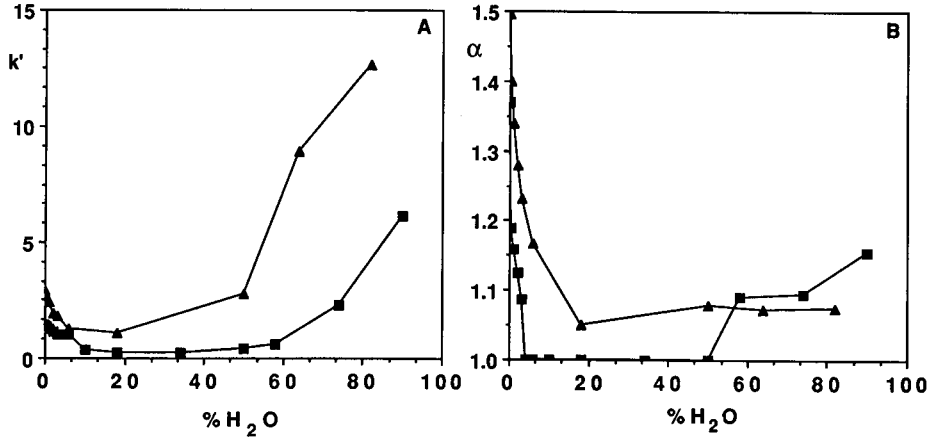

Fig. 1. Influence of water concentration in the mobile phase on (A) the retention and (B) enantioselectivity obtained on AC-β-CD (■) and RN-β-CD (▲) column for D, L-proline. Eluent: acetonitrile–water–0.6% triethylamine–0.4% acetic acid. Flow-rate: 1 ml/min.

referred to as the "polar organic mobile phase".

As can be seen in Figs. 1 and 2, for proline, separations done with polar organic mobile phase are generally preferable to those done with a hydro-organic mobile phase. This is because the enantioselectivity (α) is significantly greater with a polar organic mobile phase, while retention times are less. Fig. 1 also shows that the *R*-(−)-1-(1-naphthyl)-ethyl carbamoylated-β-cyclodextrin column is generally more selective for the FMOC–imino acids than is the acetylated-β-CD column. It is also interesting to note that in the reversed-phase mode, the large increases in retention with mobile phases containing more than 50% buffer did not produce corresponding improvements in the separation or the enantioselectivity (Fig. 1).

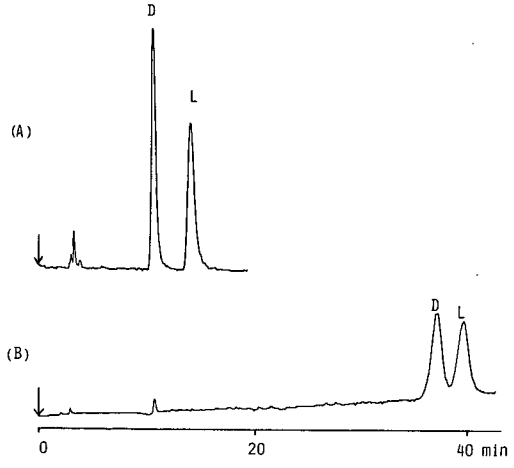

Fig. 2. Enantioseparation of D, L-proline obtained on RN-β-CD column in: (A) nonaqueous system, eluent: acetonitrile–triethylamine–acetic acid (1000:6:4); (B) under optimal conditions in aqueous system. Eluent: water–acetonitrile–triethylamine–acetic acid (850:150:6:4). Flow-rate: 1 ml/min. The time scale at the bottom of the figure applies to both chromatograms (A) and (B).

In the case of the acetylated-β-CD stationary phase, the addition of as little as 4% (v/v) water to the mobile phase negated the enantioselectivity (Fig. 1B). These results indicate that the chiral recognition mechanism may be dependent on the mobile phase composition. In the case of 1-(1-naphthyl)ethyl carbamoylated-β-cyclodextrin columns, this phenomenon has been previously reported and discussed in detail [12,39,40]. The aforementioned conclusion is also supported by the results shown in Fig. 3. The addition of water into an acetonitrile mobile phase influences not only the selectivity, but also efficiency of the column. The plots shown in Fig. 3 can give some information on the molecular recognition mechanism. Following the general non-equilibrium theory developed by Giddings [42], the overall plate height (H) for liquid–solid chromatography (LSC) can be expressed as:

$$H = A + \frac{B}{u} + C_m\bar{u} + C_k\bar{u} \quad (1)$$

Zone spreading is due to three independent

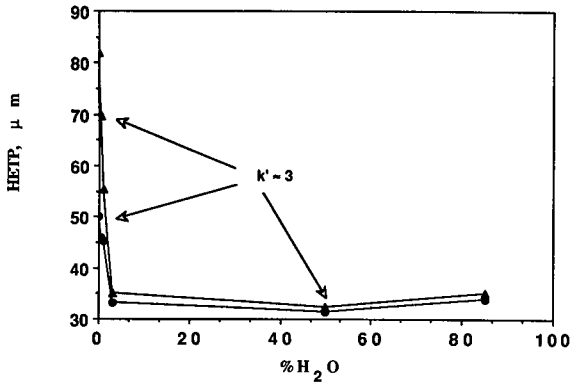

Fig. 3. Influence of water concentration in the mobile phase on efficiency of RN-β-CD column, ▲ = L-proline, ● = D-proline. Chromatographic conditions as in Fig. 1.

sources: flow pattern effects (A), longitudinal diffusion (B) and mass transfer effects (C). Flow pattern effects depend on the structure of the porous support material and are independent of the eluent velocity (u). Ordinary molecular diffusion in the flow direction contributes most at low velocities and in LC the term B/u is small. Mass transfer effects contribute most in high-speed runs. In adsorption chromatography they are controlled by two basically different mechanisms or some combination thereof: diffusion-controlled sorption and desorption rates originating in the mobile phase (C_m) and adsorption–desorption kinetics (C_k).

For the same chromatographic system, the contribution of the first three terms to H is the same for both enantiomers.

According to:

$$C_k = \frac{2q}{k_d} \cdot \frac{k'}{(1 + k')^2} \quad (2)$$

where: q is the geometrical parameter, k_d is the desorption rate and k' is the capacity factor; the significant differences in column efficiency observed for proline enantiomers in the non-aqueous system indicates that there is a considerable difference in adsorption–desorption kinetics for both enantiomers. Indeed, for the stronger retarded L-enantiomer, the rate of the adsorption–desorption process is about 2 times lower than for the D enantiomer.

The change in the eluent composition influences the mass-transfer effects controlled by diffusion in the mobile phase.

Since:

$$C = \frac{wd_p^2}{D_m} \quad (3)$$

where: w is a dimensionless constant, d_p is the particle size and D_m is the diffusion coefficient in the mobile phase. The change in the eluent composition also influences the diffusion velocity because of changes in the solvent viscosity ($D_m \approx 1/\eta$, where η = viscosity). However, the dramatic decrease of the height equivalent to a theoretical plate (HETP) values for both proline enantiomers cannot be attributed to the mass transfer effects in the mobile phase. The effect observed is just opposite to that which should be expected from theory: the addition of water induces a large increase in the solvent viscosity which should also increase the contribution of C_m term of the plate height. Moreover, the addition of water significantly decreases capacity factors in the discussed region [0–4% (v/v) water]. Because $k'/(1 + k')^2$ (eqn. 2) is an increasing function with decreasing k' values ($k' > 1$), the reduction in the HETP values also cannot be due to changes in the capacity factors. Despite a large increase in solvent viscosity [η (water) = 1 cP, η (acetonitrile) = 0.34 cP] in the true reversed-phase mode, the plate heights for both enantiomers are similar, and only slightly dependent on eluent composition in the range studied.

Interpretation of the data leads to the assumption that the addition of water to the eluent changes the chiral recognition mechanism and influences the kinetic process of sorption–desorption in the stationary phase which results in narrower peaks. The HETP values obtained in aqueous systems are lower (for the similar capacity factor as indicated in Fig. 3) compared with HETP found in the nonaqueous system. The results suggest the existence of at least two types of recognition mechanisms which differ in the rate of adsorption–desorption process.

It should be mentioned that in contrast to traditional aqueous systems, the recognition mechanism in nonaqueous systems is still not clear. It has been postulated that an inclusion complexation may not be occurring in these conditions [43]. Rather, a more external adsorption at the mouth of the cyclodextrin cavity could account for the observed separations.

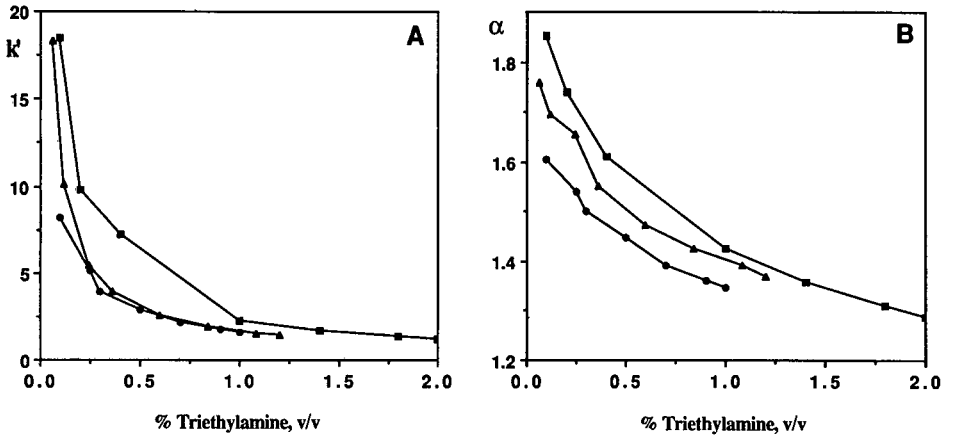

Fig. 4. Dependence of (A) the retention and (B) enantioselectivity on total amount of triethylamine and acetic acid and their relative ratio added to neat acetonitrile. Test compound: D, L-proline. Column: RN-β-CD. Eluent: acetonitrile–triethylamine–acetic acid. Triethylamine: acetic acid: ■ = 2:1, ● = 2:3, ▲ = 1:2.

including the apparent size selectivity between α, β and γ-cyclodextrin [43].

Fig. 2 shows the enantioseparation of a proline racemate obtained on RN-β-CD column in the nonaqueous mode and under optimal conditions in a water-rich system. The preliminary investigations have shown that the water-free system has several advantages over the aqueous one including: greater resolution, faster equilibration of the column, more stable base-line and lower detection limits.

Thus, the RN-β-CD column which exhibited high selectivity toward FMOC–D, L-proline, and a non-aqueous eluent was chosen for the detailed study on the optimization of enantioseparation of secondary amino acids.

As indicated in Fig. 4, retention and selectivity of nonaqueous systems can be effectively regulated by changes in two parameters of the mobile phase: the total amount of triethylamine and acetic acid added and their relative ratios. Fig. 4 presents the typical dependence for all imino acids investigated. This behavior may be used for an optimization of separation factors for any analogous separation problem. Fig. 5 shows the influence of triethylamine and acetic acid concentration on the enantioseparation of pipecolic acid racemate.

Selectivity and sensitivity of the method

The chromatographic data for all racemic mixtures investigated are summarized in Table I. The selectivity of the system was regulated by adjusting the mobile phase composition to achieve base-line resolution with a reasonable retention time. The combination of good selectivity (≈1.15–1.50) and high efficiency results in high resolution factors for FMOC proline enantiomers and its analogues.

The enantioseparation of pipecolic acid was achieved with an eluent containing lower concentrations of triethylamine and acetic acid, which resulted in a longer analysis time. The separation of nipecotic acid (an analogue of pipecolic acid) was not possible.

It should be mentioned that high selectivities and resolutions listed in Table I are more than adequate

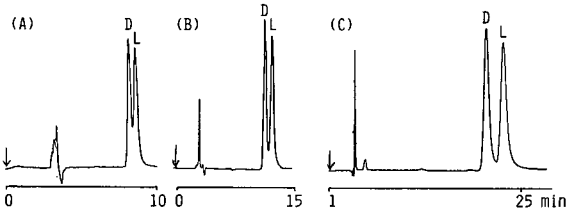

Fig. 5. Effect of total amount of triethylamine and acetic acid per 1000 ml of acetonitrile in the mobile phase on the resolution of D, L-pipecolic acid obtained on RN-β-CD column. Flow-rate: 1 ml/min. Eluent: (A) acetonitrile–0.6% triethylamine–0.9% acetic acid; (B) acetonitrile–0.3% triethylamine–0.45% acetic acid; (C) acetonitrile–0.12% triethylamine–0.18% acetic acid.

TABLE 1

SEPARATION DATA FOR RACEMIC MIXTURES OF SECONDARY AMINO ACIDS ON RN-β-CD COLUMN OPERATED WITH A NONAQUEOUS MOBILE PHASE

Name	Structure	Eluent[a]	k'_D	k'_L	α	R_s[c]
Proline	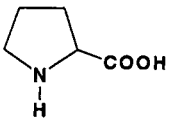	6:4:1000	2.9	4.4	1.5	4.1
trans-4-Hydroxyproline	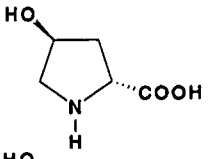	6:4:1000	7.3	9.6	1.3	2.3
cis-4-Hydroxyproline	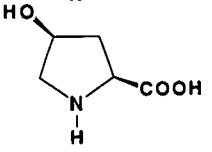	6:4:1000 3:2:1000	1.8 3.2	2.2 4.1	1.2 1.3	1.7 2.7
Pyroglutamic acid[b]	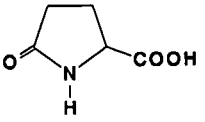	6:4:1000	1.9	2.4	1.3	3.3
3,4-Dehydroproline	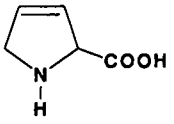	6:4:1000	2.6	3.6	1.4	3.5
Thiaproline	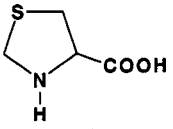	6:4:1000	1.9	2.2	1.2	2.6
Penicillamine acetone adduct	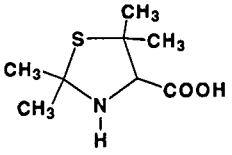	6:4:1000 3:2:1000	1.2 1.9	1.4 2.3	1.2 1.2	1.5 2.0
Pipecolic acid	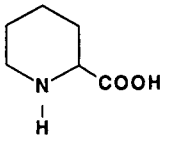	6:4:1000 3:2:1000 1.5:1:1000	2.2 3.5 6.2	2.3 3.8 6.9	1.1 1.1 1.1	1.1 1.4 1.7

[a] Triethylamine–acetic acid–acetonitrile.

[b] Although this is an amide it is known to react with a variety of acid chlorides [49,50]. In this work, we found that it reacts with FMOC-Cl as well.

[c] R_s = Resolution.

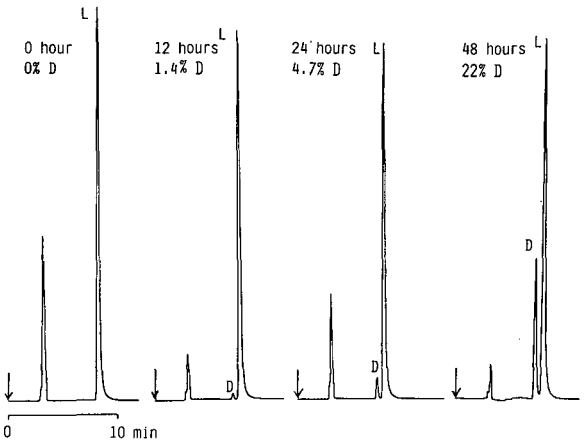

Fig. 6. Change of enantiomeric ratio of thiaproline during the racemization reaction (see Experimental). Eluent: acetonitrile–triethylamine–acetic acid (1000:6:4). Flow-rate: 1 ml/min.

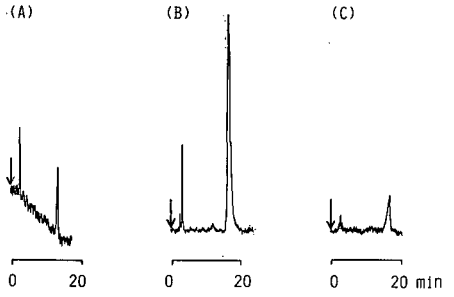

Fig. 7. Comparison of detectability of L-proline in (A) aqueous eluent: [water–acetonitrile–triethylamine–acetic acid (530:470:6:4)] and (B, C) nonaqueous eluent: [acetonitrile–triethylamine–acetic acid (1000:6:4)]. Column: RN-β-CD. Flow-rate: 1 ml/min. Injected amount: (A) 7.4 fmol, (B) 7.4 fmol and (C) 1.4 fmol.

for determinations of racemic mixtures. However, as has recently been reported [44], the requirement for trace analysis are more rigorous. Resolution factors greater than 2 for the racemic mixture is an appropriate criterion for quantitative trace analysis applications.

The elution order was checked by the injection of pure enantiomers or mixtures with different enantiomeric ratios. Since for thiaproline and *trans*-4-hydroxyproline, only L enantiomers were available, the enantiomers were prepared via racemization and epimerization reactions, respectively, according to the procedure described in the Experimental section. The degree of racemization was checked by HPLC. Fig. 6 shows the change of ratio of thiaproline enantiomers during the racemization reaction.

The D enantiomer was eluted prior to the L enantiomer for all the FMOC–imino acids examined, which is an advantage because the L enantiomer is the dominant component in most biological samples. It has been shown that when traces are eluted before the major enantiomer the quantitative determination of chiral composition becomes more accurate and precise [45,46], and trace detectability can be improved tremendously [47].

The detection limits were calculated using a signal-to-noise ratio of 2. The detection limits for all enantiomers investigated are in the low femtomole range. It was found that the sensitivity of the method depends on eluent composition. The detection limit for FMOC L-proline, estimated in the nonaqueous system, was 5 times lower than was found for the system with a mobile phase containing 53% of water (see Fig. 7). This is probably due to the fact that for many aromatic and/or heteroaromatic compounds water has a quenching effect on the fluorescence [48]. In addition, as shown in Fig. 7, the noise and baseline shifting is more prevalent in a water-rich system.

Practical applications

This method was used for determination of enantiomeric contamination in a number of commercial imino acid standards. The results are collected in Table II. The chromatographic conditions are given in Table I. Some level of enantiomeric contamination was found in all commercial amino acid samples. As can be seen from the results in Table II the method enables trace and ultra-trace determination of optical purity for both L and D enantiomers.

Quantitative analysis of contaminating D enantiomers in L-amino acids at 1, 0.1 and 0.01% gave very high precision (R.S.D. for 4 measurements) of 0.3% (pyroglutamic acid), 2.6% (*cis*-4-hydroxyproline) and 4.5% (FMOC-L-proline), respectively.

For the L enantiomer, as the trace component, the situation is more complicated. The problem associated with tailing from the enantiomerically rich component results in quantitative determinations with lower precision. This is shown in Fig. 8B. The precision in quantitative analysis for optical purity of proline enantiomers at the 0.1% level is 1.2% and

TABLE II

OPTICAL PURITY OF COMMERCIAL SAMPLES OF L- AND D-AMINO ACIDS

Chromatographic conditions as in Table I.

Name	Source	Concentration of opposite enantiomer (%)	Eluent[a]	Standard deviation[d]
D-Proline	ICN	0.7	A	0.08
L-Proline	Aldrich	0.5		0.006
FMOC-L-proline	Fluka	0.02	A	0.0008
trans-4-Hydroxy-L-proline[b]	Sigma	0	A	
		0.09[b]		0.008
cis-4-Hydroxy-D-proline	Sigma	0.4	B	0.009
cis-4-Hydroxy-L-proline	Sigma	1.5	B	0.007
D-Pyroglutamic acid[c]	Sigma	2.5	A	0.04
L-Pyroglutamic acid[c]	Sigma	1.3	A	0.004
L-Thiaproline	Sigma	0.3	A	0.009
L-Penicillamine acetone adduct	Sigma	0.3	B	0.01
3,4-Dehydro-L-proline	Aldrich	0.4	A	0.04
L-Pipecolic acid	Aldrich	0.3	C	0.007

[a] Eluent: acetonitrile–triethylamine–acetic acid: A = 1000:6:4; B = 1000:3:2; C = 1000:1.5:1.

[b] *cis*-4-Hydroxy-D-proline; according to [43], *trans*-4-hydroxy-L-proline epimerizes to *cis*-4-hydroxy-D-proline.

[c] Although this is an amide it is known to react with a variety of acid chlorides [49,50]. In this work, we found that it reacts with FMOC-Cl as well.

[d] $n = 5$.

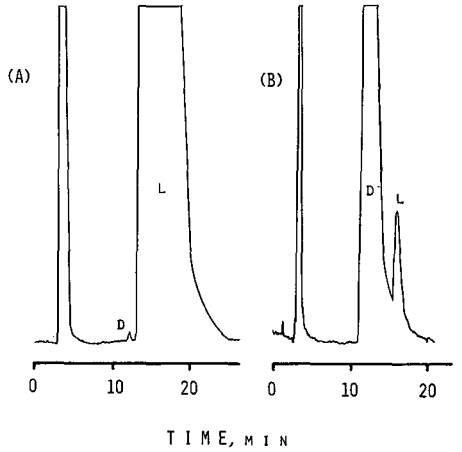

Fig. 8. Chromatograms used to evaluate the enantiomeric purity of: (A) L-proline (a purified mixture) and (B) D-proline (ICN). Eluent: acetonitrile–triethylamine–acetic acid (1000:6:4). Column: RN-β-CD. Flow-rate: 1 ml/min.

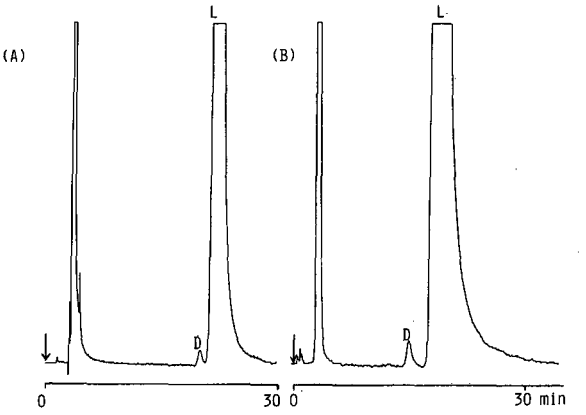

Fig. 9. Chromatograms used to evaluate the enantiomeric purity of: (A) L-pipecolic acid (Aldrich). Eluent: acetonitrile–triethylamine–acetic acid (1000:1.5:1); (B) *cis*-4-hydroxy-L-proline (Sigma). Eluent: acetonitrile–triethylamine–acetic acid (1000:3:2). The other conditions as in Fig. 8.

11.1% for the D and L enantiomer, respectively. The trace analysis precision for the L enantiomer found in this study was 1.8% (pyroglutamic acid) at the 1% level and 11.1% (proline) at the 0.1% level.

In conclusion, the present method gives high sensitivity and precision for the evaluation of trace levels of D imino acids in the presence of large amounts of the corresponding L enantiomer. Fig. 9 shows the chromatographic separation of contaminating D enantiomers in L-pipecolic acid and *cis*-4-hydroxy-L-proline samples.

This technique can be easily adopted to routine analysis and has been used extensively in this laboratory to quantitate the D-proline content in physiological fluids down to the ppm level (Fig. 8A).

ACKNOWLEDGEMENT

Support of this work by the National Institute of General Medical Science (BMT 1R01 GM36292-04) is gratefully acknowledged.

REFERENCES

1 T. J. Ward and D. W. Armstrong, *J. Liq. Chromatogr.*, 9 (1986) 407.
2 A. M. Krstulovic (Editor), *Chiral Separation by HPLC*, Ellis Horwood, Chichester, 1989.
3 S. Ahuja (Editor), *Chiral Separations by LC (ACS Symposium Series*, No. 471), American Chemical Society, Washington, DC, 1991.
4 R. S. Fager, G. B. Kutina and E. W. Abrahamson, *Anal. Biochem.*, 53 (1973) 290.
5 M. Ahnoff, I. Grundvik, A. Arfwidsson, J. Fonselius and B. A. Persson, *Anal. Chem.*, 53 (1981) 485.
6 N. Nimura, A. Toyama and T. Kinoshita, *J. Chromatogr.*, 234 (1982) 482.
7 S. Weinstein and S. Weiner, *J. Chromatogr.*, 303 (1984) 244.
8 E. Bayer, D. Gram, B. Katteneggar and R. Uhnam, *Anal. Chem.*, 48 (1976) 1106.
9 W. Lindner, I. N. le Page, G. Davies, D. E. Seitz and B. L. Karger, *J. Chromatogr.*, 185 (1979) 323.
10 K. Fujimura, S. Suzuki, K. Hayashi and S. Mosuda, *Anal. Chem.*, 62 (1990) 2198.
11 S. Allenmark and S. Andersson, *J. Chromatogr.*, 351 (1986) 231.
12 M. L. Hilton, S. Chang, M. P. Gasper and D. W. Armstrong, *J. Liq. Chromatogr.*, (1992) in press.
13 S. A. Cohen and D. J. Strydouz, *Anal. Biochem.*, 174 (1988) 1.
14 R. L. Heinrikson and S. C. Meredith, *Anal. Biochem.*, 136 (1986) 65.
15 S. Gunawan, N. Y. Walton and D. M. Freiman, *J. Chromatogr.*, 503 (1990) 177.
16 M. Roth, *Anal. Chem.*, 43 (1971) 880.
17 E. Gil, A. Tishbee and P. E. J. Hare, *J. Am. Chem. Soc.*, 102 (1980) 5115.
18 N. Nimura, T. Suzuki, Y. Kasahara and T. Kinoshita, *Anal. Chem.*, 53 (1991) 1380.
19 I. Moretti, M. Biranelli, C. Carducci, A. Poniecorvi and I. Antonozzi, *J. Chromatogr.*, 511 (1990) 131.
20 D. W. Armstrong, J. D. Duncan and S. H. Lee, *Amino Acids*, 1 (1991) 97.
21 S. Einarsson, B. Josefsson and S. Lagerkvist, *J. Chromatogr.*, 382 (1983) 609.
22 S. Einarsson, *J. Chromatogr.*, 384 (1985) 213.
23 S. Einarsson, S. Folestad, B. Josefsson and S. Lagerkvist, *Anal. Chem.*, 58 (1986) 1638.
24 M. F. Molnar and L. A. S. Schroeder, *J. Chromatogr.*, 514 (1990) 227.
25 V. Buetikofer, D. Fucks, J. O. Bosset and W. Gmuer, *Chromatographia*, 31 (1991) 441.
26 R. G. Caelson, K. Srinivasachar, R. S. Givens and B. K. Matuszewski, *J. Org. Chem.*, 51 (1986) 3978.
27 P. De Montigny, C. M. Riley, L. A. Sterson and J. F. Stobaugh, *J. Pharm. Biomed. Anal.*, 8 (1990) 419.
28 D. J. Neadle and R. J. Pollitt, *Biochem. J.*, 97 (1965) 607.
29 S. Lam and A. Karger, *J. Liq. Chromatogr.*, 9 (1986) 291.
30 A. Meister, *Science (Washington, DC)*, 130 (1973) 33.
31 E. Giacobini, Y. Namura and T. Schmidt-Glenewinkel, *Cell. Mol. Biol.*, 26 (1980) 135.
32 G. Bellon, A. Malgras, R. Rondoux and J. P. Borlel, *J. Chromatogr.*, 278 (1983) 167.
33 S. Einarsson, B. Josefsson, P. Moeller and D. Sanchez, *Anal. Chem.*, 59 (1987) 1191.
34 L. A. Schilb, V. D. Fiegel and D. R. Knighton, *J. Liq. Chromatogr.*, 13 (1990) 57.
35 H. Nishio and T. Segawa, *Anal. Biochem.*, 135 (1983) 312.
36 Y. Okano, M. Kataoka, T. Miyata, H. Morimoto, K. Takahama, T. Hitoshi, Y. Kase, I. Matsumoto and T. Shinka, *Anal. Biochem.*, 117 (1981) 196.
37 E. Bousgnet, G. Romeo and L. I. Giannola, *J. Chromatogr.*, 344 (1985) 325.
38 R. Dimaline and J. R. Reeve, Jr., *J. Chromatogr.*, 257 (1983) 355.
39 A. M. Stalcup, S. Chang and D. W. Armstrong, *J. Chromatogr.*, 540 (1991) 113.
40 D. W. Armstrong, S.-D. Chang and S. H. Lee, *J. Chromatogr.*, 539 (1991) 83.
41 D. D. Dziewiatkowski, V. C. Mascall and R. I. Riolo, *Anal. Biochem.*, 49 (1972) 550.
42 J. C. Giddings, *Dynamics of Chromatography*, Dekker, New York, 1965.
43 D. W. Armstrong, S. Chen, C. Chang and S. Chang, *J. Liq. Chromatogr.*, 15 (1992) 545.
44 T. D. Doyle, in S. Ahuja (Editor), *Chiral Separations by LC (ACS Symposium Series*, No. 471), American Chemical Society, Washington, DC, 1991, p. 27.
45 E. Busker, K. Guenter and J. Martens, *J. Chromatogr.*, 350 (1985) 179.
46 K. G. Feitsma, B. F. H. Drenth and R. A. de Zeeuw, *J. Chromatogr.*, 387 (1987) 447.
47 J. A. Perry, J. D. Rateike and T. J. Szczerba, *J. Chromatogr.*, 389 (1987) 57.
48 H. Lingeman, W. J. M. Underberg, A. Takadate and A. Hulshoff, *J. Liq. Chromatogr.*, 8 (1985) 789.
49 K. Imaki, H. Niwa, S. Sakuyama, T. Okada, M. Toka and M. Hayashi, *Chem. Pharm. Bull.*, 29 (1981) 2699.
50 K. Imaki, S. Sakuyama, T. Okada, M. Toda, M. Hayashi, T. Miyamoto, A. Kawasaki and T. Okegawa, *Chem. Pharm. Bull.*, 29 (1981) 2210.

Journal of Chromatography, 623 (1992) 43–47
Elsevier Science Publishers B.V., Amsterdam

CHROM. 24 444

Determination of glycerol in wines by high-performance liquid chromatography: comparison with enzymatic method☆

G. Sánchez Muñoz, E. Garcia Romero and M. S. Pérez Coello

Estación de Viticultura y Enología, Carretera de Torrenueva, s/n, 13.300 Valdepeñas, Ciudad Real (Spain)

P. J. Martín Alvarez

Instituto de Fermentaciones Industriales, C.S.I.C., Juan de la Cierva 3, 28006 Madrid (Spain)

(First received February 23rd, 1992; revised manuscript received June 16th, 1992)

ABSTRACT

A method for determining glycerol in wines by high-performance liquid chromatography has been developed using three 250 × 8 mm columns based on a sulphonated styrene–divinyl benzene polymer (SHODEX S-801/S,S-802/S,S-802/S) in series. This polymer combines cation-exchange mechanisms with molecular exclusion. The columns were thermostated at 75°C using water as the mobile phase. A refraction index detector was used and the samples were directly injected. The method is reproducible (coefficient of variation above 1%) and accurate. Linear regression analysis and Student's *t*-test for comparison of the mean show that the results are comparable with those obtained by an enzymatic method (differences less than 4%).

INTRODUCTION

Glycerol is the major component of wine (after water and ethanol) and is a secondary product of alcoholic fermentation. It contributes to the sensory properties of wine, such as body, smoothness and sweetness.

The official chemical method of analysis [1] requires a long and tedious sample preparation, with non-quantifiable losses of glycerol occurring [2] and anomalous higher values attributable to mannitol and sorbitol. However, enzymatic methods [3] are specific, accurate and reproducible [4] and can be applied in segmented continuous-flow analysers [5].

Gas chromatographic determination of glycerol in wines can be carried out by direct injection on packed columns [6,7]. However, problems sometimes arise because the desorption is not quantitative when porous polymers are used as stationary phases.

These problems are avoided by using capillary columns, but it is necessary to prepare the sample by extraction with organic solvents [8] or the formation of derivatives before analysis [9].

Different procedures have been developed using high-performance liquid chromatography (HPLC) with columns of the amino type [10,11], or based on cation-exchange mechanisms [12]; a cation-exchange column (Aminex HPX-87H, Bio Rad, Richmond, CA, USA) has been used by several

Correspondence to: D. G. Sanchez Muñoz, Estación de Viticultura y Enología, Carretera de Torrenueva s/n, 13.300 Valdepeñas, Ciudad Real, Spain.

☆ Presented at the *20th Annual Scientific Meeting of the Group of Chromatography and Related Techniques of the Spanish Royal Society of Chemistry, San Sebastián, October 29–31, 1991*. The proceedings of this meeting have been published in *J. Chromatogr.*, Vol. 607, No. 2 (1992).

0021-9673/92/$05.00

workers [13,14] without sample preparation, although one study [15] suggested passing the wine through ion-exchange resins to avoid interference from the organic acids present, an aspect which has also been reported by Flak [10].

In all these instances a refraction index detector was used. Conductivity detectors [16] and post-column reactors with fluorimetric [17] or pulsed amperometric [18] detectors have also described. A method using ^{13}C nuclear magnetic resonance spectroscopy has also been reported [19].

An HPLC method of determining glycerol in wines by direct sample injection is presented in this paper. Various columns are used, combining the mechanisms of molecular exclusion and cation-exchange chromatography. In this way neither compounds with a higher molecular mass nor organic acids (mobile phase, water) are retained. Carbohydrates and polyalcohols are also separated.

EXPERIMENTAL

Samples and reagents

All the chemicals used were of analytical-reagent grade. Glucose, fructose, glycerol and ethanol were supplied by Panreac (Barcelona, Spain); butan-2,3-diol and tartaric, malic, lactic, acetic, citric, succinic and fumaric acids were from E. Merck (Darmstadt, Germany); shikimic and citramalic acids were from Fluka (Buchs, Switzerland) and Millipore (Bedford, MA, USA) Milli-Q water was used.

The wine samples were injected directly after filtration through 0.2-μm membranes (Dynagard, 0.8 cm^2; Microgon, Laguna Hills, CA, USA).

Chromatographic method

The equipment consisted of a solvent chamber (SEC-4, Perkin-Elmer, Norwalk, CT, USA), a pump (Series-10, Perkin-Elmer), injection valve (7125, Rheodyne, Cotati, CA, USA), a column furnace (220-DW, Croco-Cil, Saint Foy La Grande, France), a refraction index detector (LC-25, Perkin-Elmer) and a data processing system (450-MT2, Kontron Instruments, Milan, Italy).

The samples were injected through a 6-μl loop into a system made up of three columns 250 × 8 mm in series (Shodex S-801/S, S-802/S, S-802/S; Showa Denko, Tokyo, Japan) and a Shodex S-800P pre-column controlled by thermostat at 75°C, using water as the mobile phase; the flow-rate was 1 ml/min and a refractive index detector.

Enzymatic method

The enzymatic determinations were carried out with a UV–visible scanning spectrophotometer (GBC 911, GBC Scientific Equipment, Dandenong, Australia).

Boehringer Mannheim enzymatic kits were used. The wines were diluted 1:25 to obtain glycerol concentrations between 0.03 and 0.4 g/l [3].

Data treatment

Data were processed using the BMDP statistical package [20], using Student's *t*-test for comparisons of the mean (BMDP3D program) and linear regression (BMDP1R program). These programs were run on a VAX 9200 computer.

RESULTS AND DISCUSSION

Chromatographic separation

The three molecular exclusion columns connected in series provided high resolution without an excessively long analysis time.

Fig. 1 shows the chromatogram of a red wine obtained under the described conditions. The first group of compounds (A) observed are those with the highest molecular mass and those with an acid character. Glucose, fructose, glycerol, butan-2,3-diol and ethanol (the last peak) are then eluted. The next sample can be injected without waiting for the elution of later peaks. Peak 4 results from the addition of 0.8 g/l butan-2,3-diol to the initial wine to show its presence more clearly. The separation observed between peaks 3 and 4 is not complete, but in practice has no influence on the results for glycerol.

Fig. 2 is a chromatogram of a standard mixture of acids usually present in wine and shows how they eluted in zone A of Fig. 1, and therefore do not interfere in the determination of glycerol. This is an advantage compared with other procedures [13–15]; in this instance previous preparation of the sample is not necessary.

Comparison of the proposed HPLC method and the enzymatic method

Two wines, one red and one white, to which were

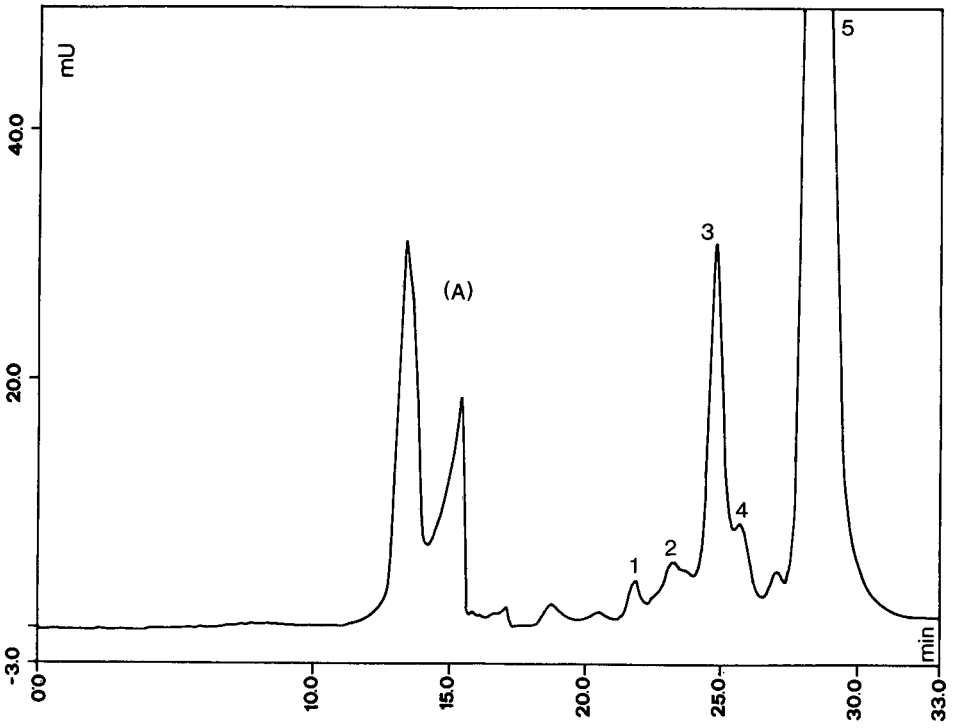

Fig. 1. Chromatogram of a red wine using Shodex S-801/S and S-802/S columns at 75°C with a mobile phase of water at a flow-rate of 1 ml/min and using a refraction index detector. Peaks: A = see text; 1 = glucose; 2 = fructose; 3 = glycerol; 4 = butan-2,3-diol (0.8 g/l added to the initial wine); 5 = ethanol.

added increasing amounts of glycerol (0.5, 1.0, 1.5 and 2.0 g/l) were analysed. The distribution of the data obtained (mean values, four replicates) is shown in Table I.

The regression lines for the results of both methods [y (mean values of glycerol recovered, g/l) *versus* x (g/l of glycerol added)] are $y = 0.9524x$ ($r^2 = 0.9962$; $s = 0.090$) for the HPLC method and $y = 1.0030x$ ($r^2 = 0.9998$; $s = 0.020$) for the enzymatic method.

The slopes do not differ significantly from unity in either instance ($p < 0.05$); a greater dispersion is observed in the results obtained by HPLC (0.09 *versus* 0.02).

Fig. 3 shows the regression line (HPLC method *versus* enzymatic method) referred to the whole set of mean values from Table I. The data fit fairly well ($r^2 = 0.9999$), although significant differences ($p < 0.05$) between the two methods were detected: less than 4.2% (mean differences about 2%) according to Student's t-test.

When ten different wines (five white and five red) were analysed by the two methods (five replicates), the values shown in Table II were obtained. The differences between the values from the two methods by Student's t-test were less than 4%, an acceptable margin in practice.

Tables I and II give the standard deviations and the coefficients of variation in each instance. The coefficients of variation are not generally greater than 1% in either method.

Influence of butan-2,3-diol

As the chromatographic resolution of the peaks of glycerol and butan-2,3-diol is not complete (Fig. 1), a study was carried out to determine the influence of butan-2,3-diol in the quantification of glycerol. One white and one red wine, to which were added 0.4 and 0.8 g/l butan-2,3-diol, were analysed in quadruplicate. The results suggest that the incomplete separation does not have an appreciable influence; the differences were less than 2.3%.

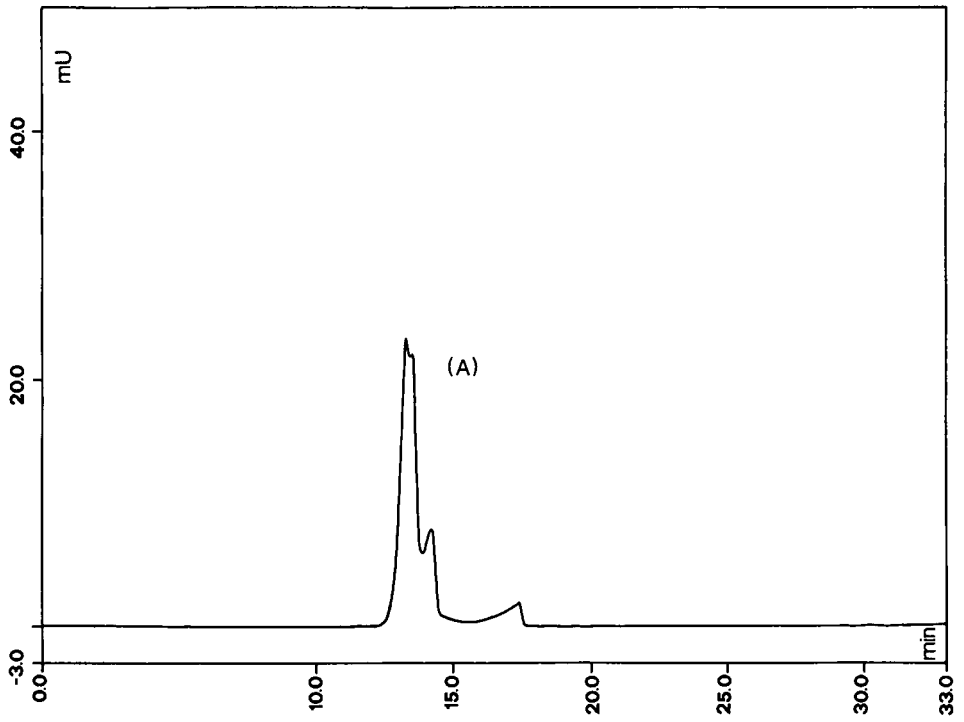

Fig. 2. Chromatogram of a standard mixture of tartaric, malic, shikimic, lactic, acetic, citric, succinic, citramalic and fumaric acids in concentrations similar to those of the wines analysed. Chromatographic conditions as in Fig. 1.

TABLE I

COMPARISON OF THE RESULTS FROM THE DETERMINATION OF GLYCEROL BY THE ENZYMATIC METHOD AND THE PROPOSED HPLC METHOD AFTER THE ADDITION OF VARIOUS AMOUNTS OF GLYCEROL

Values in parentheses are coefficients of variation (%).

Glycerol added (g/l)	Glycerol found (mean ± S.D., n = 4) (g/l)	
	Enzymatic method	HPLC method
White wine		
0.0	6.08[a] ± 0.01 (1.3)	5.92 ± 0.01 (0.2)
0.5	6.67[a] ± 0.08 (1.3)	6.39 ± 0.04 (0.6)
1.0	7.15[a] ± 0.06 (0.8)	7.05 ± 0.02 (0.3)
1.5	7.64[a] ± 0.04 (0.5)	7.42 ± 0.06 (0.8)
2.0	8.21[a] ± 0.06 (0.7)	8.01 ± 0.10 (1.2)
Red whine		
0.0	7.64 ± 0.05 (0.7)	7.60 ± 0.01 (0.1)
0.5	8.18 ± 0.03 (0.4)	8.23 ± 0.05 (0.6)
1.0	8.70 ± 0.04 (0.4)	8.55 ± 0.17 (2.0)
1.5	9.16[a] ± 0.00 (0.0)	8.96 ± 0.05 (0.6)
2.0	9.71[a] ± 0.04 (0.4)	9.48 ± 0.05 (0.5)

[a] Significant differences (p < 0.05) between the mean values obtained by the two methods.

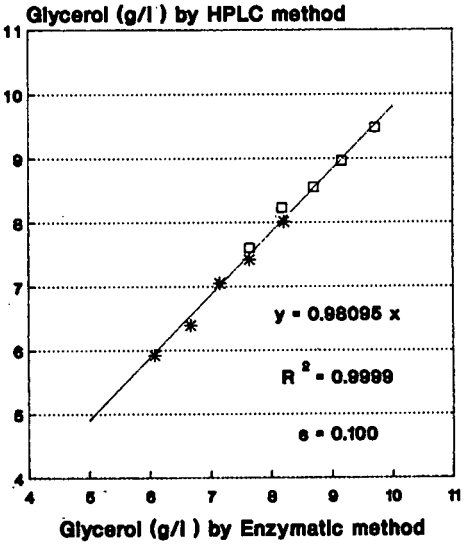

Fig. 3. Regression line for the comparison of the results from the determination of glycerol by the HPLC method and by the enzymatic method in the wines listed in Table I. (✱) White wine; (□) red wine.

TABLE II

COMPARISON OF THE RESULTS OF THE DETERMINATION OF GLYCEROL BY THE ENZYMATIC METHOD AND THE PROPOSED HPLC METHOD IN FIVE WHITE WINES AND FIVE RED WINES

Values in parentheses are coefficients of variation (%).

Wine type	Glycerol found (mean ± S.D., n = 5) (g/l)	
	Enzymatic method	HPLC method
White wine		
1	6.08[a] ± 0.01 (1.3)	5.92 ± 0.01 (0.7)
2	8.24[a] ± 0.06 (1.3)	8.48 ± 0.03 (1.0)
3	5.69[a] ± 0.05 (0.8)	5.92 ± 0.03 (0.9)
4	5.44[a] ± 0.05 (0.5)	5.52 ± 0.04 (0.9)
5	5.96[a] ± 0.03 (0.7)	6.17 ± 0.02 (0.5)
Red whine		
1	7.64 ± 0.05 (0.7)	7.60 ± 0.01 (0.1)
2	7.11[a] ± 0.07 (1.0)	7.31 ± 0.05 (0.7)
3	6.39[a] ± 0.04 (0.7)	6.49 ± 0.05 (0.8)
4	7.02 ± 0.10 (1.4)	7.07 ± 0.03 (0.4)
5	7.10[a] ± 0.04 (0.5)	7.19 ± 0.04 (0.6)

[a] Significant differences ($p < 0.05$) between the mean values obtained by the two methods.

Other applications

This HPLC method can also be applied to the simultaneous determination of ethanol in wine; the coefficients of variation found were 0.4% for ten determinations of the same wine and the recovery values ranged from 98 to 102%, giving a good correlation with the official method of alcoholic degree analysis by distillation. The method is also applicable to the determination of sucrose at concentrations greater than 2 g/l. In the same way it can be used to determine the glucose/fructose ratio in musts and has been used to follow the kinetics of alcoholic fermentation in cellars [21].

CONCLUSIONS

The proposed method of determining glycerol in wines is reproducible and gives results comparable with those obtained by the enzymatic method; the differences are about 2%.

As a result of the two separation mechanisms used in this study, interference from the organic acids present in wine is avoided and highly retained compounds are not eluted after the chromatogram has been completed. This allows the sample to be injected without previous preparation. This method has the advantage, characteristic of chromatographic methods, of allowing various compounds to be analysed simultaneously.

ACKNOWLEDGEMENT

The authors thank Dr. M. D. Cabezudo for her very useful guidance on the approach to and execution of this study.

REFERENCES

1 *Recueil des Méthodes Internationales d'Analyse des Vins*, Office International de la Vigne et du Vin, Paris, Annexe A21, 1969.
2 A. Joyeux, M. Lafitte and S. Lafon-Lafourcade, *Office International de la Vigne et du Vin*, F.V. 643 (1977) 1–5.
3 *Methods of Enzymatic Food Analysis 82/83*, Boehringer Mannheim, Munich, 1982.
4 E. Walter and P. Kohler, *Z. Lebensm.-Unters.-Forsch.*, 180 (1985) 121.
5 A. S. Curvelo-Garcia and M. C. Godinho, *Rev. Fr. Oenol.*, 123 (1990) 47.
6 W. Postel, L. Adam and M. Rustler, *Dtsch. Lebensm.-Rundsch.*, 78 (1982) 170.
7 M. A. Lage Yusty, C. M. Garcia Jarés, J. Simal Lozano and M. E. Alvarez Piñeiro, *An. Bromatol.*, 41 (1989) 375.
8 N. Gelsomini, F. Capozzi and C. Faggi., *J. High Resolut. Chromatogr.*, 13 (1990) 352.
9 E. G. Moruno and R. Di Stefano, *Vini Ital.*, 31 (1989) 41.
10 W. Flak, *Mitt. Klosterneuburg*, 31 (1981) 204.
11 R. Piccaglia and G. C. Galletti, *J. Sci. Food Agric.*, 45 (1988) 203.
12 A. Rapp and A. Ziegler, *Dtsch. Lebensm.-Rundsch.*, 75 (1979) 396.
13 P. Pfeiffer and F. Radler, *Z. Lebensm.-Unters. Forsch.*, 181 (1985) 24.
14 R. F. Frayne, *Am. J. Enol. Vitic.*, 37 (1986) 281.
15 P. Beaud, V. Marie and J. D. Aubort, *Mitt. Geb. Lebensmittel unters. Hyg.*, 80 (1989) 420.
16 K. Tanaka and J. S. Fritz, *J. Chromatogr.*, 409 (1987) 271.
17 N. Kiba, H. Maruyama and M. Furusawa, *J. Chromatogr.*, 456 (1988) 398.
18 J. Haginaka and T. Nomura, *J. Chromatogr.*, 447 (1988) 268.
19 A. Rapp, A. Markowetz, M. Spraul and E. Humpfer, *Dtsch. Lebensm.-Rundsch.*, 83 (1987) 375.
20 W. J. Dixon, *Biomedical Computer Programs*, University of California Press, Los Angeles, CA, 1983.
21 G. Sánchez Muñoz, E. Garcia Romero, M. S. Pérez Coello and P. J. Martín Alvarez, *Aliment. Equipos Tecnol.*, 10 (1991) 79.

Journal of Chromatography, 623 (1992) 49–53
Elsevier Science Publishers B.V., Amsterdam

CHROM. 24 420

Composition analysis of carboxymethylcellulose by high-pH anion-exchange chromatography with pulsed amperometric detection

Eddy A. Kragten, Johannis P. Kamerling and Johannes F. G. Vliegenthart

Bijvoet Center, Department of Bio-Organic Chemistry, Utrecht University, P.O. Box 80.075, NL-3508 TB Utrecht (Netherlands)

(First received February 25th, 1992; revised manuscript received June 4th, 1992)

ABSTRACT

A rapid method for the determination of the substituent distribution in carboxymethylcellulose has been developed, involving hydrolysis of carboxymethylcellulose in 1.2 *M* perchloric acid and analysis of the mixture of carboxymethylated glucose residues and glucose by high-pH anion-exchange chromatography with pulsed amperometric detection. The peaks in the chromatogram were identified by combined gas–liquid chromatography–mass spectrometry after pertrimethylsilylation. Molar response factors for each of the constituent monomers were established by ^{1}H NMR spectroscopy. The degrees of substitution for three carboxymethylcellulose preparations determined by the proposed method and by a standard titration method were found to be in excellent agreement.

INTRODUCTION

Sodium carboxymethyl (CM)-cellulose, prepared by conversion of cellulose with sodium chloroacetate, is an industrially important polymer that has found widespread use in the food and coatings industry and in oil-well drilling. The average degree of substitution (DS) of commercial, water-soluble CM-cellulose lies in the range 0.4–1.3 [1]. Being only partially carboxymethylated, CM-cellulose can be regarded as a copolymer of unsubstituted (D-glucose), monosubstituted (2-, 3- and 6-O-CM-D-glucose), disubstituted (2,3-, 2,6- and 3,6-di-O-CM-D-glucose), and trisubstituted (2,3,6-tri-O-CM-D-glucose) glucose.

Knowledge of the relative amounts of the constituent monomers of CM-cellulose is important in product control, and is essential for understanding structure–property relationships. So far, analysis of the intact polysaccharide by ^{13}C NMR spectroscopy has only resulted in information on the molar ratio of the substituents at HO-2, HO-3 and HO-6 [2]. For the determination of the monomer composition in solvolysates of CM-cellullose, different approaches have been developed. Mixtures of monomers, obtained by hydrolysis or methanolysis, have been analysed by carbon column chromatography [3], gas–liquid chromatography (GLC) [4–7], ^{13}C NMR spectroscopy [1,8] and ^{1}H NMR spectroscopy [9]. Recently, the substitutent distribution in CM-cellulose has been determined by GLC using a reductive cleavage procedure to obtain mixtures of the constituent monomers [10]. These methods are elaborate and time consuming. Recent advances in the separation of unmodified carbohydrates using high-pH anion-exchange chromatography (AEC) in combination with pulsed amperometric detection (PAD) [11] prompted us to devise a simple and rapid method for the determination of the substituent distribution in CM-cellulose.

Correspondence to: Professor Dr. J. F. G. Vliegenthart, Bijvoet Center, Department of Bio-Organic Chemistry, Utrecht University, P.O. Box 80.075, NL-3508 TB Utrecht, Netherlands.

0021-9673/92/$05.00

EXPERIMENTAL

Materials

CM-Cellulose samples, A, B and C were obtained from AKZO Research (Arnhem, Netherlands).

Hydrolysis procedure

Hydrolysis was carried out according to ref. 1 in modified form. CM-Cellulose (5 mg) in 0.1 ml of 70% $HClO_4$ was kept for 10 min at room temperature and, after addition of 0.9 ml of doubly distilled water affording 1.2 *M* $HClO_4$, heated for 16 h at 100°C. The solution was then neutralized with 2 *M* KOH, the precipitated $KClO_4$ was removed by centrifugation (2500 *g*, 5 min) and the supernatant was collected. The residue was washed twice with 0.5 ml of doubly distilled water and the supernatants were pooled.

High-pH anion-exchange chromatography with pulsed amperometric detection

Separation and quantification of the mixture of carboxymethylated glucose residues and glucose was carried out by high-pH AEC–PAD on a Dionex LC system consisting of a Dionex Bio-LC quaternary gradient module, a Model PAD-2 detector, a CarboPac PA-1 pellicular anion-exchange column (25 × 0.9 cm I.D.), (Dionex, Breda, Netherlands) and a Shimadzu C-R3A integrator. An aliquot (25 μl) of the pooled supernatants was applied to the column and elution was carried out starting with 0.1 *M* NaOH (eluent A)–0.1 *M* NaOH containing 1 *M* sodium acetate (eluent B) (95:5, v/v) for 0.3 min, followed by a linear gradient to eluent B in 15 min, at a flow-rate of 4.0 ml/min and ambient temperature. Detection was performed by PAD with a gold working electrode and triple-pulse amperometry with the following pulse potentials and durations: E_1 = 0.05 V, 300 ms (sampling); E_2 = 0.65 V, 60 ms (cleaning); E_3 = −0.95 V, 180 ms (reduction), and a response time of 1 s. For structural identification, fractions were isolated, neutralized with 4 *M* HCl, lyophilized and desalted on a column (40 × 1.5 cm I.D.) of Bio-Gel P-2 (200–400 mesh, Bio-Rad Labs.) using doubly distilled water. The eluent was monitored by UV detection at 206 nm with an LKB 2238 Uvicord S II absorbance detector. Residual sodium acetate was removed by conversion into acetic acid on a column (3 × 0.5 cm I.D.) of Dowex 50W-X8 (H^+) resin (100–200 mesh, Bio-Rad Labs.) and repeated lyophilization of the resulting solutions.

GLC and GLC–electron impact mass spectrometry (EI-MS)

Aliquots of the desalted high-pH AEC fractions were pertrimethylsilylated using pyridine–hexamethyldisilazane–trimethylchlorosilane (5:1:1, v/v/v). GLC was carried out on a Perkin-Elmer Model 8410 gas chromatograph equipped with a SE-30 bonded-phase, fused-silica capillary column (25 m × 0.32 mm I.D.) (Pierce) and a flame ionization detector, and connected to a Shimadzu C-R3A integrator. The temperature of the column was increased from 150 to 250°C at 4°C/min, and then kept at 250°C for 5 min. GLC–EI-MS was performed on a Carlo Erba GC–Kratos MS 80–Kratos DS 55 system (electron energy, 70 eV; accelerating voltage, 2.7 kV; ionizing current, 100 μA; ion-source temperature, 225°C; BP-1 capillary column). The initial temperature of the column was 200°C for 2 min, then increased to 300°C at 4°C/min.

^1H NMR spectrocopy

Prior to ^1H NMR spectroscopic analyses, samples were repeatedly treated with ^2H_2O (99.9 atom% ^2H) (MSD Isotopes), finally using 99.96 atom% ^2H at $p^2H \geqslant 7$. 300-MHz ^1H NMR spectra were recorded using a Bruker AC-300 spectrometer at a probe temperature of 20°C. Chemical shifts (δ) are expressed in ppm downfield from the signal for internal sodium 4,4-dimethyl-4-silapentane-1-sulphonate, but were actually measured by reference to the signal for internal acetone (δ 2.225) with an accuracy of 0.002 ppm. To obtain quantitatively reliable results, no resolution enhancement was applied, the HO^2H signal was not suppressed and a repetition delay of 5 s was used.

RESULTS AND DISCUSSION

For a reliable analysis of its substituent distribution, solvolysis of CM-cellulose has to be complete and the occurrence of side-reactions during solvolysis has to be avoided. A brief incubation with 70% $HClO_4$ at room temperature was applied to improve the solubility of the material, thereby making it accessible for complete hydrolysis in 1.2 *M*

$HClO_4$ (16 h, 100°C) without browning of the hydrolysate. Then, most of the $HClO_4$ was removed as $KClO_4$ after precipitation with KOH. This procedure gave samples that could be analysed directly by high-pH AEC–PAD.

A typical high-pH AEC–PAD trace for a hydrolysate separated on CarboPac PA-1 is shown in Fig. 1. For identification purposes fractions 1–8 were collected, neutralized, desalted on Bio-Gel P-2, pertrimethylsilylated and identified by GLC–EI-MS. Fraction 1 was found to correspond to D-glucose. Fractions 2, 3 and 4 contained 6-, 2- and 3-O-CM-D-glucose, respectively. Fractions 5, 6 and 7 corresponded to 2,6-, 3,6- and 2,3-di-O-CM-D-glucose, respectively, whereas fraction 8 contained 2,3,6-tri-O-CM-D-glucose. Apart from some minor differences in relative peak intensities, the mass spectra were in agreement with reference mass spectra of these derivatives [4,12]. It is evident that the compounds elute in groups according to the number of substituents, indicating that the interaction with the anion-exchange resin is dominated by the carboxymethyl groups. Completely resolved peaks were obtained for the positional isomers within each group, with the exception of 2-O- and 3-O-CM-D-glucose. However, the fractionation was sufficient to allow accurate integration (Fig. 1). The order of elution of the carboxymethylated glucose residues on CarboPac PA-1 was identical with that of the corresponding sulphoethylated glucose residues, separated on the same resin [13]. This suggests that the type of interactions of these compounds with the anion-exchange beads is similar, irrespective of the character of the anionic substituent. However, compared with the sulphoethylated glucose residues, a lower concentration of sodium acetate is sufficient for the elution of the carboxymethylated glucose residues, probably reflecting the weaker binding of the less acidic carboxymethyl group to the anion-exchange beads.

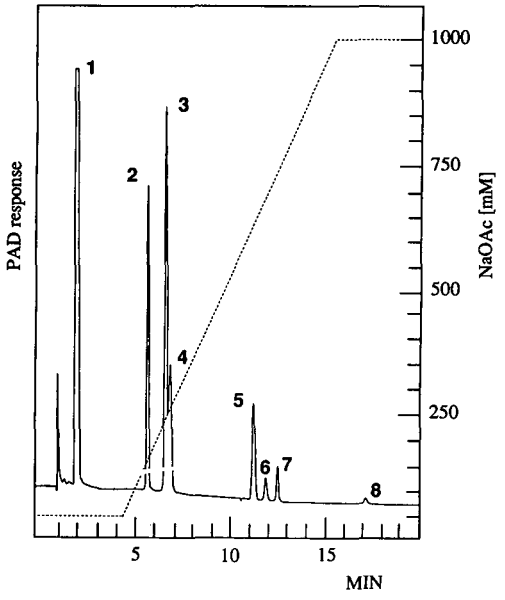

Fig. 1. Typical high-pH AEC trace of a CM-cellulose hydrolysate separated on a CarboPac PA-1 anion-exchange column (250 × 9 mm I.D.) using a gradient of sodium acetate (NaOAc) (dotted line) in 0.1 *M* NaOH at a flow-rate of 4 ml/min and PAD. Peaks: 1 = D-glucose; 2 = 6-O-CM-D-glucose; 3 = 2-O-CM-D-glucose; 4 = 3-O-CM-D-glucose; 5 = 2,6-di-O-CM-D-glucose; 6 = 3,6-di-O-CM-D-glucose; 7 = 2,3-di-O-CM-D-glucose; 8 = 2,3,6-tri-O-CM-D-glucose.

The high-pH AEC–PAD trace shows no additional peaks, suggesting that the formation of O-CM-glucoselactones (*ca.* 3 mol%) [5], which occurred during hydrolysis (6 *M* HCl, 2 h, room temperature, and subsequently 2 *M* HCl, 30 min, 120°C) or sample concentration, does not take place in the present procedure. In the method presented here the hydrolysis conditions are milder. However, when a higher concentration of $HClO_4$ (2 *M*) or a longer treatment (30 min) with 70% $HClO_4$ was supplied, minor additional peaks were observed on the high-pH AEC–PAD trace, which probably originate from O-CM-glucoselactones. This suggests that lactonization takes place only when carboxymethylated glucoses are exposed to strongly acidic conditions for a prolonged period of time.

For the determination of the substituent distribution in CM-cellulose from the peaks on the high-pH AEC–PAD trace, the molar response of each monomer to the pulsed amperometric detector was obtained from 300-MHz ^1H NMR spectra, recorded without resolution enhancement, of solutions containing one of the monomers and a defined amount of methyl β-cellobioside as an internal standard. In each instance the molar ratio of monomer to methyl β-cellobioside was determined by integration of the signals for the respective anomeric protons in the ^1H NMR spectra [14]. Then, each of the mixtures of monomer and methyl β-cellobioside was lyophilized, dissolved in doubly distilled water

TABLE I

CALCULATED PAD RESPONSE FACTORS OF THE MONOMERS OF CARBOXYMETHYL- AND SULPHOETHYLCELLULOSES

Monomer	PAD response[a]	
	R = CM[b]	R = SE[b]
D-Glucose	1.00	1.00
2-O-R-D-glucose	0.71	0.71
3-O-R-D-glucose	0.37	–
6-O-R-D-glucose	0.77	0.77
2,3-Di-O-R-D-glucose	0.26	0.16
2,6-Di-O-R-D-glucose	0.38	0.36
3,6-Di-O-R-D-glucose	0.24	0.17
2,3,6-Tri-O-R-D-glucose	0.20	–

[a] Relative to D-glucose.
[b] CM = Carboxymethyl; SE = sulphoethyl.

and subjected to high-pH AEC–PAD on CarboPac PA-1. Molar PAD responses under the conditions described under Experimental were calculated by matching the relative peak areas obtained by PAD with the relative amounts determined by ^{1}H NMR spectroscopy (see Table I). The general effect of substitution is a decrease in PAD response with an increasing number of carboxymethyl groups in the glucose residue. Although little is known about the actual electrochemical reactions taking place at the gold electrode, it is likely that the response to the pulsed amperometric detector mainly results from the oxidation of unsubstituted hydroxyl groups and of the hemiacetal group in the glucose residue. It is interesting that, within the group of monocarboxymethylated glucose residues, substitution of HO-3 results in the largest decrease in PAD response. A similar effect is observable for the dicarboxymethylated glucose residues. However, the response factors of the di- and tricarboxymethylated glucose residues cannot be calculated simply by addition of the effects of monocarboxymethylation on the PAD response. For comparison, previously established molar response factors of some sulphoethylated glucose residues [13] are included in Table I. Similar response factors for carboxymethylated and sulphoethylated glucose residues are observed when substituents occur at O-2 or O-6. The decrease in molar response is, however, larger with a sulphoethyl group than with a carboxymethyl group at O-3.

The high-pH AEC–PAD procedure was applied twice to samples A and B and four times to sample C, and in Table II the calculated substituent distribution for each of the samples is shown. The degrees of substitution (DS) of A, B and C, calculated using the data in Table II, were found to be 0.80, 0.81 and 0.68 ± 0.03, respectively. The determined DS values were in excellent agreement with the degree of substitution [(A) 0.77, (B) 0.80 and (C) 0.67]

TABLE II

SUBSTITUENT DISTRIBUTIONS IN THREE CARBOXYMETHYLCELLULOSES DETERMINED BY HIGH-pH AEC–PAD

Monomer	Distribution (mol%)		
	Sample A[a]	Sample B[a]	Sample C[b]
D-Glucose	37.0	36.7	44.5 ± 1.0[c]
2-O-CM-D-glucose[d]	21.4	21.7	21.0 ± 0.3
3-O-CM-D-glucose	12.5	11.9	9.2 ± 0.2
6-O-CM-D-glucose	12.7	13.0	13.0 ± 0.3
2,3-Di-O-CM-D-glucose	4.4	4.5	3.0 ± 0.3
2,6-Di-O-CM-D-glucose	8.1	8.2	6.4 ± 0.2
3,6-Di-O-CM-D-glucose	3.1	3.3	2.4 ± 0.2
2,3,6-Tri-O-CM-D-glucose	0.8	0.7	0.5 ± 0.1

[a] Average results of two individual analyses.
[b] Average results of four individual analyses with standard deviation.
[c] This larger standard deviation probably results from contamination of the sample with glucose from external sources.
[d] CM = Carboxymethyl.

provided by the manufacturer, based on a standard acid wash procedure [15].

From the data in Table II, the order of reactivity of the hydroxyl groups in cellulose towards carboxymethylation was calculated to be HO-2 > HO-6 > HO-3, in agreement with several other reports on CM-cellulose solvolysates using ^{13}C NMR spectroscopy [1], ^{1}H NMR spectroscopy [9] or GLC [5,6,10]. In two studies employing ^{13}C NMR spectroscopy [2,16] directly on the polymer it was reported that the reactivities of HO-3 and HO-6 are equal. Using a statistical model for the etherification of cellulose [17], which has been confirmed for CM-cellulose [1], the relative reaction rate constants for HO-2, HO-3 and HO-6 were calculated to be $k_2:k_3:k_6$ = 1.8:1:1.2, 1.9:1:1.3 and 2.3:1:1.5 for samples A, B and C, respectively. Comparison of these data with results from other studies is complicated by the fact that relative reaction rate constants, especially that of HO-3, depend to some extent on the reaction conditions used [8]. However, the relative reaction constants presented here are similar to previously reported data [1,6,9,10], with the exception of one study presenting higher values [5].

The method for the determination of the substituent distribution of CM-cellulose reported here offers important advantages over other procedures. There is no need for derivatization as required for GLC. Further, contrary to the appearance in ^{13}C and ^{1}H NMR spectra and gas–liquid chromatograms, each monomer is represented by a single peak on the high-pH AEC–PAD trace, making quantification more easy.

ACKNOWLEDGEMENTS

We thank A. C. van der Kerk-van Hoof (Bijvoet Center, Department of Mass Spectrometry, Utrecht University) for recording the GLC–EI-MS data. This investigation was carried out with financial aid from AKZO Research Arnhem and the Netherlands Foundation for Chemical Research (NWO/SON).

REFERENCES

1 J. Reuben and H. T. Conner, *Carbohydr. Res.*, 115 (1983) 1.
2 S. N. K. Chaudhari, K. C. Gounden, G. Srinivasan and V. S. Ekkundi, *J. Polym. Sci., Part A*, 25 (1987) 337.
3 J. Croon, *Sven. Papperstidn.*, 8 (1960) 247.
4 K. Niemelä and E. Sjöström, *Carbohydr. Res.*, 180 (1988) 43.
5 K. Niemelä and E. Sjöström, *Polym. Commun.*, 30 (1989) 254.
6 F. A. Buytenhuys and R. Bonn, *Papier*, 31 (1977) 525.
7 S. Ukai, A. Honda, K. Nagai and T. Kiho, *J. Chromatogr.*, 513 (1990) 338.
8 A. Parfondry and A. S. Perlin, *Carbohydr. Res.*, 57 (1977) 39.
9 F. F.-L. Ho and D. W. Klosiewicz, *Anal. Chem.*, 52 (1980) 913.
10 S. G. Zeller, G. W. Griesgaber and G. R. Gray, *Carbohydr. Res.*, 211 (1991) 41.
11 Y. C. Lee, *Anal. Biochem.*, 189 (1990) 151.
12 D. C. DeJongh, T. Radford, J. D. Hribar, S. Hanessian, M. Bieber, G. Dawson and C. C. Sweeley, *J. Am. Chem. Soc.*, 91 (1969) 1728.
13 E. A. Kragten, J. P. Kamerling, J. F. G. Vliegenthart, H. Botter and J. G. Batelaan, *Carbohydr. Res.*, (1992) in press.
14 E. A. Kragten, B. R. Leeflang, J. P. Kamerling and J. F. G. Vliegenthart, *Carbohydr. Res.*, 228 (1992) 433.
15 Monograph D 1439 (78), American Society for Testing and Materials, Philadelphia, PA.
16 A. Talvitie and J. Paasivirta, *Finn. Chem. Lett.*, 1 (1984) 18.
17 H. M. Spurlin, *J. Am. Chem. Soc.*, 61 (1939) 2222.

Journal of Chromatography, 623 (1992) 55–62
Elsevier Science Publishers B.V., Amsterdam

CHROM. 24 311

Determination of hydroxy acids as their copper(II) complexes by reversed-phase liquid chromatography with UV detection

Da Shi Lu, Wen Yu Feng, Da Hui Ling and Wang Zhog Hua

Department of Chemistry, Wuhan University, Wuhan 430072 (China)

(First received February 13th, 1991; revised manuscript received January 28th, 1992)

ABSTRACT

A method for the liquid chromatographic separation and UV detection of hydroxy acids without any pretreatment of derivatization is described. An aqueous solution containing copper ion, alkylsulphonate and acetate buffer is used as the mobile phase in conjunction with a conventional reversed-phase column. Detection is carried out at 254 nm. The influence of pH and the concentrations of copper ion, alkylsulphonate and buffer on the retention and detection response has been investigated. These parameters were found to provide powerful means of selectivity and response manipulations.

INTRODUCTION

The separation and determination of hydroxy acids, such as lactic, citric, malic, tartaric and α-hydroxybutyric acids, are important problems in physiology, biochemistry, food, beverages, health and related areas. For example, the concentration of lactic acid in the plasma of patients with leukaemia is much higher than that of healthy persons [1]. These compounds are present as major acid components in fruit, vegetable, milk and wine [2].

Ion-exchange chromatography is suitable for analyses for hydroxy acids [3]. There are several difficulties with the direct separation and determination of hydroxy acids by gas or reversed-phase liquid chromatography with UV detection because of their low volatility, strong polarity, ionicity and lack of appreciable UV absorption. Derivatizations for improved separation and detectability have been utilized. Derivatization with phenacyl bromide has been applied to the determination of hydroxy acids in wines using reversed-phase chromatography with UV detection [4]. Rigas and Pietrzyk [5] described an indirect spectrometric chromatographic method for the determination of lactic and α-hydroxybutyric acids, etc., using iron(II)–phenanthroline as a detection reagent. In our laboratory, the reversed-phase chromatographic separation and indirect UV spectrophotometric detection of hydroxy acids were studied using various detection reagents [6].

Levin and Grushka [7] reported a new approach to the determination of amino acids on a reversed-phase column using an aqueous mobile phase containing copper ion. In this approach, the detection of amino acids was accomplished by the *in situ* formation of their complexes. The determination of citric acid in milk using UV spectrophotometry with the formation of a complex with copper ion has been reported [8]. None of studies has investigated in detail the use of copper ion in high-performance liquid chromatography for the separation and determination of hydroxy acids.

This paper describes a method that allows the determination of hydroxy acids as their Cu(II) com-

Correspondence to: Dr. D. S. Lu, Department of Chemistry, Wuhan University, Wuhan 430072, China.

0021-9673/92/$05.00

plexes on a conventional reversed-phase column in conjunction with a UV detector. In order to ascertain the possibility of applying UV detection, the UV absorption spectra of hydroxy acid–Cu(II) mixtures in aqueous solution were determined. A reversed-phase chromatographic system for the separation and determination of hydroxy acids with an aqueous mobile phase containing copper ion and alkylsulphonate was investigated. An hydrophobic alkylsulphonate was added to the mobile phase as an ion-pair reagent and spectrophotometric sensitizing agent in order to increase the retention and detection response. Acetate buffer was used to maintain a suitable pH and ionic strength. The effects of various factors on retention and detection response were studied, especially pH and the concentrations of copper ion, alkylsulphonate and buffer. Guidelines are given for optimization of the separation and detection. The calibration graphs of peak area *versus* sample amount, detection sensitivity and minimum detectable amounts were also studied.

EXPERIMENTAL

Apparatus

A Model UV-240 spectrophotometer (Shimadzu) was used. The chromatographic system consisted of a Model LC-6A pump (Shimadzu), a Model 7125 injector with a 20-μl loop (Rheodyne), a Model DZ-1 fixed-wavelength (254 nm) UV detector (Shanghai Scientific Instrument Factory), a Type 3056 recorder and a Model C-R2A digital integrator (Shimadzu). The column used was Zorbax-ODS (250 × 4 mm I.D.) (DuPont). A precolumn made in our laboratory, packed with 5-μm YWG.CH (Tianjing Second Chemical Reagent Factory), was connected between the pump and the injector. The pH measurements were performed with a pH-3E digital pH meter (Jiansu Electroanalysis Instrument Plant). A Model CQ-50 ultrasonic cleaner (Shanghai Ultrasonic Instrument Plant) was used.

Reagents and solvents

Analytical-reagent grade or equivalent chemicals and water doubly distilled in a quartz still were used. Acetate buffer was prepared with acetic acid and sodium hydroxide. Copper(II) acetate was obtained from Shanghai Chemical Reagent Factory and sodium hexanesulphonate from Beijing Chemical Reagent Institute.

Samples

The following hydroxy acids (HA) were chosen as sample solutes: lactic (LA), citric (CA), tartaric (TA), malic (MA) and α-hydroxyisobutyric acid (HBA). Stock standard solutions of the samples (0.1–0.01 *M*) were prepared and diluted as needed.

Procedures

The solutions of the HA–Cu(II) complexes for determination of UV absorption spectra were made with appropriate volumes of stock of samples, copper(II) acetate and buffer, then diluted to 25 ml with water. The UV absorption spectra of the solutions were determined in the range 330–190 nm. The absorbances at 254 (A_{254}) and 230 nm (A_{230}) were recorded.

The mobile phases were prepared by dissolving known amounts of hexanesulphonate and copper (II) acetate in the acetate buffer, adjusted to the desired pH, then filtered and degassed in an ultrasonic bath before use. The flow-rate of the mobile phase was set at 1 ml/min. The eluent was passed through the column for about 1 h until equilibrium was observed by recording the breakthrough curve due to the background absorption by copper ions. To protect the instrument, prolong the lifetime of the column and obtained reproducible results for the retention and detection sensitivity, at the end of each working day the chromatographic system was flushed with 0.01 *M* EDTA in the buffer solution (pH 5.6), water and methanol in that order.

RESULTS AND DISCUSSION

UV absorption spectra of hydroxy acid–Cu(II) complexes in acetate buffer solution

In the reversed-phase chromatographic system with a UV detector using buffer solution without copper ion as the mobile phase, no detection response of the HAs was observed. Copper ion is known to form complexes with HAs, which have similar stability constants to amino acid–copper ion complexes [9]. Fig. 1 shows the UV absorption spectra of the HA–copper ion mixture in acetate buffer solution. For comparison the absorption curves of LA, MA and copper(II) acetate are also given. No

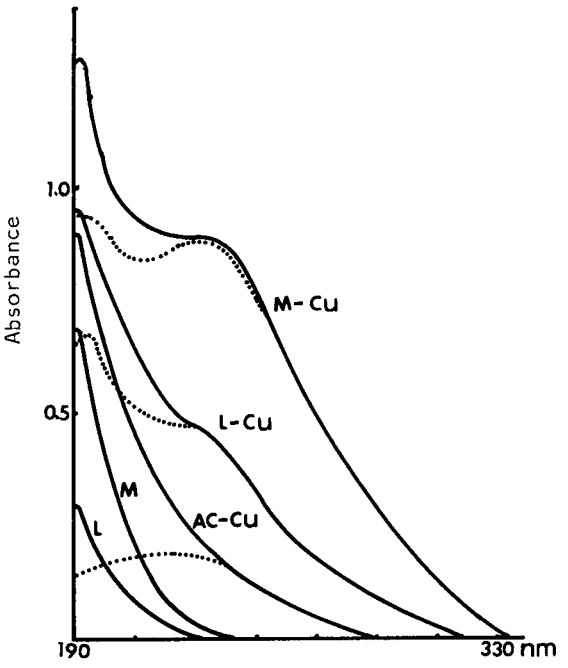

Fig. 1. UV absorption spectra of HA–Cu(II) mixture in solution of acetate buffer (5 m*M*, pH 5.6). L, M and AC refer to LA, MA and acetate, respectively; Cu refers to copper ion. Water was used as a reference for solid lines and acetate buffer (5 m*M*) for dotted lines.

appreciable absorption is observed above 210 nm for the HAs. In the presence of copper ion the absorption of the HA solutions is much stronger in the range 190–330 nm because of the formation of HA–Cu(II) complexes. For the spectra of the complexes, shoulder peaks between 230 and 240 nm are observed and the absorbances at 254 nm are also very high.

Table I lists the absorbances at 230 and 254 nm for the mixture solutions. The absorbances of the complexes of the HAs having multiple hydroxy or carboxy groups, such as MA, CA and TA, are higher than those of the monobasic HAs, possibly because the former have a stronger complexing capacity than the latter for copper ion.

Factors that affect the retention and detection response

The HAs with strong polarity and weak hydrophobicity show hardly retention on conventional reversed-phase columns and the separation selectivity based on solvophobic interaction is very poor. It is believed that the formation of HA–Cu(II) complexes will occur in the chromatographic system. According to evaluation of the dilution factors arising from the column, which can be expressed as a function of the column efficiency, the injection volumes and the retention volumes of the solutes [10], it is found that the concentrations of HAs in the mobile phase are slightly lower than that of copper ion, assuming that all the complexes have 1:1 composition and are positively charged, making it possible to form ion pairs of ternary complexes with hexanesulphonate. Probably the reactions can be written as

$$HA + Cu^{2+} \rightleftharpoons [ACu]^{+} + H^{+} \quad (1)$$

$$[ACu]^{+} + R^{-} \rightleftharpoons ACuR \quad (2)$$

where R^{-} represents the anion of hexanesulphonate. Interaction of species should enhance the retention via a dynamic ion-exchange, ion-pair partition or ion-interaction mechanism. In order to compare the sensitivities under different conditions the response value, *R*, of detection is represented by the area of the peak produced per unit concentration of the solute injected, in units of $m^2/mmol$.

Influence of Cu(II) concentration

The retention and detection response of the HAs as a function of copper ion content in the mobile

TABLE I

ABSORBANCES OF HA–Cu(II) MIXTURE IN BUFFER SOLUTION

In each case the solution contained 5 m*M* acetate buffer, 0,4 m*M* HA and 0.4 m*M* copper ion (pH 5.6).

Absorbance	LA	LA–Cu	HBA	HBA–Cu	MA	MA–Cu	CA	CA–Cu	TA	TA–Cu
A_{320}	0	0.357	0.005	0.408	0.011	1.004	0.008	1.120	0.008	0.894
A_{254}	0	0.162	0.004	0.200	0.002	0.760	0.005	0.936	0.006	0.600

phase are illustrated in Fig. 2. It can be seen that the capacity factors, k', for TA and MA show a maximum values with increase in copper ion concentration, whereas there is a gradual increase for LA and HBA a smaller increase for CA, with three carboxy groups, whose hydrophobicity is less changed by complex formation. When the Cu(II) concentration reaches a certain level (about 0.5 mM), no further marked increase or even a decrease in k' is observed, which can been explained by the lack of a further increase in the concentration of the complexes, and by the increase in the eluting power of the mobile phases as further increase in the concentration of copper ion, which is a participant in the dynamic ion-exchange process.

Fig. 2 demonstrates that the concentration of Cu (II) has a much greater effect on the detection response of polybasic acids than on that of monobasic HAs, owing to the great differences between the absorption values of the two kinds of complexes. In the range of Cu(II) concentration from 0.05 to 1 mM the detection response for polybasic HAs first increases sharply to a maximum and then tends to decrease, whereas for monobasic HAs it first increases slowly between 0.05 and 0.5 mM and then decreases slightly with further increase in the concentration of copper ion.

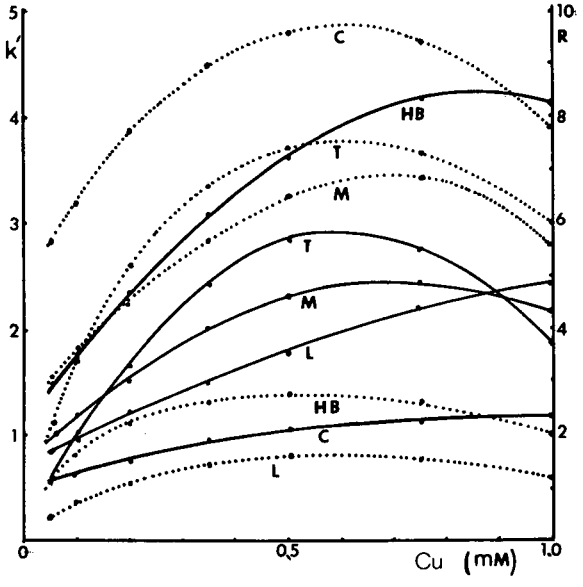

Fig. 2. Effect of copper ion concentration on the retention and detection response of HAs. The mobile phase contained 2 mM acetate buffer (pH 5.6) and 5 mM hexanesulphonate; temperature, 30°C; flow-rate, 1.0 ml/min; UV detection at 254 nm. L, HB, C, M and T refer to LA, HBA, CA, MA and TA, respectively. Solid lines, variation of retention; dotted lines, variation of detection response.

Influence of hexanesulphonate concentration

Fig. 3 illustrates the relationship between the retention, response of the solutes and hexanesulphonate concentration. It is obvious that the addition of hexanesulphonate has a considerable influence on the retention and detection response for the HAs, consequently modifying their separation selectivity. When hexanesulphonate is absent from the mobile phase the retention is lower and tends to be similar for all the HAs, owing to their weak hydrophobicity. The k' values first increase rapidly for all the HAs, and then remain relatively constant for LA and HBA and tend to decrease for CA, MA and TA with increase in hexanesulphonate concentration from 0 to 10 mM. The decrease in the retention of polybasic hydroxy acids with further increase in the concentration of hexanesulphonate may be due to electrostatic repulsion between the anion of hexanesulphonate adsorbed on the stationary phasae and negatively charged solutes with multiple carboxy groups. The results show that the

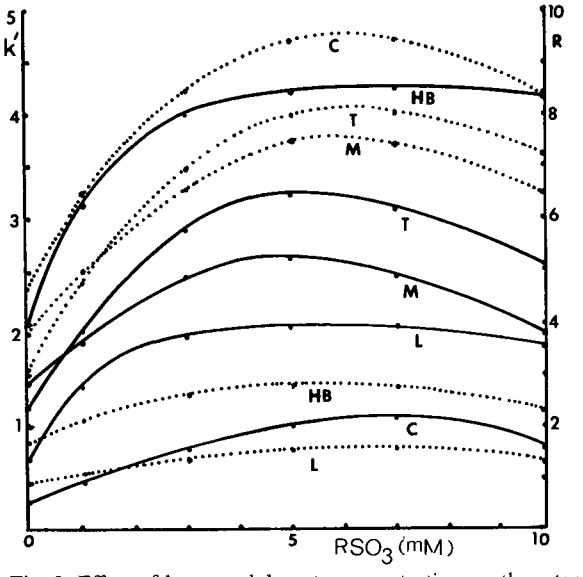

Fig. 3. Effect of hexanesulphonate concentration on the retention and detection response of HAs. Chromatographic conditions as in Fig. 2 except 0.5 mM Cu(II). Lines as in Fig. 2.

retention of HAs at lower concentrations of hexanesulphonate can be regulated by the controlled addition of the latter.

Fig. 3 shows that the R values of polybasic HAs increase sharply as the concentration of hexanesulphonate increases from 0 to 5 mM, and then decrease with further increase in from 5 to 10 mM. No significant effect of hexanesulphonate on the R values of monobasic HAs is observed, as could be expected owing to their lower capacity to form ternary complexes and their smaller absorbances.

Influence of buffer concentration

The concentration of acetate buffer has an important effect on the retention and detection response under conditions of constant pH and copper ion concentration, as shown in Fig. 4. The retention of polybasic HAs increases initially as the acetate buffer concentration increases from 1 to 4 mM, and then decreases slowly with further increase in concentration. For monobasic HAs the retention always decreases with increase in acetate concentration from 1 to 50 mM. The increase in the retention may be explained by the simultaneous formation of mixed complexes with acetate radical ion as a secondary ligand or solvation of HA–Cu(II) complexes by acetate buffer, therefore leading to the increase in the hydrophobicity of the solutes. Presumably, the decrease in k' is produced by an increase in the solvent strength, which is a function of acetate content in the mobile phase, and by a decrease in the tendency of the solutes to interact by ion exchange with residual Si–OH groups on the surface of the packing [11]. Experiments have shown that phosphate buffer is unusable when copper ion is present in the mobile phase. The check valves of the reciprocating pump often became blocked by copper ion when phosphate buffer was used because of precipitation of copper ion by the anion of the phosphate buffer.

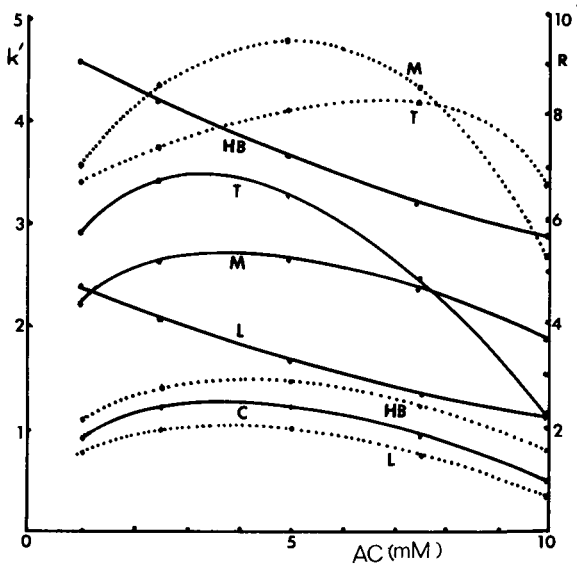

Fig. 4. Effect of acetate buffer concentration on retention and detection response of HAs. Chromatographic conditions as in Fig. 2 except 0.5 mM Cu(II) and buffer concentration at pH 5.6. Lines as in Fig. 2.

Comparing the variations in R values in Figs. 3 and 4, it can be seen that acetate has a similar effect to hexanesulphonate on the detection response. The increase and decrease in response can probably be explained by the solvation of the complexes and the background absorptyion of copper(II) acetate. Fig. 4 shows that the optimum buffer concentration for the detection of the HAs is between 2 and 8 mM. It is unnecessary to use concentrations above 10 mM with regard to either the separation selectivity or the detection response. An important factor is that when the acetate concentration is above 10 mM, the system peak produced by acetate is so large that it will interfere seriously in the determination of the sample peaks. It was found that the system peak due to acetate almost disappears if the acetate concentration is below 5 mM. In addition, the column lifetime will decrease as the buffer concentration increases.

Influence of pH

It is possible to change the complexation equilibria by varying the pH and therefore to influence the hydrophobicity and UV absorbance of the solutes. The changes in k' and R values of the HAs with variation of pH in the mobile phase containing copper ion and hexanesulphonate are demonstrated in Fig. 5. The retention of polybasic HAs increases slowly in the pH range 3.5–5 and increase sharply at pH $>$ 5. It is obvious that the formation of the complexes as the dissociation of the HAs increases enhances the hydrophobicity of the solutes. The decrease in k' values of monobasic HAs with increase in pH may be caused by a lower hydrophobicity of

the complexes than that of the molecular HAs at lower pH, and by increasing the eluting power of the mobile phase with increase in concentration of OH^- ions.

Fig. 5 shows that the response values of all the hydroxy acids are relatively low at pH < 5, owing to a lower capability of copper ion complexing with the molecular HAs and a shift of eqn. 1 to the right with increasing pH, leading to an increase in the response. The drastic increase in the response at pH > 5 results from the formation of complexes which have high UV absorbances. The background absorption produced by copper ion in the presence of acetate, hexanesulphonate and an excess of OH^- ion with further increase in pH causes the *R* values to decrease.

On the basis of the above investigation, the HAs were chromatographed with UV detection at 254 nm using an aqueous mobile phase containing Cu (II), hexanesulphonate and acetate buffer. In this way chromatograms with high resolution and good peak symmetry for the HAs studied were obtained. Typical chromatograms obtained with different mobile compositions are given in Figs. 6 and 7. The HAs are eluted in different orders depending on the chromatographic conditions. The system peaks S_1, S_2 and S_3 are due to copper ion, acetate and hexanesulphonate respectively. Peak S_1 is negative in all the chromatograms. Peak S_2 disappears gradually with decreasing concentration of acetate buffer. Peak S_3 is positive or negative depending on the concentration of hexanesulphonate. At pH < 4.5 peak S_3 is not eluted within 30 min.

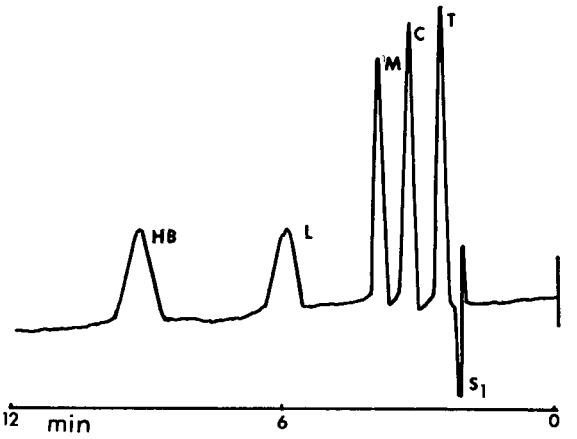

Fig. 6. Chromatogram of a mixture of HAs. Mobile phase, 0.5 m*M* Cu(II)–5 m*M* hexanesulphonate–2 m*M* acetate buffer (pH 4.2), flow-rate 1 ml/min; detection, UV at 254 nm, 0.08 a.u.f.s.; temperature, 30°C; concentration of samples, 0.1–1 m*M*. Peaks: S_1 = system peak; C = CA; T = TA; M = MA; L = LA; HB = HBA.

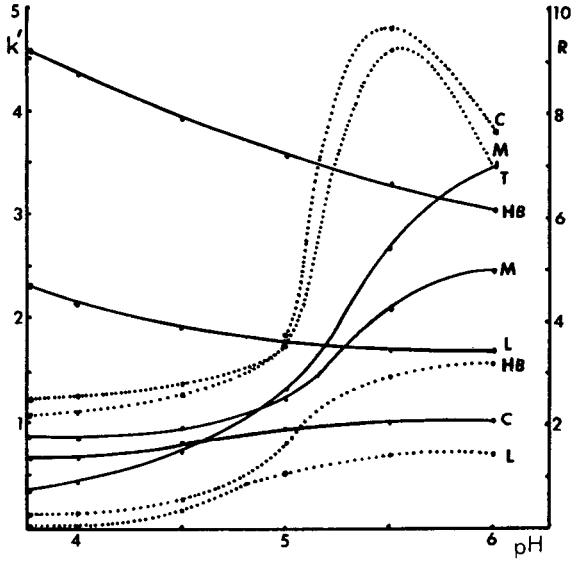

Fig. 5. Effect of pH on the retention and detection response of HAs. Conditions as in Fig. 2 except 0.5 m*M* Cu(II) and pH 5.6. Lines as in Fig. 2.

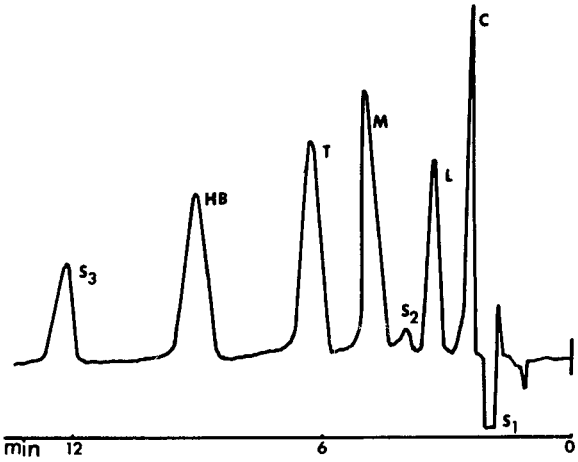

Fig. 7. Chromatogram of a mixture of the HAs. Mobile phase, 0.5 m*M* Cu(II)–5 m*M* hexanesulphonate–5 m*M* acetate buffer (pH 5.6); detection, UV at 254 nm, 0.16 a.u.f.s.; concentration of HAs, 0.1–0.5 m*M*. Peaks: S_1, S_2, S_3 = system peaks. Other conditions and peaks as in Fig. 6.

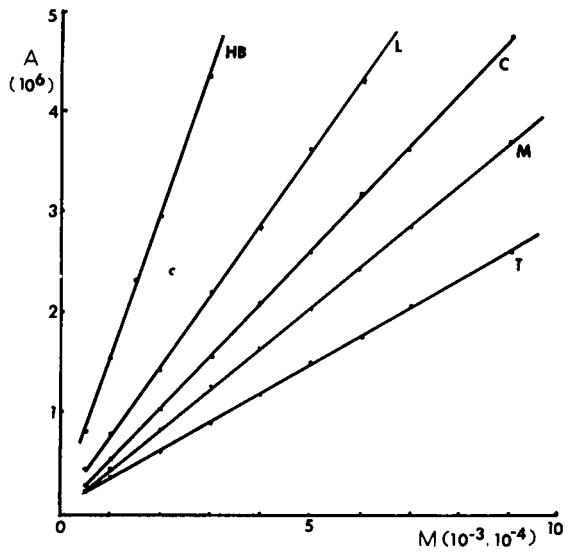

Fig. 8. Calibration graphs of integral peak area values (A) *versus* HA concentrations injected. Concentration coordinate is $\times 10^{-3}$ M for HBA and LA and $\times 10^{-4}$ M for CA, MA and TA. Chromatographic conditions as in Fig. 7.

Determination of hydroxy acids

If the mobile phase conditions are optimized and held constant, determination of the HAs is possible with Cu(II)-aided UV detection. Calibration graphs were obtained for HAs in the range of sample amounts from 10^{-6} to 10^{-4} mmol under the same conditions as in Fig. 7. No attempt was made to determine linearity above 10^{-4} mmol. Typical calibration graphs of integral peak areas *versus* the sample concentration injected are shown in Fig. 8. Owing to the background absorbance of the mobile phase and the background noise of the instrument, the calibration graphs do not pass through the origin. The graphs can be fitted to a linear regression equation:

$$A_i = a + bm_i \quad (3)$$

where A is the integral peak area value, a is the intercept, b is the slope and m is solute amount. The slopes should be related to the detection sensitivity of the HAs, which may be defined as the change in response intensity per unit change in solute amount, that is

$$S = \Delta R/\Delta m_i \quad (4)$$

With a UV detector for concentration-sensitive detection, the sensitivity is given in units of absorbance × ml/mM and can be calculated from the absorbance corresponding to full-scale deflection of the recorder at maximum detector sensitivity. Table II gives the intercepts a, slopes b, correlation coefficients r and detection sensitivity S for the HAs. The correlation coefficients are over 0.99 for all the samples, showing good linearity of the calibrations.

Minimum detectable amount

The minimum detectable amount is defined as the amount of solute that produces a response of the chromatographic peak height equal to three times the noise level. The minimum detectable amounts of the HAs under the chromatographic conditions used were calculated and are given in Table II. Most of them are below 1 nmol and hence trace analyses for the HAs are practicable.

TABLE II

DATA FOR DETERMINATION, SENSITIVITY AND MINIMUM DETECTABLE AMOUNT

HA	Intercept, a[a]	Slope, b[a]	Correlation coefficient, r	Sensitivity, S (absorbance ml/mM)	Q_{min}[b] (mol)
LA	30	$3.6 \cdot 10^6$	0.9972	464	$4.2 \cdot 10^{-10}$
BHA	15	$7.3 \cdot 10^6$	0.9989	928	$2.5 \cdot 10^{-10}$
CA	30	$2.8 \cdot 10^7$	0.9993	3520	$7.9 \cdot 10^{-11}$
MA	20	$2.1 \cdot 10^7$	0.9981	2720	$6.3 \cdot 10^{-11}$
TA	17	$1.3 \cdot 10^7$	0.9967	2240	$3.5 \cdot 10^{-10}$

[a] Integral values.
[b] Minimum detectable amount.

CONCLUSIONS

The proposed method allows the separation and determination of multi-functional HAs by reversed-phase chromatography with the aid of copper ion in the mobile phase containing acetate buffer and hexanesulphonate. The dynamic ion exchange and ion-pair partition of HA–Cu(II) complexes formed in the chromatographic process can offer significant advantages over fixed-site ion exchangers of a bonded phase for the separation of ion interaction and hydrophobicity and also for detection sensitivity of the HAs. Detection is performed at 254 nm, avoiding interferences that occur at lower wavelengths. The analysis is simple and rapid. Also, the sensitivity, accuracy and precision appear to be comparable to those in alternative methods.

REFERENCES

1 Z.-C. Xu and X. Yin, *Chin. J. Chromatogr.*, 4 (1986) 321.
2 Wuxi Institute of Light Industry, *Analysis of Food*, Light Industry Publishing House, Beijing, 1987, p. 100.
3 S. Rokushika, Z. L. Sun and H. Hatano, *J. Chromatogr.*, 253 (1982) 87.
4 E. Mentasti, M. C. Gennaro, C. Sarzanini, C. Baiocchi and M. Savigliano, *J. Chromatogr.*, 322 (1985) 177.
5 P. G. Rigas and K. Pietrzyk, *Anal. Chem.*, 59 (1987) 1388.
6 S.-L. Da and Z.-H. Wang, *Chem. J. Chin. Univ.*, 11 (1990) 1081.
7 S. Levin and E. Grushka, *J. Chromatogr.*, 384 (1987) 249.
8 A. Pierre and G. Brule, *Lait*, 63, Nos. 623–624; *C.A.*, 99 (1983) 51931.
9 S. Kotrly and L. Sucha, *Handbook of Chemical Equilibria in Analytical Chemistry*, Ellis Horwood, Chichester, 1985, p. 157–162.
10 R. Rosset, M. Caude and A. Jardy, *Manual Pratique de Chromatographie en Phase Liquide*, Masson, Paris, 2nd ed., 1982, p. 82.
11 L. R. Snyder and J. J. Kirkland, *Introduction to Modern Liquid Chromatography*, Wiley-Interscience, New York, 2nd ed., 1979, p. 295.

Journal of Chromatography, 623 (1992) 63–67
Elsevier Science Publishers B.V., Amsterdam

CHROM. 24 412

Determination of diaminopimelic acid in biological materials using high-performance liquid chromatography

R. Puchała, Hanna Pióor and G. W. Kulasek

Department of Animal Physiology, Warsaw Agricultural University, Nowoursynowska 166, 02-766 Warsaw (Poland)

J. A. Shelford

Department of Animal Science, University of British Columbia, Vancouver (Canada)

(First received March 3rd, 1992; revised manuscript received June 2nd, 1992)

ABSTRACT

A method for the determination of diaminopimelic acid (DAPA) concentrations in feeds and rumen digesta by reversed-phase high-performance liquid chromatography using precolumn derivatization with *o*-phthaldialdehyde and fluorimetric detection was developed. Samples were oxidized and hydrolysed prior to analyses by HPLC. Hydrogen peroxide and formic acid were used for oxidation; hydrolyses were performed using 3 *M* hydrochloric acid under vacuum at 120°C for 17 h. Oxidation allowed more space for DAPA–OPA peak elution and hydrochloric acid hydrolysis reduced sample clean-up and extended the column life. Hydrolysates were diluted, adjusted to pH 7 and filtered. A Beckman Model 507 autosampler with a precolumn derivatization cassette was used for the derivatization process and fluorimetric detection was used to measure the OPA derivatives. Samples were prepared in order to have on-column DAPA concentrations in the range 10–100 pmol. The relative recovery of the standard solutions added to the feed samples ranged from 98.4 to 102.8%. The reproducibility of the method was evaluated by the analysis of eight alfalfa hay samples and eight alfalfa hay samples incubated in the rumen for 48 h and they yielded relative standard deviations of 2.04% and 2.02%, respectively.

INTRODUCTION

Diaminopimelic acid (DAPA) is a component of bacterial cell walls. It has been established that in bacteria the DAPA/protein ratio is relatively constant [1]. Therefore, DAPA has been used as a indirect marker for the measurement of bacterial contamination in biological materials, *e.g.*, silages and rumen contents [2,3]. The traditional method for determining DAPA in digesta or in feeds employed ion-exchange chromatography and ninhydrin [4,5]. This method requires an expensive amino acid analyzer and high levels of methionine in the sample can interfere with DAPA determination. Czerkawski [1] proposed a method that is less costly, but it is labour intensive and interference from proline may occur. The method proposed by Webster *et al.* [6] using high-performance liquid chromatography (HPLC) requires costly purification of samples and the individual sample running time is similar to that in the normal amino acid analyzer method.

The objective of this study was to develop a rapid, inexpensive, sensitive and reliable HPLC method for determination of the DAPA content in biological samples with utilization of oxidation, hydrolysis, precolumn *o*-phthaldealdehyde (OPA) derivatization and fluorimetric detection.

EXPERIMENTAL

Reagents and standards

HPLC-grade methanol, 2-mercaptoethanol and

Correspondence to: Dr. R. Puchała, Department of Animal Physiology, Warsaw Agricultural University, Nowoursynowska 166, 02-766 Warsaw, Poland.

0021-9673/92/$05.00

tetrahydrofuran were purchased from Merck (Darmstadt, Germany), sodium acetate from BDH (Poole, UK) and DL-α,ε-diaminopimelic acid, OPA and ethanolamine from Sigma (St. Louis, MO, USA). All other chemicals were purchased from POCH (Gliwice, Poland).

HPLC configuration

A System Gold (Beckman, San Ramon, CA) HPLC system was employed. The apparatus consisted of a Model 126 gradient solvent-delivery module, a Model 507 autosampler with precolumn derivatization cassette, a Waters (Milford, MA, USA) Model 420-AC fluorescence detector (excitation filter, 338 nm interference; emission filter, 425 nm long pass), a Model 166 UV detector and a Model 406 analogue interface. Analytical method development, data collection and data integration were performed by using Beckman Gold Chromatograph software on a PC-AT computer. Data from the fluorescence and UV detectors were collected simultaneously. The column used was a Eurospher 80 C_{18}, 5 μm (250 × 4.6 mm I.D.) (Knauer, Berlin, Germany) in conjunction with a Eurospher 80 C_{18} precolumn (Knauer).

Analytical solvents and gradient composition

A binary gradient was used. Solvent A was tetrahydrofuran–methanol–buffer (5:95:900) and solvent B was methanol. The buffer in solvent A was prepared from 0.1 *M* sodium acetate adjusted to pH 7.0 with phosphoric acid. All components of solvent A were mixed and the pH was adjusted to 7.0. Solvents were filtered (0.45 μm) and flushed with helium prior to use. The gradient composition is shown in Table I.

Preparation of standard and derivatizing solutions

DL-α,ε-Diaminopimelic acid stock standard solution was prepared at a concentration of 2.63 m*M* (0.5 mg ml^{-1}) in 0.1 *M* sodium acetate adjusted to pH 7.0 and stored at 4°C. The stock standard solution was further diluted with 0.1 *M* sodium acetate.

Ethanolamine was dissolved in 0.1 *M* sodium acetate so that the concentration was 1 μ*M* and the pH was adjusted to 7.0. This solution was used for final sample dilution.

The derivatizing solution was prepared by dissolving 50 mg of OPA crystals in 1.25 ml of methanol. To this solution 11.2 ml of 0.4 *M* borate buffer (pH 9.5) and 50 μl of 2-mercaptoethanol were added. The contents were mixed, transferred into a dark flask and flushed with nitrogen.

TABLE I

GRADIENT COMPOSITION

Time (min)	Flow-rate (ml min^{-1})	Composition (%)		Gradient duration (min)[a]
		A	B	
0.00	1.00	70	30	
1.00	1.00	54	46	16.00
17.00	1.00	0	100	5.00
24.00	1.00	70	30	1.00
28.00[b]	1.00	70	30	

[a] Isocratic pumping if cell is empty.
[b] Sample injection.

Sample preparation

Feeds and rumen incubated feeds [7] were dried and finely ground prior to analysis. Samples corresponding to 2 mg of nitrogen were weighed into 50-ml round-bottom flasks and oxidized with 2 ml of oxidizing reagent (0.2 ml of 30% hydrogen peroxide + 1.8 ml of 98% formic acid). The oxidizing reagent was allowed to stand at 50°C for 3 min before being added to the sample. Oxidation proceeded at 50°C for 15 min and was terminated by adding 0.3 ml of 40% bromic acid before the oxidizing mixture was evaporated on a Büchi rotary evaporator. The oxidized samples were hydrolyzed in the same flasks with 5 ml of 3 *M* hydrochloric for 17 h at 120°C. Prior to hydrolysis the flasks were jointed with a glass adapter flow control (Kontes, Vineland, NJ, USA) and air was evacuated from the flasks with a vacuum pump. Following hydrolysis, the vacuum was released from the flasks. Hydrolysates were transferred into 50-ml beakers and adjusted to pH 7 with 10 *M* NaOH and made up to 50 ml. The hydrolysates were stored at −27°C until analysis. A 1-mol volume of the hydrolysate was mixed with 4 ml of 0.1 *M* sodium acetate, adjusted to pH 7.0 and filtered though a 0.22-μm filter into the autosampler vial.

Sample derivatization

Derivatization of DAPA and other amino acids was performed with the Beckman Model 507 auto-

sampler using a precolumn derivatization cassette. A 50-μ volume of sample from the vial was mixed with 50 μl of derivatizing solution and after reaction for 2 min it was injected into the analytical column.

RESULTS AND DISCUSSION

The use of hydrochloric acid for sample hydrolysis followed by pH adjustment resulted in a much longer column life in comparison with the same procedure using methanesulphonic acid. Comparison of these two hydrolyzing agents showed that column life was approximately tripled when using the former procedure.

In regular amino acid analysis, tyrosine is eluted prior to DAPA and methionine; consequently, methionine often overlaps with DAPA. This is particularly true with non-oxidized samples where the DAPA peaks are eluted very close to methionine and hence are difficult to integrate. In order to allow more elution space for the DAPA peaks and because the DAPA–OPA derivative peaks were very small, oxidation of the samples was performed. This caused the tyrosine peak to disappear and methionine to be converted into methionine sulphone, which is eluted much earlier. This allowed for better integration of the DAPA peaks in comparison with non-oxidized samples. It was found that oxidation did not change the DAPA content in oxidized samples; the mean recovery was 103.6 ± 2.8% in comparison with non-oxidized samples. In summary, the oxidation of the samples overcame the problems discussed above and also allowed the analysis time to be decreased to less than 30 min (Table I).

Webster *et al.* [6] proposed the use of a UV detector for the determination of DAPA. To determine DAPA–OPA derivatives using a UV detector, higher sample concentrations are required. This results in the loading of highly concentrated samples on to the column, which decreases its performance and lifetime. To avoid these problems, a special clean-up procedure is required, which increases the cost of analysis. In addition, high sample concentrations resulted in more time being required to elute the sample from the column and thus increased the analysis time. Even though the concentration of other amino acids was too high for their accurate determination with a fluorescence detector, it was still impossible to determine DAPA using the UV detector as was proposed by Webster *et al.* [6] (Fig. 1). The sensitivity of the fluorescence detector is approximately eight times higher than that of the UV detector set at 340 nm.

Samples were prepared such that the on-column amino acid concentration was about ten times higher than that for the regular hydrolysate used for amino acid analyses [8] and so that the DAPA concentration was in the 10–100-pmol range. In this range the response of the fluorescence detector was

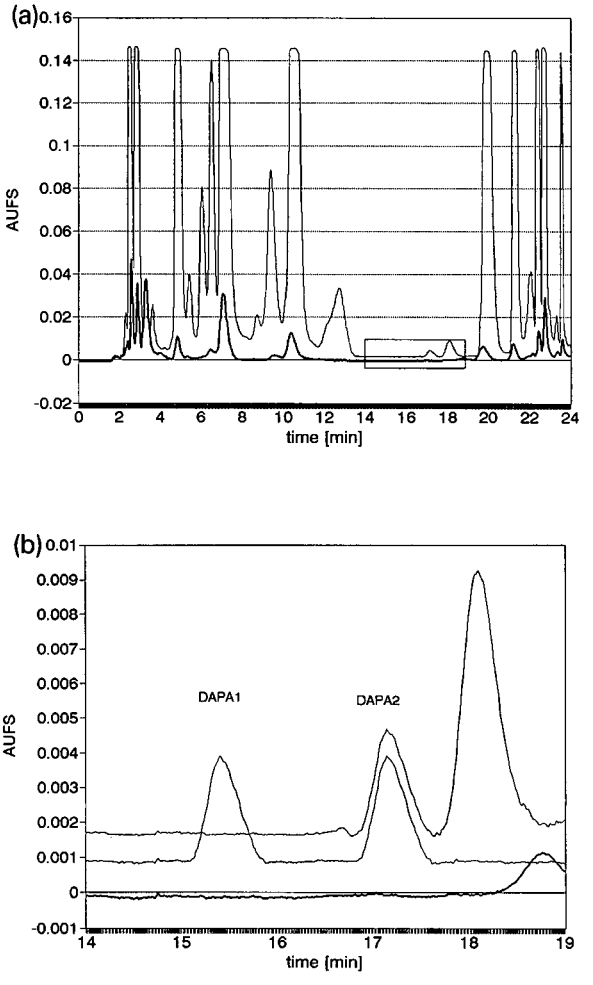

Fig. 1. Chromatogram of grass hay for DAPA determination showing data from two detectors. (a) Upper line, - fluorescence detection; lower line, UV detection (340 nm). (b) Expanded area from chromatogram (a) with added chromatogram of DAPA standard (20 pmol) with fluorescence detection (centre line).

linear with respect to the DAPA–OPA concentration.

As reported by Webster *et al.* [6], the DAPA standard was eluted in two peaks having very similar areas (Figs. 1 and 2). Zanol and Gastaldo [9], using a reversed-phase column and 1-fluoro-2,4-dinitrophenylalaninamide, reported that the same standard yielded three peaks. They identified them as D,L-, D,D- and L,L-DAPA. In this paper the peaks will be referred as DAPA1 and DAPA2 as there are no isolated stereoisomers available commercially. Both DAPA peaks were assumed to have equal fluorescence detector responses so the amount of each stereoisomer present in the standard were determined from its contribution to the peak area. The form DAPA2 occurred in forages such as grass hay or alfalfa hay, which according to Webster *et al.* [6] represented the D,L-stereoisomer. However, in grass silage and corn silage both peaks occurred. For the rumen incubated feeds, DAPA1 appeared on the chromatogram (Fig. 2) and the concentration of both DAPA peaks was increased with increasing time of incubation. Our observations show that bacteria colonizing the feed particles contain all DAPA isomers which is in agreement with the work of Zanol and Gastaldo [9].

The amounts of DAPA found in feed samples incubated in the rumen are shown in Table II. The concentration of DAPA increased despite the digestive processes which occurred during rumen incubation. During rumen fermentation ingested feedstuffs are digested and converted into microbial biomass. Adherence of these microorganisms to the feed particles causes an increase in DAPA concentration. It was found that the relationship between DAPA-N (μg g^{-1} DM) and time of incubation in the rumen of cows was best described by the exponential regression $y = 6.81 + 10.42\ [1 - \exp(-0.05t)]$, where t (h) is the time of incubation in the rumen. According to this equation, the onset of bacterial contamination of grass hay occurred largely within the first 12 h of rumen incubation. It is interesting that the same type of regression was used to describe the rate of disappearance of feedstuffs in the rumen [10].

TABLE II

CONTENT OF DIAMINOPIMELIC ACID IN GRASS HAY INCUBATED IN THE RUMEN OF COWS

Rumen incubation (h)	DAPA (nmol g^{-1} DM)[a]	DAPA-N (μg g^{-1} DM)[a]
0	243.2 ± 23.5	6.81 ± 0.65
2	274.2 ± 7.3	7.68 ± 0.20
4	299.2 ± 8.1	8.38 ± 0.23
8	395.2 ± 12.3	11.06 ± 0.35
12	408.5 ± 18.6	11.43 ± 0.52
24	474.1 ± 1.4	13.27 ± 0.04
48	615.4 ± 11.4	17.23 ± 0.32

[a] Mean ± standard error from five different grass hays used.

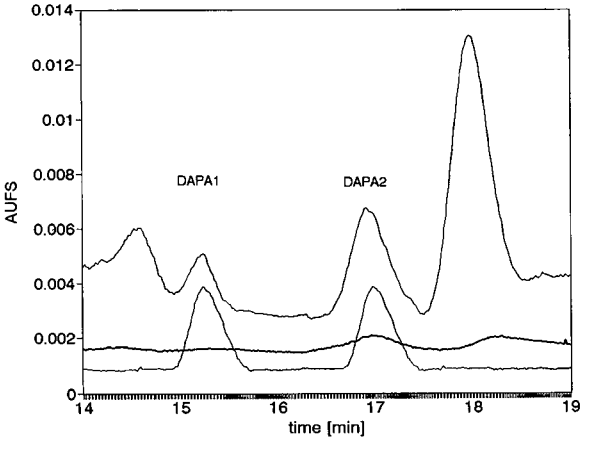

Fig. 2. Part of chromatogram with DAPA peaks of grass hay incubated in the rumen for 24 h. Upper line, fluorescence detection; centre line. UV detection (340 nm); lower line, fluorescence detection for DAPA standard.

Recovery of DAPA was performed by adding the DAPA standard to the feed samples and rumen incubated feed samples prior to oxidation and hydrolysis. The mean recovery of the standard solution added to the feed samples was 99.8 ± 1.4% and ranged from 98.4 to 102.8% for seven feeds. To check the accuracy of the autosampler, ethanolamine (internal standard) was added to the samples at the time of injection. It must be noted that this causes an increase in analysis time. The reproducibility of the method was evaluated by analyzing eight alfalfa hay samples (227.9 ± 4.67 nmol g^{-1} DM) and eight samples of alfalfa hay that had been incubated for 48 h in the rumen (940.14 ± 19.02 nmol g^{-1} DM), which yielded relative standard deviations of 2.04% and 2.02%, respectively.

REFERENCES

1 J. W. Czerkawski, *J. Sci. Food. Agric.*, 25 (1974) 45–55.
2 D. E. Beever, D. G. Harrison, D. J. Thomson, S. B. Cammell and D. F. Osbourn, *Br. J. Nutr.*, 32 (1974) 99–112.
3 J. R. Ling and P. J. Buttery, *Br. J. Nutr.*, 39 (1978) 165–179.
4 K. Hutton, F. J. Bailey and E. F. Annison, *Br. J. Nutr.*, 25 (1971) 165–173.
5 M. J. Ulyatt, J. C. Macrae, C. J. Clarke and P. D. Pearce, *J. Agric. Sci.*, 84 (1975) 453–458.
6 P. M. Webster, W. H. Hoover and T. K. Miller, *Anim. Feed Sci. Technol.*, 30 (1990) 11–20.
7 G. de Boer, J. J. Murphy and J. J. Kennelly, *Agric. For. Bull.*, 9 (1986) 18–21.
8 B. N. Jones and J. P. Gilligan, *J. Chromatogr.*, 266 (1983) 471–482.
9 M. Zanol and L. Gastaldo, *J. Chromatogr.*, 536 (1991) 211–216.
10 E.R. Ørskov and I. McDonald, *J. Agric. Sci.*, 92 (1979) 499–503.

Journal of Chromatography, 623 (1992) 69–74
Elsevier Science Publishers B.V., Amsterdam

CHROM. 24 406

High-performance liquid chromatography with electrochemical detection for the simultaneous determination of vitamin A, D_3 and E in milk

M. M. Delgado Zamarreño, A. Sánchez Perez, C. Gómez Pérez and J. Hernández Mendez

Departamento de Química Analítica, Nutrición y Bromatología, Facultad de Química, Universidad de Salamanca, 37008 Salamanca (Spain)

(First received February 3rd, 1992; revised manuscript received May 20th, 1992)

ABSTRACT

A high-performance liquid chromatographic electrochemical detection for the rapid and simultaneous determination of the vitamin A, D_3 and E is described. The separation is carried out by using a C_{18} reversed-phase column and 0.1 *M* $LiClO_4$ in methanol–water (99:1, v/v) as the mobile phase. The compounds are eluted with good resolution in the above order within about 15 min and are determined by amperometric detection with a glassy carbon electrode at +1050 mV (*vs.* Ag/AgCl). The method gave reproducible results and the detection limits were of the order of 0.07, 4 and 0.2 ng of vitamin A, D_3 and E, respectively. The method was successfully applied to the determination of vitamin A, D_3 and E in liquid cow milk and milk powder samples. After saponification, fat-soluble vitamins were extracted with hexane and a methanolic solution of the dried extract was injected directly into the chromatographic system, avoiding the clean-up step that is necessary for vitamin D_3 when electrochemical detection is not used. Good recoveries were obtained.

INTRODUCTION

In recent years, much research has been devoted to developing sensitive, selective, rapid and reliable methods for the determination of fat-soluble vitamins in foods [1] because a deficiency of these vitamins causes serious nutritional diseases. The absence from the diet of significant levels of vitamin A, D_3 and E leads to certain eye diseases, rickets and fertility disorders, respectively. The determination of vitamin A, D_3 and E in milk is of major importance as dairy foods play a vital role in nutrition and these vitamins have additional roles such as in protecting against cancer, avoiding dental caries and osteomalacia and avoiding neuropathological and neuromuscular disorders, respectively.

In addition to the determination of naturally occurring vitamin A, D_3 and E in milk and milk-based foods, there is also a need for the determination of these substances in processed low-fat and skimmed milk products and dairy foods fortified with these fat-soluble vitamins. There are numerous reports relating to the determination of lipid-soluble vitamins in milk, although methods for the simultaneous determination of these three vitamins are lacking. In recent years there have been increasing reports on the determination of fat-soluble vitamins using high-performance liquid chromatography (HPLC) in the normal-phase [2–11] and reversed-phase [12–14] modes with UV or fluorimetric detection. HPLC with electrochemical detection (HPLC–

Correspondence to: Dr. M. M. Delgado Zamarreño, Departamento de Química Analítica, Nutrición y Bromatología, Facultad de Química, Universidad de Salamanca, 37008 Salamanca, Spain.

0021-9673/92/$05.00

ED) appears to be promising for fat-soluble vitamin determination. Electrochemical methods have been published for the determination of vitamin A, D_3 and E [15–22] in different samples, pharmaceuticals (A and D_3) and biological samples.

In this paper, a rapid method is proposed for the simultaneous determination of vitamin A, D_3 and E using reversed-phase HPLC and amperometric detection with a glassy carbon electrode. The method was applied to the determination of these vitamins in milk samples. In this procedure the clean-up step, after extraction of vitamins from the unsaponificable phase, which is usually used in the determination of vitamin D_3 in milk, butter and other samples, was avoided.

EXPERIMENTAL

Apparatus

The liquid chromatograph consisted of an SP 8800 ternary pump (Spectra-Physics, San Jose, CA, USA) equipped with a Rheodyne (Berkeley, CA, USA) valve with an injection loop of 10 μl. The detectors were a Spectra-Physics SP8450 UV detector and an EG & G PAR (Princeton, NJ, USA) Model 400 electrochemical detector. Peak areas were measured with an SP 4290 integrator (Spectra-Physics).

The chromatographic columns used were an RP-18 precolumn (15 × 3.2 mm I.D., 7-μm film thickness (Brownlee Labs., Santa Clara, CA, USA) and an OD-224 RP-18 column (220 × 4.6 mm I.D., 5-μm film thickness) (Brownlee Labs.).

A Büchi (Flawil, Switzerland) RE 121 rotavapor with a Büchi 461 water-bath was used.

Reagents

All-*trans*-retinol, vitamin A was obtained from Sigma Química (Madrid, Spain), cholecalciferol, vitamin D_3 from Fluka Química (Madrid, Spain), α-tocopherol, vitamin E from Aldrich Quimica (Madrid, Spain), $LiClO_4$ (analytical-reagent grade) from Panreac (Barcelona, Spain) and methanol (LC grade) from Carlo Erba (Milan, Italy). Water was purified in a ElgaStat water-purification system (Elga, High Wycombe, UK).

The mobile phase was a 0.1 *M* solution $LiClO_4$ as supporting electrolyte in methanol–water (99:1, v/v). Alcoholic potassium hydroxide solution was prepared by mixing 50 ml of ethanol and 15 ml of 60% KOH solution. The extractants used were hexane and hexane–chloroform–ethanol (6:3.5:0.5).

Samples were commercial powdered milk and commercial liquid cow milk.

Procedure

The mobile phase was degassed with helium and pumped at a flow-rate of 1.0 ml/min. Standards of vitamins or sample extracts dissolved in methanol were injected through a Rheodyne valve. The glassy carbon elctrode was pretreated daily by cathodic polarization (−600 mV for 10 min) followed by anodic polarization (+1200 mV for 30 min), both in

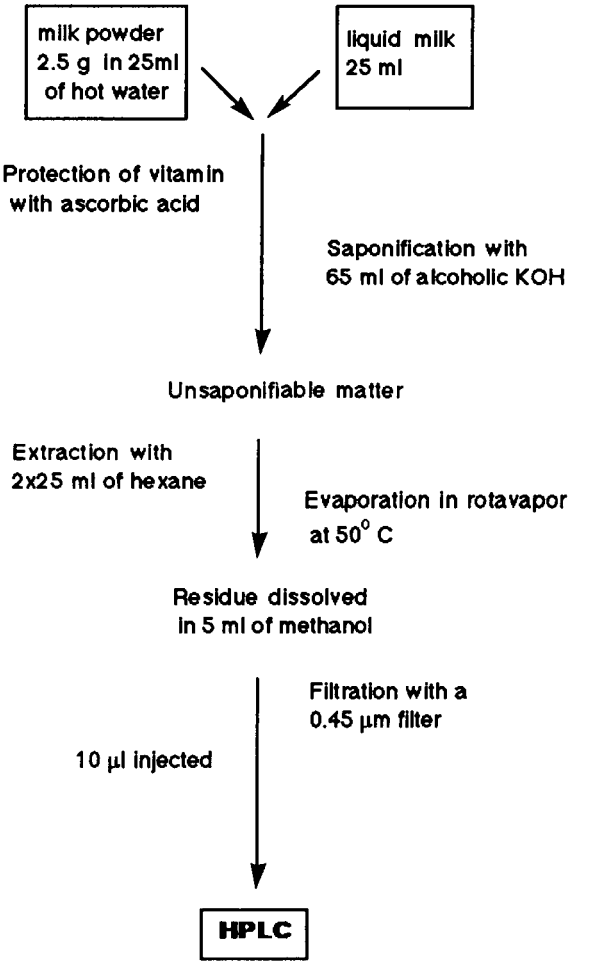

Fig. 1. Procedure for the determination of vitamin A, D_3 and E in powdered and liquid milk samples.

a flowing stream of mobile phase. The applied potential for detection was +1050 mV. For the simultaneous UV detection of three vitamins a compromise wavelength of 280 nm was chosen. The procedure for the determination of the vitamins in milk samples is detailed in Fig. 1.

RESULTS AND DISCUSSION

Optimization of the method

The influence of the applied potential, mobile phase composition, flow-rate and concentration of the supporting electrolyte was studied. In order to determine the optimum applied potential for the detection of the three vitamins, their hydrodynamic voltammograms were obtained by injecting fixed amounts of standard solutions of vitamins and varying the applied potential in 50-mV steps (Fig. 2). Higher voltages produce higher signals, especially with vitamin D_3, but also an increase in background signal. The working potential chosen was +1050 mV.

The amount of water in the mobile phase was varied from 0 to 6%. For all the water/methanol ratios tried good separations between the three vitamins were obtained, but at 3% water the retention times increased considerably (up to 22 min for vitamin E). Therefore, methanol–water (99:1, v/v) was chosen.

From the study of the effect of flow-rate a value of 1.0 ml/min was chosen. The chromatograms showed

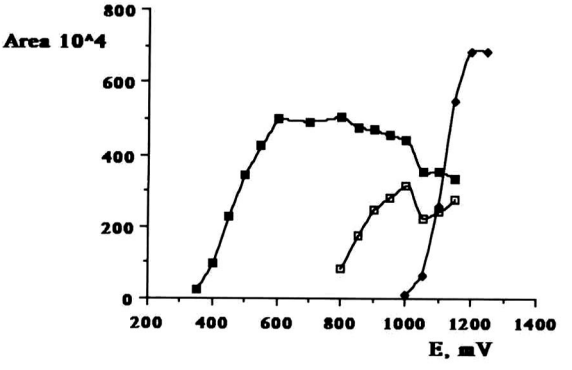

Fig. 2. Hydrodynamic voltammograms. Mobile phase, methanol–water (99:1, v/v) containing 0.1 *M* $LiClO_4$; flow-rate, 1.0 ml/min; Amounts injected, (□) vitamin A 2.5, (◆) vitamin D_3 19.3 and (■) vitamin E 10.8 ng.

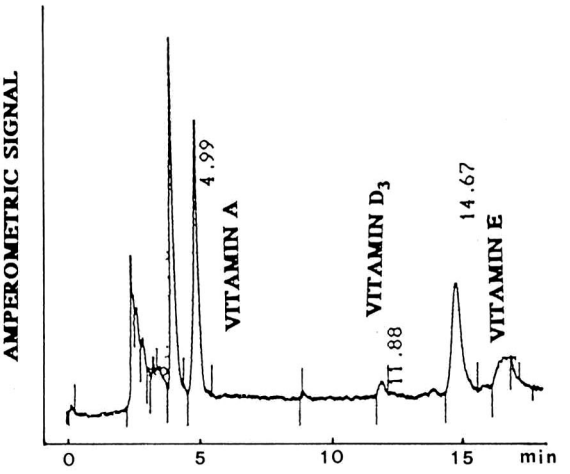

Fig. 3. Chromatogram obtained after application of the proposed method to a sample of liquid cow milk.

good resolution and acceptable retention times for the three vitamins (4, 12 and 14 min for A, D_3 and E, respectively) (Fig. 3).

The influence of $LiClO_4$ concentration in the mobile phase was studied in the range 0.02–0.18 *M*. The peak areas increased with increasing electrolyte concentration, reaching a constant value for concentrations >0.05 *M*. Hence an $LiClO_4$ concentration of 0.1 *M* was chosen for the proposed procedure.

Analytical characteristics of the HPLC–ED method

The relationships between chromatographic peak area and vitamin concentration injected were linear in the ranges $4.62 \cdot 10^{-8}$–$2.31 \cdot 10^{-6}$ *M* vitamin A, $2.06 \cdot 10^{-6}$–$3.24 \cdot 10^{-5}$ *M* vitamin D_3 and $4.48 \cdot 10^{-8}$–$1.55 \cdot 10^{-6}$ *M* vitamin E. The equations relating peak areas to concentration are shown in Table I.

The limits of detection (signal-to-noise ratio = 3) obtained were $3.7 \cdot 10^{-8}$, $1.1 \cdot 10^{-6}$ and $4.4 \cdot 10^{-8}$ *M* (0.07, 4.3 and 0.19 ng injected) for vitamin A, D_3 and E, respectively; relative standard deviations of 4.2, 3.1 and 5.7% were obtained when amounts of 0.66, 25 and 1.15 ng of vitamin A, D_3 and E were injected ($n = 10$).

Table II shows the calibration fittings for UV detection at 280 nm. The detection limits obtained were $6.48 \cdot 10^{-8}$, $2.1 \cdot 10^{-6}$ and $7.7 \cdot 10^{-7}$ *M* (0.12, 10

TABLE I

LINEARITY BETWEEN VITAMIN CONCENTRATIONS AND CHROMATOGRAPHIC PEAK AREAS USING THE HPLC–ED METHOD

Calibration fitting: $A = a + bx$.

Vitamin	Concentration range (M)	$a \cdot 10^{-3}$	$b \cdot 10^{-10}$	r ($n = 10$)
A	$(0.46–23) \cdot 10^{-7}$	150 ± 70	359 ± 7	0.998
D_3	$(2.1–32) \cdot 10^{-6}$	-80.4 ± 39	15.6 ± 0.2	0.999
E	$(0.45–16) \cdot 10^{-7}$	3.9 ± 0.1	446 ± 13	0.997

TABLE II

LINEARITY BETWEEN VITAMIN CONCENTRATIONS AND CHROMATOGRAPHIC PEAK AREAS USING THE HPLC–UV METHOD

Calibration fitting: $A = a + bx$.

Vitamin	Concentration range (M)	$a \cdot 10^{-3}$	$b \cdot 10^{-10}$	r
A	$(0.46–23) \cdot 10^{-7}$	0.73 ± 0.49	2.41 ± 0.05	0.997 ($n = 10$)
D_3	$(2.1–32) \cdot 10^{-6}$	-1.07 ± 2.0	1.61 ± 0.01	0.999 ($n = 7$)
E	$(8.9–18) \cdot 10^{-7}$	5.8 ± 1.4	1.20 ± 0.16	0.991 ($n = 5$)

and 3.3 ng injected) for vitamin A, D_3 and E, respectively, the relative standard deviation being 1% for the three vitamins. As shown by the detection limits and slope values, electrochemical detection provides higher sensitivity for the determination of these vitamins.

Analytical applications

The determination of fat-soluble vitamins usually includes saponification, extracction and clean-up of the samples before injection into the HPLC system. In order to avoid the saponification step, direct extraction of the vitamins from the milk powder,

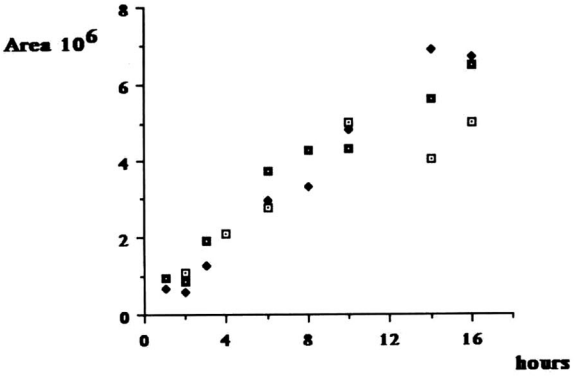

Fig. 4. Influence of extraction time in the extraction of vitamins from milk powder with hexane–chloroform–ethanol (6.0:3.4:0.5). □ = Vitamin A; ◆ = vitamin D_3; ■ = vitamin E.

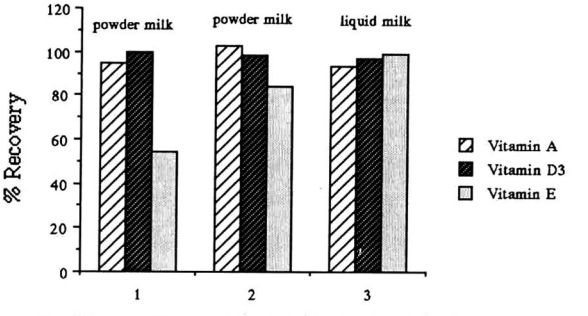

1: without hydrolysis, 2 and 3: with hydrolysis

Fig. 5. Recoveries of the proposed method for samples of milk (1) without and (2 and 3) with hydrolysis.

TABLE III

DETERMINATION OF VITAMIN A, D_3 AND E IN DIFFERENT MILK SAMPLES

Results from three replicate analyses.

Milk sample	Powdered milk					
	A (μg per 100 g)		D_3 (μg per 100 g)		E (mg per 100 g)	
	Found	Quoted by supplier	Found	Quoted by supplier	Found	Quoted by supplier
1	362 ± 0.5	450	10.3 ± 0.4	7.5	2.90 ± 0.1	2.7
2	441 ± 2	450	10.8 ± 3.6	10	2.65 ± 1.4	2.7
3	553 ± 3	450	3.9 ± 1.5	3	4.94 ± 1.3	4.4
	Liquid milk (found)					
	A (μg per 100 ml)		D_3 (ng per 100 ml)		E (μg per 100 ml)	
1	18.7 ± 0.4		296 ± 4		331 ± 1	
2	45.5 ± 0.4		388 ± 1		285 + 2	
3	36.5 ± 1.7		383 ± 3		185 ± 1	
4	35.3 ± 1.3		311 ± 1		67 ± 2	
5	66.1 ± 1.4		224 ± 2		50 ± 1	

using the procedures included in different reports [23], was tried. The samples (2.5 g of powder milk, three replicates) were extracted with 25 ml of hexane–chloroform–ethanol (6.0:3.5:0.5), with constant stirring in the dark. From the study of the extraction time a value of 10 hours is proposed (Fig. 4). After centrifugation, the organic phase was removed in a rotavapor at 50°C, the remaining residue being dissolved in 5 ml of methanol. After filtration an aliquot of this solution was injected into the chromatographic system. Data for the recoveries were obtained by spiking the samples of milk with standard solutions of vitamins in amounts of the same order as contained in the samples ($1 \cdot 10^{-6}$–$6 \cdot 10^{-6}$ *M*). Although good recoveries were obtained for vitamin A and D_3, they were not for vitamin E (Fig. 5); moreover, the amounts found in all the samples were lower than those specified by the manufacturer. Therefore, we conclude that milk powder samples must be saponified prior to the determination of vitamins.

The samples (2.5 g of powdered milk or 25 ml of liquid milk) were saponified with an alcoholic solution of potassium hydroxide. After extraction of the vitamins with hexane and evaporation of the solvent, the residue was dissolved in methanol and injected into the chromatograph after filtration (0.45-μm filter) without any clean-up step (Fig. 3). By applying this procedure the recoveries (Fig. 5) were in the ranges 84–103% (milk powder) and 93–99% (liquid cow milk). The amounts found for each vitamin in the different samples are summarized in Table III. The day-to-day precision was obtained by replicate analyses ($n = 5$) of standard solutions, the values found being 6.6, 5.21 and 6.68% for vitamin A, D_3 and E, respectively.

The vitamin contents obtained in the milk powder were compared with those stated by the manufacturer but it was not possible to do so for the liquid milk because this value is not available for the commercial products. In all instances good reproducibility in the analysis and acceptable relative standard deviations were found.

CONCLUSION

The proposed method allows the simultaneous determination of vitamin A, D_3 and E in milk,

avoiding the clean-up steps usually necessary in vitamin D_3 determination. No interferences were found with either detector (UV or electrochemical) and no washing step between samples is necessary. Moreover, the high sensitivity of the electrochemical detection allows the determination of vitamin D_3 in unenriched liquid milk, which is not possible using UV detection without a preconcentration step. Both the precision and the accuracy of the method make it suitable for routine milk (liquid and powder) analysis.

ACKNOWLEDGEMENT

Financial assistance from the CICYT (PB89-0397) is gratefully acknowledged.

REFERENCES

1 P. J. Van Niekerk, in R. Macrae (Editor) *HPLC in Food Analysis*, Academic Press, London, 2nd ed., 1988, pp. 133–184.
2 E. J. De Vries and B. Borsje, *J. Assoc. Off. Anal. Chem.*, 65 (1982) 1228–1233.
3 R. S. Mills, *J. Assoc. Off. Anal. Chem.*, 68 (1985) 56–58.
4 D. C. Sertl and B. E. Molitor, *J. Assoc. Off. Anal. Chem.*, 68 (1985) 177–182.
5 X. Li, L. Zhang and J. Zuo, *Yingyang Xuebabo*, 5 (1983) 103–111.
6 H. Johnsson and H. Hessel, *Int. J. Vitam. Nutr. Res.*, 57 (1987) 357–365.
7 S. F. O'Keefe and P. A. Murphy, *J. Chromatogr.*, 445 (1988) 305–309.
8 W. O. Landen, *J. Assoc. Off. Anal. Chem.*, 68, 183–187 (1985).
9 V. K. Agarwal, *J. Assoc. Off. Anal. Chem.*, 71 (1988) 19–22.
10 W. Knifel, F. Ulberth and U. Winkler-Macheiner, *Dtsch. Lebensm. Rundsch.*, 83 (1987) 137–139.
11 C. J. Lammi-Keefe, *J. Pediatr. Gastrenterol. Nutr.*, 5 (1986) 934–937.
12 S. L. Reynolds and H. J. Judd, *Analyst (London)*, 109 (1984) 489–492.
13 A. F. Wickroski and L. A. McLean, *J. Assoc. Off. Anal. Chem.*, 67 (1984) 62–65.
14 J. Ballester, E. Cortes, M. Moya and M. J. Campello, *Clin. Chem.*, 33 (1987) 796–799.
15 J. P. Hart, *Electroanalysis of Biologically Important Compounds*, Ellis Horwood, Chichester, 1990, pp. 137–187.
16 S. S. Atuma, J. Lindquist and K. Lundström, *Analyst (London)*, 99 (1974) 683–689.
17 S. A. Wring, J. P. Hart and D. W. Knight, *Analyst*, 113 (1988) 1785–9.
18 H. Iwahashi, Y. Negoro, A. Ikeda and R. Kido, *J. Chromatogr.*, 391 (1987) 199–205.
19 J. Hernandez Mendez, A. Sanchez Perez, M. Delgado Zamarreño and M. L. Hernandez Garcia, *J. Pharm. Biomed. Anal.*, 6 (1988) 737–741.
20 A. Sanchez Perez, M. Delgado Zamarreño, J. Hernandez Mendez and R. M. Sanchez Rodriguez, *Anal. Chim. Acta*, 225 (1989) 247–251.
21 O. Hiroshima, S. Ikenoya, M. Ohmae and K. Kawabe, *Chem. Pharm. Bull.*, 29 (1981) 451–455.
22 L. L. Darryl and M. B. Alan, *Talanta*, 38 (1991) 65–72.
23 R. R. Elton-Bott and C. I. Stacey, *Anal. Chim. Acta*, 127 (1981) 213–218.

Journal of Chromatography, 623 (1992) 75–82
Elsevier Science Publishers B.V., Amsterdam

CHROM. 24 279

Application of high-performance liquid chromatography in the kinetic study of α-methyldopa

Mohammed El-Sayed Metwally and Fathalla F. Belal

Department of Analytical Chemistry, Faculty of Pharmacy, Mansoura University, Mansoura 35516 (Egypt)

(First received November 13th, 1991; revised manuscript received April 10th, 1992)

ABSTRACT

A reversed-phase high-performance liquid chromatographic (HPLC) method was developed for use in kinetic studies of α-methylopa (MD). The proposed method was further applied to the determination of MD in sustained release capsules and in the presence of its industrial impurity, 3-O-methylmethyldopa (MMD). The detector response was linear in the range 0.5–200 μg/ml for MD and MMD. Replicate injections of both compounds gave relative standard deviations of 0.54 and 0.62%, respectively. The mean recoveries of MD from raw material and sustained release capsules were 99.71–100.2% and 99.5–100.1%, respectively. The proposed HPLC method was used to study the kinetics of degradation of MD in raw material and in sustained release capsules as a function of temperature, pH, humidity and exposure to UV radiation. MD degradation followed first-order kinetics and gave a linear relationship, in agreement with the Arrhenius theory, for all the incubation media studied. The activation energy for MD degradation was 93.36–105.92 kJ $l\ mol^{-1}$. The disappearance of MD followed pseudo-first-order kinetics in buffered distilled water over the experimental pH range 2–13. Above pH 7.96, a base-catalysed degradation dominates, with a second-order rate constant of 190.72 ± 14.5 $l\ mol^{-1}\ day^{-1}$. Below pH 7.96, degradation is independent of pH, with a disappearance rate constant of 6.65 (± 1.07) · $10^{-4}\ day^{-1}$ at 25°C. Degradation of MD raw material or ground MD beads was not enhanced by exposure to 80% humidity or to UV radiation for 21 days.

INTRODUCTION

L-α-Methyldopa, [L-3-(3,4-dihydroxyphenyl)-2-methylalanine] (MD) is a competitive inhibitor of DOPA-decarboxylase [1] and can also serve as a substrate for pigment formation in the melanocytes of hair follicles [2]. Owing to its phenolic nature, MD degrades easily under unfavourable storage conditions [3] and can undergo oxidation in alkaline media to a polymeric melanin-like pigment [4].

Only speculations have been made with respect to the study of MD degradation in raw material or in pharmaceutical preparations. In this respect, Lippold and Jaeger [5] used a conventional UV spectrophotometer to study MD degradation. They showed that the MD degradation rate increases with increasing supply of oxygen and increasing pH, but with decreasing starting concentration of the drug. In addition, they found that on changing the pH, MD degrades to different products with different absorption maxima.

Using the official USP method [6], Gupta and Gupta [3] claimed that although there was no difference in the stability of MD tablets after storage for 8 weeks in counting machine cells, the colour of the tablets was duller than that of the control tablets. The electrochemical kinetics of MD were studied by Young *et al.* [7] using an electrochemical cell. They demonstrated that a melanoid pigment was formed as a final oxidation product. It is, evident, therefore, that there is still a need for a comprehensive kinetic study of MD, especially in the sustained release forms owing to the exposure of the beads to a high temperature during the coating step. In such kinetic studies, a stability-indicating method is essential to

Correspondence to: Dr. M. E.-S. Metwally, Department of Analytical Chemistry, Faculty of Pharmacy, Mansoura University, Mansoura 35516, Egypt.

0021-9673/92/$05.00

determine whether peaks of MD degradation products overlap with MD peaks.

The USP method [8] for the determination of MD in tablets does not appear to be stability indicating since an almost-degraded sample indicated that 53% of the drug was still intact compared with 0% using a high-performance liquid chromatographic (HPLC) method [9]. MD has been determined in dosage forms by fluorimetry [10,11], UV spectrophotometry [12], colorimetry [13–16], PMR spectroscopy [17], potentiometry [18], thin-layer chromatography [19], ion-exchange chromatography [20], HPLC [21,22] and gas chromatography [23]. These methods are not specific, are lengthy and time consuming, may require rigid experimental conditions such as pH adjustment and temperature control and/or cannot be used for the separation of MD from its degradation products.

The method previously developed by Metwally [9] using a cyano-bonded column succeeded in separating MD from its degradation products and its industrial impurity, MMD. Although this method would be suitable for the determination of MD in the presence of its degradation products and MMD, the half-life of the column was short, as expected [24], as the efficiency of the column decreased with time, necessitating frequent changes of the column.

The aim of this work was to study the degradation kinetics of MD using a stability-indicating HPLC method. The method was applied to the determination of MD in sustained release capsules and in the presence of MD degradation products and the industrial impurity MMD. In addition, the data presented provide a detailed description of the kinetic behaviour of MD at different pH and humidity, after exposure to UV radiation and at different temperatures (25–80°C). Degradation rate constants, the half-lifes and the activation energies of the degradation reaction were investigated. The kinetic data were compared under different media conditions.

EXPERIMENTAL

Chemicals

USP reference standards of MD and MMD were used (Sigma, St. Louis, MO, USA). MD raw material (checked according to the USP [8]) and MD sustained release microcapsules were supplied by Elan Pharmaceutical (Gainesville, GA, USA). Methanol (HPLC grade), acetonitrile (HPLC grade), acetic acid and sodium 1-hexanesulphonate were purchased from Aldrich (Milwaukee, WI, USA). All other chemicals were of high purity and used as received.

Liquid chromatograph

A Waters (Milford, MA, USA) Model 590 solvent pump, a Rheodyne (Berkeley, CA, USA) Model 7125 20-μl loop and a Kratos Spectroflow 757 variable-wavelength detector (Schoeffel Instrument, Westwood, NJ, USA) set at 280 nm were used. Compounds were separated on a 150 $\times$ 4.6 mm I.D. μBondapak C_8 (5 μm) analytical column (Waters). The eluted peaks were integrated by a Hewlett-Packard (Avondale, PA, USA) Model 3392A integrator.

Mobile phase

A solution of methanol in water containing 2% (v/v) acetic acid and 0.005 *M* sodium 1-hexanesulphonate (18:82) was used. The pH of solutions was 2.60 $\pm$ 0.05. The mobile phase was filtered by passing it through a 0.45-μm Millipore filter and degassed before use. The mobile phase flow-rate was 1.5 ml/min and the temperature was ambient.

Determination of water content

The water content in MD bulk powder and in the MD sustained release capsules was found to be 12.3 and 13.0%, respectively [9].

Preparation of stock solution

Stock solutions (0.1%, w/v) of MD and MMD were prepared in 0.05 *M* sulphuric acid using a simple solution method.

Preparation of calibration graphs

An accurately weighed 50-mg sample of USP MD or MMD was transferred into a 100-ml volumetric flask and 50 ml of 0.05 sulphuric acid were added. The flask was sonicated for 15 min, and then brought to volume with 0.05 *M* sulphuric acid. Serial dilutions of MD or MMD standards covering the concentration range 0.5–200 μg/ml were made. Concentrations of MD and MMD were determined in the acidified aqueous solutions using the HPLC conditions given above, and the peak heights of the standards (calibration graphs) were recorded.

Quantification

All measurements were done using peak heights. Concentrations of sample solutions containing MD were calculated using the slope and the intercept of the calibration graph prepared under the same conditions. The slope and the intercept of the calibration graph were obtained by linear regression of peak height *vs.* concentration ($y = ax + b$), where a is the slope, b is the intercept and y is the response of the analyte.

Concentrations of MD and MMD were determined in the acidified aqueous solutions using the HPLC conditions listed above. Concentrations were calculated by comparing the peak height with standard concentrations (calibration graphs) of both compounds. The plots of the peak height *versus* concentration were linear over the range 0.5–200.0 μg/ml with a regression coefficient of over 0.999 for both compounds.

Extraction of MD from sustained release microcapsules

Beads equivalent to 500 mg of MD were ground to a fine powder and transferred into a 100-ml volumetric flask, then 50 ml of 0.05 *M* sulphuric acid were added. The flask was sonicated for 15 min and then brought to volume with 0.05 *M* sulphuric acid, then filtered. The first 10.0 ml of the filtrate were rejected and 10 ml of the clear filtrate were diluted to 100.0 ml with 0.05 *M* sulphuric acid.

Kinetic studies

pH–rate profile. Kinetic studies were made in aqueous solutions containing 0.1 *M* buffer solutions [25] covering the pH range 2–12. A kinetic run at pH 13 was conducted in 0.1 *M* NaOH solution. In all kinetic runs, 10-mg samples of MD were dissolved in 100 ml of the appropriate buffer solution in a 100-ml volumetric flask. The flasks were kept in a thermostated water-bath at 25 ± 0.5°C. At appropriate time intervals, 5 ml of sample were transferred into a 25-ml flask and 5 ml of 0.1 *M* sulphuric acid were added. The mixture was adjusted to volume with deionized water and then analysed.

Effect of heat on the degradation rate of MD in raw material and in solid formulations. MD raw material and MD beads (finely ground) were stored at ambient temperature (25 ± 0.2), 40, 50, 60, 70 and 80°C. Zero-time sample measurements were carried out when the study began only on samples from bottles to be stored under ambient conditions. All original and re-bottled samples stored under accelerated conditions were not opened until the first analysis. The bottles were re-closed tightly by hand between sampling. For all storage conditions, the entire study was performed on duplicate bottles of MD raw material or MD microcapsules. For aqueous solutions, samples equivalent to 100 mg of MD raw material were dissolved in 100 ml of 0.1 *M* buffer (pH 6) [25]. Samples were diluted 1:20 using the same buffer and poured into 10-ml vials and sealed. The vials were placed in ovens set at appropriate temperatures, and at specified time intervals individual samples were taken for analysis.

Effect of humidity and UV radiation. The effect of humidity was observed by exposing finally ground beads in an open petri dish to 80% humidity in an oven held at 60°C for 60 days, and the results were compared with those obtained with closed bottles. The effect of UV radiation on MD degradation was observed by exposing finally ground beads in an open petri dish to strong UV radiation in an oven held at 25°C for 60 days, and the results were compared with those obtained with unexposed bottles.

RESULTS AND DISCUSSION

The fact that MD can easily be oxidized in alkaline media, or when stored under unfavourable condition [3,5], necessitates a detailed study of its kinetics under different conditions using a stability-indicating procedure. The proposed reversed-phase HPLC method utilizes a C_8 column coupled with an acidic methanol–water mobile phase containing hexanesulphonate and UV detection for the separation of MD from its degradative products and its industrial impurity, MMD (Fig. 1). Under identical separation conditions, the retention times (t_R) were MD 4.35 min, MMD 8.93 min and MD degradation products 10.54, 8.12, 5.96, 5.43, 4.04, 3.41, 2.57, 1.577, 1.25, 1.15, 1.01 and 0.88 min on a 150 × 4.6 mm I.D. μBondapak C_8 (5 μm) analytical column.

As has been observed with the CN bonded column [9], using acetonitrile as an organic modifier resulted in overlapping of one of the peaks of the degradation products of MD with that of MMD. Accordingly, methanol was chosen as an organic

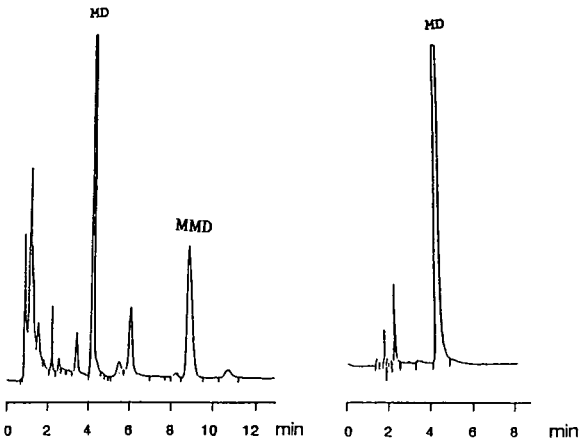

Fig. 1. Chromatogram obtained from a mixture of MD (10 μg/ml, t_R = 4.35 min), MMD (10 μg/ml, t_R = 8.93 min) and degraded MD (100 μg/ml), 30 min degradation time in 0.1 *M* NaOH at 25°C, t_R = 10.54, 8.12, 5.96, 5.43, 4.04, 3.41, 2.57, 1.577, 1.25, 1.15, 1.01 and 0.88 min). Column, 150 × 4.6 mm I.D. μBondapak C_8 (5 μm); mobile phase, methanol–water (18:82, v/v) containing 2% (v/v) acetic acid and 0.005 *M* sodium 1-hexanesulphonate; pH, 2.60 ± 0.05; flow-rate, 1.5 ml/min; detector wavelength, 280 nm.

Fig. 2. Chromatogram obtained for MD sustained release capsules (t_R = 4.35 min, 90 μg/ml). Chromatographic conditions as in Fig. 1.

solvent modifier, whence all the degradation peaks were successfully separated from MD and MMD. On the other hand, on using heptanesulphonate as a counter ion each analysis requires over 20 min, and the analysis time was shortened to 11 min by using hexanesulphonate as a counter ion.

Based on the peak-height responses of standards, the method was linear in the range 0.5–200 μg/ml with regression coefficients of 0.999 for both MD and MMD.

The reproducibility of the measurement of 100 μg/ml based on ten determinations showed relative standard deviations of 0.54 and 0.62% for MD raw material and MD sustained release formulations, respectively. The corresponding value for the injection of 1 μg/ml were 0.92 and 1.05%, respectively.

An overnight decomposed sample of MD in 0.1 *M* NaOH solution showed zero recovery by the proposed HPLC method and 53.4% by the USP spectrophotometric method, an indication of the precision of the proposed method. This is in agreement with previously published data [9]. Another advantage of the proposed HPLC ion-pairing method appears in the separation of MMD from MD. The separation without the ion-pairing reagent was impossible. In addition, the presence of excipients common to sustained release capsules [critic acid, fumaric acid, sodium lauryl sulphate, non-pareils, talc, polyvinylpyrrolidone (PVP) and shellac] did not interfere in the determination of MD in the sustained release capsules. Fig. 2 illustrates the separation of the active ingredients in MD sustained release capsules from excipients. No MMD was found in any of the studied MD batches.

In Table I, the percentage of the labelled values obtained when the proposed HPLC method was applied to the determination of MD in sustained release capsules in five different batches are compared with those obtained with the USP method with standard deviations of 0.80 and 0.94%, respectively. No noticeable discrepancies were observed. The mean recovery of MD from raw material and sustained release capsules ranged from 99.71 to 100.2% and from 99.5 to 100.1%, respectively.

Kinetics

The short analysis time using HPLC allowed a precise study of the MD degradation with a large number of determinations per curve. The kinetic studies were performed on MD raw material and on formulated beads to observe the effect of pH, manufacturing and storage temperatures, humidity and UV radiation on the degradation rate constants.

pH–rate profile. In the pH-rate profile study, the retention times of MD, MMD and MD degradation products were recorded every time to ensure the reproducibility and to monitor peak disappearance peak formation behaviour. The patterns of the chromatograms were not stable with time (Fig. 3). MD degradation products with retention times of 10.54, 8.12,5.96 and 5.43 min (which are apparently more lipophilic than MD) disappear with time with a subsequent increase in the area of the more hydrophilic products with retention times of 2.57, 1.577, 1.25, 1.15, 1.01 and 0.88 min. This is consistent with Young *et al.*'s findings [7], with a melanin-like pigment as the final oxidation product of MD. The degradation pathway of MD became increasingly complex with time. The chromatograms were carefully examined to ensure that none of the MD degradation products interfered with MD or MMD at any time during the study.

TABLE I

DETERMINATION OF MD IN DIFFERENT BATCHES OF SUSTAINED RELEASE CAPSULES USING THE PROPOSED HPLC METHOD AND THE USP SPECTROPHOTOMETRIC METHOD [8]

Batch No.	Sample weight[a] (μg/ml)	MD found (%)	
		HPLC method	USP method
C821	5.03	59.44	59.78
	17.94	58.58	58.83
	89.99	58.70	58.32
	165.29	58.80	59.01
	218.50	58.54	58.56
C934	3.01	59.80	59.63
	20.03	58.31	58.45
	75.01	58.29	58.07
	149.21	58.25	58.19
	250.25	58.38	58.29
C1040	20.45	58.68	59.15
	66.98	58.39	58.63
	117.43	57.99	58.21
	190.00	58.29	58.34
	298.99	59.18	59.34
176A/40	9.35	55.94	56.01
	35.10	57.04	56.23
	87.56	57.32	57.21
	187.90	57.47	57.18
	275.92	57.64	57.90
21B/11	3.29	59.27	60.00
	21.27	57.59	58.76
	69.98	57.82	57.72
	159.33	57.73	58.32
	249.57	57.71	57.67
Mean		58.21	58.31
S.D.		0.80	0.94

[a] Each 100 mg of beads contains 58 mg of MD.

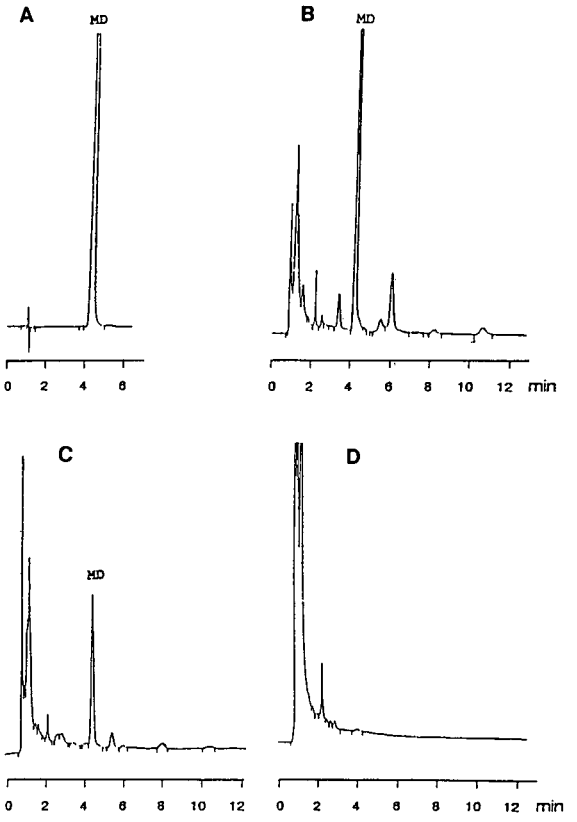

Fig. 3. Chromatograms shows MD degradation products in 0.1 *M* NaOH at 25°C after time = (A) 0, (B) 30 min, (C) 2 h and (D) 8 h. MD initial concentration, 100 μg/ml. Retention times and chromatographic conditions as in Fig. 1.

The effect of initial concentration on the pH–rate profile was first studied. Degradation of 5, 25, 50 and 100 μg/ml of MD in 0.1 *M* NaOH at 25°C proceeded with the same degradation rate. This is different from the early findings of Lippold and Jaeger [5], who used UV spectrophotometry to study MD degradation. For the remaining experiments, an initial concentration of 100 μg/ml was used to permit a longer time course.

The observed first- or pseudo-first-order disappearance rate constants and the corresponding second-order disappearance rate constants for MD in 0.1 *M* non-sterile buffers in the pH range 2–13 and at 25°C are listed in Table II. Fig. 4 shows logarithmic concentration (ln *C*) *versus* time (*t*) for the disappearance of MD in 0.1 *M* NaOH aqueous solution and indicates a first-order degradation behaviour with a rate constant (k_{obs}) of 16.21 ± 0.14 day^{-1} and a regression coefficient of 0.994. The pseudo-first-order disappearance rate constants were calculated using a non-linear regression according to

$$\ln (C_t/C_0) = -k_{obs}t \quad (1)$$

where C_0 and C_t are the MD concentrations at time zero and t, respectively. The rate constant was taken as the slope of the line obtained by a linear least-squares analysis of the data. The second-order rate constant (k_2) was calculated from the equation

TABLE II

OBSERVED FIRST-ORDER OR PSEUDO-FIRST-ORDER DISAPPEARANCE RATE CONSTANTS FOR MD IN NON-STERILE BUFFERED DISTILLED WATER, USING A BUFFER CONCENTRATION OF 0.1 *M* AT 25°C

pH	r^{2a}	$k_{obs}{}^{b}$ (day^{-1})	$t_{1/2}{}^{c}$ (day)	$k_2{}^{d}$ (day^{-1} l mol^{-1})
13.00	0.994	16.21	0.043	162.10
11.98	0.995	1.810	0.383	189.53
10.88	0.995	0.150	4.621	197.74
9.91	0.991	$1.600 \cdot 10^{-2}$	43.322	196.84
9.15	0.982	$2.800 \cdot 10^{-3}$	247.553	198.22
8.69	0.780	$9.790 \cdot 10^{-4}$	708.016	199.89
7.96	0.701	$6.010 \cdot 10^{-4}$	1153.323	[e]
7.54	0.701	$7.010 \cdot 10^{-4}$	988.798	[e]
7.00	0.695	$5.190 \cdot 10^{-4}$	1335.543	[e]
6.09	0.691	$8.340 \cdot 10^{-4}$	831.112	[e]
4.10	0.689	$7.016 \cdot 10^{-4}$	987.952	[e]
1.98	0.700	$6.327 \cdot 10^{-4}$	1095.538	[e]

[a] r^2 = Regression coefficient.
[b] k_{obs} = Observed first-order rate constant.
[c] $t_{1/2}$ = Half-life of the reaction.
[d] k_2 = Second-order rate constant.
[e] pH-independent degradation reaction.

$$k_2 = k_{obs}/[OH^-] \quad (2)$$

where $[OH^-]$ is the hydroxyl ion concentration.

The pH–rate profile for the degradation of MD is shown in Fig. 5, which indicates that MD undergoes a neutral (pH-independent) degradation reaction over the pH range 2–7.5 with a first-order rate constant of 6.65 ($\pm$1.07) $\times$ 10^{-4} day^{-1} (n = 5) at 25°C. Above pH 7.96, a base-promoting degradation reaction dominates and the reaction is first order with respect to the hydroxyl ion concentration. The second-order rate constant was 190.72 $\pm$ 14.50 l mol^{-1} day^{-1} based on using data covering the pH range 8.69–13.0. The data obtained at pH 7.96 were not included in calculating k_2 because the neutral degradation rate constant still contributes seriously to the overall rate constant. The data indicate the importance of incorporating acidic excipients as diluents in the sustained release formulation to prevent such degradation.

Rate constants measured at room temperature and in the pH range 2–7.96 show considerable variation, presumably mainly owing to the difficulties inherent in measuring rate constants for very slow reactions.

Heating. Disappearance rate constants for MD in raw materials and in sustained release capsules were measured at elevated temperatures to obtain more accurate values for degradation rates at room temperature and to indicate the effect of high temperature of the manufacturing, storage and shipping conditions on the stability of MD.

Activation energy. The activation energy (E_a) and the frequency factor (A) were calculated using the data presented in Table III according to the Arrhenius equation:

$$\ln k_{obs} = \ln A - (E_a/RT) \quad (3)$$

where R is the molar gas constant (8.3143 J^{-1} l mol^{-1}) and T is the absolute temperature. The behavior of MD degradation follows the general

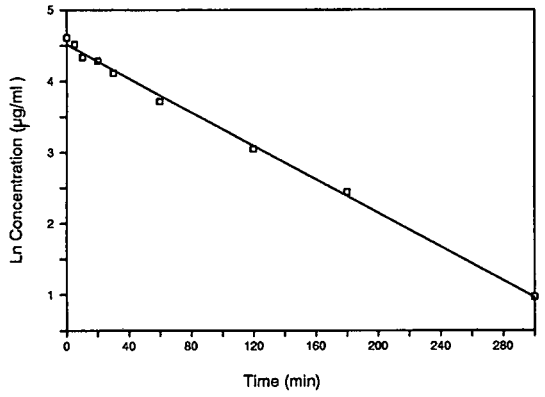

Fig. 4. Plot of ln (concentration) *versus* time for the degradation of MD in 0.1 *M* NaOH at 25°C.

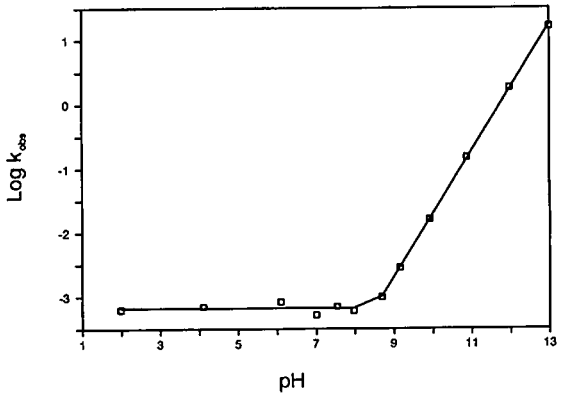

Fig. 5. Plot of log (observed rate constants) *versus* pH for the degradation of MD in 0.1 *M* buffered distilled water at 25°C.

TABLE III

VALUES FOR EXPERIMENTAL AND CALCULATED DEGRADATION RATE CONSTANTS AND HALF-LIFES FOR THE DISAPPEARANCE OF MD IN DIFFERENT MEDIA AND AT DIFFERENT TEMPERATURES

Sample	Temperature (°C)	r^2 [a]	k_{obs} [b] (day^{-1})	k'_{obs} [c] (day^{-1})	$t_{1/2}$ [d] (day)	$t'_{1/2}$ [e] (day)
MD aqueous solution	25	0.710	$8.34 \cdot 10^{-4}$	$6.20 \cdot 10^{-4}$	831.11	1117.80
	40	0.895	$3.91 \cdot 10^{-3}$	$5.01 \cdot 10^{-3}$	177.28	138.39
	50	0.987	$2.91 \cdot 10^{-2}$	$1.81 \cdot 10^{-2}$	23.82	38.29
	60	0.993	$5.39 \cdot 10^{-2}$	$6.06 \cdot 10^{-2}$	12.86	11.44
	70	0.998	0.190	0.189	3.65	3.67
	80	0.997	0.602	0.552	1.15	1.26
MD raw material	25	0.695	$1.04 \cdot 10^{-4}$	$7.08 \cdot 10^{-5}$	6664.88	9786.99
	40	0.845	$6.79 \cdot 10^{-4}$	$4.47 \cdot 10^{-4}$	1020.84	1552.11
	50	0.913	$9.89 \cdot 10^{-4}$	$1.39 \cdot 10^{-3}$	700.86	500.08
	60	0.962	$3.26 \cdot 10^{-3}$	$4.02 \cdot 10^{-3}$	212.62	172.46
	70	0.988	$1.40 \cdot 10^{-2}$	$1.10 \cdot 10^{-2}$	49.51	63.29
	80	0.989	$4.03 \cdot 10^{-2}$	$2.82 \cdot 10^{-2}$	17.20	24.58
MD beads	25	0.694	$1.01 \cdot 10^{-4}$	$5.83 \cdot 10^{-5}$	6862.84	11886.84
	40	0.897	$4.39 \cdot 10^{-4}$	$3.89 \cdot 10^{-4}$	1578.92	1782.34
	50	0.904	$8.93 \cdot 10^{-4}$	$1.25 \cdot 10^{-3}$	776.20	554.79
	60	0.963	$3.57 \cdot 10^{-3}$	$3.74 \cdot 10^{-3}$	194.16	185.23
	70	0.992	$1.31 \cdot 10^{-2}$	$1.05 \cdot 10^{-2}$	52.91	65.93
	80	0.994	$4.01 \cdot 10^{-2}$	$2.79 \cdot 10^{-2}$	17.29	24.88

[a] r^2 = Regression coefficient.
[b] k_{obs} = Observed first-order rate constant.
[c] k'_{obs} = Estimated first-order rate constant.
[d] $t_{1/2}$ = Half-life of the reaction.
[e] $t'_{1/2}$ = Estimated half-life of the reaction.

Arrhenius relationship because linear plots of ln (rate) *versus* $1/T$ were obtained for MD raw material in both the aqueous and solid forms and for MD solid dosage forms, with regression coefficients of 0.988, 0.977 and 0.981, respectively. The activation energies and the frequency factors are summarized in Table IV.

Arrhenius plots (ln k_{obs} *vs.* $1/T$) for the disappearance of MD in aqueous solutions and in solid forms are shown in Fig. 6. Use of more precise data from runs at 40, 50, 60, 70 and 80°C to calculate the least-squares line permits extrapolation to lower temperatures, and resulted in calculating more precise rate constant estimates. Values of 6.20×10^{-4}, 7.08×10^{-5} and 5.83×10^{-5} day^{-1} for the disappearance of MD at 25°C in aqueous solution, solid-form of materials and in sustained release capsules, respectively, were obtained.

It is obvious that MD degrades at a faster rate in aqueous solutions than in solid forms. This could be due to the presence of dissolved oxygen in aqueous solution, which is necessary for oxidation.

On heating solid beads the colour changed,

TABLE IV

ACTIVATION ENERGIES AND FREQUENCY FACTORS FOR THE DISAPPEARANCE OF MD IN DIFFERENT MEDIA

Sample	E_a [a] (kJ)	A [b] (day^{-1})	r^2 [c]
MD aqueous solution	105.92	35.38	0.989
MD raw material	93.36	28.21	0.977
MD beads	96.21	29.16	0.981

[a] E_a = Activation energy.
[b] A = Frequency factor.
[c] r^2 = Regression coefficient.

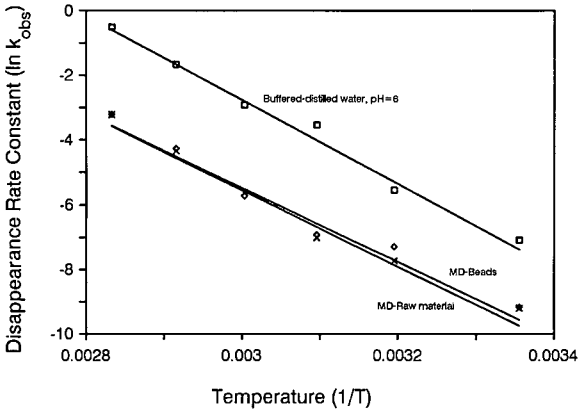

Fig. 6. Arrhenius plot for the degradation of MD in (□) aqueous solution, (◇) raw material and (×) sustained release capsules.

ranging from light yellow through yellow and light brown to dark brown. Because only a 7% decrease in potency over 21 days at 60°C was observed, this dramatic colour change could be attributed to some sort of oxidation of the excipients rather than of the drug itself.

Effect of humidity and UV radiation. Kinetic runs on finely ground powder of batch C-821 sustained release capsules were conducted at 60°C and at 80% humidity. It was found that changing the humidity to 80% has no effect on the kinetics of degradation of MD beads. The same conclusion was also obtained for the effect of UV radiation. The exposure time in both experiments was 60 days.

In conclusion, the degradation of MD is a function of both pH and temperature. The faster degradation rate of MD in aqueous solution than in solid form may be interpreted by the presence of dissolved oxygen in the aqueous solution. In addition, the proposed method is accurate, rapid, selective and precise. It gave results for MD in sustained release capsules that were in excellent agreement with those obtained by the official USP method. The method was superior, however, in application to kinetics studies.

REFERENCES

1 A. G. Gilman, L. S. Goodman and A. Gilman, *The Physiological Basis of Therapeutics*, Macmillan, New York, 6th ed., 1980, pp. 795–803.
2 R. J. Yu and E. Van Scott, *J. Invest. Dermatol.*, 60 (1973) 234–238.
3 V. S. Gupta and A. Gupta, *Am. J. Hosp. Pharm.*, 36 (1979) 1539–1541.
4 R. Sassetti and H. Fundenberg, *Biochem. Pharmacol.*, 20 (1971) 57–62.
5 B. C. Lippold and I. Jaeger, *Arch. Pharm. (Weinheim)*, 306 (1973) 106–117.
6 *The United States Pharmacopeia XIX Revision*, United States Pharmacopeial Convention, Rockville, MD, 1975, p. 320.
7 T. E. Young, B. W. Babbitt and L. A. Wolfe, *J. Org. Chem.*, 45 (1980) 2899–2902.
8 *The United States Pharmacopeia XXII Revision and The National Formulary XVI*, United States Pharmacopeial Convention, Rockville, MD, 1990, pp. 865–867.
9 M. E.-S. Metwally, *J. Chromatogr.*, 549 (1991) 221–228.
10 R. Leverty and K. M. Tylor, *Anal. Biochem.*, 22 (1968) 269–279.
11 B. K. Kim and R. T. Koda, *J. Pharm. Sci.*, 68 (1977) 1632–1634.
12 R. G. Bhatkar and V. N. S. Nevreckar, *Indian Drug Pharm. Ind.*, 15 (1980) 45–47.
13 S. K. Wahba-Khalil and R. B. Salma, *J. Pharm. Pharmcol.*, 26 (1974) 972–974.
14 N. El-Rabbat and N. M. Omer, *J. Pharm. Sci.*, 67 (1978) 779–781.
15 M. I. Walash, A. A. Abou Ouf and F. B. Salem, *J. Assoc. Off. Anal. Chem.*, 68 (1985) 91–95.
16 P. B. Issopoulos, *Fresenius' Z. Anal. Chem.*, 336 (1990) 124–128.
17 A. M. Farina, M. A. Iorio and A. Doldo, *Spectrosc. Lett.*, 21 (1988) 455–487.
18 E. M. Athanasiou-malaki and M. A. Koupparis, *Anal. Chim. Acta*, 161 (1984) 349–353.
19 J. Martens, K. Guenther and M. Schickedanz, *Arch. Pharm. (Weinheim)*, 319 (1986) 572–574.
20 R. Chu, *J. Assoc. Off. Anal. Chem.*, 54 (1971) 603–608.
21 S. Ting, *J. Assoc. Off. Anal. Chem.*, 66 (1983) 1436–1442.
22 A. G. Ghanekar and V. Das Gupta, *J. Pharm. Sci.*, 67 (1978) 1247–1250.
23 J. R. Watson and R. C. Lawrence, *J. Chromatogr.*, 103 (1975) 63–70.
24 L. R. Snyder and J. J. Kirkland, *Introduction to Modern Liquid Chromatography*, Wiley, New York, 1979, pp. 270–321.
25 J. Heyrovsky and P. Zuman, *Practical Polarography*, Academic Press, London, 1968, p. 179.

Journal of Chromatography, 623 (1992) 83–91
Elsevier Science Publishers B.V., Amsterdam

CHROM. 24 395

Inverse gas chromatography: the use of Laffort solubility factors and topological indices in structure–polarity relationships

Adam Voelkel

Poznań Technical University, Institute of Chemical Technology and Engineering, Pl. M. Skłodowskiej-Curie 2, 60-965 Poznań (Poland)

(First received February 12th, 1992; revised manuscript received June 2nd, 1992)

ABSTRACT

Inverse gas chromatography was used in the physico-chemical characterization of 1,3-bis[ω-alkoxyoligo(oxyethylene)]-2-propanols. Laffort solubility factors were examined as polarity measures and topological indices as structural parameters. Relationships between Laffort solubility factors and polarity index were examined. It was found that Laffort solubility factor *O* and factor *E* may be usesd as polarity measures. Topological indices were used as structural parameters in polarity–structure relationships, which were evaluated and are discussed. A higher discriminating power of the Balaban index and Wiener number was found in comparison with the valence connectivity indices.

INTRODUCTION

Numerous efforts have been made to characterize properly liquid stationary phases used in gas chromatography [1–5]. The term "stationary phases" is used here both for commercial liquid phases and the large group of organic (polymeric and non-polymeric) compounds examined by the procedures of inverse gas chromatography [6–8]. The solubility parameter, defined as the square root of cohesive energy density [9–12], seems to be a powerful tool in the description of intermolecular solute–solvent interactions. However, the lack of physico-chemical data for most liquid phases owing to their low vapour pressure has limited the use of solubility parameters in the characterization of organic compounds.

An interesting attempt to overcome these difficulties is the use of Laffort's solubility factors [13,14]. Laffort and Patte [14] described a procedure for their determination and found close relationships between solubility factors and solubility parameters for solutes used in the chromatographic process. They expressed the retention indices of carefully selected standard solutes according to the following equation:

$$I_i = \alpha_i A + \omega_i O + \varepsilon_i E + \pi_i P + \beta_i B + 100 \qquad (1)$$

where I_i denotes the retention index of solutes i as measured on a given stationary phase, α_i and β_i are solubility factors of solute i and A, O, E, P and B are Laffort solubility factors for the examined liquid phase.

The physical meaning of solute solubility factors is as follows: α is an apolar factor proportional to the molar volume of solute at the boiling point, ω is an orientation factor proportional to dipole moments for simple molecules, ε is an electron factor, π is a proton donor factor, also called acidity factor, and β is a basicity factor proportional to the ability to accept protons [14].

The physico-chemical interpretation of solubility

Correspondence to: Dr. Adam Voelkel, Poznań Technical University, Institute of Chemical Technology and Engineering, Pl. M. Skłodowskiej-Curie 2, 60-965 Poznań, Poland.

0021-9673/92/$05.00

factors *A*, *O*, *E*, *P* and *B* remained unclear. Recently, Voelkel and Janas [15] described an attempt to use of Laffort solubility factors in the characterization of some thioethylene derivatives. They indicated the existence of statistically significant relationships between some of the Laffort factors and the differences in retention indices for McReynolds probes (*e.g.*, $\Delta I_{\text{benzene}}$ *vs* factor *E* and $\Delta I_{\text{2-pentanone}}$ *vs.* factor *O*).

The polarity parameters, thermodynamic functions of solution and dispersive interactions parameters for 1,3-bis[ω-alkoxyoligo(oxyethylene)]-2-propanols of general formula

$$R(OCH_2CH_2)_nOCH_2CH(OH)CH_2O(CH_2CH_2O)_mR$$

where R,R′ = C_4H_9, C_6H_{13}, C_8H_{17}; R = R′ or R ≠ R′; *n*,*m* = 0–3; *n* = *m* or *n* ≠ *m*, were published earlier [16,17]. Variations in R and R′ alkyl groups and in *n* and *m* cause significant differences in the properties of examined compounds [16–18].

The polarity index, *PI*, was proposed by Huebner [19] to characterize surface-active agents examined by gas–liquid chromatography and is calculated from the experimental relationship

$$PI = 100\log(C - 4.7) + 60 \quad (2)$$

where *C* is an apparent carbon number equal to the number of carbon atoms in a hypothetical *n*-alkane having the same retention time as a polar solute (alcohol).

Thermodynamic functions of solution, *i.e.*, partial molal Gibbs free energy of solution for a methylene group, $\Delta G_s^m(CH_2)$, or functional group FG, ΔG_s^m (FG), were introduced by Risby and co-workers [20–23] and were used to characterize liquid stationary phases [23] and also surfactants and extractants [16–18]. The criterion *A* developed by Ševčik and Löwentap [24] and the partial molar excess Gibbs free energy of solution per methylene group, ΔG^E (CH_2) [25], parameters of dispersive interactions, were used in the characterization of surfactants and extractants [17,26]. Poole and Poole [27] suggested the usefulness of criterion *A* and $\Delta G^E(CH_2)$ as solvent strength parameters.

It has been shown that topological indices can be used as structural parameters [28–33]. These parameters were developed for saturated hydrocarbons, but the procedures proposed by Balaban [34] and Barysz *et al.* [35] made them useful for describing the structures for all groups of compounds. Topological indices are sensitive to the length of the alkyl chain, the length of the oxyethylene and thioethylene chain and the presence of different heteroatoms. Hence they could be used to characterize the structure of organic compounds. However, the discriminating power of any topological index may be limited to an examined group of compounds. It has been shown [36] that for the group of oligooxyethylene derivatives of alcohols, thioalcohols and alkylamines the best retention–structure correlations were obtained when the valence molecular connectivity indices were used as structural parameters. The relationships which use the Balaban index I_B and $W(G)$ were characterized by only moderate statistical characteristics.

The aim of this paper is to discuss the usefulness of Laffort's solubility factors in the characterization of examined compounds used as GC stationary phases. Parameters to be used in physico-chemical characterization should be sensitive to any changes in the structure of examined substances. It is of interest to check whether solubility factors obey such a condition. Topological indices generally change with increase in the number of exyethylene units in the oligooxyethylene chain. Do they indicate the changes in the distribution of oxyethylene units in two oligooxyethylene chains?

EXPERIMENTAL

Thirty pure model 1,3-bis[ω-alkoxyoligo(oxyethylene)]-2-propanols were used as liquid stationary phases in a GC column. The method of synthesis, some physico-chemical data and the conditions of chromatographic measurements were described previously [16,17].

Retention data collected earlier were used to calculate solubility factors according to Laffort's idea following the procedure described by Voelkel and Janas [15]. Topological parameters were calculated according to the procedure of Barysz *et al.* [35], which has been used in earlier papers [36,37].

RESULTS AND DISCUSSION

The examined compounds were divided into three groups according to the differences in the alkyl groups, *viz.*, (i) R = R′ = C_4H_9; (ii) R = R′ = C_6H_{13};

TABLE I

LAFFORT SOLUBILITY FACTORS FOR $Bu(EO)_nCH_2CH(OH)CH_2(OE)_mOBu$

Formula		Solubility factors					Polarity index[a]
n	*m*	*A*	*O*	*E*	*P*	*B*	
0	0	–	–	–	–	–	92.3
	1	203	214	238	259	339	96.2
	2	210	221	252	272	394	99.5
	3	196	195	254	253	525	103.2
	4	194	244	268	289	399	105.7
1	1	207	209	243	269	399	98.9
	2	206	251	259	295	305	102.9
	3	195	201	262	208	503	105.4
	4	213	198	264	264	521	107.7
2	2	205	166	256	230	624	104.5
	3	193	192	269	245	598	107.5
	4	205	243	281	295	429	108.9
3	3	198	237	278	282	468	109.1
	4	201	253	284	297	425	110.0

[a] 70°C, ethanol as polar solute. Taken from ref. 16.

and (iii) $R \neq R'$ and R or R′ = C_4H_9, C_6H_{13}, C_8H_{17}. The estimated Laffort solubility factors for these three groups of oxyethylates are presented in Tables I–III. Polarity indices at 70°C (ethanol as a polar solute) taken from refs. 16 and 17 are also given for comparison. The polarity index has been discussed as a polarity parameter for a large group of surface-active agents and extractants [38–41]. The term "polarity of liquid stationary phases" has often been used and discussed, but is often misunderstood. According Poole and to Poole [5,27], solvent strength (polarity) could be defined as the capacity to enter into various solute–solvent interactions, whereas solvent selectivity is a measure of relative capacity of a solvent for a particular solute–solvent interaction.

Anyway, the empirical "polarity index" has been successfully used to characterize the properties of surface-active agents and surfactants [36–41]. Strong correlations existing between the polarity index, *PI*, and *HLB* number, well known in surfactant physico-chemistry or *HLB* (calculated from *PI*) and extraction rate of copper [42–45], have been reported. The *HLB* (hydrophile–lipophile balance) number is the ratio of the effective molecular masses of the hydrophilic groups to the sum of the molecular masses of the lipophilic (hydrophobic) groups in the surfactant molecule [46]. For non-ionic surfactants the *HLB* number is between 1 and 20. Compounds with $HLB > 10$ are hydrophilic and exhibit a high affinity for the aqueous phase, and those with $HLB < 10$ are hydrophobic. Hence the *HLB* number characterizes different properties of organic molecules containing both polar and non-polar groups. As an example, surface-active agents with $HLB = 1$–6 will stabilize water-in-oil emulsions, whereas more hydrophilic compounds with

TABLE II

LAFFORT SOLUBILITY FACTORS FOR $Hex(EO)_nCH_2CH(OH)CH_2(OE)_mOHex$

Formula		Solubility factors					Polarity index[a]
n	*m*	*A*	*O*	*E*	*P*	*B*	
0	0	202	169	219	216	384	82.9
	1	194	137	225	199	545	89.4
	2	194	284	246	271	288	92.5
	3	193	232	260	268	306	95.4
1	1	198	229	244	275	278	93.6
	2	197	206	248	257	392	96.2
	3	192	213	255	264	416	99.1
2	2	182	150	255	168	639	100.2
3	3	189	246	271	282	364	103.1

[a] 70°C, ethanol as polar solute. Taken from ref. 16.

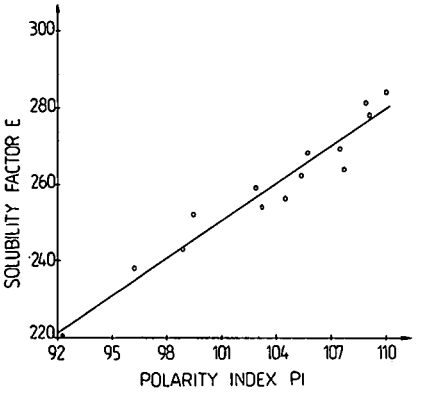

Fig. 1. Laffort solubility factor *E* *vs.* polarity index (ethanol as polar agent) relationship for 1,3-bis[ω-alkoxyoligo(oxyethylene)]-2-propanols.

TABLE III

LAFFORT SOLUBILITY FACTORS FOR $R(EO)_nCH_2CH(OH)CH_2(OE)_mOR'$

Formula				Solubility factors					Polarity index[a]
R	R'	*n*	*m*	*A*	*O*	*E*	*P*	*B*	
C_8H_{17}	C_8H_{17}	0	0	194	148	215	197	401	74.4
		0	1	192	165	225	214	397	81.8
		0	2	191	151	232	208	495	86.2
C_8H_{17}	C_4H_9	0	0	188	323	248	321	−94	81.9
		0	1	196	318	253	327	−50	88.6
		1	1	213	201	235	257	309	90.0
C_6H_{13}	C_4H_9	0	1	202	183	229	236	407	92.6

[a] 70°C, ethanol as polar solute. Taken from ref. 16.

HLB = 8–18 tend to stabilize oil-in-water emulsions.

For the group of 1,3-bis[butoxyoligo(oxyethylene)]-2-propanols, the best relationship with polarity index has been found for the solubility factor *E* (Fig. 1). It is statistically significant: the correlation coefficient $R = 0.9695$ and the F ratio = 187.97. The same relationship for the second group of compounds examined is as follows:

$$E = 9.2064 + 2.5107PI \quad (3)$$

where *E* = solubility factor and *PI* = polarity index, with $R = 0.9316$ and $F = 45.99$.

Both correlations are statistically valid, but several deviations from the straight line in Fig. 1 suggest that the examined parameters, at least in some instances, behave differently with the structural changes of oxyethylates. There are four structural elemets that could influence the properties of our compounds: (i) the length of alkyl groups R and R'; (ii) the number of oxyethylene units (*n,m*) in oligooxyethylene chains; (iii) asymmetry in R and R'; (iv) asymmetry of two oxyethylene units. The variations of the discussed polarity and topological parameters caused by the changes in the above-mentioned structural elements are presented in Table IV. The deviations from the straight line in Fig. 1 are the result of different sensitivities of the factor *E* and polarity index *PI* on changing the asymmetry in both alkyl chains and oligooxyethylene chains. The polarity index decreases with increasing asymmetry in R and R' but with decreasing asymmetry in

TABLE IV

VARIATION OF POLARITY INDEX, LAFFORT SOLUBILITY FACTOR *E* AND TOPOLOGICAL INDICES WITH CHANGES IN THE STRUCTURE OF THE EXAMINED COMPOUNDS

Structural element	Polarity index, *PI*	Laffort solubility factor, *E*	Balaban index, I_B	Wiener number, *W(G)*	Connectivity index, $^1\chi^v$
No. of carbon atoms in alkyl group(s)	↓[a]	↓	↓	↑	↑
No. of EO units in *m* (*n* = constant)	↑	↑	↑	↑	↑
Asymmetry in R and R'	↓	↑	↓	↑	No change
Asymmetry	↑	↓	↓	↑	No change

[a] The arrows ↑ and ↓ indicate an increase or decrease of a given parameter with a rising change of structural parameter.

TABLE V

TOPOLOGICAL INDICES FOR $Bu(EO)_nCH_2CH(OH)CH_2(OE)_mOBu$

Formula		Topological parameter				
n	m	I_B	$W(G)$	$^1\chi^v$	$^2\chi^v$	$^3\chi^v$
0	0	3.4567	373.625	5.6436	3.5108	2.0340
	1	3.5312	667.000	6.7210	4.1231	2.4060
	2	2.5663	1087.875	7.7983	4.7355	2.7780
	3	3.5882	1658.750	8.8757	5.3479	3.1501
	4	3.6025	2402.125	9.9530	5.9602	3.5221
1	1	3.5967	1081.875	7.7983	4.7354	2.7780
	2	3.6256	1646.750	8.8757	5.3479	3.1501
	3	3.6425	2384.125	9.9530	5.9602	3.5221
	4	3.6512	3316.500	11.0304	6.5726	3.8941
2	2	3.6550	2378.125	9.9530	5.9602	3.5221
	3	3.6708	3304.500	11.0304	6.5726	3.8941
	4	3.6797	4448.375	12.1077	7.1850	4.2661
3	3	3.6859	4442.375	12.1077	7.1850	4.2661
	4	3.6958	5820.258	13.1851	7.7974	4.6381

oligooxyethylene chains. Factor E, in contrast to PI, is highest for compounds with strong asymmetry of alkyl groups and having equal oligooxyethylene chains. Hence the discussed physico-chemical parameters are not completely equivalent.

Topological parameters calculated for the examined oxyethylates are presented in Table V–VII. To examine the sensitivity of topological indices to structural changes, several data have been extracted and are shown in Tables VIII and IX. The Balaban index decreases with increasing number of carbon atoms in alkyl chains, but increases with increasing length of oligooxyethylene chains. Asymmetry of any structural element causes a decrease in this topological index. The Wiener number always increases when all the discussed structural elements

TABLE VI

TOPOLOGICAL INDICES FOR $HexO(EO)_nCH_2CH(OH)CH_2(OE)_mOBu$

Formula		Topological parameter				
n	m	I_B	$W(G)$	$^1\chi^v$	$^2\chi^v$	$^3\chi^v$
0	0	3.4102	826.625	7.6436	4.9250	3.0340
	1	3.4880	1299.000	8.7210	5.5373	3.4060
	2	3.5328	1928.875	9.7983	6.1497	3.7780
	3	6.5646	2738.750	10.8757	6.1497	3.7780
1	1	3.5512	1922.875	9.7983	6.1493	3.7780
	2	3.5880	2726.750	10.8759	6.7621	4.1501
	3	3.6105	3733.125	11.9530	7.3745	4.5221
2	2	3.6192	3727.125	11.9530	7.3745	4.5221
3	3	3.6610	6419.375	14.1077	8.5992	5.2661

TABLE VII

TOPOLOGICAL INDICES FOR $R(EO)_nCH_2CH(OH)CH_2(OE)_mOR'$

Formula				Topological parameter				
R	R'	n	m	I_B	$W(G)$	$^1\chi^v$	$^2\chi^v$	$^3\chi^v$
C_8H_{17}	C_8H_{17}	0	0	3.3705	1551.625	9.6436	6.3392	4.0340
		0	1	3.4464	2247.000	10.7210	6.9516	4.4060
		0	2	3.4965	3129.750	11.7983	7.5639	4.7780
C_8H_{17}	C_4H_9	0	0	3.3643	934.625	7.6436	4.9250	3.0340
		0	1	3.4680	1305.000	8.7210	5.5373	3.4060
		1	1	3.5236	1934.875	9.7983	6.1497	3.7780
C_6H_{13}	C_4H_9	0	1	3.5100	948.000	7.7210	4.8302	2.9060

"increase". Valence molecular connectivity indices are less useful as they are not sensitive to asymmetry of the examined compounds. This is also shown in Table IV. In any case, physico-chemical and topological parameters change in the same way with changes in structural elements.

Let us consider derivatives having $R = R' = C_4H_9$. In this instance, one can omit the influence of this element. In relationships of *PI vs.* I_B, *PI vs.* $W(G)$, *E vs.* I_B and *E vs.* $W(G)$, changes of only two structural elements (*i.e.*, length of oligooxyethylene chains and their asymmetry) cause similar behaviour of both physico-chemical and topological parameters. As an examole, both the polarity index and Balaban index increase with increasing number of oxyethylene units and decrease with increasing asymmetry of the alkyl group. However, asymmetry of oligooxyethylene chains causes an increase in *PI* whereas the Balaban index decreases the *PI vs.* I_B relationship is given in Fig. 2. Significant deviations from a straight line can be seen although the correlation coefficient (R) = 0.9524 and F = 117.26. A similar situation is observed for the relationship between polarity index and Wiener number, $W(G)$. In this instance much better fits to the multiplicative model

$$PI = aI_B^b; \quad R = 0.9938, \quad F = 965.9$$

are presented in Fig. 3a. The same results were obtained for hexoxy derivatives (Fig. 3b).

A similar situation is observed for relationships between the Laffort solubility factor E and both topological indices. The linear relationship for *E vs.* $W(G)$ (Fig. 4) is characterized by R = 0.9124, F = 59.6, but also in this instance deviations from the straight line are considerable. Much better statistical relationships were obtained for multiplicative models for both butoxy and hexoxy derivatives (Fig. 5a, R = 0.9729, F = 212.7; Fig. 5b, R = 0.9529, F = 69.2). The regression of factor E on the Balaban index was characterized by R values well below 0.9.

TABLE VIII

EFFECT OF COMPOUND ASYMMETRY ON TOPOLOGICAL INDICES FOR $R(EO)_nCH_2CH(OH)CH_2(OE)_mOR'$

n	m	$R = R' = C_6H_{13}$			$R = C_8H_{17}$, $R' = C_4H_9$		
		I_B	$W(G)$	$^1\chi^v$	I_B	$W(G)$	$^1\chi^v$
0	4	3.4102	826.625	7.6436	3.3643	834.625	7.6436
0	1	3.4880	1299.000	8.7210	3.4680	1305.000	8.7210
1	1	3.5512	1922.875	9.7983	3.5236	1934.875	9.7983

TABLE IX

EFFECT OF ASYMMETRY IN DISTRIBUTION OF OXYETHYLENE UNITS FOR $BuO(EO)_nCH_2CH(OH)CH_2(OE)_mOBu$

n	m	Topological parameter		
		I_B	$W(G)$	$^1\chi^v$
0	4	3.6025	2402.125	9.9530
1	3	3.6425	2384.125	9.9530
2	2	3.6550	2378.125	9.9530

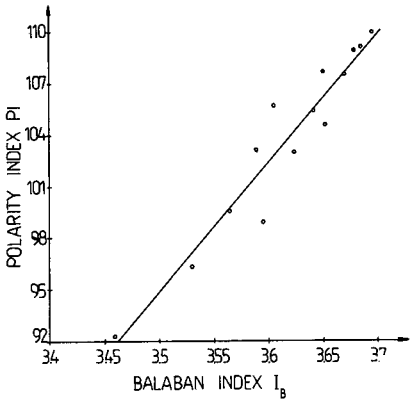

Fig. 2. Linear relationship between polarity index (PI) and Balaban index (I_B).

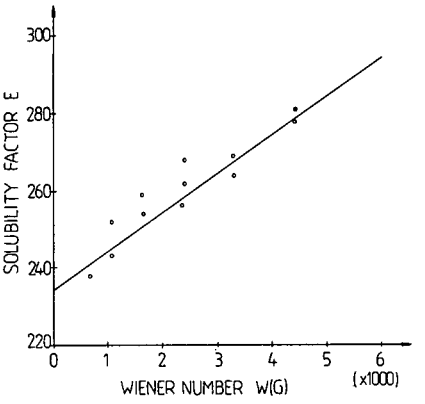

Fig. 4. Linear relationship between solubility factor E and Wiener number $W(G)$ for 1,3-bis[ω-butoxyoligo(oxyethylene)]-2-propanols.

Let us reconsider Table IV. For all 30 compounds examined, *i.e.*, taking into account also the changes in alkyl groups, the most statistically significant correlations should be obtained for the polarity index and Balaban index. In this instance three or four arrows are in the same direction, indicating that the influence of structural elements on PI an I_B is similar.

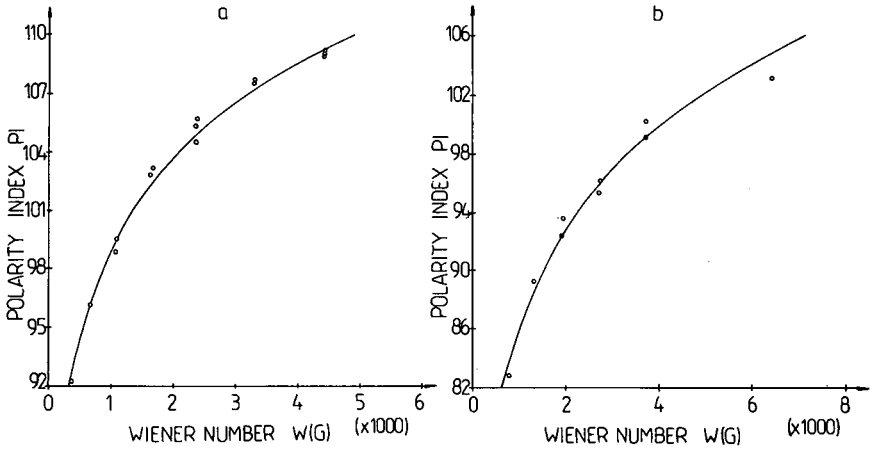

Fig. 3. Relationship between polarity index PI and Wiener number $W(G)$ for (a) 1,3-bis[ω-butoxyoligo(oxyethylene)]-2-propanols and (b) 1,3-bis[ω-hexoxyoligo(oxyethylene)]-2-propanols.

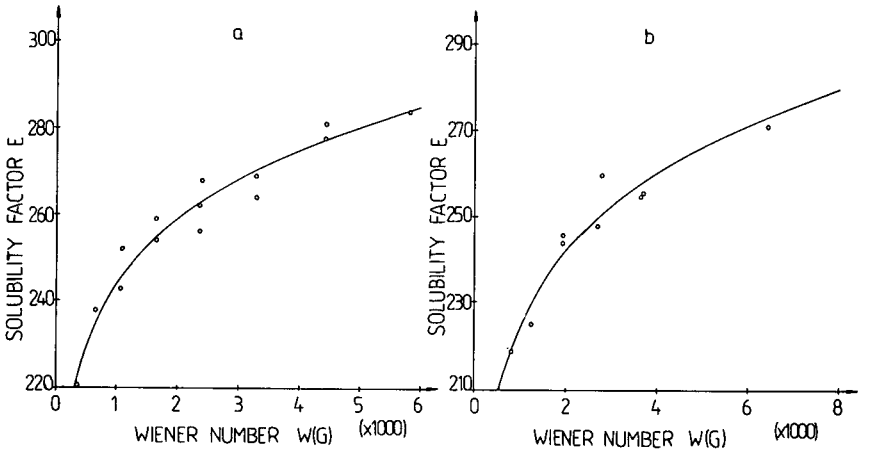

Fig. 5. Relationship between Laffort's solubility factor E and Wiener number $W(G)$ for (a) 1,3-bis[ω-butoxyoligo(oxyethylene)]-2-propanols and (b) 1,3-bis[ω-hexoxyoligo(oxyethylene)]-2-propanols.

CONCLUSIONS

It has been shown that Laffort's solubility parameters could be determined by the technique of inverse GC. The direction of change of some of them (factors E and O) is generally similar to that of the polarity index, an accepted measure of surfactant polarity. The most important difference is the opposite influence of the asymmetry of structural fragments on these two groups of physico-chemical parameters. However, factors E and O could be used as polarity parameters.

The examined topological parameters are generally sensitive to changes in the structure of compounds with the exception of valence molecular connectivity indices, which do not distinguish between symmetric and asymmetric homologues. This means that the Balaban index and Wiener number exhibit a higher discrimination power, *i.e.*, lower degeneracy in comparison with valence connectivity indices.

There is not complete agreement between the changes in physico-chemical and topological parameters caused by the changes in structural fragments (Table IV). However, several statistically satisfactory relationships were derived for polarity index and Wiener number $W(G)$ or Balaban index I_B, and also for factor E and $W(G)$.

Topological indices are sensitive and useful measures of the structure of organic compounds. They could be used in the examination of the influence of structure on, *e.g.*, polarity parameters, such as polarity index and Laffort's solubility factor E.

REFERENCES

1 W. O. McReynolds, *J. Chromatogr. Sci.*, 8 (1970) 685.
2 J. K. Haken, *Adv. Chromatogr.*, 14 (1976) 367.
3 R. V. Golovnya and T. A. Misharina, *J. Chromatogr.*, 190 (1980) 1.
4 C. E. Figgins, B. L. Reinbold and T. H. Risby, *J. Chromatogr. Sci.*, 15 (1977) 208.
5 C. F. Poole and S. K. Poole, *Chem. Rev.*, 89 (1989) 373.
6 Z. Y. Al-Saigh and P. Munk, *Macromolecules*, 17 (1984) 803.
7 E. Fernandez-Sanchez, A. Fernandez-Torres, J. A. Garcia-Dominguez and J. M. Santiuste, *J. Chromatogr.*, 457 (1988) 55.
8 K. Surowiec and J. Rayss, *Chromatographia*, 27 (1989) 412.
9 A. Voelkel, *Crit. Rev. Anal. Chem.*, 22 (1991) 411.
10 B. L. Karger, L. R. Snyder and C. Eon, *J. Chromatogr.*, 125 (1976) 71.
11 B. L. Karger, L. R. Snyder and C. Eon, *Anal. Chem.*, 50 (1978) 2126.
12 J. R. Conder and C. L. Young, *Physicochemical Measurement by Gas Chromatography*, Wiley, New York, 1979.
13 F. Patte, M. Etcheto and P. Laffort, *Anal. Chem.*, 54 (1982) 2239.
14 P. Laffort and F. Patte, *J. Chromatogr.*, 406 (1987) 51.
15 A. Voelkel and J. Janas, *J. Chromatogr.*, 555 (1991) 205.
16 A. Voelkel, J. Szymanowski, J. Beger and K. Ebert, *J. Chromatogr.*, 398 (1987) 31.
17 A. Voelkel, J. Szymanowski, J. Beger and K. Ebert, *J. Chromatogr.*, 409 (1987) 29.
18 A. Voelkel, *J. Chromatogr.*, 435 (1988) 35.
19 V. R. Huebner, *Anal. Chem.*, 34 (1962) 488.

20 T. H. Risby, P. C. Jurs and B. L. Reinbold, *J. Chromatogr.*, 99 (1974) 173.
21 B. L. Reinbold and T. H. Risby, *J. Chromatogr. Sci.*, 13 (1975) 372.
22 C. E. Figgins, T. H. Risby and P. C. Jurs, *J. Chromatogr. Sci.*, 14 (1976) 453.
23 C. E. Figgins, B. L. Reinbold and T. H. Risby, *J. Chromatogr. Sci.*, 15 (1977) 208.
24 J. Ševčik and M. S. H. Löwentap, *J. Chromatogr.*, 217 (1981) 139.
25 M. Roth and J. Novak, *J. Chromatogr.*, 234 (1982) 337.
26 A. Voelkel, *J. Chromatogr.*, 450 (1988) 291.
27 S. K. Poole and C. F. Poole, *J. Chromatogr.*, 500 (1990) 329.
28 I. Gutman and N. Trinajstič, *Top. Curr. Chem.*, 42 (1979) 49.
29 L. Ekiert, J. Bojarski and J. L. Mokrosz, *Wiad. Chem.*, 40 (1986) 65.
30 M. Razinger, J. R. Chretien and J.-E. Dubois, *J. Chem. Inf. Comput. Sci.*, 25 (1985) 23.
31 A. Voelkel, *Chromatographia*, 25 (1988) 655.
32 R. Kaliszan, in P. R. Brown and R. A. Hartwick (Editors), *High Performance Liquid Chromatography* (*Chemical Analysis Series of Monographs*, Vol. 22), Wiley, New York, 1989, p. 563.
33 R. Kaliszan, *Crit. Rev. Anal. Chem.*, 16 (1986) 323.
34 A. T. Balaban, *Chem. Phys. Lett.*, 89 (1982) 399.
35 M. Barysz, G. Jashari, R. S. Lall and V. Shrivastava, *Stud. Phys. Theor. Chem.*, 28 (1983) 222.
36 A. Voelkel, *J. Chromatogr.*, 464 (1989) 251.
37 A. Voelkel, *J. Chromatogr.*, 547 (1991) 247.
38 J. Szymanowski, *Crit. Rev. Anal. Chem.*, 21 (1990) 407.
39 J. K. Haken, *Adv. Chromatogr.*, 17 (1979) 163.
40 I. G. Fineman, *J. Am. Oil Chem. Soc.*, 46 (1969) 296.
41 J. Szymanowski, *Tenside Deterg.*, 26 (1989) 198.
42 J. Szymanowski, M. Cox, C. G. Hirons, *J. Chem. Technol. Biotechnol.*, 34A (1984) 218.
43 J. Szymanowski, *Polyhedron*, 4 (1985) 269.
44 J. Szymanoski, A. Voelkel and Z. A. Rashid, *J. Chromatogr.*, 402 (1987) 55.
45 J. Szymanowski and A. Voelkel, *J. Chem. Technol. Biotechnol.*, 54 (1992) 19.
46 W. C. Griffin, *J. Soc. Cosmet. Chem.*, 1 (1949) 311.

Journal of Chromatography, 623 (1992) 93–103
Elsevier Science Publishers B.V., Amsterdam

CHROM. 24 437

Thermal desorption cold trap-injection in high-resolution gas chromatography: multivariate optimization of experimental conditions

Anna-Lena Sunesson, Carl-Axel Nilsson and Barbro Andersson

Analytical Chemistry Division, National Institute of Occupational Health, P.O. Box 7654, S-907 13 Umeå (Sweden)

Rolf Carlson

Department of Organic Chemistry, University of Umeå, S-901 87 Umeå (Sweden)

(First received March 2nd, 1992; revised manuscript received June 17th, 1992)

ABSTRACT

In studies of low concentrations of volatile compounds in air, the method of adsorption on porous polymers and determination by thermal desorption cold trap-injection high-resolution gas chromatography is finding increasing application. Factors considered important for injection and chromatographic separation of volatile compounds by this method were investigated with the use of multivariate techniques. For the amount injected on to the chromatographic column, the factors of main importance were found to be the temperature of the injection block, the thickness of the internal coating of the cold trap and the flow-rate. Strong interaction effects were noted. For the sharpness of the chromatographic peaks, the flow-rate was the most important factor.

INTRODUCTION

Thermal desorption cold trap-injection high-resolution gas chromatography is an effective method for the determination of low concentrations of volatile compounds in air. Some studies have been reported concerning the important factors controlling desorption [1,2], but the injection step has not yet been well examined. As many factors presumably exert a joint action both on the injection and on the chromatographic performance, this study was performed using multivariate methods, which take possible interaction effects into account. Such interaction effects are common in chemistry, and a traditional approach, *i.e.*, considering the factors one at a time, is bound to fail if interaction effects are present [3].

Microorganisms such as various species of moulds and bacteria are often found to be the source of contamination of water-damaged buildings, often giving rise to health problems for the inhabitants. The aim of this study was to optimize analytical conditions for the determination of volatile metabolites produced by such microorganisms in affected buildings as well as in laboratory studies. These studies were performed on a test mixture consisting of eight different compounds, selected as being representative of compounds arising from culture media and of some compounds expected to be produced by microorganisms. These compounds also differ sufficiently in polarity and volatility to make these studies of general interest.

Correspondence to: Dr. Anna-Lena Sunesson, Analytical Chemistry Division, National Institute of Occupational Health, P.O. Box 7654, S-907 13 Umeå, Sweden.

0021-9673/92/$05.00

OPTIMIZATION

The various experimental factors must be assumed to have a joint action, and it is therefore necessary to approach the problem by multivariate methods. The overall strategy was (a) first to identify the most important experimental factors by a screening experiment and (b) then to adjust these factors by a response surface technique to an optimum chromatographic performance. For evaluation of the results, we considered it necessary to consider both the amounts of injected material and the chromatographic separation.

Attempts at using various chromatographic response functions (CRFs) [4,5,6] which compress the multi-dimensional response into a single criterion were considered unsuitable. Such single-criterion response functions over-emphasize short retention times and assume that the eluted peaks are fairly evenly distributed over the whole chromatogram and occur to some extent close to each other. The composition of our test mixture did not fulfil this requirement. A minimum retention time was not considered necessary because, in this study, the chromatographic separation is not the most time-consuming part of the whole procedure. Moreover, in the application of the procedure to real samples, it could not be expected that samples will contain volatile components fulfilling the above-mentioned criteria. Instead, in order to achieve a more general optimization, our objective was to obtain a maximum of injected desorbed material and acceptable peak shapes over the whole chromatogram.

EXPERIMENTAL

Chemicals and adsorbent

The chemicals used in the test mixture were *n*-hexane (FSA Laboratory Supplies, HPLC grade), dimethyl disulphide (Janssen, p.a.), 3-methyl-2-pentanone (Aldrich, 99%), benzaldehyde (Kebo, puriss), n-decanal (Aldrich, 98%), *n*-tetradecane (Fluka, puriss) and geosmin, synthesized according to Hansson and co-workers [7,8]. Tenax TA (60–80 mesh) (Chrompack, 90 mg per sampling tube) was used as adsorbent in the experiments. The sampling tubes were made of glass (159 mm × 6 mm O.D. × 3 mm I.D.).

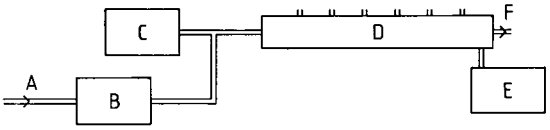

Fig. 1. Generation of samples. A = compressed air cleaned through oil filters and molecular sieve; B = moisturizing outfit consisting of three water-filled dispersion bottles in a thermostated water bath; C = microinjection pump for continuous injection of the test mixture; D = sampling chamber (Teflon, 900 × 80 × 60 mm^3) with six outlets for sampling; E = Relative humidity meter; F = air outlet.

Generation of samples

A sampling atmosphere of the test mixture in low concentration (see Table I) was dynamically generated according to Fig. 1. The test mixture was slowly injected (25 nl/min) into a stream of air by means of a microinjection pump (Carnegie Medicin CMA/100). A 50 μl gas-tight syringe (SGE) was used for the injection. The air flow-rate was maintained at 40 l/min and the relative humidity of the air was adjusted to 60%. Samples were sorbed on Tenax by pumping the sampling atmosphere through the tubes at 100 ml/min for 5 min. Three generations were made, and six analyses were run from each generation to check the repeatability and standard deviation before further use of the spiked tubes in the optimization experiments.

Injection and chromatographic separation

The experiments were run on a commercial thermal desorption injector (Chrompack 16400 purge and trap injector, modified for thermal desorption injection according to the Chrompack modification manual M-16420-85-2).

The sample, adsorbed on Tenax, was desorbed by heating the sampling tube in the desorption oven. A flow of helium transferred the desorbed substances to a cold trap (Fig. 2), a fused-silica capillary coated with a 5% phenyl and 95% methyl polysiloxane phase (Chrompack CP-TM-Sil-8CB). Sub-ambient trap temperatures were created by passing a stream of nitrogen cooled by liquid nitrogen through the trap compartment. The cold trap was then rapidly heated (15°C/s) in order to inject the sample onto the chromatographic column.

Desorption was performed at 220°C for 15 min, using a desorption gas flow-rate of 20 ml/min. The measurements were carried out on an HP 5890 gas

TABLE I

TEST MIXTURE SUBSTANCES AND CONCENTRATIONS IN TEST ATMOSPHERE

No.	Substance	Concentration ($ng\ l^{-1}$)	B.p. (°C)[a]	R.S.D. (%)[b]
1	Hexane	70	68	7
2	Dimethyl disulphide	70	109	6
3	3-Methyl-2-pentanone	82	118	4
4	Toluene	80	111	6
5	Benzaldehyde	72	178	9
6	Decanal	73	208–209	15
7	Tetradecane	68	254	9
8	Geosmin	68	[c]	11

[a] B.p. = Boiling point at atmospheric pressure.
[b] R.S.D. = Relative standard deviation, due to exposure, sample generation, sampling and analysis, based on 18 runs.
[c] Data not available.

chromatograph with a fused-silica column (HP Ultra 2, 50 m × 0.2 mm I.D., coated with cross-linked 5% phenylmethylsilicone, 0.33 μm) and a flame ionization detector. The detector temperature was 200°C. The starting temperature of the chromatographic separation was 30°C and the final temperature was 200°C. An HP 3392A integrator was used as a recorder.

Experimental factors and responses

Many factors may influence the results. Some factors were known *a priori* to be important and the task was to determine the trend and magnitude of their influence. Other factors presumably exert an influence, but their roles remained to be ascertained.

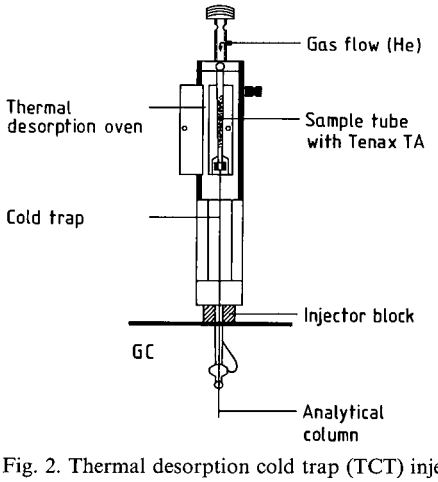

Fig. 2. Thermal desorption cold trap (TCT) injector.

The following nomenclature will be used: x_i denotes the coded setting of factor i. The response models described below are expressed in the coded variables. The following factors were studied:

(1) final temperature of the cold trap (see Fig. 2); this setting thus defines the temperature of the sample when transferred to the injection block;

(2) initial temperature of the cold trap;

(3) temperature of the injection block;

(4) thickness of the internal coating of the cold trap;

(5) duration of injection;

(6) additional time during which the chromatographic column was maintained at its starting temperature value;

(7) temperature rise during the chromatographic separation;

(8) flow-rate; this defines the flow-rate both through the cold trap during injection and through the chromatographic column at its starting temperature;

(9) temperature setting of the cold trap after the injection was completed.

The range of variations of the experimental factors is specified in Table II. Using coded normalized factor settings instead of their natural value has the advantage that the relative importance of each variable can be evaluated directly from the model [3].

The measured results of the chromatographic procedure are called responses. For each constitu-

TABLE II

RANGE OF VARIATIONS OF EXPERIMENTAL FACTORS

Factor No.	Low level (−)	Medium level (0)	High level(+)
1	+130°C	+160°C	+200°C
2	−100°C	−125°C	−150°C
3	+150°C	+200°C	+250°C
4	A[a]	A[a,b]	B[a]
5	1 min	3 min	5 min
6	$1 \cdot t_0$	$1.5 \cdot t_0$	$2 \cdot t_0$
7	3°C/min	6.5°C/min	10°C/min
8	10 cm/s	22 cm/s	34 cm/s
9	<0°C	Room temperature[b]	Room temperature

[a] A = CP-TM-SIL-8CB, d_f = 1.2 μm, I.D. = 0.32 mm. B = CP-TM-SIL-8CB, d_f = 5.0 μm, I.D = 0.5 mm.
[b] Only two levels tested for these factors.

ent (k = 1–8, Table I), two characteristics were measured: A_k, the area of the chromatographic peak, and W_k, the width of the peak at half its maximum height.

Experimental design

The overall strategy for the study presented in this paper was as follows:

(A) run a pilot experiment to validate the experimental domain;

(B) vary the experimental factors considered to be important in a screening experiment with a view to identifying the most important factors;

(C) perform additional experiments to find optimum performance.

The pilot experiment consisted of two experimental runs, one in which all experimental factors were set at their upper value, and another in which all experimental factors were set at their lower value. This was done to ensure that the responses show a significant variation within the domain and that none of the extreme points yields non-useful responses.

To ensure an orthogonal variation of the nine experimental factors, a replicated two-level fractional design 2^{9-5} was used in the screening (entries 1–32, Table III). These experiments were employed to fit a response surface model, containing linear terms $b_i x_i$ and cross-produced terms $b_{ij} x_{ij}$. The coefficients of the cross-product terms are aliased two-factor interactions [9]; see Appendix. Results are given in the next section.

Based on the results from the screening, additional experiments were carried out with a view to further optimization of the experimental conditions. One significant factor, 4 (thickness of the internal coating of the cold trap), was set at its upper level. The following factors were maintained at their average setting throughout the experimental study: 3 (temperature of the injection block), 6 (additional time during which the chromatographic column was maintained at its starting temperature) and 7 (temperature rise during the chromatographic separation). One variable, 9 (temperature setting of the cold trap after the injection was completed), was not further varied as its variation was found insignificant in the screening. For the remaining factors (1, 2, 5 and 8), experiments were run to complete a variation of these factors on three levels (−1, 0, +1), entries 33–50. This also permits square terms for these factors to be included in the model to describe non-linear effects, *i.e.*, curvature of the response surface.

Mathematical methods

Principles of response surface technique. It is reasonable to assume that the variation of the observed responses y ($y = A_k$ and W_k) is functionally related to the detailed settings of the experimental factors. However, as the responses are experimentally determined, there will always be an experimental error component (e). We therefore write the functional relationship between the observed response and the experimental factors as

$$y = f(x_1 \ldots x_9) + e$$

TABLE III

EXPERIMENTAL DESIGN FOR SCREENING AND OPTIMIZATION

1–9 are the experimental factors, and their settings (+, − or 0) corresponds to the values specified in Table II.

Entry	1	2	3	4	5	6	7	8	9	Entry	1	2	3	4	5	6	7	8	9
1	−	−	−	−	−	−	−	−	+	28	+	+	−	+	−	+	−	−	−
2	+	−	−	−	+	+	+	−	−	29	−	−	+	+	+	+	−	−	+
3	−	+	−	−	+	+	−	+	−	30	+	−	+	+	−	−	+	−	−
4	+	+	−	−	−	−	+	+	+	31	−	+	+	+	−	−	−	+	−
5	−	−	+	−	+	−	+	+	−	32	+	+	+	+	+	+	+	+	+
6	+	−	+	−	−	+	−	+	+	33	0	0	0	+	0	0	0	0	+
7	−	+	+	−	−	+	+	−	+	34	+	0	0	+	0	0	0	0	+
8	+	+	+	−	+	−	−	−	−	35	−	0	0	+	0	0	0	0	+
9	−	−	−	+	−	+	+	+	−	36	0	+	0	+	0	0	0	0	+
10	+	−	−	+	+	−	−	+	+	37	0	−	0	+	0	0	0	0	+
11	−	+	−	+	+	−	+	−	+	38	0	0	0	+	+	0	0	0	+
12	+	+	−	+	−	+	−	−	−	39	0	0	0	+	−	0	0	0	+
13	−	−	+	+	+	+	−	−	+	40	0	0	0	+	0	0	0	+	+
14	+	−	+	+	−	−	+	−	−	41	0	0	0	+	0	0	0	−	+
15	−	+	+	+	−	−	−	+	−	42	0	0	0	+	0	0	0	0	+
16	+	+	+	+	+	+	+	+	+	43	+	0	0	+	0	0	0	0	+
17	−	−	−	−	−	−	−	−	+	44	−	0	0	+	0	0	0	0	+
18	+	−	−	−	+	+	+	−	−	45	0	+	0	+	0	0	0	0	+
19	−	+	−	−	+	+	−	+	−	46	0	−	0	+	0	0	0	0	+
20	+	+	−	−	−	−	+	+	+	47	0	0	0	+	+	0	0	0	+
21	−	−	+	−	+	−	+	+	−	48	0	0	0	+	−	0	0	0	+
22	+	−	+	−	−	+	−	+	+	49	0	0	0	+	0	0	0	+	+
23	−	+	+	−	−	+	+	−	+	50	0	0	0	+	0	0	0	−	+
24	+	+	+	−	+	−	−	−	−	51	−	0	+	+	0	0	+	+	0
25	−	−	−	+	−	+	+	+	−	52	−	0	+	+	0	0	+	+	0
26	+	−	−	+	+	−	−	+	+	53	−	0	+	+	0	0	+	+	0
27	−	+	−	+	+	−	+	−	+	54	−	0	+	+	0	0	+	+	0

It is not possible to derive an analytical expression for f from purely theoretical considerations. It is reasonable to assume, however, that f can be approximated by a Taylor expansion when the range of variation in the independent factors x_1–x_9 is limited. A Taylor expansion will take the form of a polynomial in the independent factors:

$$y = b_0 + \Sigma b_1 x_1 + \Sigma\Sigma b_{ij} x_i x_j + \Sigma\Sigma\Sigma b_{ijk} x_i x_j x_k + \ldots + e$$

A sufficiently good approximation can often be obtained if the Taylor expansion is truncated after the second degree terms. The polynomial coefficients (model parameters) can be estimated by least squares multiple regression of the polynomial to the observed responses.

The systematic variation induced by changing the experimental conditions is thus described by the coefficients of the polynomial model. In order to be considered significant, an experimental factor must produce a variation in the response above the noise level e, caused by the experimental error. The error variation can be assumed to be normally and independently distributed. Hence, significant variables can be identified by plotting the corresponding coefficients on normal probability paper. A normally distributed random error variation will be depicted by a straight line. Significant model coefficients will appear as outliers. To the right of the line in the upper right quadrant, or to the left in the lower left quadrant, such effects are either too small or too large to be error variations. For details of this technique, see ref. 10.

Principal component (PC) analysis. To analyse the systematic variation of the responses over the entire set of the responses, the response matrices

were subjected to principal component decomposition. There are two kinds of responses. A PC model was established for each of them separately. Detailed accounts of PC analysis have been given elsewhere [11–13]. Here, it is sufficient to say that principal components partition the response matrix into two parts: *scores* and *loadings*. The scores describe the systematic between-objects variation over the entire set. Hence the score vector can be used as a response vector for the entire set of experiments. The score value is a linear combination of the original response variables, and thus the error will also have an approximately normal distribution. Significant experimental factors can therefore be discerned by a normal probability plot of estimated model parameters obtained by fitting the response model to the score vector. A thorough discussion of this technique in screening experiments is given in ref. 14, and its application to response surface modelling has been described by Bratchell [15]. To avoid overfitting, the principal component models were established through cross-validations [16]. Prior to computing the principal components, the original response variables were scaled to unit variance. In this way, an equal importance of each response is assumed and blow-up of the variance because of differences in magnitude in the recorded responses is avoided. For a discussion on scaling in principal component analysis, see ref. 13. The loadings describe how the response variables take part in this systematic variation.

RESULTS AND DISCUSSION

The experimental design is shown in Table III. The observed responses in these experiments are summarized in Tables IV and V.

Analysis of the residuals after fitting a second-order interaction model to the screening design (entries 1–32) indicated a systematic lack of fit. Plotting the residuals against the response value predicted by the model showed a U-shaped scatter plot. This indicated that an improved model fit was likely to be expected if square terms were also included in the model.

Principal component analysis and response model fitting to the score vectors

Peak surfaces. Principal component analysis of the data in Table IV afforded one highly significant component and two additional components of borderline significance (72 + 12 + 6% explained variance). Taking into account the fact that the measured peak areas differ in magnitude, this result was to be expected. Because of this and because peak areas cannot be negative, a logarithmic transformation of the original data could be expected to yield an improved principal component model fit. Principal component analysis of the logarithmically transformed peak areas afforded one significant component which accounted for 70% of the total variance. The corresponding score values are summarized in Table IV (t-values). The loadings (p-values) are given as the bottom line in the table.

The following response model was obtained by least squares fitting to the score values given in Table IV:

$$t_1(\log \text{ area}) = -4.04 + 0.004x_1 - 0.18x_2 + 1.16x_3 + 2.02x_4 - 0.01x_5 + 0.50x_6 + 0.26x_7 + 0.22x_8 - 0.14x_9 + 0.02x_1x_2 + 0.17x_1x_3 - 0.08x_1x_4 - 0.27x_2x_3 + 0.27x_2x_4 + 0.86x_3x_4 + 1.32x_1^2 - 0.41x_2^2 + 0.31x_5^2 + 2.37x_8^2$$

The estimated cross-product coefficients represent aliased two-factor interactions; see Appendix. A normal probability plot of the estimated coefficients is shown in Fig. 3. A plot of the residuals against the estimated score value is shown in Fig. 4. The plot does not indicate a lack of fit [17,18]. Fig. 5–7 show three-dimensional plots of the response surface.

Peak widths. A one-component PC model was significant according to cross-validation and accounted for 90% of the total variance of the responses in Table V. The following response model was determined from the score vector:

$$t_1(\text{peak width}) = -1.56 - 0.06x_1 + 0.03x_2 + 0.11x_3 - 0.05x_4 + 0.16x_5 + 0.08x_6 - 0.58x_7 - 2.90x_8 + 0.06x_9 - 0.14x_1x_2 + 0.03x_1x_3 - 0.01x_1x_4 + 0.08x_2x_3 - 0.05x_2x_4 - 0.03x_3x_4 + 0.23x_1^2 + 0.15x_2^2 + 0.15x_5^2 + 2.19x_8^2$$

A normal probability plot of the estimated coefficients is shown in Fig. 8.

Evaluation of each response separately

When each response variable was fitted separately with the response functions given above, the results were almost identical to those obtained from the score vectors.

TABLE IV

OBSERVED RESPONSES; PEAK AREAS (INTEGRATOR COUNTS)

Entry	A_1	A_2	A_3	A_4	A_5	A_6	A_7	A_8	t_1
1	13 592	4 482	12 917	19 630	8 427	3 844	9 948	7 485	−4.12
2	13 559	4 607	13 945	19 334	11 849	6 922	12 752	10 381	−1.79
3	15 381	5 067	15 208	22 185	12 495	5 039	10 843	8 561	−2.17
4	14 129	3 540	13 558	28 952	13 116	5 422	11 436	8 890	−2.20
5	15 413	5 623	17 807	24 935	13 986	4 967	12 816	10 284	−0.82
6	13 339	4 933	14 987	21 778	11 229	4 438	11 648	9 013	−2.44
7	16 808	5 297	16 011	22 075	11 710	4 230	10 930	8 500	−2.27
8	13 790	4 695	14 010	22 115	10 416	4 236	9 646	7 104	−3.49
9	21 902	6 518	19 217	27 540	13 089	7 568	15 033	12 221	0.90
10	15 919	5 616	16 765	25 260	13 616	8 597	12 875	10 129	−0.28
11	16 733	5 302	15 682	23 122	14 860	7 053	13 288	10 638	−0.53
12	19 294	5 706	16 673	24 584	10 191	5 436	10 497	8 240	−1.87
13	19 367	10 147	30 002	46 446	15 729	7 305	13 426	10 507	2.69
14	19 518	11 376	33 282	43 578	23 107	6 898	14 143	11 044	3.59
15	23 641	7 723	23 590	35 052	18 124	7 386	13 867	11 005	1.98
16	25 281	8 249	25 085	38 009	23 454	10 524	19 763	16 183	4.45
17	14 053	4 600	13 480	19 450	9 082	4 557	10 647	8 068	−3.47
18	–	–	–	–	–	–	–	–	–
19	15 518	5 240	15 893	24 493	12 233	5 337	10 337	7 973	−2.07
20	15 886	4 721	14 366	22 948	11 266	4 287	9 652	7 597	−4.47
21	16 069	5 599	16 967	24 771	12 437	4 030	10 367	7 859	−2.16
22	15 652	6 451	19 078	29 427	16 252	5 739	13 050	10 148	0.14
23	20 424	5 545	16 149	23 914	8 820	3 803	8 786	6 317	−3.39
24	12 232	4 368	13 156	19 135	11 679	4 154	12 096	9 364	−2.96
25	21 156	6 392	18 583	27 056	11 708	7 656	13 378	10 755	0.19
26	14 842	4 994	15 042	21 782	11 082	4 757	10 450	8 352	−2.61
27	17 808	5 573	16 551	24 439	15 320	6 166	13 247	10 157	−0.48
28	20 545	6 456	18 991	28 121	14 424	8 366	14 701	12 142	1.06
29	19 867	11 161	33 232	49 767	22 167	9 795	18 069	15 087	5.12
30	19 117	10 441	30 765	50 515	21 619	7 044	14 756	11 387	3.61
31	23 017	7 729	23 443	34 746	19 408	8 870	16 515	14 086	3.01
32	27 282	8 363	25 444	40 163	21 582	9 806	19 025	14 880	4.21
33	18 876	6 717	19 947	30 280	13 331	8 068	15 788	12 072	1.21
34	18 501	6 619	19 126	26 977	12 294	8 412	15 087	12 418	0.76
35	20 496	7 311	21 355	32 270	14 078	8 021	14 940	12 268	1.59
36	18 339	6 717	19 817	31 283	13 790	7 339	14 647	11 063	0.88
37	19 098	6 872	18 330	29 199	13 367	–	10 587	9 089	−0.46
38	16 853	6 322	17 935	27 160	10 949	7 039	10 115	8 786	−1.09
39	20 079	7 220	21 112	35 534	17 127	8 147	14 720	11 333	1.82
40	22 667	7 414	22 270	38 325	19 736	10 851	16 873	12 924	3.16
41	24 007	6 907	20 827	32 459	15 047	8 050	14 041	10 726	1.34
42	15 107	5 942	16 732	25 363	11 366	6 206	12 696	9 390	−1.03
43	18 596	7 219	20 516	31 667	13 563	7 596	15 293	12 279	1.34
44	20 048	7 294	20 872	32 380	15 308	8 311	15 585	12 654	1.84
45	18 261	6 087	19 066	29 063	12 541	8 562	11 338	9 944	−0.04
46	17 576	6 231	17 318	27 658	9 581	6 390	8 968	7 603	−1.89
47	18 305	6 596	18 401	28 514	11 425	7 515	9 653	8 351	−0.89
48	18 230	7 241	20 924	31 270	19 402	7 985	14 138	10 824	1.55
49	–	–	–	–	–	–	–	–	–
50	23 114	9 640	28 681	41 745	15 081	6 887	13 548	11 249	2.51
51	16 974	5 841	18 496	27 673	12 747	6 839	12 956	9 939	–
52	20 474	7 008	22 463	34 328	15 559	7 951	14 260	11 173	–
53	22 291	6 484	20 647	33 335	17 065	9 061	14 729	12 114	–
54	18 827	6 412	20 260	29 463	13 358	7 484	12 798	10 285	–
p	0.2491	0.3676	0.3788	0.3726	0.3665	0.3473	0.3606	0.3681	

TABLE V

OBSERVED RESPONSES; PEAK WIDTHS (MM)

Entry	W_1	W_2	W_3	W_4	W_5	W_6	W_7	W_8	t_1
1	8.0	11.5	10.25	11.25	13.25	12.5	13.5	17.75	4.33
2	10.5	9.0	8.5	8.75	12.75	11.5	12.75	17.5	3.67
3	2.75	5.25	5.5	5.5	5.5	5.25	5.75	6.0	−0.91
4	2.25	2.75	2.75	–	3.0	2.75	3.0	3.5	−2.97
5	3.25	3.0	3.25	3.0	3.0	2.75	3.25	3.5	−2.44
6	3.5	4.5	4.75	4.75	5.75	5.0	5.75	5.75	−1.09
7	11.0	9.0	8.5	9.0	13.5	12.0	13.25	18.5	3.97
8	9.5	12.5	11.0	11.75	13.5	12.75	14.0	18.5	4.91
9	3.25	3.0	3.0	–	3.0	2.75	3.0	3.75	−2.47
10	3.0	4.75	5.0	5.0	5.75	5.0	5.5	5.75	−1.08
11	7.25	9.0	8.75	9.5	15.5	11.75	13.0	18.0	3.69
12	10.5	11.5	11.75	11.5	13.5	12.75	13.25	17.5	3.98
13	10.5	12.5	12.0	12.25	13.25	11.75	13.0	17.5	4.95
14	6.75	9.5	9.0	9.25	11.75	11.75	12.75	17.0	3.28
15	3.0	4.0	4.5	4.5	5.75	5.5	5.75	6.0	−1.20
16	3.25	3.75	4.0	3.75	3.5	2.75	3.25	3.5	−2.14
17	8.0	11.5	10.25	11.0	13.25	12.25	13.25	17.5	4.25
18	–	–	–	–	–	–	–	–	–
19	–	–	–	–	–	–	–	–	–
20	2.25	2.75	3.0	3.0	3.0	2.75	3.0	3.25	−2.67
21	–	–	–	–	–	–	–	–	–
22	–	–	–	–	–	–	–	–	–
23	–	–	–	–	–	–	–	–	–
24	–	–	–	–	–	–	–	–	–
25	3.0	2.75	3.0	3.0	3.0	3.0	3.0	3.5	−2.54
26	3.25	5.0	5.0	5.25	5.25	5.5	5.5	6.0	−0.98
27	–	–	–	–	–	–	–	–	–
28	–	–	–	–	–	–	–	–	–
29	–	–	–	–	–	–	–	–	–
30	–	–	–	–	–	–	–	–	–
31	–	–	–	–	–	–	–	–	–
32	3.0	3.75	4.0	3.75	3.5	2.75	3.25	3.75	−2.16
33	4.25	4.5	4.0	4.25	4.5	4.25	4.5	5.5	−1.44
34	4.0	4.25	4.0	4.25	4.5	4.25	4.5	5.5	−1.50
35	4.0	4.5	4.0	4.0	4.25	4.25	4.5	5.75	−1.50
36	4.0	4.25	4.0	4.25	4.5	4.0	4.25	5.5	−1.54
37	4.0	4.25	4.0	4.0	4.25	4.25	4.5	5.5	−1.54
38	4.0	4.5	4.0	4.25	4.5	4.0	4.5	5.5	−1.49
39	3.5	4.25	3.75	4.0	4.5	4.0	4.5	5.5	−1.64
40	3.0	3.5	3.25	3.5	3.75	3.5	3.5	3.75	−2.20
41	9.5	9.75	8.75	–	12.0	12.75	13.0	18.0	2.91
42	4.0	4.5	4.0	4.25	4.5	4.0	4.5	5.5	−1.49
43	4.25	4.25	4.0	4.25	4.5	4.25	4.5	5.5	−1.47
44	4.0	4.5	4.25	4.5	4.5	4.25	4.5	5.5	−1.41
45	4.0	4.25	4.0	4.25	4.5	4.25	4.5	5.5	−1.50
46	4.0	4.25	4.0	4.0	4.5	4.0	4.5	5.75	−1.53
47	–	–	–	–	–	–	–	–	–
48	–	–	–	–	–	–	–	–	–
49	–	–	–	–	–	–	–	–	–
50	9.5	–	–	9.0	11.25	11.5	12.75	17.25	3.69
51	–	–	–	–	–	–	–	–	–
52	–	–	–	–	–	–	–	–	–
53	3.5	3.0	3.25	–	3.0	2.75	3.25	3.25	–
54	3.25	3.25	3.0	3.0	3.0	2.75	3.25	3.5	–
p	0.3487	0.3671	0.3656	0.3160	0.3633	0.3338	0.3657	0.3647	

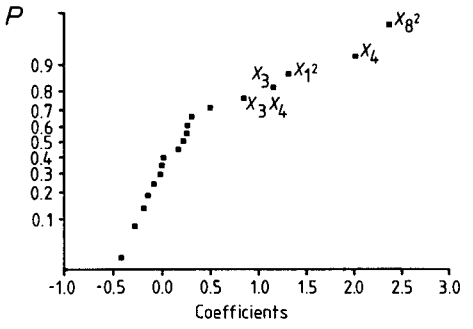

Fig. 3. Normal probability plot of estimated coefficients; log peak areas.

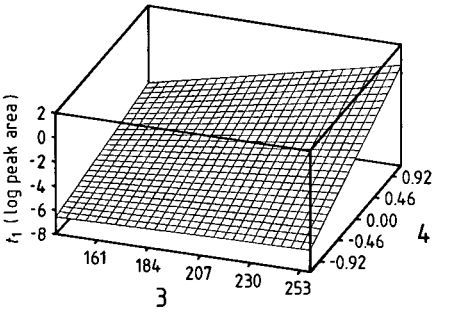

Fig. 5. Response surface of log peak areas against temperature of injection block against thickness of internal coating of cold trap.

Interpretations

From the results presented above, we conclude that the following experimental factors exert a significant influence on chromatographic performance.

Peak areas: a weak influence of factor 1 (final temperature of the cold trap); a strong linear influence of 3 (temperature of the injection block) and 4 (inner coating of the cold trap) and a strong interaction effect between 3 and 4; and a strong significant non-linear influence of the flow-rate (8).

Peak widths: as expected, the most important factor is 8 (flow-rate); an influence (however weak) of 7 (temperature rise) is also found.

Preferred settings of the experimental factors

For obtaining the desired result, maximum injected sample (maximum peak area) and sharp peaks, the following settings of the experimental factors can be inferred from the results above:

(1) the final temperature of the cold trap should be at its lower setting;

(2) the initial temperature of the cold trap could be set at any value in the explored range of variation;

(3) because of the strong interaction effect with factor 4, the temperature of the injection block should be set at its upper value;

(4) a cold trap with a thick-layered inner coating should be used (see 3.);

(5,6) the duration of the injection and the additional time during which the chromatographic column is maintained at its starting temperature can be set at any value in the explored domain;

(7) the temperature rise during chromatography should be at its higher value to ensure sharp peaks;

(8) the flow-rate should be set at its higher level;

(9) the temperature of the cold trap after injection is completed has no significant influence within the experimental domain.

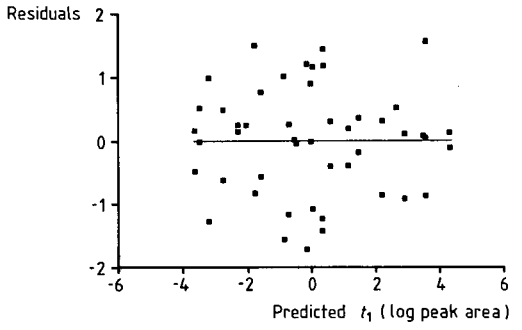

Fig. 4. Residuals against estimated score value; log peak areas.

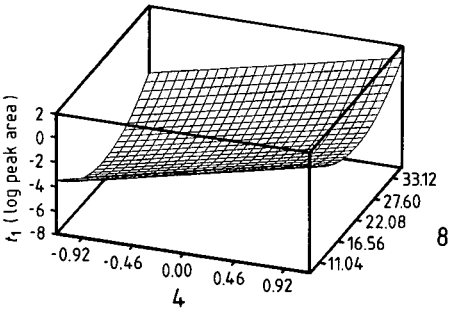

Fig. 6. Response surface of log peak areas against thickness of internal coating of cold trap against flow-rate.

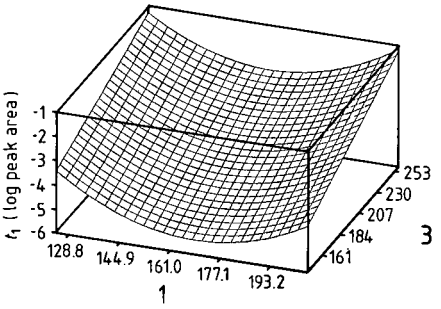

Fig. 7. Response surface of log peak areas against final temperature of cold trap against temperature of injection block.

Replicated experiments carried out under the conditions indicated above are shown in Table III, entries 51–54. The corresponding results are shown in Tables IV and V. These results confirm the conclusions with regard to the sharpness of the chromatographic peaks. For the peak areas, the results are good but are not at their possible maximum value as predicted by the model. An unexpected observation is that the integrated peak areas show a minimum along the flow-rate variation. This observation was made for all compounds in the test mixture and is not an artifact. The reason for this is not yet fully understood. The best results were found at the extremes of the flow-rate variation. The flow-rate variation was chosen in order to cover the minimum of the Van Deemter relationships, as determined for geosmin and 3-methyl-2-pentanone.

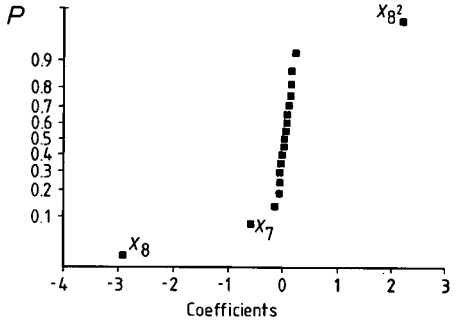

Fig. 8. Normal probability plot of estimated coefficients; peak widths.

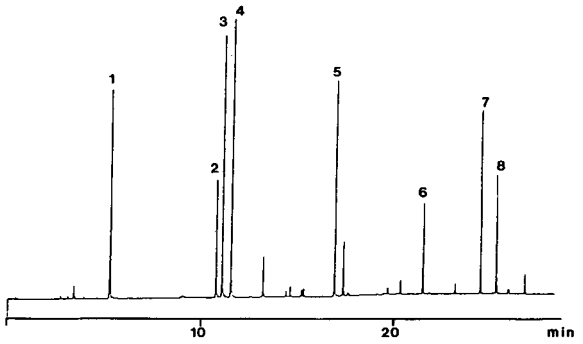

Fig. 9. Chromatogram of the test mixture after optimization. Substances 1–8 according to Table I. Chromatographic conditions are given under Experimental.

CONCLUSIONS

The results obtained provided the information required for establishing the optimum conditions for the thermal desorption injection and chromatography. The advantages of a multivariate strategy are evidenced by the finding of strong interaction effects between the experimental factors. We note that a traditional approach, *i.e.*, considering the factors one at a time, would have failed because of the presence of interaction effects [3].

To simplify the problem of multiple responses, that is, characteristics of all peaks in the chromatograms, we used principal component modelling to obtain a description of the *systematic* variation over the set of experiments. This variation is described by the score vectors. In all instances the different characteristics were described by one significant component, which thus served as a single criterion. Contrary to different chromatographic response functions, the multivariate information is not lost in the principal component model. It is always possible to go back to the original responses.

One important consequence of the optimized procedure is that the total time of analysis can be kept conveniently short without loss of quality of the eluted peaks (see Fig. 9).

ACKNOWLEDGEMENTS

Generous funding by the Centre for Environmental Research (CMF) for this project is gratefully acknowledged. We also acknowledge financial sup-

port by the Swedish Natural Science Research Council to one of us (R. C.).

APPENDIX

The 2^{9-5} fractional design used in the screening experiment was constructed from a complete two-level, four-factor factorial design. The independent generators [3,9] of the fractional design were 5 = 123, 6 = 124, 7 = 134, 8 = 234, 9 = 1234.

The confounding pattern of the aliased two-factor interactions will thus be

12 = 35 = 46 = 78
13 = 25 = 47 = 68
14 = 26 = 58
23 = 15 = 48
24 = 16 = 38 = 57
34 = 28 = 17 = 56

The response model used in the screening experiment thus contained the following terms:

$$y = b_0 + \Sigma b_i x_i + b_{12}x_1x_2 + b_{13}x_1x_3 + b_{14}x_1x_4 + b_{23}x_2x_3 + b_{24}x_2x_4 + b_{34}x_3x_4$$

REFERENCES

1 P. Werkhoff and W. Bretschneider, *J. Chromatogr.*, 405 (1987) 87
2 P. Werkhoff and W. Bretschneider, *J. Chromatogr.*, 405 (1987) 99
3 G. E. P. Box, W. G. Hunter and J. S. Hunter, *Statistics for Experimenters*, Wiley, New York, 1978.
4 M. W. Watson and P. W. Carr, *Anal. Chem.*, 51 (1979) 1835
5 J. C. Berridge and E.G. Morrissey, *J. Chromatogr.*, 316 (1984) 69
6 T. D. Schlabach and J. L. Excoffier, *J. Chromatogr.*, 439, (1988) 173
7 L. Hansson, R. Carlson and A.-L. Sjöberg, *Acta Chem. Scand.*, 44 (1990) 1036
8 L. Hansson and R. Carlson, *Acta Chem. Scand.*, 44 (1990) 1042
9 G. E. P. Box and J. S. Hunter, *Technometrics*, 3 (1961) 311
10 C. Daniel, *Application of Statistics to Industrial Experimentation*, Wiley, New York, 1976.
11 I. T. Jolliffe, *Principal Component Analysis*, Springer, New York, 1986
12 R. G. Brereton, *Chemometrics Applications of Mathematics and Statistics to Laboratory Systems*, Ellis Horwood, New York, 1990.
13 S. Wold, K. Esbensen and P. Geladi, *Chemometr. Intell. Lab. Syst.*, 2 (1987) 37
14 R. Carlson, Å. Nordahl, T. Barth and R. Myklebust, *Chemometr. Intell. Lab. Syst.*, 12 (1992) 237.
15 N. Bratchell, *J. Chemometr.*, 3 (1989) 579
16 S. Wold, *Technometrics*, 20 (1978) 396
17 N. Draper and H. Smith, *Applied Regression Analysis*, Wiley, New York, 2nd ed., 1981, pp. 141*ff.*
18 R. Carlson, *Design and Optimization in Organic Synthesis, Elsevier*, Amsterdam, 1992, pp. 159*ff.*

Journal of Chromatography, 623 (1992) 105–113
Elsevier Science Publishers B.V., Amsterdam

CHROM. 24 373

Solvent elimination rate in temperature-programmed injections of large sample volumes in capillary gas chromatography☆

J. Staniewski

Faculty of Chemical Engineering, Laboratory of Instrumental Analysis, Eindhoven University of Technology, P.O. Box 513, 5600 MB Eindhoven (Netherlands) and Institute of Chemical Technology and Engineering, Poznań Technical University, Pl. M. Skłodowskiej-Curie 2, 60-965 Poznań (Poland)

J. A. Rijks

Faculty of Chemical Engineering, Laboratory of Instrumental Analysis, Eindhoven University of Technology, P.O. Box 513, 5600 MB Eindhoven (Netherlands)

(First received October 1st, 1991; revised manuscript received May 27th, 1992)

ABSTRACT

Temperature-programmed sample introduction is a very useful approach for the injection of large sample volumes in capillary gas chromatography and also holds promise for liquid chromatography–gas chromatography coupling. The optimization of a temperature-programmed injector for both these applications depends on numerous factors such as sample volume, liner design and temperature, speed of sample introduction and purge gas flow-rate. The maximum allowable speed of introduction of large sample volumes with simultaneous elimination of the solvent is determined by the solvent elimination rate. A theoretical model is proposed to predict an optimum combination of the speed of sample introduction, the initial liner temperature and the purge gas flow-rate. The validity of the model is discussed and evaluated. The solvent elimination rate is shown to depend on, amongst others, the vapour pressure of the solvent, and can be increased by an increase in the purge gas flow-rate and/or by a decrease in the inlet pressure. The observed cooling effect and the effect of the design of the liner on the solvent elimination rate are emphasized.

INTRODUCTION

Temperature-programmed sample introduction (also known as PTV injection), proposed by Abel [1] in 1964, was developed and applied for the introduction of large sample volumes (up to 20 μl) in biomedical (steroids) and environmental (pesticides) applications by Vogt and co-workers in 1979 [2–4]. Vogt and co-workers showed that the method allowed the simultaneous elimination of the solvent and selective trapping of components with a much lower volatility in the cold liner, prior to splitless transfer of the deposited fraction of the sample into the column by rapid temperature-programmed heating. Temperature-programmed sample introduction offers many advantages in comparison with hot injection methods. In 1981 Schomburg [5] and Poy *et al.* [6] showed that cold split or splitless injection greatly reduced the discrimination of less volatile components. Their observations were confirmed by others [7–15]. The quantitative performance of the PTV injection system appears to be

Correspondence to: Dr. J. A. Rijks, Faculty of Chemical Engineering, Laboratory of Instrumental Analysis, Eindhoven University of Technology, P.O. Box 513, 5600 MB Eindhoven, Netherlands.

☆ Presented at the *12th International Symposium on Capillary Chromatography, Kobe, Japan, 1990.*

0021-9673/92/$05.00

comparable to that of on-column injection [9–11, 14–18]. The negative effect of column contamination due to the presence of residue components in the sample in on-column sample introduction can be greatly avoided with temperature-programmed sample introduction [18–20].

The potential and limitations of temperature-programmed sample introduction with solvent elimination have hardly been studied so far. Some incidental trial on the optimization of this technique were reported by Herraiz and co-workers [21–23] and Termonia *et al.* [24].

Further investigations of the effects of important factors such as injection temperature, injection speed, split flow, purge time, design of the liner and the nature of the solvent on the recoveries of the components of interest are required for a proper judgement of the applicability of the temperature-programmed injector for the introduction of large sample volumes in capillary gas chromatography (GC) and to establish its potential as an interface in coupled liquid chromatography (LC)–GC.

In this paper we present a method that allows the calculation of the solvent evaporation rate in the liner of a temperature-programmed injector. Further, we discuss the effects of various operating conditions on the solvent elimination process.

EXPERIMENTAL

Instrumentation

A Model HP 5890 gas chromatograph (Hewlett-Packard, Avondale, PA, USA) equipped with a flame ionization detector and provided with a Model HP 3393A integrator and a Type KAS 502 temperature-programmed injection system (Gerstel, Mülheim a/d Ruhr, Germany) was used. Sample introduction was done either by means of an autosampler (Model HP 7673; Hewlett-Packard) or a syringe pump. Two different syringe pumps were used. The Type MF-2 "micro feeder" syringe pump (Azumadenkikogyo, Japan) allowed sample introduction with a speed corresponding with micro-bore LC mobile phase flow-rates. Using this system the speed of sample introduction could be varied between 0.7 and 83.3 μl/min. A microprocessor-controlled syringe pump (Digisampler; Gerstel) allowed the injection of defined volumes of samples up to 1000 μl with a speed between 1 and 2000 μl/min. The sample supplied by the syringe pump was transferred directly to the injector via a fused-silica or a metal capillary.

For temperature measurements inside the liner during solvent elimination a Type 870 digital thermometer (Keithley, USA) with a Type 8701 thermocouple adapter was used. Temperature changes were recorded on a BD-40 recorder (Kipp & Zonen, Delft, Netherlands). The temperature was measured at three different positions in the liner at 15, 35 and 55 mm below the injection point, which coincides with the top of a 13-mm glass-wool plug inside the liner.

Operating conditions

Helium was used as the carrier gas at an inlet pressure of 100 kPa (linear gas velocity $\approx$ 60 cm/s). Selective solvent elimination was performed either at the normal carrier gas inlet pressure or at a reduced inlet pressure of 5–20 kPa. The purge gas flow-rate was varied between 210 and 620 ml/min. The sequence of events during sample introduction, solvent elimination and sample transfer is depicted schematically in Fig. 1. The split valve was open

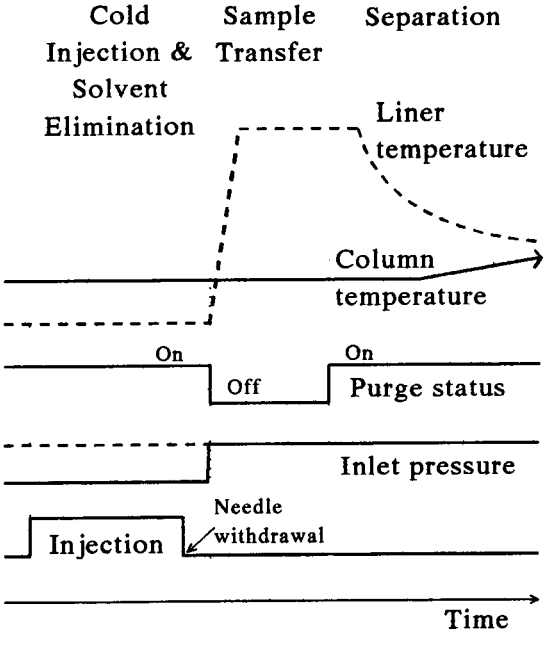

Fig. 1. The sequence of events during sample introduction, solvent elimination and sample transfer.

during the injection period and an additional time of 10–60 s (the additional purge time). Thereafter, simultaneously the inlet pressure was increased to 100 kPa (only if the introduction and solvent elimination were performed at decreased inlet pressure), the split valve was closed, the temperature programme of the column was started and the injector was heated to its final temperature (300°C) with a heating rate of 12°C/s. The injection system was kept at this temperature for 1–3 min and then cooled to 50–60°C.

For the GC separation, two 25 m × 0.32 mm I.D. non-polar fused-silica capillary columns (Chrompack, Middelburg, Netherlands) were used. Column A was coated with CP-Sil 5 and had a film thickness of 2.33 μm and column B was coated with CP-Sil 5 CB and had a film thickness of 1.21 μm. The GC oven temperature programme for column A was initial temperature 40°C for 4 min (isothermal), then increased at 10°C/min to 140°C and at 15°C/min to 250°C (held for 10 min isothermal). In the experiments with column B the initial temperature was 40°C (2 min isothermal) and was then increased at 10°C/min to 280°C.

Test mixtures

Synthetic standard mixtures were prepared that contained *n*-alkanes (C_9–C_{20}) and components of different polarity and volatility. The concentrations of the solutes in samples A and B and the retention times of the components on columns A and B, respectively, under standard operating conditions are given in Table I. Freshly distilled *n*-hexane was used as the solvent for preparing the standard samples and for subsequent dilution of the samples.

Procedure for calculation of recoveries

Normalized peak areas (expressed in area counts per ng of injected component) were used for recovery calculations throughout. As a reference, standard normalized peak areas were used, which were determined by the cold splitless injection of 1 μl of the standard solution. The amounts of components introduced into the columns correspond to 20–40 ng

TABLE I

SYNTHETIC STANDARD SAMPLES

Compound	Sample A		Sample B	
	Concentration (ng/μl)	Retention time[a] (min)	Concentration (ng/μl)	Retention time[b] (min)
n-Nonane	35.1	11.85	10.9	7.55
2-Octanone	41.0	13.41	10.7	8.92
n-Decane	28.0	14.01	11.4	9.48
2,6-Dimethylphenol	31.5	15.75	10.5	10.98
2,6-Dimethylaniline	31.6	16.76	12.1	11.98
n-Dodecane	22.6	17.50	11.3	12.94
1-Aminodecane	39.2	18.03	–	–
n-Tridecane	23.4	18.83	10.5	14.50
(−)-Nicotine	42.4	19.43	10.9	14.97
n-Tetradecane	23.8	20.02	11.5	15.96
2-Tridecanone	28.0	20.94	10.1	17.06
Fluorene	23.2	22.29	–	–
n-Hexadecane	–	–	10.8	18.66
n-Heptadecane	24.6	23.20	11.7	19.89
n-Octadecane	26.6	24.38	9.1	21.07
Anthracene	26.2	24.90	–	–
Methyl palmitate	21.0	25.95	10.3	22.29
n-Eicosane	27.4	27.47	9.3	23.25

[a] On column A under standard operating conditions.
[b] On column B under standard operating conditions.

per compound for sample A and to about 10 ng per compound for sample B.

Liner design

Three different liners were used (Fig. 2): (1) an empty, baffled liner; (2) a baffled liner with a plug (length 13 mm) of silanized glass-wool in the upper part; and (3) a straight liner packed with silanized glass-wool (plug length 40 mm).

THEORETICAL

Selective solvent elimination is an attractive way to introduce large amounts of dilute samples into a capillary GC column. Independent of the method used for this purpose (retention gap with or without so-called concurrent solvent evaporation, cold trapping, temperature-programmed injection or a combination of these techniques), the speed of sample introduction and the rate of solvent elimination have to be matched.

The saturated vapour volume (V_g) at a given temperature (T), which corresponds to a defined liquid volume (V_l), can be calculated according to the following equation:

$$V_g = \frac{V_l \rho RT}{Mp_j} \quad (1)$$

where ρ = density of the solvent, M = molecular weight of the solvent, R = gas constant and p_j = partial pressure of the solvent. In deriving this equation it is assumed that the solvent vapour exhibits ideal gas behaviour. Fig. 3 shows the calculated saturated vapour volumes as obtained from eqn. 1 for a number of different solvents. These values show the minimum volume of gas required to remove the solvent as vapour from the liner. The values of the partial pressures of the solvents were calculated from Antoine's equation [25]. The saturated vapour volumes of different solvents at 20°C vary between 0.4 ml for *n*-pentane and 60 ml for water. For very polar solvents, *e.g.*, methanol, acetonitrile and water used in reversed-phase liquid chromatography, the vapour volumes ar much larger than for non-polar or medium polarity solvents with similar boiling points.

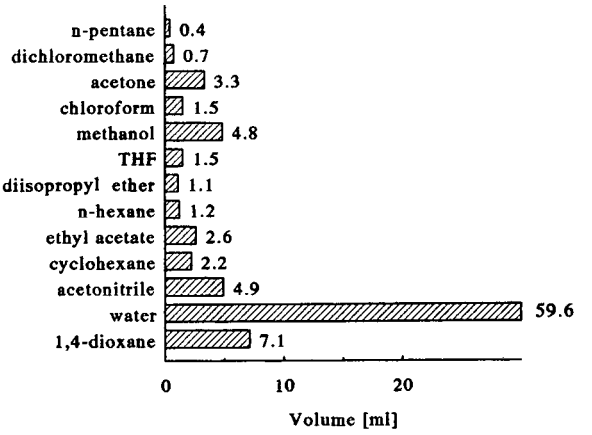

Fig. 3. Saturated vapour volumes of 1 μl of different solvent at 20°C.

During the introduction of large sample volumes the speed of sample introduction into the liner of the injector should not exceed the solvent elimination rate. In the steady state the mass flow of liquid solvent entering the liner (or interface) equals the mass flow of the corresponding solvent vapour at the exit of the liner, *i.e.*, the amount of liquid solvent in the liner remains constant. Assuming isothermal evaporation conditions and further assuming that the gas leaving the liner is saturated with solvent vapour, the maximum injection speed which equals the solvent elimination rate can be calculated as follows:

$$V_{inj,max} = V_{el} = \frac{Mp_j}{\rho RT_o} \cdot \frac{p_o}{p_i} \cdot V_{t,o} \quad (2)$$

where $V_{inj,max}$ = maximum speed of sample introduction, V_{el} = solvent elimination rate, $V_{t,o}$ = total gas flow-rate at outlet conditions (T_o and p_o) and p_i = inlet pressure of the liner.

Eqn. 2 indicates that the solvent evaporation rate

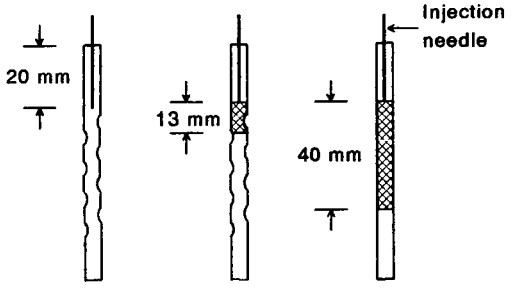

Fig. 2. Schematic design of the liners. Hatched part: silanized glass-wool, liner length 92 mm, I.D. 1.3 mm.

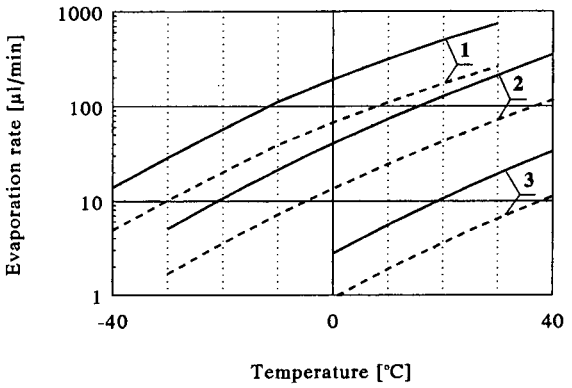

Fig. 4. Dependence of the evaporation rate on the initial liner temperature at different gas flow-rates (dashed lines, 210 ml/min; solid lines, 620 ml/min) for (1) hexane, (2) methanol and (3) water. Values calculated for $p_o/p_i = 1$.

is proportional to the gas flow-rate in the liner given by $V_{t,o}p_o/p_i$. Therefore, reducing the pressure in the liner and/or increasing the total gas flow-rate increases the solvent evaporation rate. The influence of the liner temperature on the evaporation rate is illustrated in Fig. 4 for hexane, methanol and water. A temperature increase of 10°C increases the evaporation rate by a factor of 1.5–2.

The approach described above permits the calculation of the elimination rate and, hence, the maximum acceptable speed of sample introduction as a function of the liner temperature and the purge gas flow-rate for various solvents. In deriving this equation it is assumed that the evaporation process takes place under isothermal conditions and that the purge gas is saturated by solvent vapour.

RESULTS AND DISCUSSION

In temperature-programmed introduction of large sample volumes in capillary GC and in on-line LC–GC, two main steps can be distinguished. In the first step a liquid sample is introduced into the liner of the injector. The solvent is selectively eliminated during introduction while less volatile compounds are retained in the liner. In the second step the compounds trapped in the liner are transferred splitlessly into the column. In the first step, in which selective preseparation occurs, the PTV injection of large sample volumes has to be optimized with respect to solvent elimination and component recovery. For this optimization the following factors need to be taken into account: design of the liner, inlet pressure, initial liner temperature, purge flow, speed of sample introduction, additional purge time, sample volume and physico-chemical properties of the solvent.

The effect of differences in the liner design on the solvent elimination process can be demonstrated by comparing the total amounts of solvent introduced into the column (Table II) after solvent elimination. It should be noted that this amount of solvent consist partly of solvent introduced into the column during split solvent elimination and partly of residual solvent retained in the liner after the solvent elimination process. The solvent retained in the liner is transferred into the column in the splitless mode together with compounds of interest trapped in the liner during solvent elimination. When a sample of 5.6 µl is introduced into the PTV liner at an initial liner temperature of −30°C in the solvent elimina-

TABLE II

EFFECT OF DIFFERENCES IN THE LINER DESIGN ON TOTAL AMOUNT OF SOLVENT ENTERING THE COLUMN

Operating conditions: purge gas flow-rate, 210 ml/min; additional purge time, 45 s; inlet pressure, 100 kPa.

Operating conditions	Amount of solvent (µl)		
	Liner 1	Liner 2	Liner 3
Sample volume 5.6 µl, injection time 40 s, initial liner temperature −30°C	2.7	0.5	0.2
Sample volume 21 µl, injection time 75 s, initial liner temperature −20°C	2.8	1.1	0.5

tion mode, the amounts of solvent introduced into the column correspond to about 2.7 μl, 0.5 and 0.2 μl of hexane for liners 1, 2 and 3, respectively. From these results it can be concluded that the solvent elimination rate for liner 1 is low; it is estimated to be about 2 μl/min. For liners packed with glass-wool the solvent elimination rate is increased significantly, corresponding to about 3.5 μl/min for liner 2 and about 4 μl/min for liner 3. These values are lower than the evaporation rates calculated according to eqn. 2, where it was assumed that instantaneous saturation of the purge gas with solvent vapour occurs. From the differences between the calculated and the experimental data it can be concluded that the purge gas is not fully saturated with solvent vapour. When larger samples of 21 μl were introduced at an initial liner temperature of −20°C, liner 1 again appeared to be less effective than the liners packed with glass-wool. These results indicate that the degree of saturation increases when the gas–solvent contact area in the liner is enlarged. Packing the liner with glass-wool appears to be an efficient means of increasing the contact area. Consequently, it can be expected that any modification of the liner which results in an increased gas–solvent contact area will be beneficial for the rate of solvent evaporation and, hence, the analysis time.

The solvent evaporation rate, as it is proportional to the ratio of the outlet to the inlet carrier gas pressure (see eqn. 2), can be increased by decreasing the pressure in the liner. Additionally, at a lower column inlet pressure the splitting ratio will increase, because the gas flow through the liner is mass-flow controlled and the column flow is pressure controlled (back-pressure control). A reduced amount of solvent will enter the column during split solvent venting at low column inlet pressures. This is demonstrated in Fig. 5. The shaded peaks represent the total amount of solvent entering the column. When large sample volumes of 1000 μl were injected (Fig. 5A and B), the amounts of solvent introduced into the column at the maximum obtainable purge gas flow-rate (*ca.* 600 ml/min) correspond to about 9 and 0.5 μl at inlet pressures of 100 and 18 kPa, respectively. At a lower purge gas flow-rate (210 ml/min) and for sample volumes of 250 μl (Fig. 5C and D), the amounts of solvent introduced into the column correspond to *ca.* 6 and 0.1 μl of hexane at

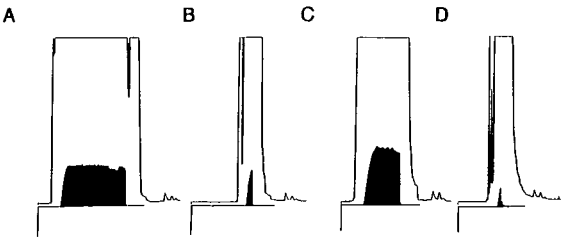

Fig. 5. Effect of inlet pressure on the size of the solvent peak. Operating conditions: inlet pressure, 100 kPa for chromatograms A and C, 18 kPa for B and 7 kPa for D; initial liner temperature, 30°C; additional purge time, 10 s; shaded solvent peaks at attenuation = 2^{16}. For more information, see text.

inlet pressures of 100 and 7 kPa, respectively. This means that by using reduced inlet pressures during solvent elimination the total fraction of solvent that enters the column is reduced to less than 0.05%. This is a considerably smaller amount than at normal column inlet pressures. Experiments showed that the stepwise increase in the pressure after solvent elimination to higher pressures during analysis does not affect the retention times of the solutes in temperature-programmed separations.

Unexpectedly, it was observed that extremely low recoveries were obtained when large sample volumes were injected at a sampling speed close to the maximum acceptable speed of sample introduction predicted according to eqn. 2. The results were significantly improved by a decrease in the speed of sample introduction and also in the sample size. The effect of the speed of sample introduction on recovery is illustrated in Fig. 6 for components with retention times between those of C_{16} and C_{20}. The calculated maximum allowable speed of sample introduction predicted by eqn. 2 under the given experimental conditions (purge gas flow-rate = 620 ml/min and initial liner temperature = 30°C) is *ca.* 700 μl/min. As the evaporation is an endothermic process, it can be expected that the temperature in the PTV liner will decrease significantly during solvent evaporation. A temperature decrease in the liner would result in a reduction in the solvent evaporation rate and might easily lead to the accumulation of an excessive amount of liquid in the liner. In this event, part of the introduced liquid sample will leave the liner in the liquid state via the split vent (right-hand part of Fig. 6), which will lead to a loss of components and incomplete recoveries.

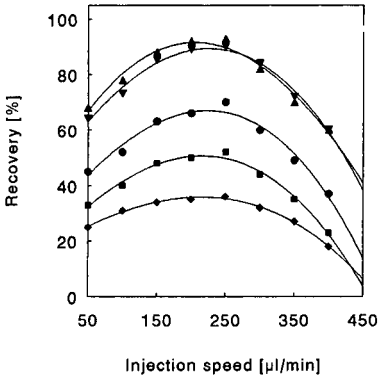

Fig. 6. Influence of injection speed on the recovery of (▼) eicosane, (▲) methyl palmitate, (●) octadecane, (■) heptadecane and (◆) hexadecane. Operating conditions: sample volume, 250 µl; initial liner temperature, 30°C; purge gas flow-rate, 620 ml/min; inlet pressure, 18 kPa; additional purge time, 10 s; liner 2.

Flooding of the liner explains the poor recoveries at high sample introduction speeds. On the other hand, at too low a speed of sample introduction no liquid film is formed in the liner. In the absence of such a liquid film the solutes are only weakly retained and might easily escape with the huge flow of purge gas (left-hand part of Fig. 6). Probably the formation of a liquid film is essential for the selective retention of the components, because this liquid will strongly incraese the retentive power of the liner. Packing of the liner with a packing material or coating of the liner with a liquid layer are possible alternatives foı a selective increase in the retention of the analytes.

The changes in temperature at different positions inside the liner during solvent elimination are shown in Fig. 7. These changes decrease from the top to the bottom part of the liner and they depend strongly on the injection speed. Obviously, the cooling effect due to vaporization of the sample is compensated for by heat transfer from the heating zone. Considering the differences in temperature drop at different positions inside the liner (*e.g.*, 12°C at the top and 0.5°C at the bottom part at an injection speed of 100 µl/min), the front of the liquid solvent film in the liner will be located nearer the exit of the liner. Moreover, the lower the actual liner temperature the smaller is the evaporation rate. It follows from the theoretical model (eqn. 2) that in order to compensate for a temperature drop of 10°C, the injection speed has to be about halved.

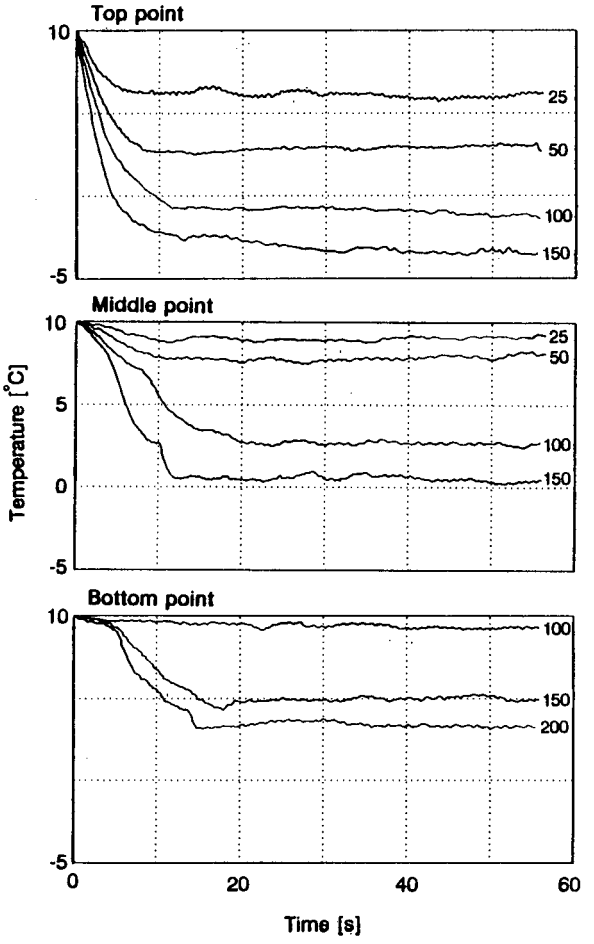

Fig. 7. Temperature at different points inside the liner during solvent elimination for various injection speeds (numbers on the right-hand side indicate injection speeds in µl/min). Operating conditions: initial liner temperature, 10°C; purge gas flow-rate, 620 ml/min; inlet pressure, 0 kPa.

The magnitude of the cooling effect depends not only on the introduction speed of the sample, but will also depend on the heat of the evaporation of the solvent. Values of the heat of evaporation for different solvents recalculated from the enthalpy of evaporation at the normal boiling point [25] are presented in Table III. The heats of evaporation vary between 50 and 100 cal/ml for most of these solvents. For the polar solvents used in reversed-phase LC, *i.e.*, methanol, acetonitrile and water, the heat of evaporation is significantly higher. This means that, in order to vaporize identical volumes of

TABLE III

HEATS OF EVAPORATION OF SOLVENTS AT NORMAL BOILING POINT

Solvent	Heat of evaporation (cal/ml)	Solvent	Heat of evaporation (cal/ml)
n-Pentane	53	*n*-Hexane	53
Dichloromethane	104	Ethyl acetate	79
Acetone	95	Cyclohexane	66
Chloroform	88	Acetonitrile	143
Methanol	208	Water	540
Tetrahydrofuran	87	1,4-Dioxane	102
Diisopropyl ether	50		

methanol and *n*-pentane, four times more energy is required for methanol. For water the difference is even more pronounced. Compared with *n*-hexane water requires ten times more energy for complete vaporization. Obviously, this also implies a different and much stronger cooling effect for methanol or water than for other solvents.

Taking into account the effects of the operating conditions on solvent elimination discussed above, a representative chromatogram for a large-volume injection of sample A (*cf.*, Table I) into a PTV injector is presented in Fig. 8. The recoveries of the components of interest are dependent on their volatilities. The more volatile components present in the sample (*n*-nonane, 2-octanone and *n*-decane) were largely lost. However, components with volatilities lower than or similar to that of *n*-heptadecane were more than 90% trapped. Selected operating conditions were preliminary optimized with respect to component recoveries. Further optimization is required to achieve quantitative trapping of components in a liner of the temperature-programmed injector with large-volume sample introduction.

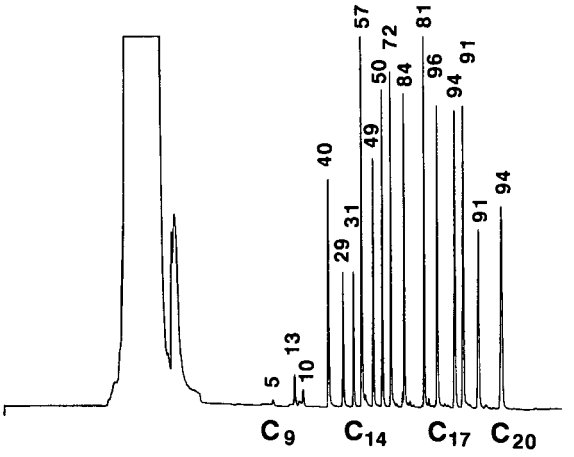

Fig. 8. Chromatogram of a large volume of test sample A [numbers on the top of peaks indicate recoveries of components (%)]; for peak identification see Table I. Operating conditions: sample volume, 150 μl; concentration, 0.08–0.16 ng/μl; injection speed, 20.8 μl/min; initial liner temperature, −20°C; purge gas flow-rate, 210 ml/min; inlet pressure, 5 kPa; additional purge time, 45 s; liner 2; column A.

CONCLUSIONS

The temperature-programmed injector is an attractive sample introduction system for large sample volumes in capillary GC and it can also be used as an interface for on-line coupling of microbore and capillary LC and capillary GC.

During the introduction of large sample volumes into a liner of the PTV injector the speed of sample introduction and solvent elimination rate have to be adjusted.

The theoretical model allows the calculation of the solvent elimination rate (the maximum allowable speed of sample introduction) for large sample volumes for different solvents under given operating conditions assuming saturation of the purge gas with solvent vapour and an isothermal evaporation process. For speeds of sample introduction up to about 50 μl/min the cooling effect during solvent evaporation inside the liner can be neglected. Under operating conditions that allow a higher injection speed to be used, the speed of sample introduction can be reliably estimated.

The solvent elimination rate can be significantly increased at increased purge gas flow-rates and a reduced pressure in the liner. Moreover, owing to a reduced pressure in the liner during split solvent elimination, the amount of solvent entering the capillary column is significantly decreased.

Enlargement of the gas–liquid contact area improves the process of saturation of the purge gas by solvent vapour, which is beneficial in the solvent elimination process.

REFERENCES

1 K. Abel, *J. Chromatogr.*, 13 (1964) 14–21.
2 W. Vogt, K. Jacob and H. W. Obwexer, *J. Chromatogr.*, 174 (1979) 437–439.
3 W. Vogt, K. Jacob, A.-B. Ohnesorge and H. W. Obwexer, *J. Chromatogr.*, 186 (1979) 197–205.
4 W. Vogt and K. Jacob, in P. Sandra (Editor), *Sample Introduction in Capillary Gas Chromatography*, Vol. 1, Hüthig, Heidelberg, 1985, pp. 99–121.
5 G. Schomburg, in R. E. Kaiser (Editor), *Proceedings of the 4th International Symposium on Capillary Chromatography, Hindelang, 1981*, Hüthig, Heidelberg, 1981, p. 921A.
6 F. Poy, S. Visani and F. Terrosi, *J. Chromatogr.*, 217 (1981) 81–90.
7 F. Poy, S. Visani and F. Terrosi, *J. High Resolut. Chromatogr. Chromatogr. Commun.*, 5 (1982) 355–359.
8 F. Poy, *Chromatographia*, 16 (1982) 345–348.
9 G. Schomburg, H. Husmann, H. Behlau and F. Schulz, *J. Chromatogr.*, 279 (1983) 251–258.
10 G. Schomburg, H. Husmann, F. Schulz, G. Teller and M. Bender, *J. Chromatogr.*, 279 (1983) 259–267.
11 G. Schomburg, in P. Sandra (Editor), *Sample Introduction in Capillary Gas Chromatography*, Vol. 1, Hüthig, Heidelberg, 1985, pp. 55–76.
12 F. Poy and L. Cobelli, in P. Sandra (Editor), *Sample Introduction in Capillary Gas Chromatography*, Vol. 1, Hüthig, Heidelberg, 1985, pp. 77–97.
13 E. Loyola, H. Herraiz, G. Reglero and P. Martin-Alvarez, *J. Chromatogr.*, 398 (1987) 53–61.
14 C. A. Saravalle, F. Munari and S. Trestianu, *J. High Resolut. Chromatogr. Chromatogr. Commun.*, 10 (1987) 288–296.
15 A. J. van Es, W. Weterings, J. P. E. M. Rijks and J. A. Rijks, in P. Sandra (Editor), *Proceedings of the 9th International Symposium on Capillary Chromatography, Monterey, 1988*, Hüthig, Heidelberg, 1988, pp. 584–596.
16 J. V. Hinshaw, Jr. and W. Seferovic, *J. High Resolut. Chromatogr. Chromatogr. Commun.*, 9 (1986) 69–72.
17 H.-J. Stan and H.-M. Müller, *J. High Resolut. Chromatogr. Chromatogr. Commun.*, 11 (1988) 140–143.
18 H.-M. Müller and H.-J. Stan, *J. High Resolut. Chromatogr.*, 13 (1990) 697–701.
19 K. Grob, Th. Läubli and B. Grechbühler, *J. High Resolut. Chromatogr. Chromatogr. Commun.*, 11 (1988) 462–470.
20 K. Grob and Z. Li, *J. High Resolut. Chromatogr. Chromatogr. Commun.*, 11 (1988) 626–632.
21 M. Herraiz, G. Reglero, E. Loyola and T. Herraiz, *J. High Resolut. Chromatogr. Chromatogr. Commun.*, 10 (1987) 598–602.
22 J. Villen, T. Herraiz, G. Reglero and M. Herraiz, *J. High Resolut. Chromatogr.*, 12 (1989) 633–635.
23 M. Herraiz, G. Reglero and T. Herraiz, *J. High Resolut. Chromatogr.*, 12 (1989) 442–446.
24 M. Termonia, B. Lacomblez and F. Munari, *J. High Resolut. Chromatogr. Chromatogr. Commun.*, 11 (1988) 890–895.
25 R. C. Reid, J. M. Prausnitz and T. K. Sherwood, *The Properties of Gases and Liquids*, McGraw-Hill, New York, 1977.

Journal of Chromatography, 623 (1992) 115–122
Elsevier Science Publishers B.V., Amsterdam

CHROM. 24 421

Gas chromatography–mass spectrometry of lipopolysaccharide 3-hydroxy fatty acids: comparison of pentafluorobenzoyl and trimethylsilyl methyl ester derivatives

Zbigniew Mielniczuk*, Srinivas Alugupalli, Eugenia Mielniczuk and Lennart Larsson

Department of Medical Microbiology, University of Lund, Sölvegatan 23, 223 62 Lund (Sweden)

(First received March 27th, 1992; revised manuscript received June 5th, 1992)

ABSTRACT

3-Hydroxytetradecanoic and 3-hydroxyhexadecanoic acids were used as chemical markers for the determination of lipopolysaccharides by gas chromatography–mass spectrometry of their pentafluorobenzoyl and trimethylsilyl methyl ester derivatives. The latter derivatives were simpler to prepare than the former, although both were chemically stable. Analysis of pentafluorobenzoyl derivatives (chemical ionization mode with negative ion detection) provided somewhat better sensitivity than analysis of trimethylsilyl derivatives (electron impact mode): 1 pg (injected amount) of pentafluorobenzoyl derivatives was detectable under routine conditions. Both types of derivative gave similar values when used to measure lipopolysaccharides in a bacteria-contaminated pharmacological product. The described methods are useful for the determination and characterization of lipopolysaccharides in various environments.

INTRODUCTION

Lipopolysaccharides (LPSs, endotoxins) are characteristic, toxic outer-membrane constituents of gram-negative bacteria [1], and they can induce several pathophysiological reactions in humans [2]. Airborne LPSs are considered to be a major occupational health problem and have been associated with, for example, development of respiratory diseases, headache, fever, and irritation of the eye [3–6].

The main method for the determination of endotoxins is the *Limulus* amebocyte lysate (LAL) test, which is very sensitive and, in the chromogenic version, provides quantitative results. Unfortunately, the specificity of the LAL test is limited since it can be activated by many chemical structures other than LPSs [7,8]. Hence, in several laboratories, ours among them, the possibility of using gas chromatography–mass spectrometry (GC–MS) for endotoxin determination has been considered. Analytes used with GC–MS are LPS-specific 3-hydroxylated fatty acids. Both methyl-trimethylsilyl (Me/TMS) derivatives (analysed by electron impact ionization (EI) [9,10]), and methyl-pentafluorobenzoyl (Me/PFBO) derivatives (analysed by chemical ionization with negative ion detection (NICI) [11,12]) have been used. However, no data comparing the GC–MS characteristics of these derivatives have been reported. Notably, most modern bench-top GC–MS instruments lack facilities for NICI.

This paper compares the Me/TMS and Me/PFBO derivatives of LPS-specific 3-hydroxy fatty acids with respect to their ease of preparation, chemical stability, and GC–MS characteristics.

Correspondence to: Dr. L. Larsson, Department of Medical Microbiology, University of Lund, Sölvegatan 23, 223 62 Lund, Sweden.

* Permanent address: Child Health Centre, Warszawa-Miedzylesie, Al. Dzieci Polskich 20, Poland.

0021-9673/92/$05.00

EXPERIMENTAL

Chemicals and glassware

Nonanoic, tridecanoic, tetradecanoic, and hexadecanoic acids hydroxylated in position 3 (3-OH 9:0, 3-OH 13:0, 3-OH 14:0, and 3-OH 16:0, respectively) were purchased from Larodan Lipids (Malmö, Sweden). Bis(trimethylsilyl)trifluoroacetamide (BSTFA, 98%), pentafluorobenzoyl chloride (PFBO-Cl, 98%), dichloromethane (p.a., stabilized with 50 ppm amylene), diethyl ether (p.a.) and acetonitrile (99%) were from Janssen Chimica (Geel, Belgium). Methanol (p.a.) and *n*-hexane (99%) were from Lab Scan (Dublin, Ireland), acetyl chloride (p.a.) and pyridine (p.a) from Merck (Darmstadt, Germany), and triethylamine (TEA) from Sigma (St. Louis, MO, USA). All chemicals were used without further purification. The glass test tubes (equipped with PTFE-lined screw-caps) were heated at 350°C overnight before use.

Reagents

Methanolic HCl (1.3 and 3.6 *M*) was prepared by adding acetyl chloride (1 or 3 ml) dropwise to methanol (9 or 7.5 ml) at 0°C; 35% PFBO-Cl solution was prepared by adding 650 μl of acetonitrile to 350 μl of PFBO-Cl; and 2% TEA solution was prepared by mixing 980 μl of acetonitrile with 20 μl TEA. All reagents were stored at 4°C in glass tubes with PTFE-lined screw caps, and used within one week of preparation.

Standard solutions

Stock solutions of the free hydroxy acids were prepared by dissolving 5 mg of each acid in 5 ml of hexane–diethyl ether (4:1, v/v). LPS stock solutions for the construction of calibration curves were prepared by diluting *Escherichia coli* serotype 055:B5 LPS (Sigma) in pyrogen-free water to concentrations of 1 and 10 ng/μl. The solutions were stored at 4 °C.

Derivatization of hydroxy acids and construction of calibration curves

The free hydroxy acids 3-OH 14:0 and 3-OH 16:0 (250 μg of each) were heated in 1 ml of 1.3 *M* methanolic HCl at 80 °C for 30 min. After the addition of 1 ml of distilled water, the samples were extracted twice with 1 ml of *n*-hexane, and the combined hexane phases were evaporated to dryness under a stream of nitrogen. Next, the samples were dissolved in 2.5 ml of hexane and divided into five equal parts, which thus each contained 50 μg of each acid. The solvent was then evaporated, and the methyl esters were subjected to TMS or PFBO derivatization as described below.

To four of the dried methyl ester samples were added 30 μl of 35% PFBO-Cl and 20 μl of 2% TEA (both in acetonitrile). To determine the influence of the reaction temperature on the yield of the PFBO derivatives, the four samples were heated for 1 h at 80°C, 100°C, 120°C and 150°C, respectively. Subsequently, *n*-hexane (1.5 ml) and distilled water (1 ml) were added and after extraction, the hexane phase was evaporated and the sample re-dissolved in 250 μl of *n*-hexane.

TMS derivatization was accomplished by adding, to the fifth sample, 50 μl of BSTFA and 5 μl of pyridine. The sample was then heated at 80°C for 15 min. After evaporation of the pyridine, using a nitrogen stream, *n*-hexane was added to achieve a final volume of 250 μl. Both the Me/PFBO and the Me/TMS derivatives were analysed by GC using flame ionization detection (see below).

To construct calibration curves, the pure 3-OH 14:0 and 3-OH 16:0 acids, plus an internal standard (250 μg of each acid), were subjected to methanolysis as above. PFBO derivatization (using 3-OH 9:0 as internal standard) was performed at 80°C for 1 h, and TMS derivatization (using 3-OH 13:0 as internal standard) was performed as described above. After serial dilution the final preparations were analysed by GC–MS in the EI (for the Me/TMS derivatives), or the NICI (for the Me/PFBO derivatives) mode.

Calibration curves for LPS analysis

To known amounts of LPS (in the range 5–1000 ng), 50 ng of either 3-OH 9:0 (for PFBO derivatization) or 3-OH 13:0 (for TMS derivatization) were added. The (dry) samples were heated overnight (about 18 h) in 3.6 *M* methanolic HCl, and the methyl esters were extracted with 1.5 ml of hexane and 1 ml of water. The hexane layer was evaporated under a stream of nitrogen, and redissolved in 1 ml of hexane–dichloromethane (1:1, v/v). Each sample was then applied to a disposable silica gel column (1 ml, Bond-Elut; Analytichem, Harbour City, CA,

USA) to separate the methyl esters of hydroxylated acids from those of non-hydroxylated acids. Prior to use the column was washed with 1 ml of diethyl ether followed by 1 ml of hexane–dichloromethane (1:1, v/v). After the methyl ester preparations had been applied to the column, 0.6 ml of hexane–dichloromethane (1:1, v/v) was added. The hydroxy fatty acid methyl esters were eluted with 1.5 ml of diethyl ether, and the solvent was evaporated. Thereafter, PFBO or TMS derivatization was performed as described above.

A calibration curve for the Me/PFBO derivative was constructed by plotting the ratios of *m/z* 452 (LPS acid 3-OH 14:0) peak areas to *m/z* 382 (internal standard 3-OH 9:0) peak areas against the amounts of endotoxin added. Analysis was performed in selected-ion monitoring (SIM) NICI mode. Similarly, for the Me/TMS derivative, the ions *m/z* 315 (LPS acid 3-OH 14:0) and *m/z* 301 (internal standard 3-OH 13:0) were used. Analysis was performed in SIM EI mode. The final preparations were brought to a volume of 100 μl with *n*-hexane, 1 μl of which was analysed by GC–MS.

Before each set of SIM analyses, a standard solution (containing *ca.* 500 pg of each derivatized acid) was injected and analysed in scan mode for determination of retention time and *m/z* values for monitoring. Injection (after the entire analytical procedure) of blanks of solvents and reagents was performed regularly to detect possible interfering compounds.

Application

Internal standards (3-OH 9:0 and 3-OH 13:0, 100 ng of each) and 1 ml of 3.6 *M* methanolic HCl were added to a dry pharmacological product suspected (by the LAL test) to contain LPSs; the sample was then heated at 100°C for 18 h. After this treatment the preparation was purified using the Bond Elut column (see above) and divided into two equal parts, one for TMS derivatization and one for PFBO derivatization (see above). These two parts were then analysed by GC–MS in the EI and the NICI mode, respectively.

Gas chromatography

A Varian Model 3500 (Los Altos, CA, USA) gas chromatograph was used, equipped with a split/splitless injector, a flame ionization detector, and a fused-silica capillary column (25 m × 0.25 mm I.D.) coated with OV-1 (SGE, Ringwood, Australia). The column temperature was programmed to rise at 8°C/min from 120°C to 260°C. The nitrogen carrier gas flow-rate through the column was 2 ml/min. The temperature of the injector was 250°C and that of the detector 270°C. The data were evaluated by using a Chrompack control and integration system with an IBM PS/2 Model 30 and a Chrompack BD 70 printer/plotter.

Gas chromatography–mass spectrometry

A VG Trio-1 S GC–MS system (Manchester, UK) was used. The gas chromatograph was a Hewlett-Packard Model 5890 (Avondale, PA, USA) equipped with a fused-silica capillary column (25 m × 0.25 mm I.D) containing cross-linked OV-1 as the stationary phase. Injections were made using a Hewlett-Packard Model 7673 autosampler in the splitless mode; the split valve was opened 1 min after the injection. Helium was used as the carrier gas, at an inlet pressure of 7 p.s.i., and the temperature of the column was programmed from 120°C to 260°C at 20°C/min. Both the injector and the interface (between GC and MS) were kept at 260°C. The Me/TMS derivatives were analysed in the EI mode (ion source temperature 220°C) and the Me/PFBO derivatives in the NICI mode (ion source temperature 150°C), using both scanning and SIM. Isobutane at a pressure of 10 p.s.i. was used as reagent gas. Ionization was performed at 70 eV.

RESULTS

Derivatization of hydroxy acids

The influence of reaction temperature on the yield of the PFBO and TMS derivatives of the hydroxy acid methyl esters was studied by GC. TMS derivatives were formed quantitatively after 15 min at 80°C, therefore longer heating did not improve the reaction yield. PFBO derivatization was complete after heating at 80°C for 1 h (Fig. 1). At a reaction temperature of 150°C, considerable decomposition of the Me/PFBO derivative was observed in the GC profile (Fig. 2); the same phenomenon was observed on GC–MS analysis (data not shown). Both the Me/TMS and Me/PFBO derivatives were chemically stable, as no decomposition was observed after several weeks of storage at 4°C.

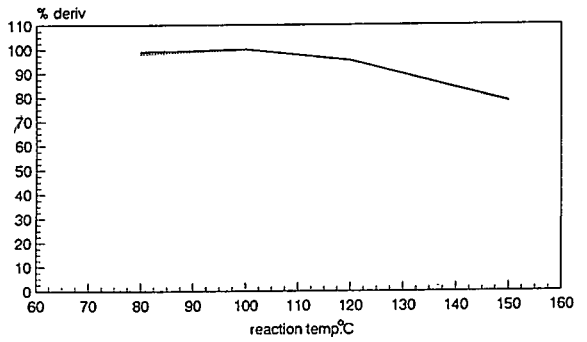

Fig. 1. Yield of PFBO methyl ester derivatives of 3-OH 14:0 (solid line) and 3-OH 16:0 (dotted line) as a function of reaction temperature (heating duration 1 h).

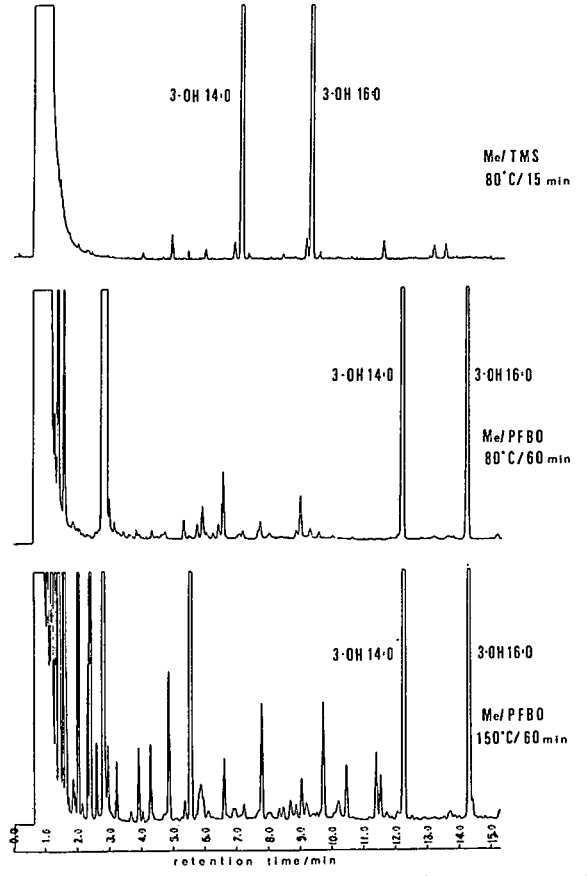

Fig. 2. Gas chromatographic analysis of TMS (upper) and PFBO (center, lower) methyl ester derivatives of 3-OH 14:0 and 3-OH 16:0 under different reaction conditions.

Mass spectra

Mass spectra of Me/TMS and Me/PFBO derivatives of 3-OH 14:0 analysed in the EI and NICI modes, respectively, are shown in Fig. 3. The spectrum of the Me/TMS derivative was characterized by two abundant peaks with m/z 315 (M − 15, loss of a CH_3 group) and m/z 175 (M − 155, cleavage of C_3–C_4 linkage); in the high-mass region, m/z 257 (M − 73, loss of a $(CH_3)_3$ Si group) was also seen. The PFBO derivative produced a mass spectrum dominated by m/z 452 (M). The Me/TMS and Me/PFBO derivatives of the other 3-hydroxy fatty acids studied produced analogous mass spectra.

Sensitivity and calibration curves

Calibration curves for the Me/TMS and Me/PFBO derivatives of the individual hydroxy acids are shown in Fig. 4. The lowest detectable injected amounts of the TMS and PFBO derivatives were, respectively, *ca.* 3 and 1 pg (signal-to noise ratio 4); these values were obtained under routine analytical conditions, using SIM focusing on m/z M − 15 (TMS derivatives) and m/z M (PFBO derivatives). When using TMS derivatization, 3-OH 13:0 was used as the internal standard, because the volatility of the 3-OH 9:0 Me/TMS derivative led to its partial evaporation, together with the pyridine, after reaction.

Calibration curves for the LPSs, obtained using 3-OH 14:0 as the analyte, are also shown in Fig. 4. Detection of a few nanograms of LPSs (starting material) was easily accomplished, when using both Me/TMS and Me/PFBO derivatization, following injection of 1 μl of a final total sample volume of 100 μl. The two curves fitted the equations $y = (4.7x - 54.4)10^{-3}$ (Me/TMS) and $y = (3.9x - 50.6)10^{-3}$ (Me/PFBO); the correlation coefficient was 0.9937 in both cases.

Application

Fig. 5 illustrates mass chromatograms of the freeze-dried pharmacological product after Me/TMS and Me/PFBO derivatization of hydroxy acids. The sample contained several 3-hydroxylated fatty acids, the identities of which (3-OH 12:0, 3-OH 14:0, 3-OH 16:0 and 3-OH 18:0) were established by GC–MS analysis in scan mode. The amount of LPSs in the sample was calculated by comparing the peak areas of the hydroxy acids of LPSs with

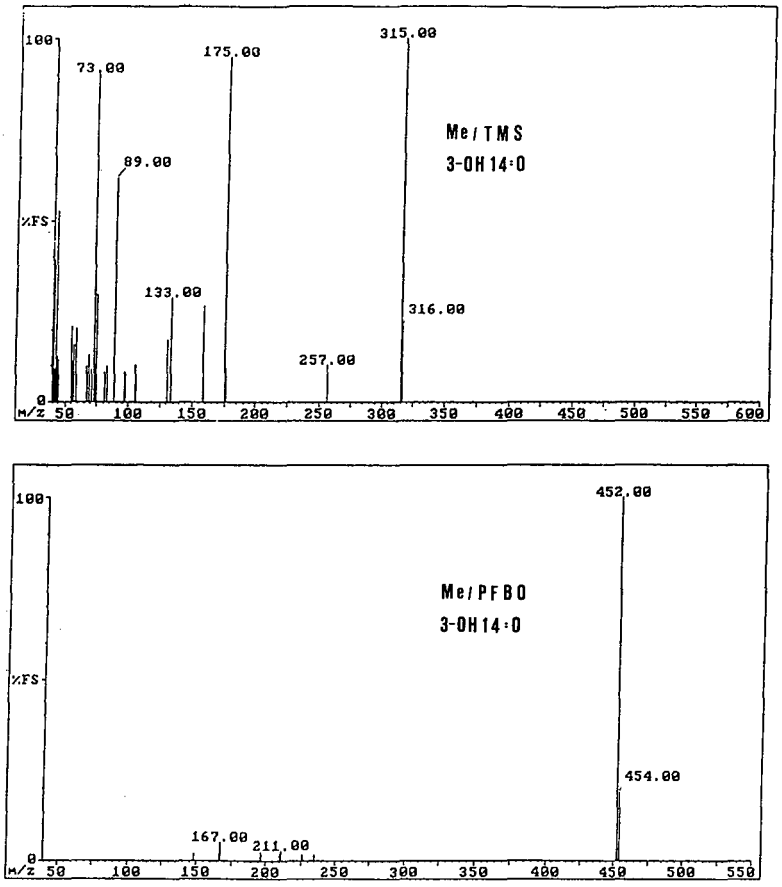

Fig. 3. Mass spectra of TMS (upper) and PFBO (lower) derivatized 3-OH 14:0 methyl ester analysed in the EI and the NICI mode, respectively.

those of the internal standards. The number of moles of the LPS-3-hydroxy acid derivatives was then calculated and subsequently divided by four, since one mole of lipid A generally contains four moles of 3-hydroxy acids. The value obtained in this manner was multiplied by an arbitrarily chosen LPS molecular mass, in this case 8000, and the amount of LPSs was thereby estimated to be 576 ng, using the Me/PFBO derivative, and 776 ng, using the Me/TMS derivative (Table I).

DISCUSSION

GC–MS analysis of 3-hydroxylated fatty acids allows accurate quantitative measurement of endotoxins, even in complex environments. These acids are present in lipid A, the part of the LPS molecule that is responsible for endotoxic effects [13]. In addition, as the distribution of the 3-hydroxylated fatty acids varies between different Gram-negative bacteria, GC–MS analysis can also supply information on the origin of LPS. For example, 3-OH 14:0 is the predominant 3-hydroxy acid in *Enterobacteriaceaea*, whereas 3-OH 10:0, 3-OH 12:0 and 3-OH 16:0 are indicative of *Pseudomonadaceae*, and several odd-numbered 3-hydroxy acids have been identified in a variety of bacterial species [14]. This information can, for instance, be useful for determining the origin of contamination caused by Gram-negative bacteria.

In the present work, we compared TMS and PFBO derivatization of 3-hydroxy fatty methyl es-

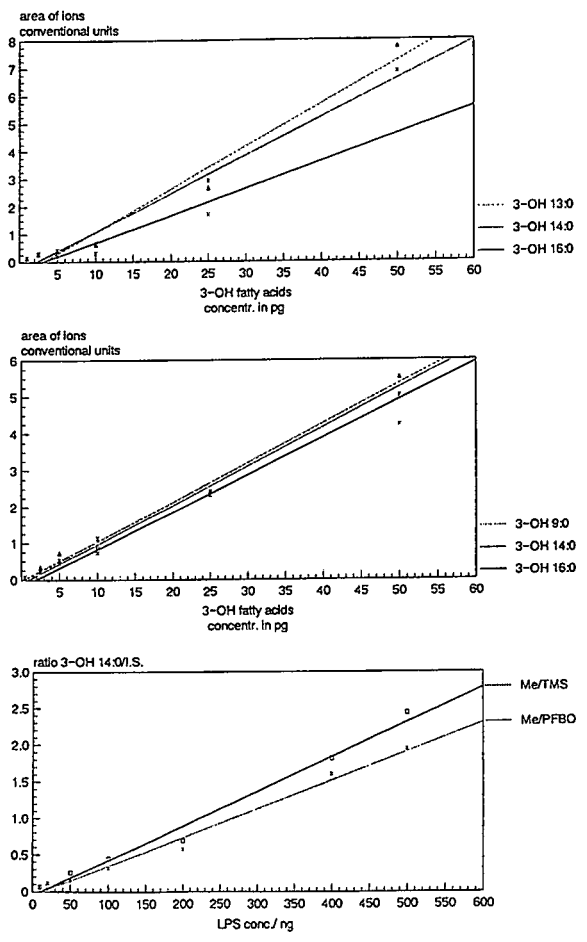

Fig. 4. Calibration curves for TMS (upper) and PFBO (centre) derivatized 3-OH acid methyl esters, and for *Escherichia coli* LPS (lower). For the latter, 3-OH 14:0 was used as an analyte, after methylation and TMS or PFBO derivatization.

ters for use in GC–MS analysis of endotoxins. TMS derivatization was also used in early studies; a minimum detectable amount (using the EI mode) of *ca.* 100 ng of LPSs per millilitre of sample was reported [9]. Recently, PFBO derivatization was found to provide superior sensitivity (using the NICI mode): an amount of only 1 ng of LPSs was detectable [11]. The present detailed comparison of the two types of derivative for LPS analysis was prompted by the fact that several of the compact, low-cost modern GC–MS instruments lack facilities for NICI analysis, and the fact that the performance of GC–MS instruments has been dramatically improved during recent years.

The sensitivity of NICI analysis of Me/PFBO derivatives was essentially the same as previously reported [11] *i.e.* the presence of a nanogram amount of LPSs in a sample was detectable under routine working conditions. The difference in sensitivity between the Me/PFBO and Me/TMS derivatives of 3-OH 14:0 was lower than expected. The reason for this is unclear, but the adsorption of subpicogram amounts of the analyte in the GC–MS system might be one explanation. In our experience, to achieve optimal sensitivity, the following are necessary: (1) PTFE-lined screw caps and clean glassware with a non-active surface must be used; (2) contamination from detergents, etc., must be carefully avoided during sample preparation; (3) the glass liner in the injection port of the chromatograph must be changed or cleaned regularly; (4) a short (1–2 m) interchangeable fused-silica pre-column should be used or 1-m lengths of the inlet part of the analytical column should be periodically removed to avoid

TABLE I

LIPOPOLYSACCHARIDE IN A PHARMACOLOGICAL SAMPLE

Values were calculated according to amounts of 3-hydroxylated fatty acids (12:0, 14:0. 16:0, and 18:0) analysed as Me/PFBO and Me/TMS derivatives. "Relative amount" refers to an internal standard.

3-Hydroxy acid	Relative amount	Mol ($\times 10^{-10}$)	Sum (mol)	Mol LPS	LPSs (ng)
Me/PFBO derivatives					
12:0	0.46	1.07			
14:0	0.73	1.50	$2.86 \cdot 10^{-10}$	$0.72 \cdot 10^{-10}$	576
16:0	0.12	0.22			
18:0	0.04	0.07			
Me/TMS derivatives					
12:0	0.40	0.93			
14:0	0.75	1.53	$3.89 \cdot 10^{-10}$	$0.97 \cdot 10^{-10}$	776
16:0	0.30	0.55			
18:0	0.53	0.88			

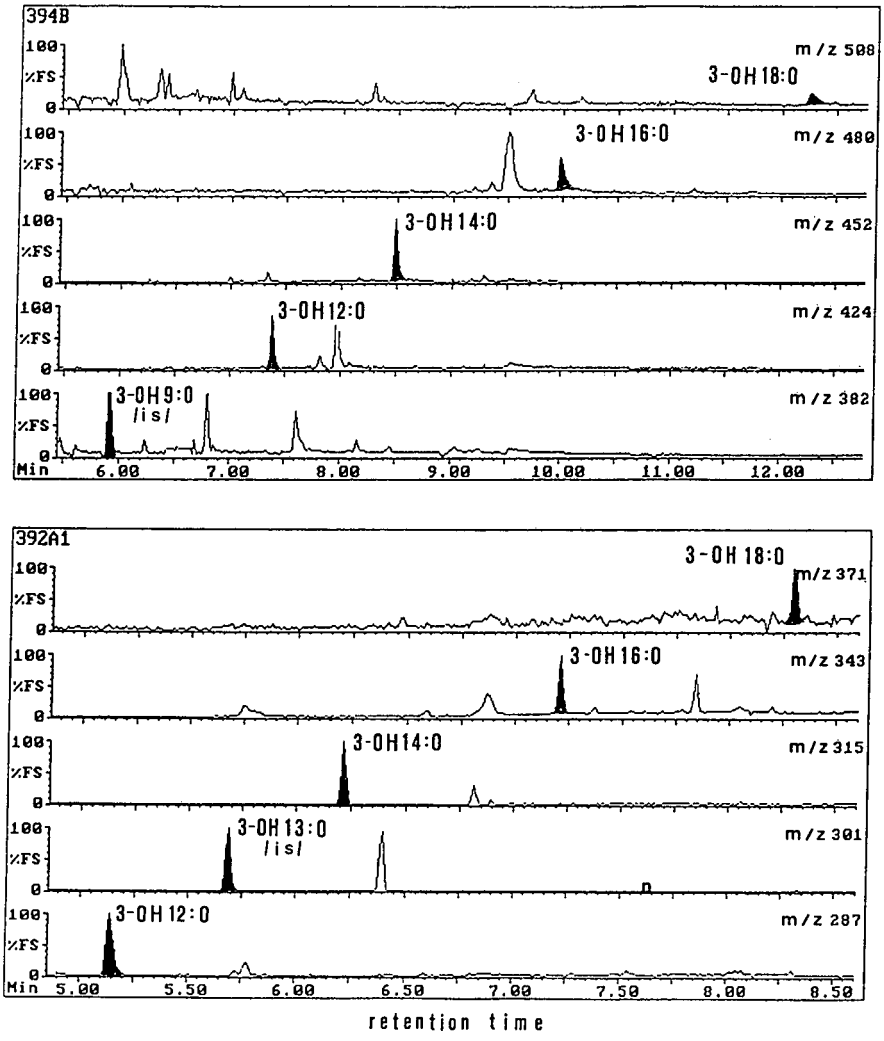

Fig. 5. Mass chromatograms of a bacteria-contaminated pharmacological sample obtained by analysing (scan mode) PFBO (upper) and TMS (lower) methyl ester derivatives of 3-hydroxylated fatty acids. For abbreviations, see text.

sample adsorption and/or decomposition on active sites formed by carbonized material; (5) the ion source should be frequently cleaned.

The amount of LPSs found in the studied pharmacological sample when using TMS derivatization differed somewhat from the amount found when using PFBO derivatization (Table I). This difference was almost exclusively represented by a much higher relative amount of 3-OH 18:0 in the former case; the adsorption of PFBO derivatives in the GC–MS system cannot be excluded.

TMS derivatization is simpler to perform, *i.e.* the reaction is quicker and requires one less extraction step than PFBO derivatization. Furthermore, the background noise was usually very low in Me/TMS mass chromatograms, even when small amounts of LPSs were analysed. Both types of derivative are chemically stable. A general advantage that EI analysis has over CI analysis is a longer filament lifetime, but for optimal sensitivity, NICI analysis of Me/PFBO derivatives is recommended.

ACKNOWLEDGEMENT

This study was supported by grants from the Swedish Work Environment Research Fund and the Swedish Council for Building Research.

NOTE ADDED IN PROOF

The results presented in this paper were achieved when the GC–MS instrument had been in use for 18 months. Thereafter the quadrupole pre-filter was cleaned. This resulted in a considerable increase in detection sensitivity of the 3-hydroxy fatty acid Me/TMS derivatives, especially in SIM mode analysis (data not shown). Thus, not only the condition of the gas chromatograph and the ion source, but also of the quadrupole pre-filter, is vital for high sensitivity.

REFERENCES

1 O. Lüderitz, M. A. Freudenberg, C. Galanos, V. Lehmann, E. T. Rietschel and D. H. Shaw, in F. Bronner, A. Kleinzeller, C. S. Razin and S. Rottem (Editors), *Current Topics in Membranes and Transport*, Academic Press, New York, Vol. 17, 1982, p. 79.
2 E. Jawetz, J. L. Melnick and E. A. Adelberg, *Review of Medical Microbiology*, Lange, Los Altos, CA, 16th ed., 1984, p. 235.
3 S. Clark, R. Rylander and L. Larsson, *Am. Ind. Hyg. Assoc. J.*, 44 (1983) 537.
4 R. Rylander and P. Haglind, *Clin. Allergy*, 14 (1984) 109.
5 A. J. deLucca, M. A. Godshall and M. S. Palmgren, *Am. Ind. Hyg. Assoc. J*, 45 (1984) 336.
6 R. Rylander, *Am. J. Ind. Med*, 10 (1986) 221.
7 F. C. Pearson, J. Bohon, W. Lee, G. Bruszer, M. Sagona, G. Jakubowski, R. Dawe, D. Morrison and C. Dinarello, *Appl. Environ. Microbiol*, 48 (1984) 1189.
8 K. Ikemura, K. Ikegami, T. Shimazu, T. Yoshioka and T. Sugimoto, *J. Clin. Microbiol.*, 27 (1989) 1965.
9 S. K. Maitra, R. Nachum and F. C. Pearson, *Appl. Environ. Microbiol*, 52 (1986) 510.
10 S. K. Maitra, M. C. Schotz, T. T. Yoshikawa and L. B. Guze, *Proc. Natl. Acad. Sci. USA*, 75 (1978) 3993.
11 A. Sonesson, L. Larsson, G. Westerdahl and G. Odham, *J. Chromatogr.*, 417 (1987) 11.
12 A. Sonesson, L. Larsson, A. Schütz, L. Hagmar and T. Hallberg, *Appl. Environ. Microbiol.*, 56 (1990) 1271.
13 C. Galanos, O. Lüderitz, E. T. Rietschel and O. Westphal, in T. W. Goodwin (Editor), *Biochemistry of lipids II —International review of biochemistry*, Vol. 14, University Park Press, Baltimore, 1977, p. 239.
14 C. Ratledge and S. G. Wilkinson. *Microbial Lipids*, Academic Press, London, Vol. 1, 1988.

Journal of Chromatography, 623 (1992) 123–127
Elsevier Science Publishers B.V., Amsterdam

CHROM. 24 387

Extraction and gas chromatographic determination of chlorinated solvents in contaminated soil

Tomaso C. Gerbino, Sandro Nadotti and Paolo Castello

Laboratorio Chimico, Castalia SpA, Via Borzoli 79A/r, I-16161 Genoa (Italy)

(Received May 26th, 1992)

ABSTRACT

The performance of a simple and reliable extraction method for the analysis of chlorinated solvents in soil was evaluated. The gas chromatographic analysis of the final extracts dissolved in acetone showed that the tested compounds (tetrachloroethylene, trichloroethylene, 1,1,1-trichloroethane and 1,2-dichloroethane) can be recovered with an efficiency ranging between 70 and 90% over a wide concentration range in the sample. The method can be used for *in situ* analysis of polluted areas, dumping sites, sediments and sands.

INTRODUCTION

The contamination of the environment by halogenated methanes, ethanes and ethenes has been widely investigated owing to the mutagenic effect of some of these compounds [1–4]. The methods used for the determination of these compounds in water samples can be grouped into three different classes: liquid–liquid extraction [5–7], static headspace [8–11] and purge and trap [12.13]. The final concentrated extracts are analysed by gas chromatography (GC) with specific electron-capture and Hall detectors that exibit a very high sensitivity to these compounds.

The extraction of halogenated compounds from soil samples is carried out with water when their expected concentration is below 1 mg/kg and with methanol (followed by dilution of the extract with water) when the expected concentration is higher [14]. The aqueous solution is then analysed using the methods mentioned above.

The use the headspace methods with solid samples has also been reported [15–19]. They require dedicated instruments and a series of replicate samplings in order to apply the so-called multiple headspace extraction. The procedures can therefore hardly be applied in field analyses. A large number of analyses carried out during the decontamination of a site polluted by tetrachloroethylene showed that the application of the described methods is complicated by the wide range of concentrations existing in the samples, which makes it difficult to predict the dilution needed to maintain the injected sample within the linearity range of the detector used. Further, the use of concentration methods for the preparation of liquid extracts that must be strongly diluted for GC analysis is time consuming and may result in unacceptable errors.

The purpose of this paper is to present a simple and reliable method for the analysis of contaminated soil for chlorinated industrial solvents.

EXPERIMENTAL

Soil samples were obtained from a site (Alessandria, Italy) contaminated by tetrachloroethylene discharged from metal-plating and degreasing operations. The soil samples were drilled and collected from various depths in the contaminated area and were transferred into amber-glass jars which were

Correspondence to: Dr. T. C. Gerbino, Laboratorio Chimico, Castalia SpA, Via Borzoli 79A/r, I-16161 Genoa, Italy.

0021-9673/92/$05.00

closed with PTFE-lined caps and transported to the laboratory in an ice-filled cooler.

A reference soil sample was taken from unpolluted area in the same site, dried at 105°C for 24 h, crushed, passed through a 0.075-mm sieve and used for the preparation of the recovery samples.

Chemicals

Stock standard and working standard solutions were prepared by dissolving aliquots of tetrachloroethylene, trichloroethylene, 1,1,1-trichloroethane, 1,2-dichloroethane (Aldrich, Steinheim, Germany) in pesticide-grade acetone (Merck, Darmstadt, Germany) and diluting with organic-free, deionized, distilled water (Millipore, Bedford, MA, USA).

The normal precautions appropriate for handling volatile analytes were employed [12] and the working standards were checked against certified standards (Supelco, Bellefonte, PA, USA) and reprepared when the deviation was greater than 1%.

In recovery studies an accurately weighed 3-g sample of clean reference soil was placed in a glass flask with a ground-glass stopper, then 100 μl of dilute aqueous standard were added with a microsyringe and the flask was stored for 12 h at 4°C to minimize the losses due to evaporation and to allow the chlorinated hydrocarbons to be absorbed by the soil. Possible inhomogeneity of the distribution in the sample is of minor importance because all the spiked amount (3 g) is subjected to the analytical procedure.

Analysis

The analyses were carried out with a Varian (Palo Alto, CA, USA) Model 3600 gas chromatograph equipped with a nickel-63 (8 mCi) electron-capture detector.

A glass column (3 m × 1/4 in. I.D.) packed with 10% SP-2100 on 80–100-mesh Supelcoport (Supelco) was used at 60°C with pure nitrogen as the carrier gas at a flow-rate of 30 ml/min. The on-column injector was maintained at 70°C and the detector at 300°C.

The pH values of aqueous soil extracts [20] were measured with an Orion Research Model 701 digital pH meter and the total organic carbon was determined by the wet combustion method [20].

Procedures

The halogenated compounds are extracted from 3 g of soil with 60 ml of acetone–water (5:1) in a 100-ml stoppered flask and agitated for 2 h on a shaker. The flask is then allowed to stand in the dark at room temperature for 24 h. The losses of volatile analytes in the extraction are minimal, as the problem may arise when the partition is between the headspace and water, where the compounds are rather insoluble. The presence of the acetone layer where the compounds are highly soluble strongly reduced the losses due to evaporation and to liquid–headspace partition.

An aliquot of clear upper layer (12 ml) is transferred into a 20-ml vial and 2 g of NaCl are added to separate the water layer from the acetone containing the compounds to be determined [21,22].

A 2-ml volume of the acetone layer is taken, dried with anhydrous $CaCl_2$ and stored in vials with PTFE-lined caps at 4°C for further GC analysis; 3 μl of this solution are injected on to the column.

Series of samples spiked with different analyte concentrations were run in duplicate. Analysis of contaminated soils for tetrachloethylene was performed in accordance with the procedure described above.

The recovery of the extracted compounds was determined by comparing the peak area from the analysis of extracts with the peak area on the calibration graph corresponding to the concentration calculated from 100% recovery of the compound in the organic layer.

RESULTS AND DISCUSSION

Tables I–IV show that the recovery of the compounds is greater then 80% (except for 1,2-dichloroethane) and seems to be independent of the concentration in the analysed soil. The lower recovery observed for 1,2-dichloroethane is probably due to the greater volatility of this compound. The lack of a quantitative recovery may be explained by the losses due to handling volatile analytes, but this situation reflects what may happen in authentic samples of contaminated soil, and it is therefore important to follow the same procedure (times, temperatures, volumes) in the calibration and in the analysis in order to minimize the fluctuations.

The incomplete recovery of the compounds is al-

TABLE I

RECOVERY OF TETRACHLOROETHYLENE (B.P. 121°C) ADDED TO REFERENCE SOIL AT DIFFERENT LEVELS

Amount added (μg/kg)	Recovery (%)	
	Replicate 1	Replicate 2
54	95	91
108	81	83
162	89	93
540	92	87
1080	86	88
1540	76	84
3080	88	84
5400	84	91
Mean ± S.D.	87.0 ± 4.9	

TABLE III

RECOVERY OF 1,1,1-TRICHLOROETHANE (B.P. 74°C) ADDED TO REFERENCE SOIL AT DIFFERENT LEVELS

Amount added (μg/kg)	Recovery (%)	
	Replicate 1	Replicate 2
40	74	70
80	76	87
120	99	99
400	76	85
800	74	80
1200	77	78
2400	84	88
4000	88	88
Mean ± S.D.	82.6 ± 8.6	

so due to the different partition coefficients between the aqueous and organic layers and to the mutual miscibility of the two solvents [23]. The salting-out effect due to the addition of NaCl increases the recovery to an extent that depends on the solubility in the two layers [24].

The pratical detection limit is about 10 μg/kg for tetrachloroetylene, 100 μg/kg for 1,1,1-trichloroethane and trichloroetylene and 1 mg/kg for 1,2-dichloroethane, owing to the different responses of the detector to these molecules [25].

The overall linearity of the method also depends on the linear dynamic range of the electron-capture detector, which is a function of the analysed compound and generally ranges within 2–3 orders of magnitude [25]. When the detector signal is above the linear range, a plateau region is observed on the sensitvity plot, an apparent concentration lower than the true value is found and the correct quantitative analysis requires a suitable diluition of the extract. If the concentrations of the various compounds differ widely, two or more samples with different dilution factors should be injected in order to detect each compound within its linearity range.

The high recovery and satisfactory reproducibility over a wide concentration range, from a few μg/

TABLE II

RECOVERY OF TRICHLOROETHYLENE (B.P. 87°C) ADDED TO REFERENCE SOIL AT DIFFERENT LEVELS

Amount added (μg/kg)	Recovery (%)	
	Replicate 1	Replicate 2
44	83	78
88	91	82
176	89	83
438	81	84
876	86	90
1314	96	94
2628	84	86
4380	79	90
Mean ± S.D.	86.0 ± 5.2	

TABLE IV

RECOVERY OF 1,2-DICHLOROETHANE (B.P. 57.2°C) ADDED TO REFERENCE SOIL AT DIFFERENT LEVELS

Amount added (μg/kg)	Recovery (%)	
	Replicate 1	Replicate 2
3750	62	56
7500	61	68
11 250	81	78
37 500	67	75
75 000	89	91
150 000	83	88
300 000	77	78
375 000	69	64
Mean ± S.D.	74.0 ± 10.7	

TABLE V

REMOVAL OF TETRACHLOETHYLENE FROM CONTAMINATED SOILS AS FUNCTION OF EXTRACTION TIME, WITH pH AND TOC VALUES OF THE SOILS EXAMINED

Sample No.	Depth (m)	pH	TOC (mg/kg)	Amount extracted (μg/kg)		
				2 h	24 h	48 h
1	1–1.40	7.76	3201	2245	5089	5239
2	2–2.40	8.00	1656	2305	4742	4775
3	3–3.40	7.66	4505	9922	28 228	26 884
4	4–4.40	7.38	3954	13 423	34 182	38 354
5	5–5.40	7.70	2878	6106	7549	7388
6	6–6.40	7.73	618	149	646	684
7	7–7.40	8.61	873	681	1238	1375
8	8–8.40	7.71	691	76	173	170
9	9–9.50	7.83	564	16	67	70

kg to hundreds of mg/kg, show that the method can be used for the extraction of chlorinated compounds from soil polluted in different environments and therefore containing variable amounts of contaminants, *e.g.*, spill-over of solvents from chemical plants, reclaimed areas contaminated by industrial wastes and dumping sites. The experiments with soil samples spiked with known amounts of standards showed that the extraction is virtually complete after 2 h of extraction on a shaker.

It has been reported [26] that the sorbed compounds in contaminated soil may be highly resistent to desorption. The slow release of trichloroethylene from contaminated soil requires an extended equilibration time for extraction; the equilibrium steady state is reached within 24 h [27,28].

Table V reports the recovery efficiency for tetrachloroethylene from various samples of contaminated soil as a function of extraction time and confirms that the equilibrium between the extracted tetrachloroethylene and that still retained in the soil is complete within 24 h. This behaviour does not depend on the pH and total organic carbon (TOC) values (Table V), which has been correlated with the sorption of organic compounds in soils and sediments [29–31]. This is expected for pH as a change in pH should not affect the desorption of non-polar tetrachloroethylene.

It has been well documented that there is a linear relationship between soil organic carbon and partition coefficients, but when the organic content is low (about 0.1%), the organic fraction is not a valid predictor of the sorption of organic compounds and other sorbent properties, such as specific surface area and cation-exchange capacity, may control the adsorption of non-polar organic compounds.

The available literature data [28] and the experimental results confirm that a 24-h extraction time is preferred in order to ensure the complete recovery of the halogenated compounds from contaminated soil.

CONCLUSIONS

The suggested method permits the determination of chlorinated compounds in polluted soil to be carried out in a short time and with high and reproducible recoveries. The compounds can be analysed over a wide range of concentrations without the problems connected with the extraction methods obtained by modifying the procedures used for the analysis of liquid samples and without requiring dedicated instruments such as for multiple headspace extraction.

The simplicity of the procedure permits its application in field conditions mainly when a rapid analysis is necessary to evaluate the performance of remedial measures by conventional treatment or biological techniques, and is independent of variable soil parameters such as pH and TOC.

Further experiments are in progress in order to evaluate whether the proposed method can be applied to the analysis of sites that have been contaminated for many years ($\geq$10 years), where the ha-

logenated compounds may be strongly adsorbed. It has in fact been reported [27,29,32] that the recovery and efficiency may depend on the age of the polluted sample.

REFERENCES

1 M. Mercier, M. Laus and J. de Garlache, in M. Kirsch-Volders (Editor), *Mutagenicicity, Carcinogenicity and Teratogenicity of Industrial Pollutants*, Plenum Press, New York and London, 1984.
2 International Agency for Research on Carcinogens, *Some Halogenated Hydrocarbons*, Monograph No. 20, IARC, Lyon, 1979.
3 V. F. Simmon and R. G. Tardiff, in R. L. Jolly, H. Gorcher and D. H. Hamilton Jr. (Editors), *Water Chlorination 2*, Ann Arbor Sci. Publ., Ann Arbor, MI, 1978, p. 471.
4 S. Kanitz, G. Castello, T. C. Gerbino, G. Gallelli and V. Patrone, Tec. Sanit., 23 (1985) 859.
5 J. P. Mieure, *J. Am. Water Works Assoc.*, 69 (1977) 60.
6 J. J. Richard and G. A. Junk, *J. Am. Water Works Assoc.*, 69 (1977) 62.
7 H. Norin and L. Ronberg, *Water Res.*, 14 (1980) 1397.
8 E. A. Dietz, Jr. and K. F. Singley, *Anal. Chem.*, 51 (1979) 1809.
9 S. L. Friant and I. H. Suffet, *Anal. Chem.*, 51 (1979) 2167.
10 J. Drozd and J. Novak, *J. Chromatogr.*, 165 (1979) 141.
11 G. Castello, T. C. Gerbino and S. Kanitz, *J. Chromatogr.*, 247 (1982) 263.
12 US Environmental Protection Agency, *Method 601, Purgeable Halocarbons, 40 CFR, Part 136 43261, Fed. Regis. 49*, No. 209 (1984).
13 T. A. Bellar and J. J. Lichtenberg, *J. Am. Water Works Assoc.*, 66 (1974) 739.
14 US Environmental Protection Agency, *Test Methods for Evaluating Solid Waste (SW 846), Method 5030*, Office of Solid Waste and Emergency Response, Washington, DC, 1986.
15 M. J. Charles and M. S. Simmons, *Anal. Chem.*, 59 (1987) 1217.
16 B. Kolb, P. Pospisil and M. Auer, *Chromatographia*, 19 (1984) 113.
17 B. Kolb and P. Pospisil, *Chromatographia*, 10 (1977) 705.
18 B. Kolb, *Chromatographia*, 15 (1982) 587.
19 M. R. Milana, A. Maggio, M. Denaro, R. Feliciani and L. Gramiccioni, *J. Chromatogr.*, 442 (1991) 205.
20 Societa Italiana della Scienza del Suolo, *Metodi Normalizzati di Analisi del Suolo*, Edagricole, Bologna, 1985.
21 S . G. Heuser and K. A. Scudamore, *J. Sci. Food. Agric.*, 20 (1969) 566.
22 Report by Panel on Fumigant Residues in Grain, *Analyst (London)*, 99 (1974) 570.
23 D. C. Legget, T. F. Jenkins, and P. H. Hyares, *Anal. Chem.*, 62 (1990) 1355.
24 T. F. Jenkins and P. H. Hyares, *Anal. Chem.*, 62 (1991) 1341.
25 G. Castello, T. C. Gerbino and S. Kanitz, *J. Chromatogr.*, 351 (1986) 165.
26 S. H. Steinberg, J. J. Pignatello and B. L. Sawhney, *Environ. Sci. Technol.*, 21 (1987) 1201.
27 J. A. Smith, C. T. Chiou, J. A. Kammer and D. E. Kile, *Environ. Sci. Technol.*, 24 (1990) 676.
28 S. G. Pavlositathis and K. Jaglad, *Environ. Sci. Technol.*, 25 (1991) 274.
29 J. W. Hamaker and J. H. Thompson, in C. A. I. Goring and G. L. Hammer (Editor), *Organic Chemicals in the Soil Environment*, Marcel Dekker, New York, 1972, p. 49.
30 S. W. Karickhoff, D. S. Brown and T. A. Scott, *Water Res.*, 13 (1979) 241.
31 R. P. Schwarzenbach and J. Westell, *Environ. Sci. Technol.*, 5 (1981) 1360.
32 W. J. Weder and T. C. Voice, *Water Res.*, 17 (1983) 1433.

Journal of Chromatography, 623 (1992) 129–137
Elsevier Science Publishers B.V., Amsterdam

CHROM. 24 450

Chiral separations in supercritical fluid chromatography: a multivariate optimization method*

Patrik Petersson, Niklas Lundell and Karin E. Markides

Department of Analytical Chemistry, Uppsala University, P.O. Box 531, S-751 21 Uppsala (Sweden)

(First received February 7th, 1992; revised manuscript received May 5th, 1992)

ABSTRACT

A multivariate optimization method, based on the method of steepest ascent, is proposed for the separation of two enantiomers on a chiral stationary phase in open-tubular column supercritical fluid chromatography. The objective of the method is to optimize start density, density gradient and temperature in order to locate a desired resolution in a first step and, if desired, minimize the retention time in a second step without decrease in resolution.

INTRODUCTION

Open-tubular column supercritical fluid chromatography (SFC) is a promising technique for chiral separations [1,2]. It possesses important advantages over gas chromatography (GC) and liquid chromatography (LC) such as combined low-temperature elution and access to a wide range of detection methods, including "universal" and sensitive flame ionization detection (FID). Low temperature is important when working with chiral separations as it will increase the chiral selectivity [3] of the chromatographic system and reduce the probability of racemization or thermal decomposition of the enantiomers.

There are several factors that simplify the optimization of a chiral separation in comparison with the separation of more complex mixtures. In most instances, the purpose of the separation is to determine the ratio of the amounts of the two enantiomers of a chiral compound and therefore only the resolution and retention times of the two enantiomers have to be monitored. This eliminates the need for the definition of more or less imaginative quality measures, often refered to as response functions [4,5]. In addition, there have been no reports, to our knowledge, of a reversal of elution order of enantiomers in SFC due to different elution temperature or density. Therefore, there should be no need for peak tracking [6] during the optimization. The number of variables that can be used to optimize a chiral separation using SFC–FID with a certain column, restrictor and mobile phase are limited to density/pressure, temprature and gradients of these, as organic modifiers (possibly with the exception for formic acid) are not suitable in combination with FID. In the method described in this paper, the start density, density gradient and temperature are the variables chosen for optimization, a compromise between the number of variables/experiments and possibilities available to achieve the desired separation.

Multivariate optimization of separations in SFC is a relatively new area where, until now, only two papers have been published, neither of which treated chiral separations. Crow and Foley [7] described the use of a modified simplex algorithm whereas Ong *et*

Correspondence to: Dr. K. E. Markides, Department of Analytical Chemistry, Uppsala University, P.O. Box 531, S-751 21 Uppsala, Sweden.

* Presented at the *European Symposium on Analytical Supercritical Fluid Chromatography and Extraction, Wiesbaden, December 4–5, 1991.*

0021-9673/92/$05.00

al. [8] chose to use overlapping resolution mapping. In the former study it was concluded that the parameters that control the separation are highly synergistic and therefore it would not be appropriate to use an univariate optimization strategy.

For the separation of two enantiomers by open-tubular column SFC–FID, a multivariate optimization method consisting of two steps is suggested: the first step locates and verifies the conditions of the desired resolution after approximately six experiments and the second step provides the possibility of continuing with a minimization of the retention time without a decrease in resolution. In this step sequential experiments are carried out until little progress is made. A minimization of retention time should result in an increase in peak height and therefore a more favourable signal-to-noise ratio for the determination of optical purity. This optimization method has been designed in a way that does not require any advanced software or skills in programming.

THEORY

Measure of resolution

The chiral resolution (*CR*) was calculated as a measure of the separation of two enantiomers. This measure was defined by Aichholz *et al.* [9] as a chiral analogy to the trennzahl (*TZ*) or separation number (*SN*):

$$CR = \frac{(t_R)_2 - (t_R)_1}{(w_h)_2 + (w_h)_1} - 1 \quad (1)$$

where t_R is retention time and w_h is peak width at half-height.

Determination of resolution

Chiral resolution was calculated from retention times and peak widths obtained by the fitting of two Gaussian functions to the recorded data. As long as the peaks have a shape that is approximately Gaussian, as in most instances in open-tubular column SFC, these variables can easily be estimated even for overlapping peaks (Fig. 1). The peak fitting of overlapping peaks is simplified by the assumption of equal widths for both peaks.

Steepest ascent

Box and Wilson first described the method of steepest ascent in 1951 [10]. In this method, a first-order polynomial is fitted from initial experiments in a subregion of the experimental domain. The response is maximized by sequential experiments in the direction that results in the largest gain in response. This is done by moving along the vector described by the coefficients of the polynomial. Subsequent experiments along the vector are continued until the curvature is considerable or little progress is made. If the former applies the optimization is ended or repeated around the experiment which resulted in the largest response.

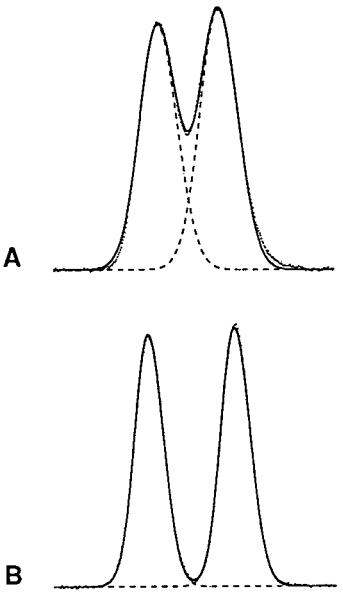

Fig. 1. Overlapping ($CR = -0.316$) and baseline-resolved ($CR = 0.274$) peaks of the enantiomers of diethyl tartrate illustrating the advantage of fitting Gaussian functions for the estimation of peak widths and retention times. Conditions: (A) CO_2, 78°C, start density 0.325 g ml^{-1}, density gradient 0.037 g ml^{-1} min^{-1}; (B) CO_2, 91°C, start density 0.175 g ml^{-1}, density gradient 0.054 g ml^{-1} min^{-1}.

Step one: location of the desired resolution

Five experiments are performed in a half-fractional factorial design [11] shaped as a cube with experiments located in the centre and in four of the corners (Fig. 2A) (the experimental domain is chosen from the result of previous "scouting", always necessary to judge if the stationary phase possess chiral selectivity for the analyte in question). From these five experiments a first-order polynomi-

al (eqn. 2) is fitted as a model of chiral resolution. The fitting is performed by the general least-squares matrix solution for linear models [11] (eqn. 3). If the variables (x_1–x_3) are coded in three levels, −1, 0 and +1, as illustrated in Table I, the fitting is simplified, and only the matrix of the response has to be changed in order to fit different models.

$$CR = \alpha_0 + \alpha_1 x_1 + \alpha_2 x_2 + \alpha_3 x_3 \quad (2)$$

$$\mathbf{A} = \begin{bmatrix} \alpha_0 \\ \alpha_1 \\ \alpha_2 \\ \alpha_3 \end{bmatrix} \quad \mathbf{X} = \begin{bmatrix} 1 & 0 & 0 & 0 \\ 1 & -1 & 1 & 1 \\ 1 & 1 & -1 & 1 \\ 1 & 1 & 1 & -1 \\ 1 & -1 & -1 & -1 \end{bmatrix} \quad \mathbf{CR} = \begin{bmatrix} CR_1 \\ CR_2 \\ CR_3 \\ CR_4 \\ CR_5 \end{bmatrix}$$

$$\mathbf{A} = (\mathbf{X}'\mathbf{X})^{-1}\mathbf{X}'\,\mathbf{CR} \quad (3)$$

The empirical coefficients of the polynomial (α_1–α_3) provide the direction which results in the largest gain in resolution, the vector of steepest ascent (Fig. 2B). The point on this vector where the desired resolution (CR^*) is obtained is given by eqns. 4–6 in coded values. The scale factor (Δ), which is related to the distance from the centre of the design, is calculated according to eqn. 7. If there is an unacceptable deviation between model and reality, the scale factor is adjusted towards higher/lower resolution.

$$x_i = \alpha_i \Delta \quad (4)$$

$$x_j = \alpha_j \Delta \quad (5)$$

$$x_k = \alpha_k \Delta \quad (6)$$

$$\Delta = \frac{CR^* - \alpha_0}{\alpha_i^2 + \alpha_j^2 + \alpha_k^2} \quad (7)$$

Step two: minimization of retention time

If the retention time is critical for the analysis, it is possible to minimize it without reducing the resolution. This is done by a modified method of steepest ascent as described below.

From five experiments, a half-fractional factorial design around the experiment which gave the desired resolution (Fig. 2C), first-order polynomials are fitted as models for the chiral resolution and the retention time of the last-eluting enantiomer (eqns. 8 and 9).

$$CR = \beta_0 + \beta_1 x_1 + \beta_2 x_2 + \beta_3 x_3 \quad (8)$$

$$(t_R)_2 = \gamma_0 + \gamma_1 x_1 + \gamma_2 x_2 + \gamma_3 x_3 \quad (9)$$

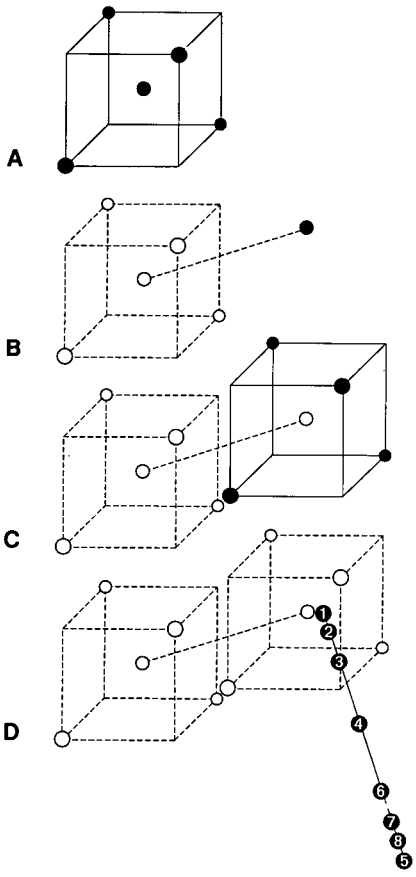

Fig. 2. Schematic illustration of the multivariate optimization method: (A) Five experiments to estimate a linear model for chiral resolution; (B) calculation of the location of the desired resolution along the vector of steepest ascent; (C) four experiments to estimate linear models for the chiral resolution and the retention time of the last-eluting enantiomer; (D) minimization of the retention time by a line search along the vector of steepest ascent for the retention time of the last eluting enantiomer. The chiral resolution is kept above a specified value.

The coefficients of eqn. 9 give the vector of steepest ascent for the retention time. However, in order to keep the resolution equal to or higher than the desired resolution during the minimization, eqn. 9 has to be modified. This is done by isolating one of the variables of eqn. 8, as a dependent variable (x_k), and including the desired resolution in this expression (eqn. 10). The dependent variable is chosen so that the starting point of the line search (see below) is located as close as possible to the centre of the experimental design (*i.e.*, $x_i = x_j = 0$). The com-

bination of eqns. 9 and 10 provides an expression (eqn. 11) that allows the minimization of the retention time without a decrease in resolution.

$$x_k = \frac{CR^* - \beta_0 - \beta_i x_i - \beta_j x_j}{\beta_k} \quad (10)$$

$$(t_R)_2 = \gamma_0 + \gamma_i x_i + \gamma_j x_j + \gamma_k \left(\frac{CR^* - \beta_0 - \beta_i x_i - \beta_j x_j}{\beta_k} \right) \quad (11)$$

To minimize the retention time, an initial step size for one of the independent variables (x_i) is chosen by the analyst while the other independent variable (x_j) is calculated by this initial step size and the coefficients of eqn. 9 (eqns. 12 and 13).

$$\delta = x_i/\gamma_i \quad (12)$$

$$x_j = \gamma_j \delta \quad (13)$$

In order to reduce the number of experiments along the vector, a method for line search is applied (Fig. 2D), *i.e.*, the step size is doubled for every step until the direction of the search is changed for the first time. From this moment the step size is halved for every step no matter what the direction is (Fig. 3). The direction of the line search is changed when the resolution decreases or the retention time increases relative to the best experiment in the line search (when a specified limit is passed, *i.e.*, the lower/upper limit of a confidence interval for the variable). The line search is ended at the point where the step size is limited by the chromatographic instrumentation. Four experiments in a half-fractional factorial design centred around the last experiment in the line search will give new linear models and another vector of steepest ascent to follow. This procedure is repeated until little progress is made.

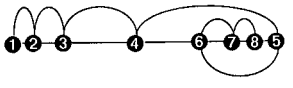

Fig. 3. Illustration of the line search along the vector of steepest ascent: the step size is doubled for every step until the direction of the search is changed (5). From this moment the step size is halved for every step. The direction of the line search is changed when the resolution decrease or the retention time increase relative to the best experiment in the line search (5 and 6). The line search is ended at the point where the step size is limited by the chromatographic instrumentation (8).

EXPERIMENTAL

Instrumentation

The chromatograms were obtained with a Series 600-D SFC system (Dionex, Salt Lake City, UT, USA) equipped with a flame ionization detector (350°C). The injector consisted of a Model CI4W.2 high-pressure four-port valve injector with a 0.2-μl sample loop (Valco Instruments, Houston, TX, USA) and a splitter (300 μm I.D.) (SGE, Austin, TX, USA). SFC-grade CO_2 (Scott Speciality Gases, Plumsteadville, PA, USA) was used as the mobile phase at an average linear velocity of *ca.* 1.5 cm s^{-1} (60°C, 0.30 g ml^{-1}) controlled by a deactivated frit restrictor (50 μm I.D.) obtained from Dionex. The chromatograms were registered with a Model SP4290 integrator (Spectra-Physics, San Jose, CA, USA) and transferred to a Macintosh IIfx computer (Apple Computer, Cupertino, CA, USA) for further treatment.

Column

An open-tubular column (5 m × 50 μm I.D.) coated with a chiral copolymeric stationary phase, poly[(1*R*)-*trans*-N,N′-1,2-cyclohexylenebisbenzamide]oligoalkylsiloxane [12] (film thickness ≈ 0.25 μm), was used.

Samples

(−)- and (+)-diethyl tartrate were purchased from Aldrich (Steinheim am Albuch, Germany). Ethyl-(2*R*,3*S*)-dihydroxyoctanoate and ethyl-(2*S*, 3*R*)-dihydroxyoctanoate were provided by K. B. Sharples (Massachusetts Institute of Technology) and (±)-mephenytoin by Sandoz (Basle, Switzerland). Ethanol was used as the solvent except for mephenytoin, which was dissolved in toluene.

Software

The chromatograms were transferred from the integrator and subsequently decoded with an in-house written routine in Microsoft QuickBasic (Microsoft, Redmond, WA, USA). A program for general graphing and data analysis, Igor (Wave Metrics, Lake Oswego, OR, USA), was used for peak fitting and Microsoft Excel was used for all other calculations.

RESULTS AND DISCUSSION

The optimization method is exemplified in Tables I–VI with the separation of ethyl-(2*R*,3*S*)-dihydroxyoctanoate and ethyl-(2*S*,3*R*)-dihydroxyoctanoate. According to the two-step theoretical discussion, a two-step optimization was performed, as follows.

Step one: conditions for the desired resolution were located as follows. The levels of the variables were coded (Table I) and five experiments performed according to a half-fractional factorial design. An experiment in the centre of the design was included to give the possibility of detecting large deviations from the linear model (Table II). Using

TABLE I

Step one: coding of variables

Coded variable[a]	−1	0	+1
D_0 Start density (g ml^{-1})	0.270	0.300	0.330
t Temperature (°C)	47	50	53
D_g Density gradient (g ml^{-1} min^{-1})	0.007	0.010	0.013

[a] $x_1 = (D_0 - 0.300)/0.030$; $x_2 = (t - 50)/3$; $x_3 = (D_g - 0.010)/0.003$.

TABLE II

Step one: half-fractional factorial design for the location of the desired resolution

Experiment No.	Coded variables[a]			D_0 (g ml^{-1})	t (°C)	D_g (g ml^{-1} min^{-1})	CR	$(t_R)_2$ (min)
	x_1	x_2	x_3					
1	0	0	0	0.300	50	0.010	0.825	17.336
2	−1	1	1	0.270	53	0.013	0.756	16.270
3	1	−1	1	0.330	47	0.013	0.516	15.077
4	1	1	−1	0.330	53	0.007	0.659	15.943
5	−1	−1	−1	0.270	47	0.007	1.219	25.980

[a] See Table I.

TABLE III

Step two: first half-fractional factorial design for the minimization of the retention time

Experiment No.	Coded variables[a]			D_0 (g ml^{-1})	t (°C)	D_g (g ml^{-1} min^{-1})	CR	$(t_R)_2$ (min)
	x_1	x_2	x_3					
6	0	0	0	0.344	52	0.013	0.281	12.251
7	−1	1	1	0.314	55	0.016	0.365	11.882
8	1	−1	1	0.374	49	0.016	0.050	11.180
9	1	1	−1	0.374	55	0.010	−0.009	10.964
10	−1	−1	−1	0.314	49	0.010	0.632	16.416

[a] In analogy with Table I, $x_1 = (D_0 - 0.344)/0.030$; $x_2 = (t - 52)/3$; $x_3 = (D_g - 0.013)/0.003$.

TABLE IV

Step two: line search along the first vector of steepest ascent for the retention time

Experiment No.	D_0 (g ml^{-1})	t (°C)	D_g (g ml^{-1} min^{-1})	δ	CR	$(t_R)_2$ (min)
11	0.343	52	0.013	0.000	0.327	12.303
12	0.338	53	0.014	−0.281	0.306	11.998
13	0.327	55	0.016	−0.842	0.283	11.423
14	0.306	59	0.020	−1.965	0.231	10.454
15	0.316	57	0.018	−1.404	0.264	10.944
16	0.311	58	0.019	−1.684	0.255	10.704

TABLE V

Step two: second half-fractional factorial design for the minimization of the retention time

Experiment No.	Coded variables[a]			D_0 (g ml^{-1})	t (°C)	D_g (g ml^{-1} min^{-1})	CR	$(t_R)_2$ (min)
	x_1	x_2	x_3					
17	0	0	0	0.311	58	0.019	0.255	10.704
18	−1	1	1	0.281	61	0.022	0.278	10.413
19	1	−1	1	0.341	55	0.022	0.086	9.734
20	1	1	−1	0.341	61	0.016	0.041	9.491
21	−1	−1	−1	0.281	55	0.016	0.547	13.629

[a] In analogy with Table I, $x_1 = (D_0 - 0.311)/0.030$; $x_2 = (t - 58)/3$; $x_3 = (D_g - 0.019)/0.003$.

TABLE VI

Step two: line search along the second vector of steepest ascent for the retention time

Experiment No.	D_0 (g ml^{-1})	t (°C)	D_g (g ml^{-1} min^{-1})	δ	CR	$(t_R)_2$ (min)
22	0.305	58	0.019	0.000	0.303	10.911
23	0.298	59	0.020	−0.385	0.284	10.738
24	0.283	61	0.022	−1.156	0.280	10.410
25	0.254	65	0.025	−2.698	0.221	9.969
26	0.269	63	0.023	−1.927	0.245	10.177
27	0.276	62	0.022	−1.542	0.265	10.293

the coefficients of the polynomial fitted for the chiral resolution (eqn. 14), the location of the desired resolution, $CR^* = 0.274$, along the vector of steepest ascent was calculated:

$$CR = 0.7949 - 0.2001x_1 - 0.0799x_2 - 0.1512x_3 \quad (14)$$

The suggested conditions (Table III, experiment 6) gave a CR value (0.281) that is within an acceptable resolution range. To estimate this standard error of resolution, a large number of experiments were carried out and it was found that $CR^* \pm 0.025$ is a reasonable range (90% confidence interval for base-

line resolution, $n = 18$). This estimate is not required in order to perform an optimization, it was merely a necessary step in the development of the method.

Step two: the retention time was minimized according to the modified method of steepest ascent. A half-fractional factorial design was located around the point of the desired resolution and the levels of the variables were coded in analogy with Table I. From the results of these five experiments (Table III), polynomials were fitted for the chiral resolution and the retention time of the last eluting enantiomer, respectively (eqns. 15 and 16).

$$CR = 0.2637 - 0.2394x_1 - 0.0815x_2 - 0.0520x_3 \quad (15)$$

$$(t_R)_2 = 12.5387 - 1.5388x_1 - 1.1875x_2 - 1.0794x_3 \quad (16)$$

The coefficients of these polynomials were used to follow the vector of steepest ascent for the retention time of the last-eluting enantiomer (Table IV). In this line search, the coded temperature (x_2) was chosen as the independent variable which determined the initial step size. The coded start density (x_1) was chosen as the dependent variable. [As a result of the definition of the dependent variable (eqn. 10), the first experiment in a line search does not necessarily result in a retention time that is shorter than in the previous experiment, as seen in Table IV.] After six experiments along the vector, the smallest possible change in temperature was reached and four experiments in a half-fractional factorial design (Table V) gave two new polynomials (eqns. 17 and 18) and a third vector to follow (Table VI).

$$CR = 0.2413 - 0.1746x_1 - 0.0786x_2 - 0.0558x_3 \quad (17)$$

$$(t_R)_2 = 10.7943 - 1.2043x_1 - 0.8648x_2 - 0.7430x_3 \quad (18)$$

After this second line search, the optimization was ended (Fig. 4). At this point the retention time had been reduced by 16% compared with the point where the desired resolution was achieved.

A more detailed investigation of the response surface around the last experiment was performed by a central composite design [11]. Second-order polynomials fitted to these results as models of resolution and retention time revealed that the area of optimum conditions had been reached.

Before deciding to use the method of steepest ascent, one alternative approach using a central composite design was evaluated. Unfortunately, the desired resolution often covered a large experimental domain and a central composite design could therefore not provide models which were good enough to locate optimum conditions. However, these experiments clearly indicated the need to optimize the start density, density gradient and temperature. Further, it showed that a first-order polynomial should be a good approximation of models for both resolution and retention time in a subregion of the experimental domain (the response surfaces obtained from the central composite designs were smooth and slightly parabolic).

Figs. 5 and 6 show two other applications of the optimization method where the enantiomers of (±)-mephenytoin, an anticonvulsant drug, and (±)-diethyltartrate were separated at retention times comparable to those of a rapid GC analysis. In the three examples the decreases in retention time, from the point of location of the desired resolution to the point of location of the area of optimum conditions, are in the range 3–19%.

One problem that often is associated with sequential methods, such as the method of steepest ascent or the simplex algorithm, is the risk of finding a local

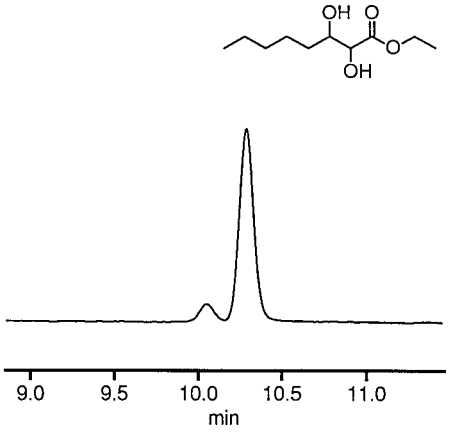

Fig. 4. Optimized separation of ethyl-(2*R*,3*S*)-dihydroxyoctanoate and ethyl-(2*S*,3*R*)-dihydroxyoctanoate. The desired resolution was located after six experiments. An additional 20 experiments resulted in a 16% decrease in the retention time of the last-eluting enantiomer. Conditions: CO_2, 62°C, start density 0.276 g ml^{-1}, density gradient 0.022 g ml^{-1} min^{-1}.

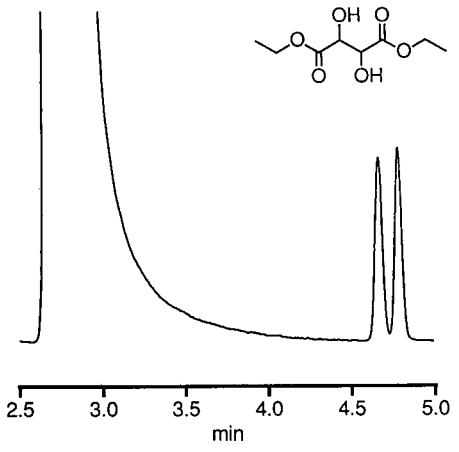

Fig. 5. Optimized separation of the enantiomers of the anticonvulsant drug mephenytoin. The desired resolution was located after seven experiments. An additional 18 experiments resulted in a 3% reduction of the retention time of the last eluting enantiomer. Conditions: CO_2, 92°C, start density 0.555 g ml^{-1}, density gradient 0.024 g ml^{-1} min^{-1}

optimum instead of the true optimum. As only the two enantiomers are to be separated and, as mentioned above, the response surfaces for both resolution and retention time are smooth and slightly parabolic, there should be no risk of hitting a local optimum with the described optimization procedure. Therefore, the minimization of retention time

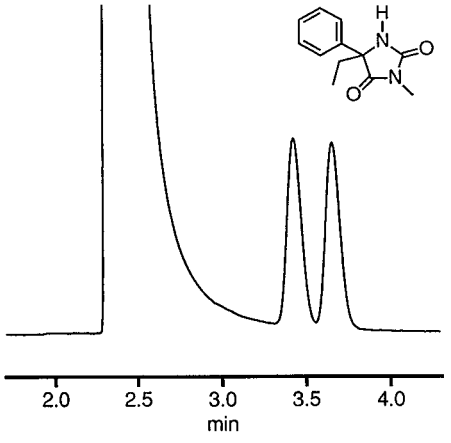

Fig. 6. Optimized separation of the enantiomers of diethyl tartrate. The desired resolution was located after seven experiments. An additional 21 experiments resulted in a 19% decrease in the retention time of the last-eluting enantiomer. Conditions: CO_2, 91°C, start density 0.175 g ml^{-1}, density gradient 0.054 g ml^{-1} min^{-1}.

in step two should also reach the optimum area sooner or later by a successive application of the method. The reliability of this location of optimum conditions is dependent on the number of experiments and therefore at least two vectors of steepest ascent ought to be followed. An assumption made in this second step, probably of no practical importance, is that the shortest possible retention time at a certain resolution increases with increasing resolution.

The method outlined is designed to optimize the separation of two enantiomers without any interfering compounds present in the sample. If interfering compounds are present a modified approach should be used. Step one provides conditions that give the desired resolution of a racemic standard solution. A central composite design, or alternatively a modified simplex algorithm, located in this limited experimental domain should then have good possibilities of finding optimum conditions.

The deterministic gradient theories that have been developed for GC [13–15] and LC [16,17] with good results may also be useful for the optimization of separations performed by SFC. There are, however, a number of complications such as changes in efficiency/mass transfer, linear velocity, etc., during a density program.

CONCLUSIONS

It has been shown that the suggested method can be used to optimize chiral separations in open-tubular column SFC. It has also been shown that it is sufficient to use three parameters, start density, density gradient and temperature, in order to reach a desired resolution within a specified range (if possible with the chromatographic system) and, if the retention time or signal-to-noise ratio is critical, minimize the retention time without a reduction in the resolution. The method was demonstrated using open-tubular column SFC, but it is also applicable to chiral separations in GC. It should be noted that all calculations are possible with commercial software and without skills in programming.

ACKNOWLEDGEMENTS

The authors would like to thank Örjan Andersson for decoding the data transferred from the integra-

tor, Rolf Danielsson and Gunnar Malmquist for fruitful discussions of chemometrical problems and ideas and the donors of the samples. This work was supported by the Swedish Natural Science Research Council, grant number K-KU 1439-300.

REFERENCES

1 V. Schurig, Z. Juvancz, G. J. Nicholson and D. Schmalzing, *J. High Resolut. Chromatogr.*, 14 (1991) 58.
2 P. Petersson, K. E. Markides, D. F. Johnson, B. E. Rossiter, J. S. Bradshaw and M. L. Lee, *J. Microcol. Sep.*, 4 (1992) 155.
3 B. Koppenhoefer and E. Bayer, *Chromatographia*, 19 (1984) 123.
4 H. J. G. Debets, B. L. Bajema and D. A. Doornbos, *Anal. Chim. Acta*, 151 (1983) 131.
5 H. K. Smith and W. L. Switzer, *J. Chromatogr.*, 27 (1989) 244.
6 J. W. Dolan, *LC·GC Int.*, 3 (1990) 17.
7 J. A. Crow and J. P. Foley, *Anal. Chem.*, 62 (1990) 378.
8 C. P. Ong, K. P. Chin, H. K. Lee and S. F. Y. Li, *J. High Resolut. Chromatogr.*, 14 (1991) 249.
9 R. Aichholz, U. Bölz and P. Fisher, *J. High Resolut. Chromatogr.*, 13 (1990) 234.
10 G. E. P. Box and K. B. Wilson, *J. R. Statist. Soc.*, Ser. B, 13 (1951) 1.
11 C. K. Bayne and I. B. Rubin, *Practical Experimental Design and Optimization Methods for Chemists*, VCH, Deerfield Beach, FL, 1986.
12 D. F. Johnson, J. S. Bradshaw, M. Eguchi, J. Curtis, B. E. Rossiter, M. L. Lee, P. Petersson and K. E. Markides, *J. Chromatogr.*, 549 (1992) 283.
13 D. E. Bautz, J. W. Dolan and L. R. Snyder, *J. Chromatogr.*, 541 (1991) 1.
14 J. W. Dolan, L. R. Snyder and D. E. Bautz, *J. Chromatogr.*, 541 (1991) 21.
15 L. R. Snyder, D. E. Bautz and J. W. Dolan, *J. Chromatogr.*, 541 (1991) 35.
16 L. R. Snyder, in Cs. Horváth (Editor), *HPLC—Advances and Perspectives*, Vol. 1, Academic Press, New York, 1980, Ch. 1, p. 207.
17 P. Jandera and J. Churáček, *Gradient Elution in Column Liquid Chromatography*, Elsevier, Amsterdam, 1985.

Journal of Chromatography, 623 (1992) 139–147
Elsevier Science Publishers B.V., Amsterdam

CHROM. 24 386

Computer-aided optimization of gradient multiple-development thin-layer chromatography

I. Two-stage development

W. Markowski and E. Soczewiński

Department of Inorganic and Analytical Chemistry, Medical Academy, Staszica 6, 20-081 Lublin (Poland)

(First received March 17th, 1992; revised manuscript received May 26th, 1992)

ABSTRACT

A theoretical model of the simplest version of gradient multiple development, the technique of two-step development, is discussed as a preliminary stage to a general theory of planar multi-step development and automated multiple development (AMD). A computer program for the calculation of final R_F values for two-step development in the gradient mode for known retention *vs.* eluent composition relationships is reported. Comparison of predicted and experimental R_F values shows satisfactory agreement; still better agreement is observed for the consecutive ΔR_F values.

INTRODUCTION

The multiple development technique in thin-layer chromatography (TLC) is a modern concept which enables high spot capacities to be attained and is suitable for the analysis of very complex mixtures [1–4]. The evolution of this method has occurred in three principal stages. The first is concerned with the formulation of the experimental technique and a better understanding of the phenomena involved in the process of multiple development. The second relates to attempts to automate the process: the method of programmed (isocratic) multiple development. The third, still in progress, is represented by the automation of multiple gradient development introduced by Burger [5].

In all techniques of multiple development, the plate is repeatedly developed in the same direction, with intermittent evaporation of the mobile phase between the consecutive developments. If the layer is developed many times to the same distance with the same eluent and the plate is removed from the chamber between the stages to evaporate the solvent, the process is called unidimensional multiple chromatography; it was applied in this form by Jeanes *et al.* [6]. A variation of this technique, called incremental multiple development, consists in the stepwise change of the development distance which is the shortest in the first step and is then increased usually by a constant increment; the last development step corresponds to the maximum development distance. If in the process of multiple development the solvent strength of the mobile phase is varied, the technique is then called gradient multiple development in either the unidimensional or the incremental version. The change in the mobile phase may concern several or all steps. Depending on the properties of the components of the mixture to be analysed, an increasing or decreasing gradient of solvent strength can be applied. The process of

Correspondence to: Dr. W. Markowski, Department of Inorganic and Analytical Chemistry, Medical Academy, Staszica 6, 20-081 Lublin, Poland.

0021-9673/92/$05.00

multiple development with an increasing gradient can be described by a model and equations reported earlier [7–12], modified to take into account intermittent evaporation of solvents. Such gradients are advantageous when the mixture is to be separated into fractions containing several components. In the simplest case of a decreasing stepwise gradient, the layer is developed to half the distance with a polar eluent that separates the most polar components in the lower part of the chromatogram; the less polar components are accumulated in the front area. Their separation occurs in the second stage when the layer is developed to the full distance with a less polar eluent. The incremental, multi-step version of this technique, with programmed, automated development and evaporation steps, is called automated multiple development [13,14]; owing to flattening of the spots at each passage of the front, increased separation efficiencies are obtained and the method is considered to be the most effective and versatile technique of TLC [15].

In spite of the advantages of multiple gradient development, there is no adequate model or theory of decreasing stepwise gradient necessary for rational optimization procedures.

In this paper, we present a basic theory of gradient multiple development (with computer assistance) limited to the simplest case of two-step development, carried out in a horizontal sandwich chamber [16–18]. A comprehensive general theory of planar gradient multiple development will be presented in a later paper [19]. It should be added that the theory of multiple development with intermittent evaporation of the solvent is inherently different from the technique of mobile phase gradients [7–12]. The theory and complete programs apply also to isocratic multiple development, assuming a constant solvent strength, *i.e.*, k' values of individual components.

THEORY

The process of two-step gradient development will be considered. The following assumptions are made: (i) a binary eluent is employed and the solvent strength is decreased in the second development; (ii) two steps are necessary to develop a plate, which corresponds to a total development time of 0.5–1 h, and the total migration distance is less than 10 cm; (iii) after the first development to a distance $z_{(1)}$ [$z_{(1)} < 1$], the layer is dried under vacuum, so that the first solvent is completely removed from the plate and the composition of the second solvent introduced in next step is not changed; (iv) the second development is to the total distance $z_{(2)} = 1.0$; and (v) a quantitative retention *vs.* solvent composition relationship of the solutes for the given adsorbent–eluent system is assumed.

For this purpose, one of the well known equations could be applied (see ref. 20 for logarithmic forms of the equations) to normal phase systems:

$$k'_{(j,i)} = \frac{k^0_{(j)}}{c^{m_{(j)}}_{(i)}} \tag{1}$$

and to reversed-phase systems:

$$k'_{(j,i)} = \frac{k^0_{(j)}}{10^{m_{(j)}c_{(i)}}} \tag{2}$$

where $k'_{(j,i)}$ is the capacity factor of solute j for the ith consecutive gradient step, $k^0_{(j)}$ is the capacity factor of solute j for unit concentration of modifier (volume fraction $c = 1$) for eqn. 1 and for unit concentration of water [$c_{(i)} = 0$] for eqn. 2 and $m_{(j)}$ is the slope of log–log plot for solute j.

Consider the diagram in Fig. 1, which shows the path migrated by the solute and the paths of the solvent fronts. In the first step of the gradient the concentration of modifier [$c_{(1)}$] is very high and the volume of the mobile phase [$v_{(1)}$] is equal to development to a partial distance $z_{(1)}$ of less than unity. For example, this distance is equal to 0.25 of the total development length. The ordinate represents the migration along the plate and the abscissa the volume of eluent absorbed by the layer. The void volume of the layer (v_0) is assumed to be equal to one (see Symbols). Under these assumptions the solvent front in the first step reaches only a fraction of the total development distance. If that distance is 0.25 then the front of the mobile phase migrated a segment of length $z_{(1)} = 0.25$ (in R_F units). The solute migrates a distance dependent on its properties. The distance can be calculated from the equation given in our earlier papers [7–11.21]:

$$y_{(j,i)} = R_{F(j,i)}z_{(1)} \tag{3}$$

where $z_{(1)}$ is the development distance in the first step [$z_{(1)} = v_{(1)}$].

The spots of the solutes are distributed along the plate according to their retention in a polar mobile

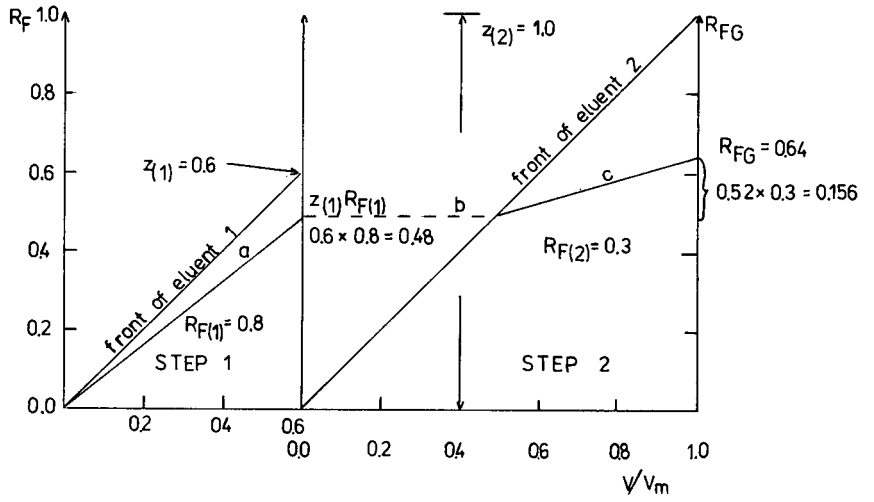

Fig. 1. Schematic diagram of migration of solute in two-stage development. (a) Migration of solute A during the first development; (b) during the second development the spot remains in the same place until it is reached by the front of the second eluent; (c) then the zone migrates in the second mobile phase.

phase: the non-polar solutes migrate near to the front but the polar solutes are separated (Fig. 2).

After the first step, the plate is dried and the first eluent is removed. The second development step begins again from the start line of the layer. The solvent front of the second step meets the spots of solutes at different positions. The volume of the mobile phase taking part in elution will be different for individual solutes and depends on their positions

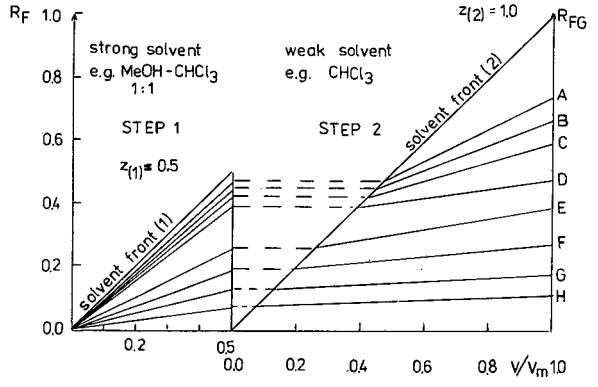

Fig. 2. Migration paths of solutes A–H during a two-step development (solid lines). In the first step polar solutes E–H are separated; the less polar solutes A–D, poorly separated during the first step, are separated during the second step.

after the first step. The volume of solvent corresponding to the process of elution in the second step is equal to

$$v_e = 1 - R_{F(j,i)} \tag{4}$$

and the distance migrated by solute j is equal to

$$y_{(j,2)} = R_{F(j,2)} v_e = R_{F(j,2)}(1 - R_{F(j,1)}) \tag{5}$$

The total distance y migrated by solute j is

$$y_{(j)} = y_{(j,1)} + y_{(j,2)} \tag{6}$$

After substitution of eqns. 3 and 5 into eqn. 6 we obtain the final form of the equation which determines the final R_F value:

$$R_{Fg(j)} = y_{(j)} \tag{7}$$

$$R_{Fg(j)} = z_{(1)} R_{F(j,1)} + [1 - R_{F(j,1)} z_{(1)}] R_{F(j,2)} \tag{8}$$

From eqn. 8, the final R_{Fg} values of solutes in two-step gradient multiple development can be calculated. This equation can be used when the values of two parameters for each solute are known, *i.e.*, the slope and k^0 from the log–log relationship.

Eqn. 8 was applied to write a computer program in GW Basic (or Pascal). The complete program is presented in the Appendix.

TABLE I

ABSOLUTE SLOPES, $m_{(j)}$, AND VALUES OF CAPACITY FACTORS, $k^0_{(j)}$, OF SIX TEST SOLUTES USED IN TWO-STAGE GRADIENT DEVELOPMENT

Code	Compound	Slope, $m_{(j)}$	Capacity factor, $k^0_{(j)}$
2	2-Hydroxynaphthalene-1-azo-(4'-chlorobenzene)	1.52	0.091
3	2-Hydroxynaphthalene-1-azo-(3'-methoxybenzene)	1.67	0.023
5	Methyl red	0.86	0.885
6	Sudan III	2.25	0.008
7	Sudan IV	1.41	0.018
9	2,6-Dinitroaniline	1.00	0.279

EXPERIMENTAL

Chromatography was performed on 100 × 100 mm glass-backed plates precoated with a 0.25-mm layer of silica gel 60 (E. Merck, Darmstadt, Germany). Solvents of analytical-reagent grade were purchased from Polish Reagents POCh (Gliwice, Poland). A mixture of six solutes was chromatographed to a distance of 2.5 cm in the first step and to 10 cm in the second step in Type DS equilibrium sandwich chambers [16,18], purchased from Chromdes (Lublin, Poland). During the isocratic analysis, to eliminate eluent demixing, the spotting of samples and elution were preceded by wetting the layer with a fraction of the void volume of the corresponding mobile phase. The spots were detected visually. In stepwise gradient experiments, fractions of the eluent of decreasing concentration of diisopropyl ether in toluene were introduced into the eluent reservoir. The solvent flow was observed by means of non-retained azobenzene marker. The plates were dried under vacuum obtained by a water pump. The calculations were made using an IBM XT computer.

RESULTS AND DISCUSSION

To illustrate the procedure and demonstrate the migration of the individual components, six compounds were chosen; their absolute slopes $m_{(j)}$ and values of capacity factors $k^0_{(j)}$ are presented in Table I.

The gradient was selected as a two-step programme (Table II) with a development distance in the first step of 0.25. The concentrations in the second step were changed. The computer programme calculated the R_F values for individual solutes corresponding to the chosen concentrations and the volumes of eluents in each step. The final $R_{Fg(j)}$ values were then calculated by computer from eqn. 8.

Comparison of experimental and calculated R_F values demonstrates that for a given set of compounds whose m and k^0 values are known, it is possible to simulate the chromatographic process for various stepwise gradient programmes in the search for the optimum conditions.

These data allow comparisons between predicted and experimental results. Results for the tested mixture show satisfactory agreement between experimental and predicted R_{Fg} values. The average errors in computer-simulated values of R_{Fg} are less than 6%. Considering the method of detection of solutes and some phenomena that disturb the migration of solutes during programmed analysis, this error could be acceptable. Application of densitometry as the method of detection would certainly improve the

TABLE II

GRADIENT PROGRAMME USED IN TWO-STAGE DEVELOPMENT RUNS

z = Development distance in R_F units; c = concentration of polar solvent in volume fraction.

No.	$c_{(1)}$	$z_{(2)}$	$c_{(2)}$	$z_{(2)}$
I	1.00	0.260	0.25	1.0
II	1.00	0.240	0.50	1.0
III	1.00	0.260	0.0[a]	1.0

[a] 100% diluent.

TABLE III

COMPARISON OF EXPERIMENTAL AND SIMULATED R_{Fg} VALUES FOR TEST MIXTURE

Conditions	Code	R_{Fg} (calc.)[a]	R_{Fg} (expt.)[a]	R_{Fg} (graph.)[a]	Error in R_{Fg} units	Error in ΔR_{Fg} units
Gradient programme I	2	0.67	0.67	0.65	0.00	0.01
	3	0.86	0.87	0.85	0.01	0.05
	5	0.36	0.30	0.33	0.06	−0.01
	6	0.89	0.94	0.90	0.05	−0.01
	7	0.92	0.96	0.93	0.04	−0.03
	9	0.52	0.59	0.59	0.01	
					Av. ±0.03 (5.45%)	±0.01 (2.04%)
Gradient programme II	2	0.84	0.73		0.11	−0.05
	2	0.95	0.89		0.06	−0.02
	5	0.46	0.42		0.04	−0.01
	6	0.97	0.94		0.03	−0.00
	7	0.97	0.94		0.03	−0.02
	9	0.71	0.66		0.05	
					Av. ±0.05 (7.52%)	±0.06 (1.89%)
Gradient programme III	2	0.27	0.24		0.03	0.01
	3	0.47	0.43		0.04	0.04
	5	0.14	0.06		0.08	−0.07
	6	0.44	0.45		0.01	0.00
	7	0.44	0.45		0.01	0.03
	9	0.34	0.30		0.04	
					Av. ±0.02 (7.6%)	+0.01 (5.01%)

[a] Calc. = values simulated; expt. = values from experiment; graph. = determined by graphical method [12].

precision of the R_F values obtained from gradient and isocratic measurements. For the purpose of the method development and optimization of the separation, however, the errors in differences in R_{Fg} values are more important because the resolution, R_s is proportional to the difference in R_F values for adjacent pairs of spots. It can be seen from Table III that the errors in ΔR_{Fg} are much smaller than those in absolute R_{Fg} values and this was observed in every instance. The experimental data demonstrate that eqn. 8 describes satisfactorily the chromatographic migration of solutes under conditions of two-step programmed reverse gradient elution. The possibility of the prediction of R_{Fg} values with the aid of a computer is a good starting point for further optimization of analysis, *i.e.*, shortening the time and improving the resolution.

It should be mentioned that even a simple two-step gradient development may lead to a satisfactory separation of complex mixtures, as demonstrated by Johansson [22] for plant waxes.

SYMBOLS

$c_{(i)}$ Concentration of modifier for the ith step

$k^0_{(j)}$ Capacity factor of solute j for unit concentration of modifier (pure modifier) for normal-phase systems and for $c_{(i)} = 0$ (pure water) for reversed-phase systems

$k_{(j,i)}$ Capacity factor of solute j for the ith step

$m_{(j)}$ Slope of log–log plot for solute j

$R_{F(j,i)}$ R_F value for solute j corresponding to ith concentration of modifier

APPENDIX

$R_{Fg(j)}$ Final value of R_F of solute j in gradient development

v_0 Void volume[a]

$v_{(i)}$ Volume of ith step[a]

v_e Elution volume[a]

$y_{(j,i)}$ Migration distance of solute j in the ith step

$y_{(j)}$ Total migration distance of solute j

$z_{(i)}$ Development distance of the ith step

GW BASIC (VBASICA version 3.20c/1.40)

```
5 'W. Markowski and E. Soczewinski
15 'DEPARTMENT OF INORGANIC AND ANALYTICAL CHEMISTRY
25 'MEDICAL ACADEMY
35 'STASZICA 6, 20-081 LUBLIN
45 'POLAND
50 OPTION BASE 1
55 '============================================================
65 'MULTIPLE DEVELOPMENT   MD
75 PRINT "THIS PROGRAM USED RELATION Rm=Rmo-n *log c":PRINT
85 '------------------------------------------------------------
90 LPRINT "MULTIPLE DEVELOPMENT ":LPRINT:LPRINT
95 PRINT "THE NUMBER OF SOLUTES"
105 INPUT "N=";N
115 DIM N$(N,10)
125 DIM KO(N):DIM M(N)
135 FOR I=1 TO N
145 PRINT "THE CODE"
150 INPUT "#";N$(I,10)
152 NEXT I
154 CLS
155 FOR I=1 TO N
160 PRINT "   # ";N$(I,10):PRINT
165 PRINT "CAPACITY FACTOR KO"
170 INPUT "KO=";KO(I)
172 PRINT "THE SLOPE m"
175 INPUT "m=";M(I)
185 PRINT "CORRECT"
195 INPUT "Y/N";Y$
205 IF Y$="N" THEN GOTO 165
210 CLS
215 NEXT I
225 '------------------------------------------------------------
235 'THE GRADIENT PROGRAM
236  '-----------------------------------------------------------
245 PRINT "THE NUMBER OF STEPS S=2"
250 INPUT "THE NUMBER OF STEPS S=";S
255 DIM C(S):DIM Z(S)
265 FOR L=1 TO S
270 PRINT "THE STEP L=";L
275 PRINT "THE CONCENTRATION OF MODIFIER C <=1"
285 INPUT "C=";C(L)
295 PRINT "THE DEVELOPMENT DISTANCE
305 INPUT "Z=";Z(L)
315 PRINT "CORRECT"
325 INPUT "Y/N";Y$
335 IF Y$="N" THEN GOTO 275
340 CLS
345 NEXT L:CLS
355 '------------------------------------------------------------
365 'THE CALCULATION OF FINAL VALUES RFG
366 '------------------------------------------------------------
370 LPRINT "THE RF VALUES IN CORRESPONDENCE TO THE STEPS OF GRADIENT"
375 DIM RG(N):DIM R(N,2)
385 FOR I=1 TO N
```

[a] All values $v_{(i)}$, v_e, v_0 are expressed as dimensionless magnitudes related to the void volume v_0 [$v_{(i)} = v_{(i)}/v_0$, $v_e = v_e/v_0$, $v_0 = v_0/v_0 = 1$].

```
395 FOR L=1 TO S
396 PRINT "THE STEP L=";L,
398 IF L=S THEN GOTO 645
405 K=KO(I)/(C(L)^M(I))
415 R(I,L)=1/(1+K)
418 LPRINT USING"\         \";N$(I,10);
420 LPRINT USING "       RF=#.##";R(I,L):LPRINT
425 NEXT L
435 NEXT I
445 'THE FOLLOWING CALCULATIONS ARE VALID FOR TWO STEPS DEVELOPMENT
446 '-----------------------------------------------------------------
455 FOR I=1 TO N
465 RG(I)=V(1)*R(I,1)+(1-V(1)*R(I,1))*R(I,2)
475 NEXT I
485 'THE PRINTOUT OF RESULTS
486 '-----------------------------------------------------------------
487 LPRINT
495 LPRINT "*********** THE FINAL VALUES OF RFG IN  MD **********"
505 LPRINT
515 LPRINT "THE GRADIENT PROGRAM "
525 LPRINT
535 FOR L=1 TO S
545 LPRINT USING "STEP    #";L;
555 LPRINT USING"              C=#.##";C(L);
565 LPRINT USING "                        Z=#.##";Z(L)
575 NEXT L
585 LPRINT
590 LPRINT "**********THE FINAL RFG VALUES**********"
591 LPRINT
592 LPRINT "CODE                          RFG"
593 LPRINT
595 FOR I=1 TO N
600 LPRINT USING "\      \";N$(I,10);
605 LPRINT USING "                        #.##";RG(I)
606 LPRINT
610 NEXT I
612 LPRINT "*************** END ****************"
615 CLS
620 PRINT "OTHER GRADIENT PROGRAM "
625 INPUT "Y/N";Y$
626 IF Y$="N" THEN GOTO 635
628 ERASE C,Z,RG,R
630 GOTO 245
635 END
645 PRINT "IF IN THE LAST STEP IS USED THE DILUENT THEN INPUT YES"
655 IF Y$="N" THEN GOTO 405
658 PRINT "CODE #";N$(I,10)
660 INPUT "VALUES RF IN PURE DILUENT RF=";RF
662 K=(1-RF)/RF
665 CLS
670 GOTO 415
```

TURBO PASCAL (version 6.0)

```
    PROGRAM PMD2;

USES
PRINTER,CRT;

CONST
S = 2;

VAR
N,I,J,L : INTEGER;
CONC : ARRAY [1..S] OF REAL ;
DIST : ARRAY [1..S] OF REAL;
  RF : ARRAY [1..20,1..S] OF REAL;
 RFG : ARRAY [1..20] OF REAL;
CODE : STRING [5];
  KO : ARRAY [1..20] OF REAL;
   M : ARRAY [1..20] OF REAL;
```

```
BEGIN
        WRITE (' NUMBER OF SOLUTES ');
        READLN (N);
        WRITELN ('NUMBER OF SOLUTES N=',N);
        FOR I:=1 TO N DO
        BEGIN
        WRITE('CODE OF SOLUTE # ');
        READ (CODE);
        END;
        FOR I:=1 TO N DO
        BEGIN
        WRITELN (' # ',I,CODE);
        WRITE (' KO= ');
        READLN (KO[I]);
        WRITELN(' KO= ',KO[I]:5:3);
        WRITE ('SLOPE M=');
        READLN (M[I]);
        WRITELN (' M= ',M[I]:4:2);
        END ;
        WRITELN ('      *** GRADIENT PROGRAM ***    ');
        FOR L:=1 TO 2 DO
        BEGIN
        WRITELN ('STEP L=',L);
        WRITE ('CONCENTRATION  OF MODIFIER C=0 OR C<=1 C=');
        READLN (CONC[L]);
        WRITE ('DISTANCE Z=');
        READLN (DIST[L]);
        END;
        FOR J:=1 TO N DO
        BEGIN
        FOR L:=1 TO S DO
        BEGIN
                        IF CONC [2]=0
                        THEN
                        BEGIN
                        WRITE (' GIVE VALUES OF RF FOR DILUENT ');
                        READLN ( RF[J,L] );
                        END
        ELSE
        RF[J,L]:=1/(1+KO[J]/(EXP(M[J]*LN(CONC[L]))));
        END;

        END;
        FOR J:=1 TO N DO
        BEGIN
        RFG[J]:=DIST[1]*RF[J,1]+(1-DIST[1]*RF[J,1])*RF[J,2]
        END;
        WRITELN  (LST, ' FINAL VALUES OF RFG ');
        FOR J:=1 TO N DO
        BEGIN
        WRITE (LST,' # ',I,' ',CODE,'    ',' RFG=',RFG[J]:4:2);
        END;
        CLRSCR;
END.
```


REFERENCES

1 U. de la Vigne and D. Jänchen, *J. Planar Chromatogr.*, 3 (1990) 6.
2 G. Lodi, A. Botti, E. Mensiani, V. Brandolini and B. Tosi, *J. Planar Chromatogr.*, 4 (1991) 106.
3 C. F. Poole, S. K. Poole, W. P. N. Fernando, T. A. Dean, H. D. Ahmed and J. A. Berndt, *J. Planar Chromatogr.*, 2 (1989) 336.
4 A. Betti, G. Lodi, N. Fuzzati, S. Coppi and S. Benedetti, *J. Planar Chromatogr.*, 4 (1991) 360.
5 K. Burger, *Fresenius' Z. Anal. Chem.*, 318 (1984) 228.
6 A. Jeanes, C. S. Wise and R. J. Dimler, *Anal. Chem.*, 23 (1951) 415.
7 E. Soczewiński and W. Markowski, *J. Chromatogr.*, 370 (1986) 63.
8 W. Markowski and W. Golkiewicz, *Chromatographia*, 25 (1988) 339.
9 W. Markowski, E. Soczewiński and G. Matysik, *J. Liq. Chromatogr.*, 10 (1987) 1261.
10 E. Soczewiński, G. Matysik and W. Markowski, *Chem. Anal. (Warsaw)*, 33 (1988) 353.

11 W. Markowski, *J. Chromatogr.*, 485 (1989) 517.
12 W. Golkiewicz, in J. Sherma and B. Fried (Editors), *Handbook of Thin-Layer Chromatography*, Marcel Dekker, New York, 1991, pp. 135–153.
13 D. E. Jänchen and H. J. Isaaq, *J. Liq. Chromatogr.*, 11 (1988) 1941.
14 D. E. Jänchen, in R. E. Kaiser (Editor), *Proceedings of the 3rd International Symposium on Instrumental HPTLC (Würzburg)*, Institut für Chromatographie, Bad Durkheim, 1985, pp. 71–82.
15 C. F. Poole and M. T. Belay, *J. Planar Chromatogr.*, 4 (1991) 345.
16 T. H. Dzido, G. Matysik and E. Soczewiński, *J. Planar Chromatogr.*, 4 (1991) 161.
17 M. Matyska, A. M. Siouffi and E. Soczewiński, *J. Planar Chromatogr.*, 4 (1991) 255.
18 E. Soczewiński, in R. E. Kaiser (Editor), *Planar Chromatography*, Vol. 1, Hüthig, Heidelberg, 1986, pp. 79–117.
19 W. Markowski, in preparation.
20 E. Soczewinski and G. Matysik, *J. Chromatogr.*, 32 (1968) 458.
21 W. Markowski, E. Soczewiński and K. L. Czapińska, *Chromatographia*, 27 (1989) 123.
22 L.-A. Johansson, *Sver. Utsådesfören. Tidskr.*, 95 (1985) 129.

Journal of Chromatography, 623 (1992) 148–152
Elsevier Science Publishers B.V., Amsterdam

CHROM. 24 487

Short Communication

Behaviour of the system peak in ion chromatography with indirect ultraviolet absorption detection and trimellitate as eluent

Yoshimasa Michigami and Yoshikazu Yamamoto

Department of Chemistry and Chemical Engineering, Faculty of Technology, Kanazawa University, 2-40 Kodatsuno, Kanazawa 920 (Japan)

(First received March 25th, 1992; revised manuscript received July 2nd, 1992)

ABSTRACT

The behaviour of the system peak has been studied using an ion chromatographic system equipped with an ultraviolet detector and an ODS column coated with cetyltrimethylammonium bromide and trimellitate (pH 4.0). The intensity of the system peak depended on the pH of the sample injected and also on the injected anion concentration, especially for the injection of an acidic anion of high concentration.

INTRODUCTION

In high-performance liquid chromatography (HPLC) or ion chromatography (IC), the injection of a sample into a eluent containing more than one component often causes the appearance of so-called system peaks [1–8] (or dip peaks [9]). Many papers have reported the formation mechanism and the simulation of the first and second system peaks. A first system peak is eluted at the solvent front and is due to ion exclusion of the sample cation from the resin and the elution of water from the sample [3–9]. The peak is referred to as the injection peak and its retention volume coincides with the void volume of the column [3–8].

A second system peak, which is simply called the "system peak" in this paper, is eluted later and may cause incorrect peak identification and waste time. Many formation mechanisms of this system peak have been discussed, with some computer simulations in IC [4,5,8,9]. It is generaly assumed that the system peak mainly results from a eluent-deficient zone formed by the sample injection and also depends on the pH of the injected sample. Samples containing no eluent anion were injected in previous studies [4,5,8,9].

In this paper, the behaviour of the system peak is reported for anion chromatography using trimellitate (TMA, pH 4.0) as the eluent and some anion samples containing TMA with ultraviolet detection.

EXPERIMENTAL

Apparatus and reagents

The IC equipment consisted of a pump (CCPD, Tosoh, Japan),a variable-wavelength ultraviolet de-

Correspondence to: Dr. Y. Michigami, Department of Chemistry and Chemical Engineering, Faculty of Technology, Kanazawa University, 2-40 Kodatsuno, Kanazawa 920, Japan.

0021-9673/92/$05.00

tector (UV-8000, Tosoh), an injector (Rheodyne, USA) with a 100-μl sample loop, a column oven (CO-8000, Tosoh) and a pen recoder (YEW Type 3066, Yokogawa, Japan).

All chemicals were of analytical-reagent grade, and deionised, distilled water, further filtered through a 0.45-μm membrane filter, was used throughout. The solutions of anions were prepared from their sodium salts. The eluent of 1 m*M* TMA was adjusted to pH 4.0 with diluted sodium hydroxide solution and filtered through a 0.45-μm membrane filter before use. Phthalate, citrate and benzoate as eluents were also compared with TMA.

Dynamically coated columns were prepared using columns (50 × 4.6 mm I.D.) packed with ODS resin (Capcell Pack C18, AG120, 5 μm particle size, Shiseido, Japan). The column was coated with cetyltrimethylammonium bromide (CTMABr) as described previously [10]. The ion-exchange capacity of the coated column was about 0.10 mequiv. per column for the eluent ion. Regeneration of the column was carried out by washing with methanol and coating with CTMABr. The commercial TSK gel IC anion SW (Tosoh) was also compared with the coated column.

The injected anions (0.4 mequiv. l^{-1} sulphate, nitrate, chloride, acetate and citrate) were dissolved in 1 m*M* TMA (pH 7.0) and showed a stable injection pH and large relative absorbance of the system peak. The chromatographic conditions used are summarized in Table I.

TABLE I

CHROMATOGRAPHIC CONDITIONS

Column	ODS column coated with cetyltrimethylammonium bromide (CTMABr)
Column temperature	35°C
Flow-rate	1.0 ml min^{-1}
Detection wavelength	275 nm
Sample loop	100 μl
Eluent	1.0 m*M* Trimellitate (TMA)
Eluent pH	4.0
Sample	0.4 mequiv. l^{-1} of sample anion in 1 m*M* TMA solution
Sample pH	7.0

RESULTS AND DISCUSSION

Effect of eluent TMA concentration

A basic equation (eqn. 1) has been published for IC in terms ofthe capacity factor (k') and the concentration of the eluent ion (E), if all other chromatographic conditions are constant except the eluent concentration [4].

$$\log k' = -a/b \log [E] + \text{constant} \quad (1)$$

where a and b are the charges on the sample ion and the eluent ion, respectively.

A slope of plots of log k' *versus* log [E] shows the ratio ($-a/b$) of the charges on the sample and eluent ions. Fig. 1 shows the plots of the log k' *versus* log [TMA] in the coated column and the non-coated column. The slopes for the system peak, nitrate and sulphate were 0.73, 0.64 and 0.96 in the coated column, respectively. The charge of the TMA eluent ion at pH 4.0 was about 1.6 as calculated from the acid dissociation constant (pK_{a1} 2.52, pK_{a2} 3.85, pK_{a3} 5.20) [11]. The slope for the nitrate (univalent) ion as sodium nitrate, 0.64 of the experimental value, agrees with the theoretical value of 0.62. Similarly, the slopes (0.94, 0.32 and 0.53) of the system peaks for phthalate, benzoate and citrate eluent were also obtained, as shown in Table II. These slopes should theoretically be 1.0 accord-

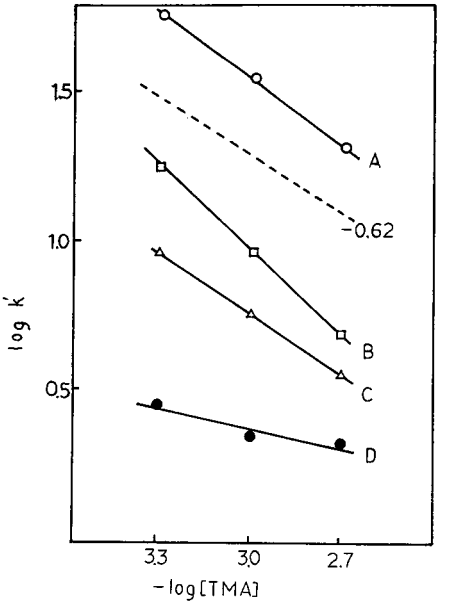

Fig. 1. Log [TMA] *versus* log k'. (A) System peak; (B) sulphate; (C) nitrate; (D) system peak on non-coated ODS column. Other chromatographic conditions as in Table I.

TABLE II

EFFECT OF ELUENT ON THE SLOPE (a/b)

Equation: $\log k' = -a/b \log [E] +$ constant. Eluent concentration 1 mM.

Eluent	Eluent pH	Eluent ion charge	Slope ($-a/b$)	
			Nitrate	System peak
TMA	4.0	1.6	0.64	0.73
			–	0.78[a]
Phthalate	4.3	1.03	0.83	0.94
Citrate	3.6	0.80	–	0.53
Benzoate	4.5	0.67	0.98	0.32

[a] Column: commercial TSK gel IC anion SW (Tosoh). The other chromatographic conditions are the same as in Table I.

ing to ion-exchange processes only. However, the experimental values were smaller than 1.0, therefore another process (probably a reversed-phase interaction) must have occurred on the resin. The behavior of system peak observed was similar to that of univalent anion by the two process (ion exchange and reversed phase interaction) for TMA and phthalate eluents. The slope ($-a/b$) of the system peak for the non-coated ODS column was 0.22. This value also suggests that another interaction occurred on the ODS resin in addition to ion exchange. It was found that nitrate and sulphate were not retained on the non-coated column.

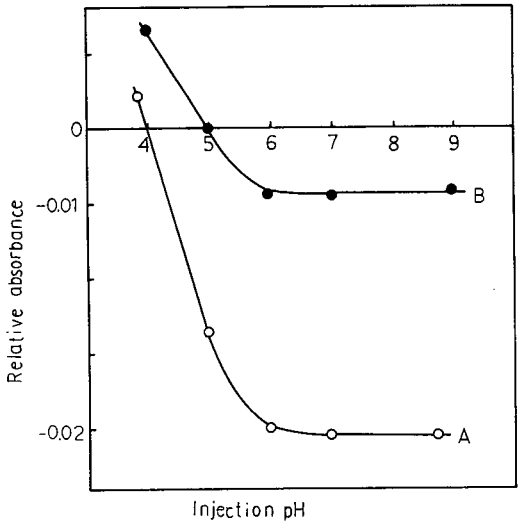

Fig. 2. Effect of injection pH on the relative absorbance of system peak. Eluent: (A) 1 mM TMA (pH 4.0); (B) 1 mM TMA (pH 5.0). Sample: 1 mM TMA. Other chromatographic conditions as in Table I.

Effects of eluent pH and injection pH

The retention times of sulphate and chloride decreased with increasing eluent pH from 4.0 to 6.0 and levelled off at pH values greater than 6, whereas that of the system peak rapidly increased at pH 4.0–5.0 and then disappeared at pH values greater than 6.0.

The effect of the injection pH on the relative absorbances of the system peak and some anions was examined in the pH range 4.0–9.0. The results obtained for the relative absorbance of the system peak are shown in Fig. 2. The system peak appeared as a negative peak when the injection pH was higher than the eluent pH (pH 4.0), whereas the system peak appeared as a positive peak when the injection pH was lower than the eluent pH. The relative absorbance of a negative or positive system peak increased with increasing difference between the injection pH and the eluent pH, although the relative absorbances of the anions did not vary for any injection pH. The absorbance of 1 mM TMA decreased with increasing pH at 275 nm and showed no decrease at pH values greater than 6.0. It is considered that the system peak results from the elution of the TMA band at increased pH (greater than pH 4.0) around the sample zone by sample injection (greater than pH 4.0) into the eluent (pH 4.0). The relative absorbances of the system peak in an aqueous solution and 1 mM TMA solution, the pH equal to the pH of the aqueous solution, pH 4.0 and pH 7.0, are shown in Table III. The relative absorbances of the anions show little variation. It is clear that the presence of TMA in the sample and the difference in pH between the sample and the eluent strongly affects the intensity of the system peak. The intensities of the system peaks by injection of the aqueous sample are smaller compared with those following injection of the sample containing TMA (pH equal to the aqueous solution pH).

Effect of injected sample concentration

The effect of the injected sample anion concentration on the relative absorbance of the system peak obtained by the injection of TMA and some anions was examined in the injected anion concentration

TABLE III

EFFECT OF SAMPLE SOLVENT ON THE RELATIVE ABSORBANCE OF THE SYSTEM PEAK

The chromatographic conditions are as shown in Table I.

Anion	Solvent	Sample pH	Relative absorbance
None	1 m*M* TMA	7.0	0.024
	1 m*M* TMA	4.0	0.002
Acetate	1 m*M* TMA	6.6	0.028
	Aqueous	6.6	0.010
	1 m*M* TMA	4.0	0.001
Chloride	1 m*M* TMA	7.0	0.022
	1 m*M* TMA	5.6	0.015
	Aqueous	5.6	0.004
	1 m*M* TMA	4.0	0.002
Sulphate	1 m*M* TMA	7.0	0.022
	1 m*M* TMA	5.8	0.019
	Aqueous	5.8	0.003
	1 m*M* TMA	4.0	0.002

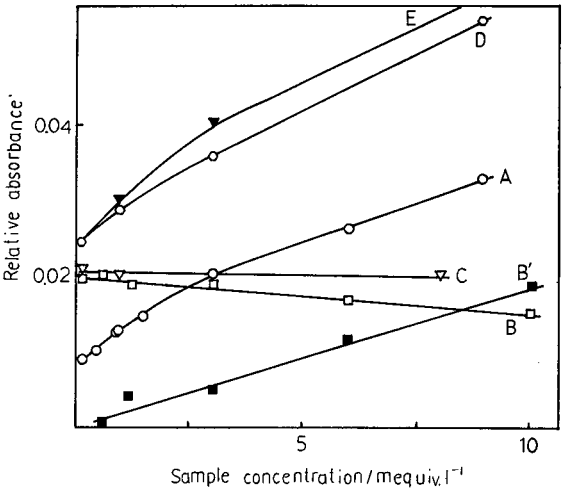

Fig. 3. Effect of sample concentrations on the relative absorbance of system peak. Negative system peak on the injection of: (A) TMA; (B) sulphate; (C) chloride; (D) acetate; and (E) citrate. (B') Positive system peak by injection of sulphate. Other chromatographic conditions as in Table I.

range 0–10 mequiv. l^{-1}. The results obtained are shown in Fig. 3. The relative absorbances of the negative system peak from acetate, citrate and TMA injections increased with increasing concentration of the injected anion, whereas those from chloride and sulphate injections gradually decreased. On injection of more than 0.6 mequiv. l^{-1} sulphate, a positive system peak appeared just in front of the negative system peak usually observed, as shown in Fig. 4, and the relative absorbance of the positive system peak increased with increasing concentration of the injected sulphate. This positive system peak may result from the excess of TMA excluded by the sample injection, as shown in Fig. 4 (lines A and C). A positive system peak also appeared at high concentrations (tens of mequivalents per litre) of chloride. The same phenomena were also observed by using a commercial TSK gel IC anion SW column. The negative system peak was obtained by the injection of hydrogencarbonate, phosphate, acetate and hippurate, and positive and negative system peaks were obtained by chloride and sulphate injections.

Injections of anions with an acid dissociation constant (pK_a) [12] of more than 4.0 (the eluent pH value), such as acetate (pK_a 4.76), citrate (pK_{a_1} 4.76, pK_{a_2} 6.40) and phosphate (pK_{a_1} 7.20, pK_{a_2} 12.35), and those of less than 4.0, such as chloride and sulphate (pK_{a_2} 1.99), give negative system peaks and both positive (at high concentrations) and negative system peaks, respectively. For the injection of the latter, when the sample anion (pH 7.0) was added the low pH eluent (pH 4.0), the charge of the sample anion did not vary, whereas that of TMA around the sample zone changed and the local pH of TMA

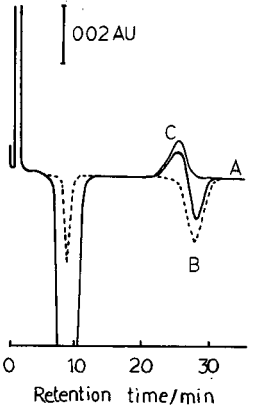

Fig. 4. Chromatogram of system peak. System peak on the injection of: (A) (solid line) 5 m*M* sulphate; (B) (broken line) 0.2 m*M* sulphate; (C) (fine line) 4 m*M* TMA (pH 4.0). Other chromatographic conditions as in Table I.

became higher than 4.0. The combination of a negative and positive contribution to the intensity of the system peak due to the higher pH and the excess of TMA by sample injection may explain the appearance of negative and positive system peaks. However, the charges of sample anion and TMA were affected by the injection; the charge of sample anion decreased, the charge of TMA became higher than that of eluent TMA and then the local TMA became more basic. When the basic TMA was eluted, only a negative system peak appeared. The contribution of the excess TMA by sample injection was smaller than that of pH. The intensity of the negative system peak only became larger for an injected anion with a basic pK_a value.

It was confirmed that system peak resulted from the elution of local TMA when the pH was varied by sample injection. The intensity of the system peak depended greatly on the difference in pH between the injected sample containing the eluent anion and eluent, and also on the injected anion concentration. The profile of the system peak on the chromatogram was varied by the injection of an acidic anion of high concentration.

REFERENCES

1 S. Levin and E. Grushka, *Anal. Chem.*, 58 (1986) 1602.
2 S. Levin and E. Grushka, *Anal. Chem.*, 59 (1987) 1157.
3 F. G. P. Mullins, *Analyst (London)*, 112 (1987) 665.
4 D. T. Gjerde and J. S. Fritz, *Ion Chromatography*, Hüthig, Heidelberg, 2nd ed., 1987, pp. 73, 154.
5 A. Yamamoto, A. Matsunaga, M. Ohto, E. Mizukami, K. Hayakawa and M. Miyazaki, *J. Chromatogr.*, 482 (1989) 145.
6 J. Ståhlberg and M. Almgren, *Anal. Chem.*, 61 (1989) 1109.
7 S. Golshan-Shirazi and G. Guiochon, *Anal. Chem.*, 62 (1990) 923.
8 H. Sato, *Anal. Chem.*, 62 (1990) 1567.
9 T. Okada and T. Kuwamoto, *Anal. Chem.* 56 (1984) 2073.
10 Y. Michigami, Y. Yamamoto and K. Ueda, *Analyst (London)*, 114 (1989) 1201.
11 K. Ohta, H. Harada, S. Nakajima and K. Tanaka, *Bunseki Kagaku*, 41 (1992) 146.
12 R. Kuroda, Y. Sugitani and M. Shibukawa, *Bunseki Kagaku*, Shokabo, Tokyo, 1989, p. 371.

Journal of Chromatography, 623 (1992) 153–158
Elsevier Science Publishers B.V., Amsterdam

CHROM. 24 459

Short Communication

Determination of tetracycline antibiotics by reversed-phase high-performance liquid chromatography with fluorescence detection

Kazuo Iwaki, Norio Okumura and Mitsuru Yamazaki

School of Pharmacy, Hokuriku University, Ho-3, Kanagawa-machi, Kanazawa-shi, Ishikawa 920-11 (Japan)

(First received March 5th, 1992; revised manuscript received June 26th, 1992)

ABSTRACT

A highly sensitive method for the determination of tetracycline antibiotics (TCs) using reversed-phase high-performance liquid chromatography with fluorescence detection is presented. This method was based on the use of disodium ethylenediaminetetraacetate (EDTA) and calcium chloride as fluorescence-increasing reagents in the mobile phase. The concentrations of each reagent in the mobile phase greatly influenced the fluorescence intensity of TCs. When the concentration of EDTA and calcium chloride were 25 and 35 m*M*, respectively, and the pH of the mobile phase was 6.5, the maximum fluorescence intensity was obtained. The column temperature hardly influenced the fluorescence intensity. At 3.75 ng of TCs injected, the precision (relative standard deviation) ranged from 1.12 to 2.20%. In the range 0.075–37.5 ng for tetracycline and oxytetracycline and 0.225–37.5 ng for chlortetracycline, a linear response was observed. The detection limits of this method were 49–190 pg for three different TCs. The proposed method was applied to the determination of one of the TCs in pharmaceuticals by the internal standard method using other TCs as internal standards and was also applied to determination of TCs added to fish tissue.

INTRODUCTION

Tetracycline antibiotics (TCs) are widely used in the stockbreeding and fishery industries and a selective and sensitive analytical method is still required for pharmacokinetic studies of TCs. Recently, various high-performance liquid chromatographic (HPLC) methods for the determination of TCs have been reported [1–9]. These methods use spectrophotometric detection of TCs, which limits the sensitivity that can be achieved. More recently, Blanchflower *et al.* [10] discussed this and other disadvantages of these methods, and developed an HPLC method for chlorotetracycline (CTC) at residual levels with fluorescence detection. This method allowed the detection of CTC at picomole levels, but it is restricted to CTC. An HPLC method for TCs with electrochemical detection was reported by Hou and Wang [11]. This allowed highly selective detection, but electrochemical detectors are not widely used compared with spectrophotometric and fluorimetric detectors.

It is well known that TCs combine with divalent metal ions to give fluorescent chelate compounds. Although only TCs show fluorescence under basic conditions, the fluorescence intensity of the chelate under neutral or alkaline conditions is stronger

Correspondence to: Dr. K. Iwaki, School of Pharmacy, Hokuriku University, Ho-3, Kanagawa-machi, Kanazawa-shi, Ishikawa 920-11, Japan.

0021-9673/92/$05.00

than that of free TCs. This suggests the possibility of their highly sensitive detection. Indeed, this has applied to the determination of TCs by the manual methods [12,13]. However, application to an HPLC–fluorescence detection method for TCs using this property has not been reported, because TCs experience problems in reversed-phase HPLC. In order to resolve these problems, an acidic mobile phase must be used, but this results in quenching of the fluorescence. The problems are a decrease in recovery from the column owing to chelation between the TCs and trace metal ions in the packing and on the surface of the column tube, and asymmetric peaks arising from interactions between TCs and residual silanols present in the packing, resulting in poor sensitivity.

In order to overcome the above problems, in this work calcium chloride (CC) and disodium ethylenediaminetetraacetate (EDTA) were added to the neutral mobile phase and a metal ion-free packing was used, resulting in a highly sensitive HPLC method for the determination of tetracycline (TC), oxytetracycline (OTC) and CTC with fluorimetric detection. The method was applied successfully to the determination of TCs present in pharmaceutical preparations and added to fish tissue.

EXPERIMENTAL

Apparatus

The HPLC system consisted of an L-6200 delivery system (Hitachi, Tokyo, Japan), a Model 7125 loop injector (Rheodyne, Cotati, CA, USA), a Capcell C_{18} type SG-120 (5-μm) prepacked column (250 × 4.6 mm I.D.) (Shiseido, Tokyo, Japan) and an L-1200 spectrofluorimeter (Hitachi). The column was thermostated at 30 ± 0.2°C. The detector excitation and emission wavelengths were set at 390 and 512 nm, respectively. Results were recorded on a D-2500 chromato-integrator (Hitachi).

Reagents

Methanol was of HPLC grade; all other reagents were of analytical-reagent grade. Water was purified by distillation, followed by final clean-up through a Milli-Q Labo system (Nihon Millipore, Tokyo, Japan). TC · HCl and OTC · HCl were obtained from Wako (Osaka, Japan) and CTC · HCl from Sigma (St. Louis, MO, USA). A 1 mg/ml stock solution of each TC was prepared with 50 m*M* HCl. The mobile phase consisted of 0.1 *M* acetate buffer (pH 6.5) containing 35 m*M* CC and 25 m*M* EDTA (buffer A) and methanol.

Procedure for standard samples

Standard solutions of each TC were prepared by diluting the stock solution to appropriate concentrations with 50 m*M* HCl. To 150 μl of the standard solution were added 250 μl of 24% trichioroacetic acid (TCA) solution in methanol. An aliquot (10 μl) of the resulting mixture was injected on to the HPLC column.

Procedure for determining OTC and TC in pharmaceutical formulations by the internal standard method

For Terramycin capsules (Pfizer). One capsule was dissolved and diluted with 50 m*M* HCl in a 250-ml calibrated flask, and this solution was centrifuged for 15 min at 2000 *g*. Further, 100 μl of the supernatant were diluted with 50 m*M* HCl in a 50-ml calibrated flask. To 150 μl of this solution and the standard solution of OTC (2 μg/ml) were added 250 μl of internal standard solution (prepared by dissolving TC in 24% methanolic TCA solution concentrated to 2 μg/ml), respectively. An aliquot (10 μl) of the each resulting mixture was injected on to the HPLC column successively. The content of OTC in the capsule was calculated by using the ratio of the peak area of OTC to that of the internal standard (TC) for each chromatogram.

For Achromycin V syrup (Lederle). A 1-ml volume of syrup was diluted with 50 m*M* HCl in a 25-ml calibrated flask and this solution was centrifuged for 15 min at 2000 *g*. Further, 100 μl of the supernatant were diluted with 50 m*M* HCl in a 50-ml calibrated flask. To 150 μl of this solution and the standard solution of TC (2 μg/ml) were added 250 μl of internal standard solution (prepared by dissolving OTC in 24% methanolic TCA solution concentrated to 2 μg/ml), respectively. An aliquot (10 μl) of the each resulting mixture was injected on to the HPLC column successively. The content of TC in the syrup was calculated by using the ratio of the peak area of TC to that of the internal standard (OTC) for each chromatogram.

Procedure for determining three TCs spiked in silver salmon tissue

A 1-g amount of tissue was homogenized with 3 ml of 1 *M* HCl, then further homogenized with 6 ml of 24% methanolic TCA solution. This mixture was centrifuged at 2000 *g* for 15 min. To 600 μl of the supernatant were added 600 μl of buffer A. After the mixture had been vortex mixed and allow to stand for 5 min, it was centrifuged at 2000 *g* for 10 min. An aliquot (50 μl) of the resulting supernatant was injected on to the HPLC column.

RESULTS AND DISCUSSION

Effects of calcium ion and EDTA on fluorescence intensity and elution from a reversed-phase column

The effects of calcium ion and EDTA on fluorescence intensity were investigated by a flow-injection method. The mobile phase containing CC alone gave fluorescence but its intensity was less than half of that when both CC and EDTA were present. With EDTA alone or no additive hardly any fluorescence was obtained. This suggests that the presence of the appropriate amount of EDTA further increased the fluorescence of the TC–calcium chelates.

Fig. 1 shows typical chromatograms of three TCs obtained with the above mobile phase systems using a reversed-phase column. The mobile phase containing both CC and EDTA gave three symmetrical peaks (Fig. 1A), whereas the three TCs could not be detected using mobile phases containing CC alone, EDTA alone or no additive (Fig. 1B–D). Undesirable interactions between TC chelates and the packing were diminished by addition of EDTA to a CC-containing mobile phase.

In order to compare with fluorescence intensity of TC–magnesium chelates, a mobile phase containing magnesium chloride instead of CC was also studied by the flow-injection method. A slightly stronger fluorescence of the three TCs was observed with CC compared with magnesium chloride.

Optimization of HPLC conditions

In order to optimize the HPLC conditions, the effects of the concentration of each additive in the mobile phase, pH and column temperature were investigated. The maximum fluorescence intensity of the TCs was obtained when the CC, EDTA and

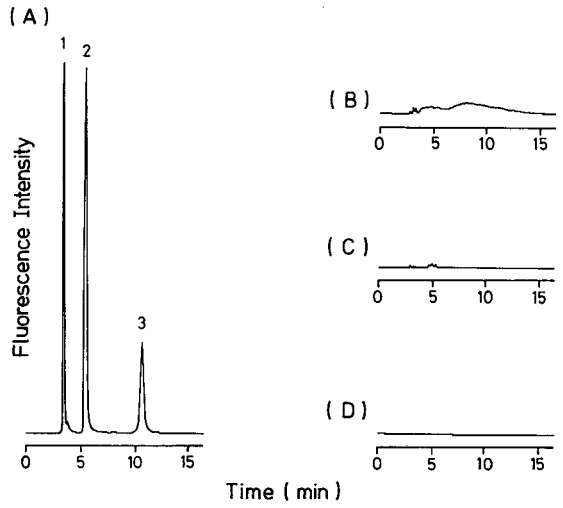

Fig. 1. Chromatographic profiles of three TCs obtained on a reversed-phase column using various mobile phases. Mobile phase: (A) methanol–buffer A (45:55); (B) without EDTA; (C) without CC; (D) without both EDTA and CC. Flow-rate, 1.0 ml/min; sample concentration, 37.5 ng per injection. Peaks: 1 = OTC; 2 = TC; 3 = CTC.

sodium acetate concentrations in the mobile phase were $\geqslant 35$ m*M*, 25 m*M* and $\geqslant 0.01$ *M*, respectively.

The mobile phases were tested in the pH range 5.0–7.5. Only OTC showed a different pattern from the other two TCs, but the fluorescence intensity of the three TCs was almost constant in the pH range 6.5–7.5; lower pH values decreased the intensity (Fig. 2). Figure 3 shows the effect of column temperature on the fluorescence intensity in the range 20–40°C. In this range, the fluorescence intensity of TC and CTC remained almost constant, whereas that of OTC decreased slightly with an increase in temperature. Consequently, the HPLC conditions given under Experimental were adopted.

Under these conditions, column packings, various kinds of conventional ODS (including end-capped types) and a few metal-free type ODS, were also investigated. A Capcell C_{18} type SG-120 (metal-free type) gave the most symmetrical peaks, and was adopted. The details are omitted. As TCA is generally used in bioanalysis as deproteinization reagent for TCs, TCA was added to the standard solution.

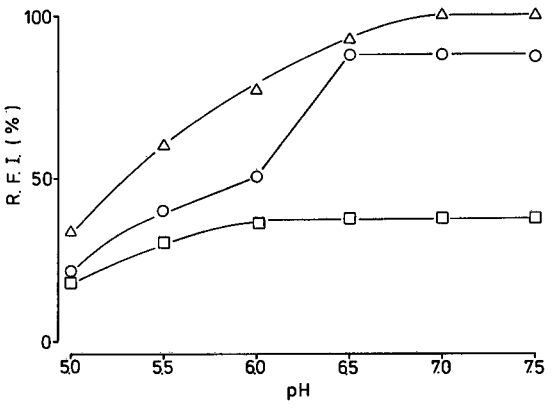

Fig. 2. Effect of pH of buffer A on the fluorescence intensity of TCs. Mobile phase, methanol–buffer A (45:55); flow-rate, 1.0 ml/min; column temperature, 30°C; sample concentration, 37.5 ng per injection. △ = TC; ○ = OTC; □ = CTC. R.F.I. = relative fluorescence intensity.

Evaluation of present method

Linear responses were observed in the range 0.075–37.5 ng for OTC and TC and 0.225–37.5 ng for CTC. The equations of the regression lines for the calibration graphs were $y = 4.787x - 0.343$ for OTC, $y = 6.245x + 0.114$ for TC and $y = 2.751x + 0.070$ for CTC (y = peak area $\cdot 10^{-5}$, x = ng). The correlation coefficient for the three TCs were > 0.9999.

Several analyses were performed to determine the reproducibility of the method. Table I gives the relative standard deviations of peak area for the three TCs at a concentration of 3.75 ng per injection. The detection limits with both fluorimetric and spectrophotometric (350 nm) detection (signal-to-noise ratio = 3) are also given in Table I. The results demonstrate that highly sensitive detection for all three TCs was achieved.

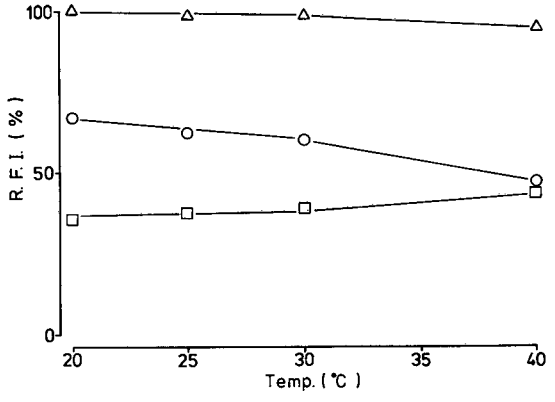

Fig. 3. Effect of column temperature on the fluorescence intensity of TCs. pH of buffer A, 6.5; other conditions and symbols as in Fig. 2.

TABLE I

REPRODUCIBILITIES OF PEAK AREA AND DETECTION LIMITS FOR TETRACYCLINES

Sample	R.S.D. (%)		Detection limit[c] (ng)	
	Intra-assay[a]	Inter-assay[b]	Fluorimetric detection	UV detection[d]
OTC	1.46	2.20	0.051	1.9
TC	1.24	1.48	0.049	3.6
CTC	1.18	1.12	0.190	9.6

[a] 3.75 ng per injection, $n = 10$.
[b] 3.75 ng per injection, $n = 5$.
[c] Signal-to-noise ratio = 3.
[d] Wavelength, 350 nm.

Application to determination of TCs in pharmaceuticals

The method was applied to the determination of OTC in Terramycin capsules and TC in Achromycin V syrup using the internal standard method as an example. TC and OTC were used as internal standards in the former and latter analyses, respectively. Fig. 4 shows chromatograms for (A) Terramycin capsules and (B) Achromycin V syrup. The mean results (± S.D., $n = 5$) were 106.7 ± 3.8% OTC in Terramycin capsules and 92.3 ± 1.1% TC in Achromycin V syrup.

Application to determination of TCs added to fish tissue

As the conventional HPLC methods for the determination for TCs mainly used spectrophotometric detection, they required concentration steps involving extraction using organic solvents or a precolumn as a pretreatment for the determination of TCs in biological fluids. These methods are generally tedious and are responsible for unsystematic errors in the analysis. In contrast, the present method allows the highly sensitive detection of TCs, suggesting the possibility of the determination of TCs in biological fluids without the need for tedious pretreatment.

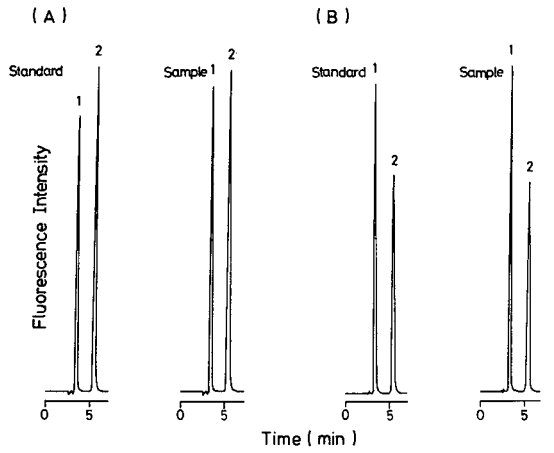

Fig. 4. Chromatograms for determining OTC in (A) Terramycin capsules and TC in (B) Achromycin V syrup by the internal standard method. Mobile phase, methanol–buffer A (45:55); flow-rate, 1.0 ml/min. Peaks: 1 = OTC; 2 = TC.

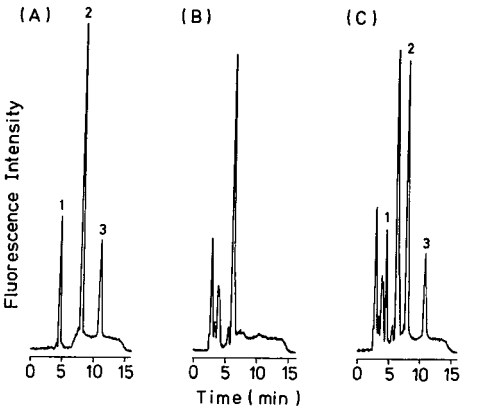

Fig. 5. Chromatograms of (A) standard TCs, (B) tissue blank and (C) TCs added to tissue. Mobile phase, mixture of 90% methanol and buffer A (using 0.3 *M* instead of 0.1 *M* sodium acetate). Gradient programme: 0–1 min, 67% buffer A; 1–8.5 min, 45% buffer A; 8.5 min onwards, 67% buffer A. Flow-rate, 1.0 ml/min; sample concentration, 1 ppm. Peaks: 1 = OTC; 2 = TC; 3 = CTC.

The effect of the extraction reagent on the recovery from silver salmon tissue is shown in Table II. The extraction conditions specified under Experimental gave maximum recoveries. Fig. 5 shows chromatograms of standard TCs, tissue blank and the three TCs added to tissue. Isocratic elution as in Fig. 1 suffered interference from endogenous materials in the detection of OTC. This problem was resolved by a combination of gradient elution as indicated in the caption of Fig. 5 and the use of 0.3 *M* instead of 0.1 *M* sodium acetate in buffer A. Under these conditions, the calibration graphs for OTC, TC and CTC were linear in the ranges of 0.08–10, 0.06–10 and 0.1–10 ppm (all with r >0.999), respectively. The recovery and reproducibility [relative standard deviation (R.S.D.)] for OTC at 0.1, 0.5 and 1.0 ppm were 73.6–91.9% and R.S.D. 2.77–4.44% (n = 7), for TC 90.6–95.5% and R.S.D. 2.62–4.63% (n = 7) and for CTC 85.6–93.4% and R.S.D. 3.48–4.70% (n = 7). The reproducibility of the retention time of each TCs was R.S.D. = 0.77–1.78% (n = 7).

TABLE II

RECOVERY OF TETRACYCLINES FROM SILVER SALMON FISH TISSUE BY THE USE OF VARIOUS EXTRACTION REAGENT SYSTEMS

Method[a]	Recovery (%)		
	OTC	TC	CTC
24% TCA in methanol, 3 ml	76.8	75.9	79.4
1 *M* HCl, 3 ml 24% TCA in methanol, 3 ml	72.6	73.4	70.9
1 *M* HCl, 3 ml 24% TCA in methanol, 6 ml	91.0	93.5	93.4
24% TCA in methanol, 9 ml	87.8	86.0	93.1

[a] For 1 g of muscle tissue; sample concentration, 1 ppm.

The detection limits for the three TCs were 32–90 ppb (signal-to-noise ratio = 3). The three TCs were stable for at least 24 h in the resulting mixture at room temperature.

Although the tedious pretreatment step discussed above was omitted, the detection limits were as good as those for the conventional methods [1,3,4]. This demonstrates the possibility of the simple determination of TCs in biological fluids and also of a more sensitive determination by a combination of the present method and concentration steps. Concentration steps that are as simple as possible and suitable for the present method are currently being studied.

REFERENCES

1 J. P. Sharma and R. F. Bevill, *J. Chromatogr.*, 166 (1978) 213.

2 J. P. Sharma, E. G. Perkins and R. F. Bevill, *J. Chromatogr.*, 134 (1977) 441.
3 H. Oka, H. Matsumoto and K. Uno, *J. Chromatogr.*, 325 (1985) 265.
4 W. A. J. Moats, *J. Chromatogr.*, 358 (1986) 253.
5 W. A. J. Moats, *J. Chromatogr.*, 366 (1986) 69.
6 J. H. Knox and J. Jurand, *J. Chromatogr.*, 110 (1975) 103.
7 K. Wolfs, E. Roets, J. Hoogmartens and H. Vanderhaeghe, *J. Chromatogr.*, 358 (1986) 444.
8 H. J. E. M. Reeuwijk and U. K. Tjaden, *J. Chromatogr.*, 353 (1986) 339.
9 K. Tsuji, J. H. Robertson and W. F. Beyer, *Anal. Chem.*, 46 (1974) 539.
10 W. J. Blanchflower, R. J. McCracken and A. Rice, *Analyst (London)*, 114 (1989) 421.
11 W. Hou and E. Wang, *Analyst (London)*, 114 (1989) 699.
12 K. W. Kohn, *Anal. Chem.*, 33 (1961) 862.
13 H. Poiger and C. Schlatter, *Analyst (London)*, 101 (1976) 808.

Journal of Chromatography, 623 (1992) 159–162
Elsevier Science Publishers B.V., Amsterdam

CHROM. 24 482

Short Communication

Direct liquid chromatographic separation of the enantiomers of a 1,3-dihydrophenylindol-2-one and of a 2,3-dihydro-2-oxo-benzofuran derivative

Salvatore Caccamese

Dipartimento di Scienze Chimiche, Università di Catania, Viale A. Doria 6, 95125 Catania (Italy)

Tiziana Benincori

Dipartimento di Chimica Organica e Industriale, Università di Milano, Via Golgi 19, 20133 Milan (Italy)

Grazia Principato

Dipartimento di Scienze Chimiche, Università di Catania, Viale A. Doria 6, 95125 Catania (Italy)

(First received April 28th, 1992; revised manuscript received June 22nd, 1992)

ABSTRACT

The enantiomers of a 1,3-dihydrophenylindol-2-one derivative were separated on a Pirkle chiral phase. This phase was unable to separate the enantiomers of a structurally similar 2,3-dihydro-2-oxo-benzofuran derivative, where an oxygen atom replaces the N-CH_3 in the hetero-ring. The enantiomers of this compound were instead separated using a Chiralpak OP(+) column.

INTRODUCTION

1,3-Dihydro-1,3,4,6-tetramethyl-3-(2-amino)phenyl-indol-2-one (**1**), 3-(2-amino)phenyl-2,3-dihydro-2-oxo-3,4,6-trimethylbenzofuran (**2**) and 3-(4-amino)-phenyl-2,3-dihydro-2-imino-3,4,6-trimethylthianaphthene (**3**) (Fig. 1) were the main racemic products of the rearrangements of 2-phenylhydrazo-1,3,4,6-tetramethylindole, 2-phenylhydrazo-3,4,6-trimethyl-benzofuran and 2-phenylhydrazo-3,4,6-trimethyl-thianaphthene, respectively, in acidic medium [1]; these new compounds are expected to show some pharmacological activity as they possess a skeleton which is known to be biologically active [2–5].

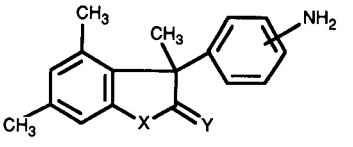

Fig. 1. Structures of compounds **1**–**3**: **1**: X = N(CH_3), Y = O, *ortho* NH_2; **2**: X = O, Y = O, *ortho* NH_2; **3**: X = S, Y = NH, *para* NH_2.

Correspondence to: Dr. S. Caccamese, Dipartimento di Scienze Chimiche, Universita di Catania, Viale A. Doria 6, 95125 Catania, Italy.

0021-9673/92/$05.00

This paper reports the direct enantiomeric resolution of compound **1** by high-performance liquid chromatography (HPLC) on a donor–acceptor chiral stationary phase (CSP) (Pirkle column) and of compound **2** on a helical column [Chiralpak OP(+)]. The resolution factor of compound **1** afforded milligram separation and circular dichroism (CD) measurement of the enantiomeric pair.

EXPERIMENTAL

Apparatus

The HPLC system consisted of a Varian 5060 liquid chromatograph with a 10-μl Valco sample loop, a Jasco Uvidec 100-III UV spectrophotometric detector operating at 240 nm and a Varian CDS 401 data system. For semi-preparative purpose repetitive injections on a 50-μl loop were performed. CD spectra were recorded on a Jasco 600 spectropolarimeter. The columns (25 cm × 4.6 mm I.D.) were packed with (*R*)-N-3,5 dinitrobenzoylphenylglycine covalently bonded to γ-aminopropylsilanized silica (DNPBG) from Regis (Morton Grove, IL, USA) and with (+)-polydiphenyl-2-pyridylmethylmethacrylate [6] coated on silica gel [Chiralpak OP(+)] from Daicel (Tokyo). The void volume (t_0) was determined by injection of 1,3,5-tri-*tert*.-butylbenzene as a non-retained sample.

Chemicals

Compounds **1–3** were prepared by treatment with acetic acid and concentrated sulphuric acid of 2-phenylhydrazo-1,3,4,6-tetramethylindole, 2-phenylhydrazo-3,4,6-trimethylbenzofuran and 2-phenylhydrazo-3,4,6-trimethylthianaphthene, respectively.

1,3,4,6-Tetramethyl-3-(2-amino)phenylindolinone (**1**) was obtained in 30% yield, m.p. 133°C; ^{1}H NMR (C^2HCl_3) δ 7.35 (1H, dd, aromatic), 7.08 (1H, m, aromatic), 6.98 (1H, m, aromatic), 6.68–6.40 (3H, m, aromatic), 3.25 (3H, s, CH_3 in position 1), 3.10 (2H, broad s exchangeable with ^2H_2O, NH_2), 2.30, 1.95 and 1.80 (3 × 3H, 3s, 3 CH_3).

3-(2-Amino)phenyl-2,3-dihydro-2-oxo-3,4,6-trimethylbenzofuran (**2**) was obtained in 58% yield, m.p. 195°C; ^{1}H NMR (C^2HCl_3) δ 7.25–6.20 (6H, m, aromatic), 4.2 (2H, broad s exchangeable with ^2H_2O, NH_2, 2.35 (2 × 3H, s, 2 CH_3 in position 4 and 6), 1.80 (3H, s, CH_3 in position 1).

3-(4-Amino)phenyl-2,3-dihydro-2-imino-3,4,6-trimethylthianaphthene (**3**) was obtained in 47% yield, m.p. 152°C; ^{1}H NMR (C^2HCl_3) δ 7.10–6.90 (3H, m, aromatic), 6.50–6.75 (3H, m, aromatic), 5.3 (3H, broad s exchangeable with ^2H_2O, NH and NH_2), 2.30 and 1.80 (9H, 2s, 3 CH_3).

RESULTS AND DISCUSSION

The chromatographic results are presented in Table I. Racemic compound **1** was completely resolved using the Pirkle-type DNBPG column, obtaining a good separation factor (α) which was slightly affected by an increase in the percentage of propan-2-ol in the mobile phase, and excellent resolution factors (*R*) as shown in Table I and Fig. 2a. This gave a quantitative separation of the enantiomers by repeated 50-μl injections of racemic

TABLE I

CSP-HPLC RESOLUTION OF ENANTIOMERIC COMPOUNDS 1–3

Compound	CSP[a]	A[b] (%)	k'[c]	α	R
1	DNBPG	3	5.25	1.44	2.5
	DNBPG	5	3.70	1.42	2.8
	DNBPG	10	2.41[d]	1.39	2.5
	DNBPG	15	1.74	1.33	2.5
	Chiralpak OP(+)	5[e]	4.32[f]	NS[g]	
2	DNBPG	0	1.74[f]	1.02	
	Chiralpak OP(+)	0[e]	4.79	1.19	0.98
	Chiralpak OP(+)	5[e]	2.61	1.16	0.69
	Chiralpak OP(+)	10[e]	2.04	1.15	0.57
	Chiralpak OP(+)	10[h]	2.12	1.16	0.68
3	DNBPG	10	6.19	NS	
	DNBPG	10[i]	4.07[f]	NS	
	DNBPG	10[i,j]	4.49[f]	1.02	
	Chiralpak OP(+)	10	6.64[f]	NS	

[a] CSPs are described under Experimental.
[b] Percentage of propan-2-ol in *n*-hexane at a flow-rate of 1.5 ml/min unless otherwise specified, t_0 = 2.37 min.
[c] Capacity factor of the first eluted enantiomer.
[d] CD-positive enantiomer, see text.
[e] Flow-rate of 1 ml/min, t_0 = 3.21 min.
[f] Shoulder in the rising edge of the peak.
[g] Not separated.
[h] Flow-rate of 0.7 ml/min.
[i] Propan-2-ol doped with 0.5% diethylamine.
[j] Flow-rate of 0.7 ml/min, t_0 = 5.50 min.

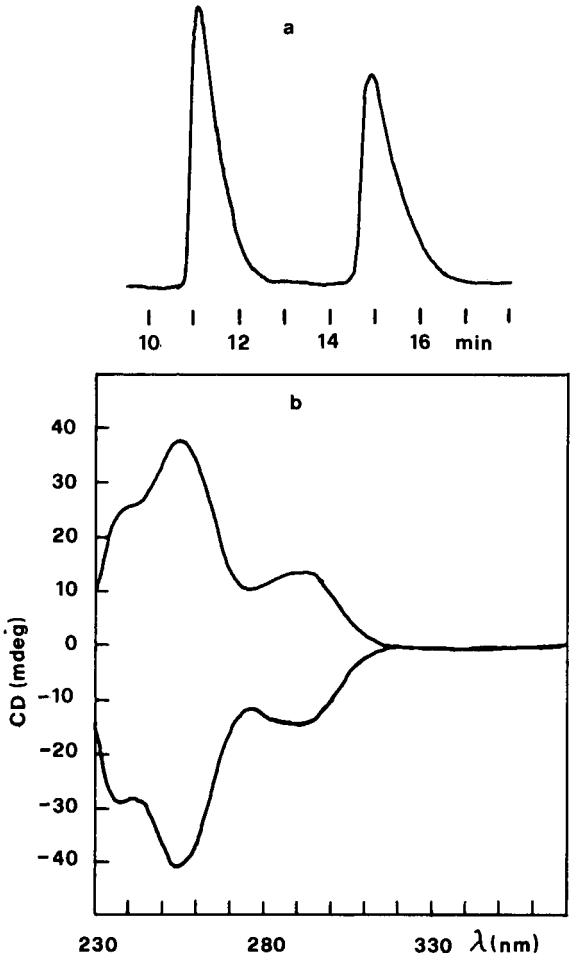

Fig. 2. (a) HPLC separation of the enantiomeric pair of compound **1** on DNBPG, mobile phase *n*-hexane–propan-2-ol (95:5, v/v) at 1.5 ml/min. (b) CD spectra of the enantiomeric pair of compound **1** obtained from the first eluted peak (positive) and from the second peak (negative) in ethanol at 22°C.

1 and collection of the eluates from the two chromatographic peaks. The CD spectra of both eluates were measured and these were mirror images of each other as shown in Fig. 2b, indicating that the two eluates are optical isomers. Analytical HPLC reruns of the eluates indicated a 100% enantiomeric purity of each peak. Their UV spectra are also identical. No separation of the enantiomers of compound **1** was achieved using the Chiralpak OP(+) column, which owes its chirality to the macromolecular helicity, as shown in Table I and from other trials with various percentages of propan-2-ol in hexane.

Compound **2** was well resolved using the Chiralpak OP(+) column, as shown in Table I. The best results were achieved by eliminating the propan-2-ol in the eluent and by decreasing the flow-rate of the mobile phase, thus obtaining a beneficial effect on the resolution factor. The Pirkle-type CSP was ineffective in the resolution of compound **2**. A single sharp peak was observed using hexane–propan-2-ol mobile phases and barely resolved peaks were observed using only *n*-hexane as the eluent, as shown in Table I.

Compound **3** was only slightly resolved using the DNBPG column and the addition of a small amount of diethylamine, combined with a low flow-rate (0.7 ml/min) was crucial to observe this poor resolution, as shown in Table I. No separation was achieved using the Chiralpak OP(+) column, as shown in Table I.

The different behaviour of compounds **1** and **2**, structurally very similar, to the DNBPG chiral stationary phase is explained using the chiral recognition model proposed by Pirkle for its DNBPG phase [7]. We envisage three simultaneous interactions for the relative configurations of compound **1**: (a) a π–π bonding interaction between the 3,5-dimethylphenyl ring of the analyte and the 3,5-dinitrobenzoyl group of the CSP; (b) a dipole-stacking [8] between the N-methyllactame moiety of compound **1** and the 3,5-DNB carboxamide group of the CSP; and (c) a stereochemically dependent steric interaction between the analyte and the CSP. The dipolar interaction in (b) is strong if the dipole moments of the N-methylpyrrolidone (4.06 D [9]) and of the *trans*-carboxamide group of the CSP (3.9 D [10]) are considered as a model.

The dipole stacking is instead much less effective between the lactone function of compound **2** and the carboxamide group of the DNBPG CSP and this results in a minor enantioselectivity with respect to compound **1**. The estereal function of analyte **2** interacts in some way with the estereal function of the Chiralpak OP(+) column, resulting in the resolution of the enantiomers.

Thus the use of the correct CSP is crucial to obtain enantioselectivity sufficient for the preparative resolution of compounds **1** and **2**.

REFERENCES

1 T. Benincori, *Ph. D. Thesis*, University of Milan, Milan, 1992.
2 W. Fischer, E. Schilling and R. Schmiedel, *Pharmazie*, 37 (1982) 858.
3 I. Virsis, B. A. Grinberg, D. Cedere and A. Prikulis, *Khim. Farm. Zh.*, 19 (1985) 953; *C.A.*, 104 225 (1986).
4 H. G. S. Rathae and V. Molla Reddy, *J. Indian Chem. Soc.*, 61 (1985) 556.
5 M. N. A. Rao and L. Harish Rau, *Indian J. Pharm. Sci.*, 47 (1985) 46.
6 Y. Okamoto and K. Hatada, *J. Liq. Chromatogr.*, 9 (1986) 369.
7 W. H. Pirkle and T. C. Pochapsky, *Chem. Rev.*, 89 (1989) 347.
8 W. H. Pirkle, *Tetrahedron Lett.*, 24 (1983) 5707.
9 O. Exner, *Dipole Moments in Organic Chemistry*, Thieme, Stuttgart, 1975.
10 A. Kotera, S. Shibata and K. Sone, *J. Am. Chem. Soc.*, 77 (1955) 6183.

Journal of Chromatography, 623 (1992) 163–167
Elsevier Science Publishers B.V., Amsterdam

CHROM. 24 520

Short Communication

Separation of the enantiomers of some potassium channel activators using an α_1-acid glycoprotein column

John M. Evans, Richard J. Smith and Geoffrey Stemp

SmithKline Beecham Pharmaceuticals, The Pinnacles, Coldharbour Road, Harlow, Essex CM19 5AD (UK)

(First received June 3rd, 1992)

ABSTRACT

The separations of the enantiomers of some 3,4-dihydro-2,2'-dimethyl-2H-1-benzopyrans and a related tetrahydronaphthalene on α_1-acid glycoprotein (Chiral-AGP) are presented, together with the results from an investigation of the effects of organic modifier and pH on the separations achieved. The general utility of Chiral-AGP in separating the enantiomers of compounds from this class of antihypertensive agents is demonstrated in this paper.

INTRODUCTION

3,4-Dihydro-2,2-dimethyl-2H-1-benzopyrans such as **1–5** and the related tetrahydronaphthalene **6** are potent antihypertensive agents which relax smooth muscle by activating potassium channels [1,2]. These compounds contain two chiral centres but the relative stereochemistry of these is fixed in the *trans* configuration, so that each compound exists as only one pair of enantiomers. The biological activity of cromakalim **1** is known to reside principally in one enantiomer [3], and it is therefore important to have analytical methods which can distinguish between the enantiomers of **1** and also between the enantiomers of its analogues. High-performance liquid chromatography (HPLC) methods have been reported previously for the separation of the enantiomers of similar compounds on a hexahelicene phase [4] and using chiral ion pairs [5] but the former method required the presence of a nitro group in the aryl group of the benzopyran for enantioselectivity and the latter required the presence of a basic nitrogen group in the molecule. Neither method was general, therefore. The separation of the enantiomers of **1** has also been reported by gas chromatography [6]. This study describes the separation of the enantiomers of **1–6** by HPLC on α_1-acid glycoprotein (Chiral-AGP), a column which appears to separate the enantiomers of a wide range of compounds from this class and thus provides a method more general than any previously described.

EXPERIMENTAL

Chemicals

The synthesis of compounds **1–6** has been described [3,7,8]. Methanol and propan-2-ol were from Romil Chemicals (Loughborough, UK); other chemicals were from Aldrich (Gillingham, UK). So-

Correspondence to: Dr. Richard J. Smith, SmithKline Beecham Pharmaceuticals, The Pinnacles, Coldharbour Road, Harlow, Essex CM19 5AD, UK.

0021-9673/92/$05.00

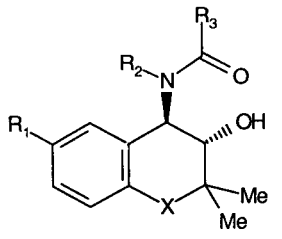

Compound	R_1	R_2	R_3	X
1	CN	-$(CH_2)_3$-		O
2	CN	-$(CH_2)_4$-		O
3	CN	H	Me	O
4	H	H	Me	O
5	CN	H	Ph	O
6	CN	H	Me	CH_2

dium phosphate buffers were prepared by dissolving the appropriate amount of sodium phosphate dibasic heptahydrate or sodium phosphate monobasic monohydrate in HPLC grade water to give 0.01 *M* solutions, adjusting to the required pH with concentrated orthophosphoric acid and filtering through a Millipore Durapore membrane (0.45 μm).

HPLC

All mobile phases were degassed with helium before use. Chromatographic analyses were performed on a Waters 991 photodiode array system equipped with a Waters M600E pump and a Gilson 231/401 autosampler. The primary detection wavelengths were 220 and 252 nm. Analyses were carried out on a Chiral-AGP column (100 × 4.0 mm I.D.), supplied by Technicol (Stockport, UK) at a flow-rate of 0.9 ml/min. Samples were prepared as 0.1 mg/ml solutions in eluent after prior dissolution in a small volume of methanol. Injection volumes were 5 μl. All analyses were performed at ambient temperature (approx. 21°C). Capacity factors (k') for the peaks were calculated using the equation $k'_1 = (t_1 - t_0)/t_0$, where t_1 was the retention time of peak 1 and t_0 was the retention time of an unretained substance. The latter was determined by injection of mobile phase with a slight difference in composition.

RESULTS AND DISCUSSION

Compounds **1–6** were chromatographed using eluents of three different pH values and with varying percentages of either methanol or propan-2-ol as organic modifiers to determine the best separation conditions for each racemate. Example chromatograms for **2** and **3** are shown in Fig. 1 and the results for all the compounds are summarized in Tables I, II and III. The data in Table I show that the k' values, and usually also the enantioselectivities (α), increase with a decrease in the percentage propan-2-ol. Compound **5** was so well retained at 5% propan-2-ol that experiments below this modifier concentration were not performed. It can be seen from the data in Table I that all the racemates in the series can be separated using an eluent consisting of propan-2-ol and phosphate buffer at pH 7, although the enantiomers of the two cyclic amides (**1** and **2**) were less well separated than those of the other compounds. The increase in retention for the series **3**, **1**, **2**, **5** appeared to correlate with the expected order of hydrophobicities of these compounds; the aromatic ring in **5** produced a particularly marked increase in retention. However, the enantioselectivities observed for these compounds did not mirror the trend in retention —it appears that processes giving rise to retention for these compounds do not necessarily also give rise to chiral discrimination. This can also be seen from a comparison of the behaviours of **3**, **4** and **6**. For this range of similar compounds, **3** was the least retained in all conditions tried, but it consistently gave the best enantioselectivity. Such observations further illustrate the documented dependence of the stereoselectivity of the Chiral-AGP column on small structural changes in the solute molecules [9,10].

Variation of mobile phase pH (using 1% propan-2-ol as organic modifier) gave the results shown in Table II. For all compounds, reducing the pH lead to decreased retention and for most of the compounds it also lead to decreased enantioselectivity. However, for **2**, decreasing the pH from 4.7 to 3 *increased* the enantioselectivity observed, in marked contrast to the result for the very similar compound **1**. The effect of pH was also investigated for **5**, using 5% propan-2-ol as the organic modifier. At pH 3 there was a decrease in retention compared to that

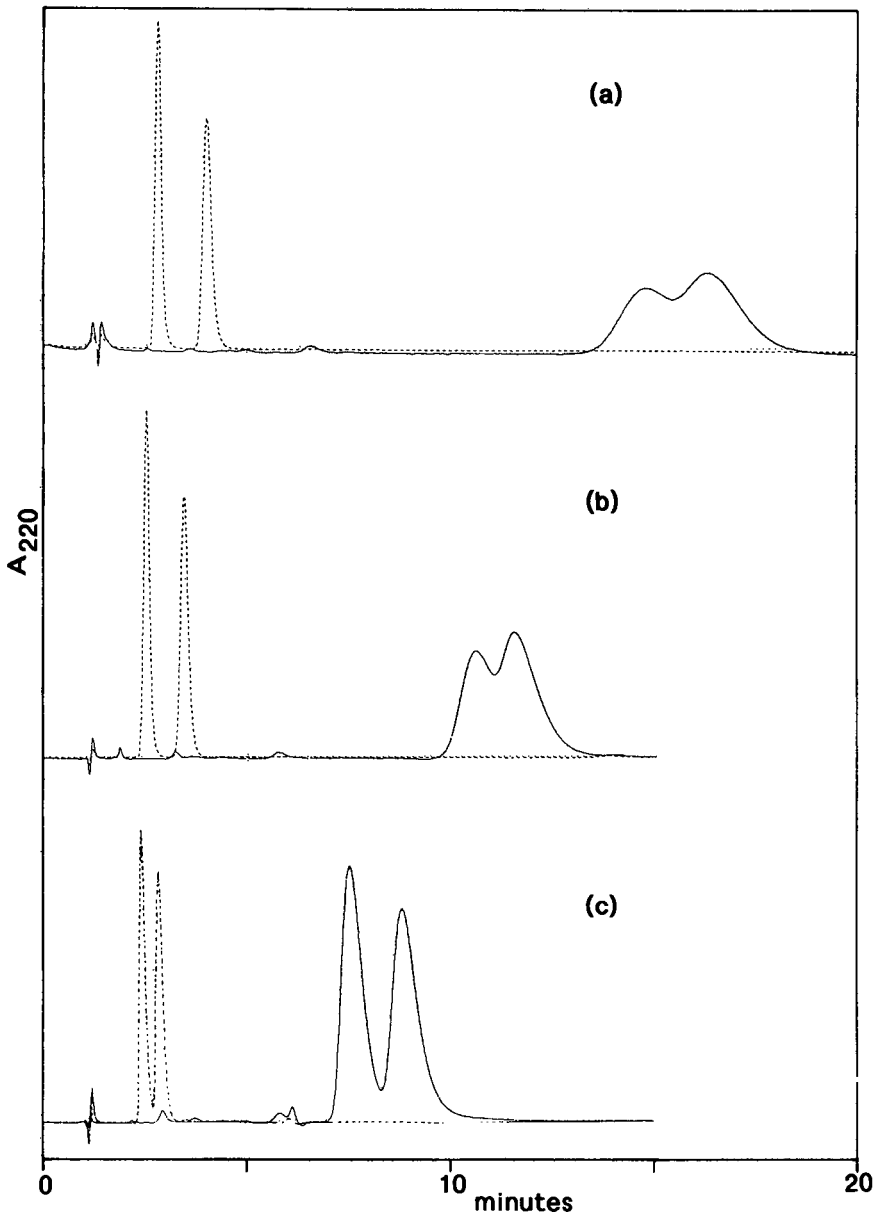

Fig. 1. Example chromatograms for **2** (solid line) and **3** (broken line) with eluent conditions as follows: (a) 1% propan-2-ol in aqueous phosphate buffer pH 7.0; (b) 1% propan-2-ol in aqueous phosphate buffer pH 4.7; (c) 1% propan-2-ol in aqueous phosphate buffer pH 3.0.

observed at pH 7 (k'_2 = 6.35 at pH 3), but the decline in enantioselectivity was less marked (α = 1.29 at pH 3).

Changing the organic modifier to 10% methanol (Table III) produced, in most cases, approximately the same enantioselectivities as observed using 1% propan-2-ol, but the retention times were reduced, thus giving shorter analysis times. Compound **2** was

TABLE I

INFLUENCE OF CONCENTRATION OF PROPAN-2-OL ON THE RETENTION AND ENANTIOSELECTIVITY FOR **1–6**

Column, Chiral-AGP (100 × 4 mm I.D.); mobile phase, 0.01 *M* phosphate buffer (pH 7.0) containing different concentrations of propan-2-ol; flow-rate 0.9 ml/min.

Compound	5% Propan-2-ol		2.5% Propan-2-ol		1% Propan-2-ol	
	k'_2	α	k'_2	α	k'_2	α
1	0.82	1.00	1.86	1.10	4.08	1.20
2	1.59	1.00	4.42	1.14	10.66	1.11
3	0.45	1.19	0.95	1.51	1.86	1.84
4	0.75	1.19	1.96	1.33	4.69	1.49
5	10.32	1.34	NP[a]		NP[a]	
6	0.78	1.00	1.60	1.11	3.16	1.29

[a] NP = Experiment not performed.

again an exception; the enantioselectivity observed for this compound was considerably reduced with methanol, except at pH 3. Again this contrasted with the behaviour of **1**, for which 10% methanol gave *improved* enantioselectivities, except at pH 3.

From the results, it can be concluded that Chiral-AGP appears to be very useful column for the separation of the enantiomers of these antihypertensive agents and that their separations can be usefully manipulated by changing the eluent pH or the organic modifier. A mobile phase pH of around 7 gives the best chance of obtaining a separation and either propan-2-ol or methanol can be used as the organic modifier, with methanol usually being preferred for the shorter analysis times it can provide (for the same selectivity). The series of compounds described in this study has shown some interesting contrasts in chromatographic behaviour and this aspect will be further investigated in the near future.

TABLE II

INFLUENCE OF BUFFER pH ON THE RETENTION AND ENANTIOSELECTIVITIES FOR **1–6** WITH PROPAN-2-OL AS ORGANIC MODIFIER

Conditions as in Table I, with 1% propan-2-ol used as the organic modifier and variation of buffer pH.

Compound	pH 7		pH 4.7		pH 3	
	k'_2	α	k'_2	α	k'_2	α
1	4.08	1.20	3.89	1.12	3.21	1.00
2	10.66	1.11	9.00	1.10	6.93	1.20
3	1.86	1.84	1.98	1.70	1.66	1.33
4	4.69	1.49	4.05	1.23	3.22	1.00
5	Experiment not performed					
6	3.16	1.29	3.10	1.17	3.00	1.06

TABLE III

INFLUENCE OF BUFFER pH ON THE RETENTION AND ENANTIOSELECTIVITIES FOR **1–6** WITH METHANOL AS ORGANIC MODIFIER

Conditions as in Table II, with methanol in place of propan-2-ol.

Compound	pH 7		pH 4.7		pH 3	
	k'_2	α	k'_2	α	k'_2	α
1	3.03	1.25	2.37	1.20	2.09	1.00
2	7.1	1.00	4.93	1.00	4.47	1.15
3	1.56	1.79	1.33	1.80	1.24	1.37
4	3.88	1.41	2.97	1.30	2.55	1.10
5	Experiment not performed					
6	2.46	1.34	2.06	1.31	2.02	1.14

REFERENCES

1 T. C. Hamilton, S. W. Weir and A. H. Weston, *Brit. J. Pharmacol.*, 88 (1986) 103.
2 J. M. Evans and G. Stemp, *Chem. Britain*, 27 (1991) 439.
3 V. A. Ashwood, R. E. Buckingham, F. Cassidy, J. M. Evans, E. A. Faruk, T. C. Hamilton, D. J. Nash, G. Stemp and K. Willcocks, *J. Med. Chem.*, 29 (1986) 2194.
4 J. M. Evans, W. J. Lough, R. S. Oliver, S. A. Matlin and V. E. Stacey, presented at the *12th International Symposium on Column Liquid Chromatography, Washington, DC, June 1988*.
5 V. de Biasi, M. B. Evans and W. J. Lough, in D. Stevenson and I. D. Wilson (Editors), *Recent Advances in Chiral Separations*, Plenum Press, New York, 1990, p. 93.
6 B. E. Davies, in E. Reid, J. D. Robinson and I. D. Wilson (Editors), *Bioanalysis of Drugs and Metabolites*, Plenum Press, New York, 1988, p. 179.
7 V. A. Ashwood, F. Cassidy, M. C. Coldwell, J. M. Evans, T. C. Hamilton, D. R. Howlett, D. M. Smith and G. Stemp, *J. Med. Chem.*, 33 (1990) 2667.
8 V. A. Ashwood, F. Cassidy, J. M. Evans, S. Gagliardi and G. Stemp, *J. Med. Chem.*, 34 (1991) 3261.
9 J. Hermansson and G. Schill, in P. R. Brown and R. A. Hartwick (Editors), *High Performance Liquid Chromatography*, Wiley-Interscience, New York, 1989, Ch. 8, p. 337.
10 E. Arvidsson, S. O. Jansson and G. Schill, *J. Chromatogr.*, 591 (1992) 55.

Journal of Chromatography, 623 (1992) 168–173
Elsevier Science Publishers B.V., Amsterdam

CHROM. 24 452

Short Communication

Liquid chromatographic determination of 2-hydroxy-3-aminophenazine and 2,3-diaminophenazine as impurities in pesticide formulations containing benomyl or carbendazim

Benny Køppen

National Environmental Research Institute, Frederiksborgvej 399, P.O. Box 358, DK-4000 Roskilde (Denmark)

(First received April 24th, 1992; revised manuscript received June 19th, 1992)

ABSTRACT

Highly mutagenic 2-hydroxy-3-aminophenazine (HAP) and 2,3-diaminophenazine (DAP) are possible impurities present in technical samples of the pesticides carbendazim and benomyl. A liquid chromatographic method with electrochemical detection was developed for the determination of HAP and DAP in technical or formulated samples of these pesticides. The method involves sample clean-up by strong cation-exchange solid-phase extraction prior to high-performance liquid chromatographic analysis. The method is relatively simple and can be used for analytical control of the contents of HAP and DAP impurities in pesticide products.

INTRODUCTION

Carbendazim and benomyl (Fig. 1, **I** and **II**, respectively) are fungicides that are used as active ingredients in pesticide formulations. The structures of these compounds are closely related and benomyl is, in fact, thought to act biologically as a precursor of carbendazim [1]. For some years it has been known that the mutagenic effects displayed by carbendazim and benomyl [2,3] are caused by the presence of phenazine impurities in the technical active ingredients, namely 2-hydroxy-3-aminophenazine (HAP) and 2,3-diaminophenazine (DAP) (Fig. 1, **III** and **IV**, respectively) [4,5].

According to information provided by DuPont, which produces the active ingredients, the Ames test for mutagenic effect is negative if the total content

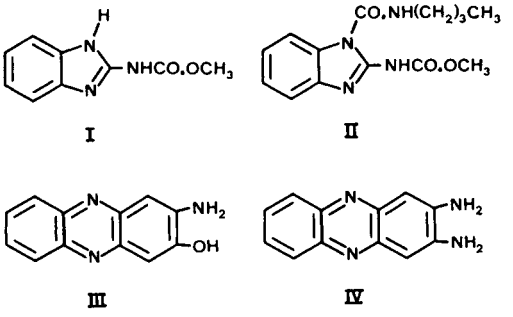

Fig. 1. Structures of the active ingredients carbendazim (**I**) and benomyl (**II**) and those of the two impurities 2-hydroxy-3-aminophenazine (**III**) and 2,3-diaminophenazine (**IV**).

Correspondence to: Dr. Benny Køppen, National Environmental Research Institute, Frederiksborgvej 399, P.O. Box 358, DK-4000 Roskilde, Denmark.

0021-9673/92/$05.00

of HAP and DAP impurities in the active ingredients is below 3.5 ppm. For authority control of the pesticide products available in Denmark, a method was needed by which the content of these two impurities in carbendazim and benomyl formulations could be determined. The method should have a detection limit below 3.5 ppm relative to the content of active ingredient (benomyl or carbendazim) in the formulation. The only published method for the determination of HAP and DAP in technical carbendazim and carbendazim-containing formulations is that of Van Damme *et al.* [6], which is a normal-phase high-performance liquid chromatographic (HPLC) method with UV–VIS absorption detection at 453 nm. The method proposed in this paper is a reversed-phase HPLC method with electrochemical detection, which offers increased sensitivity compared with absorption detection. Further, the method is also applicable to formulations containing benomyl as the active ingredient.

EXPERIMENTAL

Reagents

Phosphoric acid (85%) (Merck, Germany), sodium hydroxide (Merck) and triethylamine (Fluka, Switzerland) were of analytical-reagent grade and methanol (Merck) was of gradient grade. All chemicals were used as received. Water was purified with a Milli-Q purification system (Millipore, USA). 2,3-Diaminophenazine and 2-hydroxy-3-aminophenazine were received as a gift from Dupont.

Apparatus and chromatographic conditions

A Bransonic 52 ultrasonic bath (Branson), an Omnifuge centrifuge (Heraeus-Christ), 0.5-μm pore-size Fluoropore filters (Millipore) and Bond Elut strong cation-exchange (SCX) solid-phase extraction columns (50 mg) (Analytichem) were used.

The HPLC system consisted of a Waters Model 510 pump equipped with a Waters Model 712 WISP autosampler, a BAS LC-4 electrochemical detector (Bioanalytical Systems) and a D-2000 Chromato-Integrator (Hitachi). The applied detector voltage was +0.75 V *vs.* Ag/AgCl reference electrode. The analytical column was a Novapak C_{18} (15 cm × 3.9 mm I.D.), 4-μm particle size (Waters). The column temperature was maintained at 30.0 ± 0.1°C using a laboratory-made LC column thermostat. The mobile phase was: 0.050 *M* phosphoric acid–0.025 *M* triethylamine, adjusted to pH 6.0 with 2 *M* NaOH–methanol (68:32, v/v), at a flow-rate of 1.0 ml/min.

Preparation of standards

Standards were protected from light during preparation and analysis. Stock solutions of HAP and DAP were prepared separately by dissolving 5.0 mg of the compound in 50 ml of methanol. Volumes of 1.0 ml each of the HAP and DAP stock solutions were mixed and made up to 10 ml with methanol. The stock solutions and mixed stock solutions were stable for at least 2 months when stored at 4°C. A calibration standard solution, that was used for HPLC analysis, was prepared by diluting 100 μl of the mixed stock solution to 50 ml with mobile phase. A fresh calibration standard solution was prepared each day.

Preparation of samples

Samples were protected from light during preparation and analysis. An amount of sample corresponding to 300 mg of active ingredient was weighed and extracted with 10.0 ml of methanol by ultrasonic treatment for 15 min. Following centrifugation (*ca.* 1000 *g*, 10 min) a 3.0-ml aliquot of the supernatant was diluted with 6.0 ml of 0.2 *M* phosphoric acid. If necessary the mixture was filtered and 6.0 ml of the filtrate were applied to a Bond Elut SCX column, pre-equilibrated with 3.0 ml of 0.2 *M* phosphoric acid. The column was washed with 3 x 3.0 ml of 0.2 *M* phosphoric acid followed by 3.0 ml of water. The column was then eluted with 9.0 ml of 0.15 *M* sodium phosphate buffer (pH 9.0)–methanol (65:35). The eluate was made up to 10.0 ml with mobile phase and analysed by HPLC.

RESULTS AND DISCUSSION

In order to select the optimum detection conditions for the HPLC of HAP and DAP, a comparison between UV–VIS absorbance detection and electrochemical detection was made. Absorption spectra (200–600 nm) and response *vs.* applied voltage curves for HAP and DAP were obtained and are shown in Fig. 2. Under optimum detection conditions (electrochemical detection at +0.75 V applied voltage and absorbance detection at 254 nm), the signal-to-noise ratio was 10–15 times higher us-

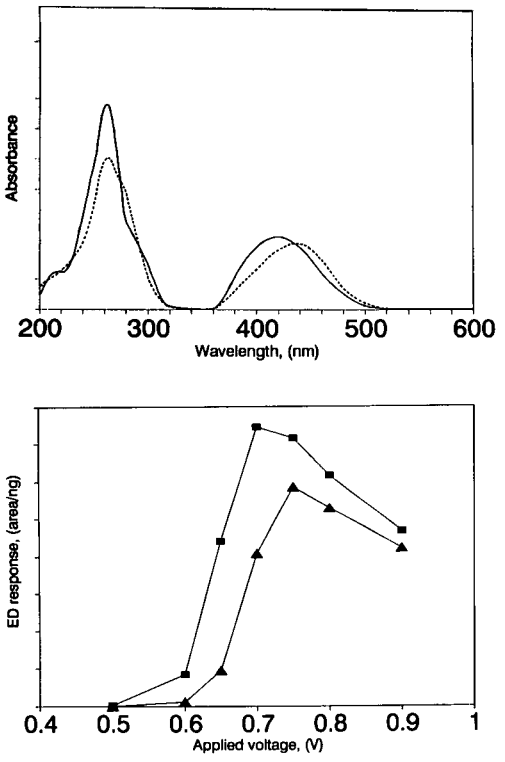

Fig. 2. Top: UV–VIS absorption spectra of (dashed line) HAP and (solid line) DAP, obtained on solutions of HAP and DAP in the HPLC mobile phase. Bottom: electrochemical detection response of (■) HAP and (▲) DAP as a function of applied voltage. Other HPLC conditions as described in the text.

ing electrochemical detection than using absorbance detection. Hence electrochemical detection was preferred.

HAP and DAP are very soluble in polar solvents such as water and methanol, but less soluble in less polar organic solvents such as dichloromethane and benzene [6,7]. Methanol was chosen as the extraction solvent because preliminary experiments indicated that the stability of HAP and DAP was better in methanolic than in aqueous solution. It was found that HAP and DAP degraded when they were exposed to light, and that degradation was faster in aqueous than in methanolic solution, in agreement with the findings of Van Damme *et al.* [6]. In order to prevent degradation of HAP and DAP, the samples were protected from light during sample preparation and analysis.

A clean-up step before HPLC analysis was found to be necessary, because sample matrix components (especially when analysing suspension formulations) interfered with the electrochemical detector signal of the analytes. Two different types of solid-phase extraction columns (C_{18} and SCX) were investigated. Allthough C_{18} columns showed an acceptable retention of the analytes, the interfering matrix components were also retained on the column and it was not possible to find a water–methanol composition of the eluting solvent that selectively eluted the analytes.

Strong-cation exchange columns were preferred because selective retention of the analytes (in the protonated ionic form) was achieved, with the possibility of washing sample matrix interferences through the column. The sample solution was therefore acidified with phoshoric acid prior to application to the SCX clean-up column. Elution of the analytes from the column was done by changing to an eluting solvent of increased pH (9.0) and containing 35% methanol. Addition of methanol to the eluting solvent was found to be necessary to optimize the elution effiency, probably because of some non-ionic adsorption of HAP and DAP on the column.

Linearity, precision and detection limits

Linearity was investigated by analysing a series of dilutions (six concentrations) of HAP and DAP standards. The relationship between peak area and HAP and DAP concentration was linear (correlation coefficients 0.9999 and 0.9997, respectively) over the concentration range 10–200 ng/ml for both compounds.

The precision of the method was evaluated by triplicate analysis of several different technical samples (TC), suspension concentrate (SC) and wettable powder (WP) formulation samples. The results are shown in Table I. As no authentic samples were available that contained the phenazine impurities, all the samples used for evaluation of the precision of the method were spiked samples. A typical chromatogram from the analysis of a spiked sample is shown in Fig. 3. The precision of the method was 5–7% for determination of both HAP and DAP in the various types of samples.

Detection limits (calculated as injected amount of analyte with a signal-to-noise ratio of *ca.* 3) was

TABLE I

PRECISION OF THE METHOD

Sample type[a]	Active ingredient	Analyte	Content[b], ppm	R.S.D.[c] (%)	
				HAP	DAP
TC	Carbendazim	HAP	7.8	6.8	
		DAP	9.4		1.2
TC	Benomyl	HAP	6.3	6.6	
		DAP	6.7		3.8
SC	Carbendazim	HAP	1.6	3.2	
		DAP	1.8		9.4
SC	Carbendazim	HAP	2.1	11.1	
		DAP	2.3		1.9
WP	Benomyl	HAP	2.8	5.3	
		DAP	2.2		9.6
Mean				6.6	4.5

[a] TC = technical; SC = suspension concentrate; WP = wettable powder.
[b] Mean of triplicate analyses.
[c] Relative standard deviation.

0.10 ng for both HAP and DAP, corresponding to a content of 0.3 ppm relative to the content of active ingredient in a typical sample (containing 50% of active ingredient). Detection limits reported by Van Damme *et al.* [6] were 0.4 and 0.8 ppm, respectively.

Recovery

The recovery of the method was evaluated by analysing samples before and after addition of known amounts of HAP and DAP. Two spike levels of each of the different sample types were investigated and the results are shown in Table II. The recoveries ranged between 62% and 112% with a mean recovery for both compounds of *ca.* 80%. The low and variable recovery for the method may be ascribed to two different parameters: non-ionic adsorption of the two analytes on the SCX cartridge column, in spite of the optimized elution conditions, and the inherent limited photostability of the analytes. Significant variation of the recovery within a sample type was seen, which might be explained as resulting from variations in the adsorption characteristics of the solid-phase extraction columns. Despite the low recovery, the method was considered acceptable for the purpose of analytical control of the contents of HAP and DAP in pesticide formulations in relation to given limits.

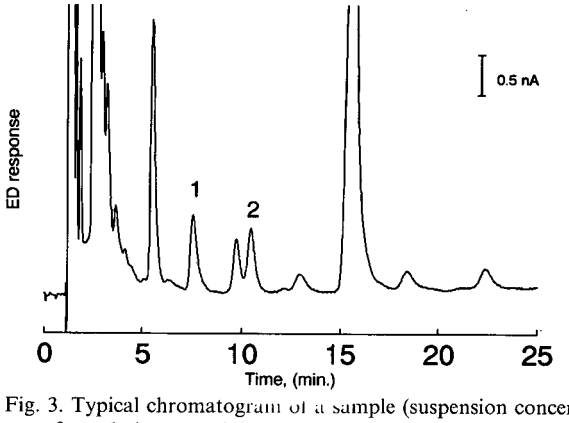

Fig. 3. Typical chromatogram of a sample (suspension concentrate formulation containing carbendazim as active ingredient) spiked with HAP (1) and DAP (2). The contents of HAP and DAP in the spiked sample were 1.56 and 1.84 ppm, respectively.

Application

The method has been used as a part of a authority control programme monitoring pesticide products available in Denmark. Seven different formulation samples (five containing carbendazim and two containing benomyl as the active ingredient) were

TABLE II

RECOVERY DATA

Sample type[a]	Active ingredient	Spike level (ppm)		Recovery[b] (%)	
		HAP	DAP	HAP	DAP
TC	Carbendazim	5.0	5.0	90	74
		50	50	94	86
TC	Benomyl	5.0	5.0	79	83
		50	50	65	65
SC	Carbendazim	2.5	2.5	65	74
		25	25	93	107
SC	Carbendazim	2.5	2.5	87	88
		25	25	78	88
WP	Benomyl	2.5	2.5	90	72
		25	25	63	71
WP	Benomyl	2.5	2.5	112	95
		25	25	62	71
Mean				82	81

[a] TC = technical; SC = suspension concentrate; WP = wettable powder.
[b] Means of duplicate analyses.

analysed. In all of the samples the contents of HAP and DAP were below the detection limit of the method. Two plausible explanations for this can be given: the contents of the synthesis impurities HAP and DAP in the active ingredients were initially very low or the impurities had degraded during the period between synthesis of the active ingredient and analysis of the commercial formulation. As discussed by van Damme *et al.* [6], who also were unable to detect HAP and DAP in newer formulations, it is very likely that any HAP or DAP initially present in the technical active ingredient will degrade during formulation production or storage, especially when formulations (such as SC formulations) contain water.

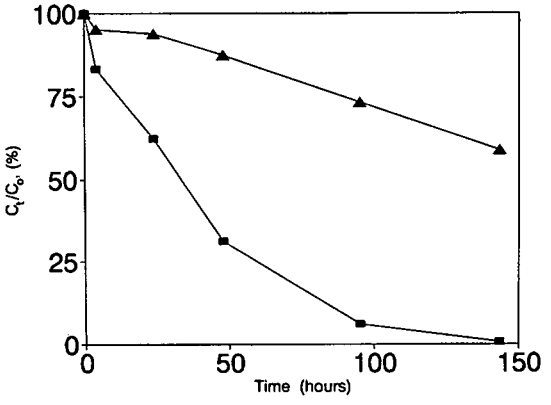

Fig. 4. Stability of (■) HAP and (▲) DAP. A sample of a suspension concentrate formulation containing carbendazim as the active ingredient was spiked with HAP and DAP (initial concentrations C_0 13.1 and 16.0 ppm, respectively) and stored at room temperature protected from light. At different times during storage, the concentrations (C_t) of HAP and DAP in subsamples were determined (single determinations) as described in the text.

This is demonstrated by the results shown in Fig. 4. A sample of an SC formulation was spiked with HAP and DAP and stored at room temperature protected from light. At different times during storage subsamples were analysed for their contents of HAP and DAP. As can be seen from Fig. 4, the stability of HAP and DAP (at least in an SC formulation) is very limited.

CONCLUSIONS

The method presented here is relatively simple and useful for the determination of HAP and DAP

impurities in pesticide formulations containing carbendazim or benomyl as the active ingredient. The precision and accuracy of the method are acceptable for use in authority pesticide formulation control.

ACKNOWLEDGEMENT

The author thanks DuPont for supplying samples of HAP and DAP.

REFERENCES

1 G. P. Clemons and H. D. Sisler, *Pestic. Biochem. Physiol.*, 1 (1971) 32.
2 J. P. Seiler, *Mutat. Res.*, 15 (1972) 273.
3 J. P. Seiler, *Mutat. Res.*, 32 (1975) 151.
4 Danish Environmental Protection Agency, Pesticide Division, personal communication.
5 F. Oesch, *Evaluation of the Genotoxicity Studies on Carbendazim (MBC), Benomyl and Thiophanate-methyl*, Department of Toxicology and Pharmacology, University of Mainz, Mainz, 1982.
6 J.-C. Van Damme, B. De Ryckel and M. Galoux, *J. Chromatogr.*, 518 (1990) 375.
7 *Merck Index*, Merck, Rahway, NJ, 10th ed., 1983, p. 431.

Journal of Chromatography, 623 (1992) 174–177
Elsevier Science Publishers B.V., Amsterdam

CHROM. 24 460

Short Communication

Sulphur compounds

CLIX☆. Determination of dithionite ($S_2O_4^{2-}$) and hydroxymethanesulphinate ($HOCH_2SO_2^-$; Rongalite) by ion-pair chromatography

Ralf Steudel and Vera Münchow

Institut für Anorganische und Analytische Chemie, Sekr. C2, Technische Universität Berlin, Strasse des 17. Juni 135, D-1000 Berlin 12 (Germany)

(First received April 9th, 1992; revised manuscript received June 30th, 1992)

ABSTRACT

Dithionite ($S_2O^{2-}_4$) and hydroxymethanesulphinate ($HOCH_2SO^-_2$) were separated from other sulphur oxyanions by ion-pair chromatography and determined using a UV absorbance detector. To circumvent the autoxidation of dithionite it was derivatized by quantitative reaction with formaldehyde to give hydroxymethanesulphinate; the UV spectrum of the latter is reported. The detection limit of $HOCH_2SO_2Na \cdot 2H_2O$ (Rongalite) was 0.5 mg l^{-1} (0.5 ppm).

INTRODUCTION

Sodium dithionite and sodium hydroxymethanesulphinate (Rongalite) are commercial chemicals widely used as powerful reducing agents, in particular in the textile, printing and paper industries [2]. The determination of dithionite is difficult owing to its extreme sensitivity to oxygen in aqueous solution and to the spontaneous decomposition of such solutions even with exclusion of oxygen [3,4]. This decomposition depends strongly on the pH and is rapid at pH < 5.5. At pH values close to 7 the main decomposition reaction can be represented by the equation [5].

$$2\ S_2O_4^{2-} + H_2O \rightarrow S_2O_3^{2-} + 2\ HSO_3^- \qquad (1)$$

So far, dithionite has been determined by iodimetric [6,7], potentiometric [8], and spectrophotometric [8] titration, polarography [9], Raman spectroscopy [10] and spectrophotometry [11]. Reports on the ion chromatographic determination of dithionite [12] will be discussed below.

Inorganic sulphide (HS^-), polysulphide (S_n^{2-}), sulphite (SO_3^{2-}), thiosulphate ($S_2O_3^{2-}$), polythionates ($S_nO_6^{2-}$) and organic S-sulphonate anions ($RSSO_3^-$) can be separated and determined by ion-pair chromatography [13–15]. This method uses an

Correspondence to: Professor Dr. R. Steudel, Institut für Anorganische und Analytische Chemie, Sekr. C2, Technische Universität Berlin, Strasse des 17. Juni 135, D-1000 Berlin 12 (Germany).

☆ For Part CLVIII, see ref. 1.

0021-9673/92/$05.00

inert organic stationary phase and a water–acetonitrile mixture containing tetrabutylammonium ions and a buffer as the mobile phase. A UV absorbance detector has been applied in all instances. We report here the analysis of aqueous dithionite and Rongalite by ion-pair chromatography. To circumvent the oxygen sensitivity of dithionite, the freshly prepared solutions were reacted with formaldehyde, which converts $S_2O_4^{2-}$ rapidly and quantitatively into the less sensitive sulphinate and sulphonate ions [6,7]:

$$S_2O_4^{2-} + 2\,CH_2O + H_2O \rightarrow HOCH_2SO_2^- + HOCH_2SO_3^- \quad (2)$$

EXPERIMENTAL

The chromatographic and spectroscopic equipment described in a previous paper [14] were used. The variable-wavelength UV detector was operated at 215 nm. As in the earlier work [14], a PRLP-S column (Polymer Labs.) (120 mm × 4 mm I.D., particle size 8 μm) connected to a PRP-100 precolumn (Knauer) (Eurogel, particle size 8 μm) was used. Two different eluent compositions were employed, depending on the accompanying ions to be determined. For mixtures of $S_2O_4^{2-}$ with $S_2O_3^{2-}$ and polythionates the eluent was water–acetonitrile (Promochem Chrom AR) (75:25, v/v) containing 1 mmol l^{-1} of Na_2CO_3 and 2 mmol l^{-1} of tetra-*n*-butylammonium hydrogenphosphate (pH of eluent = 7.7). Mixtures of $S_2O_4^{2-}$ with HS^- and $S_2O_3^{2-}$ were analysed with an eluent consisting of water–acetonitrile (93:7, v/v) containing 1 mmol l^{-1} of Na_2CO_3 and 2 mmol l^{-1} of tetra-*n*-butylammonium hydroxide. The pH of this eluent was adjusted to 11.0 by addition of H_3PO_4 (8%). The eluents were degassed and in some instances oxygen-free helium was bubbled through. However, even then it was not possible to detect $S_2O_4^{2-}$ directly [16]. The flow-rate was always 1 ml min^{-1}.

Water for sample and eluent preparation was doubly distilled. To remove dissolved oxygen, the water for samples was then refluxed under nitrogen for 10 h. The nitrogen had an oxygen content of <0.1 ppm. To avoid the intrusion of O_2 from the air, the apparatus was made from glass and copper and the use of plastic pipes was avoided as far as possible.

$Na_2S_2O_4$ (93%; containing 6.5% Na_2SO_3 and 0.5% Na_2SO_4) (BASF) and Rongalite (98.8% dihydrate) (BASF) were used as received. $Na_2S_2O_4$ was stored at −18°C under nitrogen. $Na_2S \cdot 7\text{–}9H_2O$ (Merck) was recrystallized from degassed water. Aqueous formaldehyde (37%) (Merck), Na_2SO_3 (puriss.) (Fluka) and $K_2S_2O_3 \cdot 3/2H_2O$ (purum) (Fluka) were used as received. Polythionates were prepared in almost 100% purity according to ref. 17.

To calibrate the chromatographic system, standard solutions of Rongalite and dithionite were made daily. The latter was added directly to aqueous formaldehyde of pH 8–9. To study the decomposition of aqueous dithionite (see below), the $S_2O_4^{2-}$ solution (*ca.* 20 mmol l^{-1}; 1 ml) was added to aqueous formaldehyde (2 ml) which had been adjusted to pH 8–9 with NaOH (0.1 mol l^{-1}) followed by dilution to 50 ml with doubly distilled water. After completion of reaction 2, exclusion of oxygen was no longer necessary.

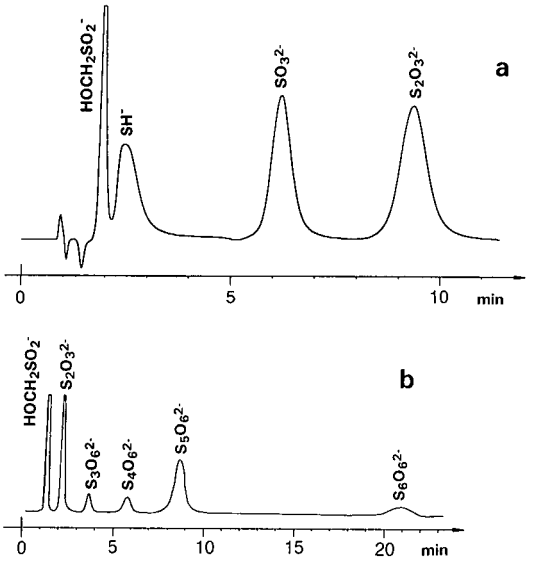

Fig. 1. Chromatograms of the following mixtures: (a) $HOCH_2SO_2^-$ (0.75 mmol l^{-1}), HS^- (0.44 mmol l^{-1}), SO_3^{2-} (0.80 mmol l^{-1}) and $S_2O_3^{2-}$ (0.70 mmol l^{-1}) using an alkaline eluent (pH 11.0); (b) $HOCH_2SO_2^-$ (0.39 mmol l^{-1}), $S_2O_3^{2-}$ (0.39 mmol l^{-1}), $S_3O_6^{2-}$ (0.90 mmol l^{-1}), $S_4O_6^{2-}$ (0.03 mmol l^{-1}), $S_5O_6^{2-}$ (0.09 mmol l^{-1}), $S_6O_6^{2-}$ (0.02 mmol l^{-1}) using an almost neutral eluent (pH 7.7).

RESULTS

Fig. 1a shows the chromatographic separation of hydroxymethanesulphinate, hydrogensulphide, sulphite and thiosulphate at pH 11.0 of eluent No. 2. In Fig. 1b the corresponding separation of hydroxymethanesulphinate, thiosulphate and the polythionates $S_nO_6^{2-}$ (n = 3–6) is shown (eluent No. 1 at pH 7.7). The different retention times on the two chromatograms are due to the different eluent compositions. The assignment of the peaks was made using pure substances and by comparison of retention times and UV absorbance spectra recorded online with a diode-array detector [14].

Fig. 2 shows the previously unknown UV spectrum of the sulphinate; identical spectra were obtained from either Rongalite or $S_2O_4^{2-}$–CH_2O mixtures. The sulphonate does not absorb at 215 nm and therefore does not show up in the chromatograms of $S_2O_4^{2-}$–CH_2O mixtures. However, when the akaline eluent was used it was observed that the sulphonate partly hydrolyzed to give sulphite and CH_2O during analysis. Whereas CH_2O does not absorb at 215 nm the sulphite peak was well separated (see Fig. 1a). As neither sulphide, thiosulphate nor polythionates react with CH_2O at 20°C in water, all these species, which have been found in decomposing dithionite solutions, can now be determined by ion-pair chromatography. However, sulphite reacts with CH_2O to give the sulphonate which, as mentioned above, does not absorb at 215 nm. Its determination requires the use of another detection technique.

The calibration functions for Rongalite and dithionite (after reaction with CH_2O) were investigated in the concentration range (c) 0.09–0.46 mmol l^{-1}. Straight lines were obtained in both instances (correlation coefficients $r \geqslant 0.999$), the slopes of which differed by only 1.6%: Rongalite, peak height = $974c - 12.2$; dithionite, peak height = $959c - 11.7$. The negative intercepts expected for $c = 0$ are caused by the negative peak preceding the sulphinate peak. In both instances the concentration of the solution was determined by iodimetric titration of the sulphinate. The results show that reaction 2 must proceed rapidly and quantitatively. Using a sample loop of 10 μl the detection limit of Rongalite ($HOCH_2SO_2Na \cdot 2H_2O$) was 0.5 mg l^{-1}.

To test the applicability of the method, we analysed an aqueous dithionite solution exposed to air simultaneously by iodimetric titration and by quantitative ion-pair chromatography. The results shown in Fig. 3 demonstrate that both methods yield virtually identical values. Owing to the reaction

$$S_2O_4^{2-} + O_2 \rightarrow 2\ SO_3^{2-} \quad (3)$$

the dithionite concentration (c) slowly decreased but in between sometimes oscillations of c occurred, as had already been observed by others [18]. A more detailed account of the dithionite decomposition will be published elsewhere.

DISCUSSION

We have demonstrated that dithionite can be determined chromatographically after derivatization

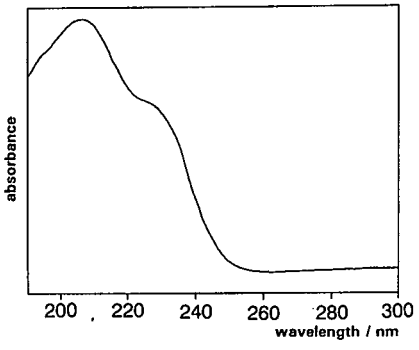

Fig. 2. Absorption spectrum of the $HOCH_2SO_2^-$ ion in water–acetonitrile (75:25, v/v) at pH 7.7 recorded with a diode-array detector. No absorptions were detected in the range 300–800 nm.

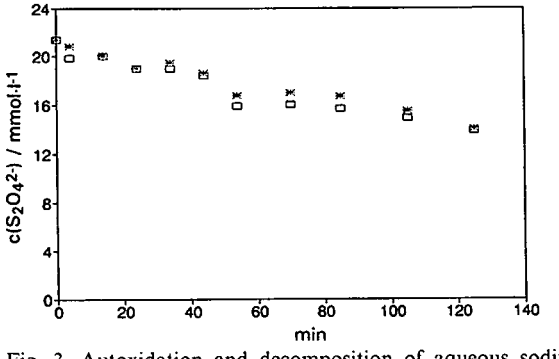

Fig. 3. Autoxidation and decomposition of aqueous sodium dithionite on exposure to air (initial pH = 7). The $S_2O_4^{2-}$ concentration was independently determined by (✱) ion-pair chromatography and (□) iodimetric titration.

to the more stable hydroxymethanesulphinate, which has absorption maxima at 206 and 225 nm and can therefore be detected using a UV absorbance detector. The dithionite anion also shows a strong UV absorption (maxima near 200 and 320 nm [19,20], but its extreme sensitivity to oxygen in solution prevented its direct chromatographic separation and UV detection. However, Stutts [12] reported the detection of $S_2O_4^{2-}$ by ion chromatography using a UV detector operating at 254 nm, although $S_2O_4^{2-}$ shows an absorption minimum near 260 nm. He added sulphite to the eluent to prevent autoxidation of the dithionite. However, Dixon [20] has demonstrated that dithionite reacts much faster with molecular oxygen than sulphite. Therefore, the use of sulphite as an antioxidant may remove the oxygen dissolved in the eluent, but oxygen diffusing into the system during sample handling will first oxidize $S_2O_4^{2-}$ rather then SO_3^{2-}. We therefore consider that our technique of immediate derivatization of dithionite and its indirect detection as sulphinate is superior. Not only is the sample handling simpler, but also the detection limit of 0.5 mg l^{-1} (0.5 ppm) is much lower than the 10 ppm reported for Stutt's method [12].

The separation of $S_2O_4^{2-}$ from other sulphur oxyanions by ion-pair chromatography reported by Weiss and Göbl [21] is in error as the peak assigned to dithionite was in fact due to sulphate [22].

ACKNOWLEDGEMENTS

We are grateful to Angela Albertsen for advice and the measurement of UV spectra. This work was supported by the Deutsche Forschungsgemeinschaft and by BASF.

REFERENCES

1 J. Buschmann, T. Koritsanszky, P. Luger, H. Schmidt and R. Steudel, *J. Phys. Chem.*, (1992) in press.
2 Ullmanns Encyklopädie der Technischen Chemie, Part 21, *Verlag Chemie, Weinheim*, 4th ed., 1982, p. 109.
3 L. Szekeres, *Talanta*, 21 (1974) 1.
4 L. V. Haff, in J. H. Karchmer (Editor), *The Analytical Chemistry of Sulfur and Its Compounds, Part I*, Wiley, New York, 1970, p. 244.
5 V. Cermák and M. Smutek, *Collect Czech. Chem. Commun.*, 40 (1975) 3241.
6 J. P. Danehy and Ch. W. Zubritzsky, III, *Anal. Chem.*, 46 (1974) 391.
7 R. Wollak, *Fresenius' Z. Anal. Chem.*, 80 (1930) 1.
8 A. Kurtenacker, *Analytische Chemie der Sauerstoffsäuren des Schwefels*, Enke-Verlag, Stuttgart, 1938, p. 166.
9 M. Wayman and W. J. Lem, *Can. J. Chem.*, 48 (1972) 782.
10 B. Meyer, M. Ospina and L. P. Peter, *Anal. Chim. Acta*, 117 (1980) 301.
11 Ch. W. Scaife and R. G. Wilkins, *Inorg. Chem.*, 19 (1980) 3244.
12 K. J. Stutts, *Anal. Chem.*, 59 (1987) 543.
13 R. Steudel and G. Holdt, *J. Chromatogr.*, 361 (1986) 379.
14 R. Steudel, G. Holdt and T. Göbel, *J. Chromatogr.*, 475 (1989) 442.
15 R. Steudel, A. Albertsen, *J. Chromatogr.*, 606 (1992) 260.
16 A. Albertsen, personal communication.
17 F. Fehér, in G. Brauer, *Handbuch der Präparativen Anorganischen Chemie, Part I*, Enke-Verlag, Stuttgart, 2nd ed., 1975, p. 397.
18 R. G. Rinker, S. Lynn, D. M. Mason and W. H. Corcoran, *Ind. Eng. Chem., Fundam.*, 4 (1965) 282.
19 S. M. Lough and J. W. McDonald, *Inorg. Chem.*, 26 (1987) 2024.
20 M. Dixon, *Biochim. Biophys. Acta*, 226 (1971) 241.
21 J. Weiss and M. Göbl, *Fresenius' Z. Anal. Chem.*, 320 (1985) 439.
22 J. Weiss, personal communication.

Journal of Chromatography, 623 (1992) 178–181
Elsevier Science Publishers B.V., Amsterdam

CHROM. 24 517

Short Communication

Dispersion and selectivity indices of *n*-alkyl- and 1-(alkyl)alkylbenzenes

J. K. Haken

Department of Polymer Science, University of New South Wales, P.O. Box 1, Kensington, NSW 2033 (Australia)

(First received June 9th, 1992; revised manuscript received July 21st, 1992)

ABSTRACT

The dispersion and selectivity indices of a series of *n*-alkyl- and 1-(alkyl)$_m$(alkyl)$_n$benzenes were determined using retention index values determined on a non-polar (DB-1) and a polar (DB-wax) fused-silica capillary column. The effect of the individual groups and the multiple alkyl substituents and their position on the alkyl chain are discussed in terms of the relevant polar interactions.

INTRODUCTION

The effect of the solute–solvent interactions in chromatography on the retention of a substance in chromatography is conveniently determined as the retention index value, this being a summation of both non-polar and polar forces, moderated by steric factors. Evans *et al.* [1] have expressed the retention index (I) as the sum of two factors:

$$I = I_m + I^*$$

where I_m the dispersion index is defined as the retention index of a hypothetical *n*-alkane having the same molecular mass as the solute and I^* is the selectivity index, which reflects the combined effects of molecular shape and functionality.

Since an *n*-alkane has a molecular formula of C_iH_{2i+2} or $(CH_2)_i + 2H$ its molecular mass is $m = 14.026i + 2.016$. Therefore I_m can be calculated from:

$$I_m = \frac{m - 2.016}{0.14026}$$

where m is the molecular mass of the solute.

The scheme has been applied to a study of the homologous carboxyl and carboxyl compounds [2,3], alkyl, chlorinated and alkenyl benzoate esters [4], *n*-alkylbenzenes [5] and chlorinated derivatives of cyclohexane, benzene and anisole [6]. This paper extends the analyses of *n*-alkylbenzenes by the use of a wider range of alkyl chain lengths than previously reported [5] and includes homologous branched chain alkylbenzenes.

DATA

The retention data used in this paper are reproduced from work reported by Peng *et al.* [7] who used Hewlett-Packard Model 5890 and 5880 A gas chromatographs, equipped with thermal conductivity detectors using non-polar and polar fused-silica

Correspondence to: Dr. J. K. Haken, Department of Polymer Science, University of New South Wales, P.O. Box 1, Kensington, NSW 2033, Australia.

0021-9673/92/$05.00

capillary columns (30 m × 0.53 mm I.D., film thickness 1.0 μm of DB-wax and 1.5 μm of DB-1 (J. & W. Scientific, Folsom, CA, USA). The temperature was linearly programmed, the initial oven temperature of 40°C was held for 4 min and then increased at a rate of 8°C/min to 280°C for DB-1 and to 200°C for the DB-wax column. The maximum oven temperature was maintained for 20 min. The retention index values were calculated using the equation of Van der Dool and Kratz [8].

RESULTS

Table I shows retention data of C_1–C_7 *n*-alkylbenzenes determined by Engewald *et al.* [9] on packed OV-1 and UCON LB550 columns and similar data of C_1–C_{13} *n*-alkylbenzenes determined by Peng *et al.* [7] on capillary columns coated with a comparable dimethylsiloxane and DB-wax. The earlier values on the OV-1 column are essentially identical with those of Peng *et al.* [7] indicating that the works should be generally comparable. With C_1–C_7 *n*-alkylbenzenes it was shown that the value of the selectivity indices I^* gradually decreased indicating a reduction in polar character as the alkyl chain length increased. With the longer chain length homologues the trend is reversed and the values increase due evidently to alteration of the configuration of the alkyl chain.

This effect was not as expected or as observed in the earlier works [4–6] where the I^* values tended to approach a constant value. However, this work differs from the earlier studies in that a much wider range of homologues was considered. A variation in the trend of properties of homologues which pass through a minimum is well known with many systems. One of the earliest studies of homologue properties considers the polyalkyl acrylates and the polyalkyl methacrylates. The brittle point and the hardness of the first eight *n*-alkyl acrylates and the first twelve *n*-alkyl methacrylates follow a linear function with the logarithm of the carbon number of the alkyl groups but with increased alkyl chain length the relationship does not continue as the values dramatically alter and the previous trend is reversed [10]. The systems which find considerable

TABLE I

RETENTION (I), DISPERSION (I_m) AND SELECTIVITY (I^*) INDICES OF *n*-ALKYLBENZENES

n-Alkylbenzenes	I_m	OV-100			DB-1			LB550X			DB-wax		
		I	I^*	$I_C^* - I_B^{*a}$	I	I^*	$I_C^* - I_B^*$	I	I^*	$I_C^* - I_B^*$	I	I^*	$I_C^* - I_B^*$
Benzene	542	664	122		654	112		759	217		947	405	
Toluene	642	767	125	3	764	122	10	862	220	3	1051	409	4
Ethylbenzene	742	859	117	−5	858	116	4	950	208	−9	1129	382	−18
n-Propylbenzene	842	950	108	−14	945	103	−9	1037	185	−22	1206	364	−41
n-Butylbenzene	942	1047	105	−17	1047	105	−7	1134	192	−25	1306	364	−41
n-Pentylbenzene	1042	1146	104	−18	–	–	–	1233	191	−26	–	–	–
n-Hexylbenzene	1142	1244	102		1254	112	0	1332	190	−27	1515	373	−32
n-Heptylbenzene	1242	1342	100		1348	106	−6				1611	369	−36
n-Octylbenzene	1342				1456	114	2				1715	373	−32
n-Nonylbenzene	1442				1560	118	6				1821	379	−26
n-Decylbenzene	1542				1664	122	10				1928	386	−19
n-Dodecylbenzene	1742				1870	128	16				2141	399	−6
n-Tridecylbenzene	1842				1958	136	24				2265	423	18

[a] $I_C^* = I^*_{\text{compound}}$; $I_B^* = I^*_{\text{benzene}}$.

TABLE II

RETENTION (I), DISPERSION (I_m) AND SELECTIVITY (I^*) INDICES OF 1-(ALKYL)ALKYLBENZENES

Compound	I_m	DB-1			DB-wax		
		I	I^*	$I_C^* - I_B^*$	I	I^*	$I_C^* - I_B^*$
Benzene, (1-butylhexyl)	1542	1526	−16	−128	1729	187	−30
(1-propylheptyl)	1542	1534	−8	−120	1743	201	−16
(1-ethyloctyl)	1542	1553	11	−101	1767	225	−2
(1-methylnonyl)	1542	1588	46	−66	1833	291	74
n-decyl	1542	1664	122	10	1928	306	169
(1-pentylhexyl)	1642	1620	−22	−134	1820	178	−39
(1-butylheptyl)	1642	1626	−16	−128	1828	186	−31
(1-propyloctyl)	1642	1636	−6	−118	1843	201	−16
(1-ethylnonyl)	1642	1656	14	−98	1873	231	14
(1-methyldecyl)	1642	1692	50	−62	1933	291	74
(1-pentylheptyl)	1742	1719	−23	−135	1918	176	−41
(1-butyloctyl)	1742	1723	−19	−131	1928	188	−29
(1-propylnonyl)	1742	1735	−7	−119	1943	201	−16
(1-ethyldecyl)	1742	1755	13	−99	1972	230	13
(1-methylundecyl)	1742	1791	49	−63	2036	294	77
n-dodecyl	1742	1870	128	16	2140	398	181
(1-pentyloctyl)	1842	1814	−28	−140	2015	173	−44
(1-butylnonyl)	1842	1821	−21	−133	2026	184	−33
(1-propyldecyl)	1842	1836	−9	−121	2046	204	−13
(1-ethylundecyl)	1842	1856	14	−63	2079	237	20
(1-methyldodecyl)	1842	1894	50	−62	2143	301	84
n-tridecyl	1842	1978	164	52	2275	433	216

industrial application have been extensively studied and other physical properties show the same trends [11].

Most of the contribution to the I^* value is due to the aromatic ring, the effect of the alkyl chain may be estimated by subtraction of I^* for benzene. The values decrease due to the reduction in polar forces with increasing chain length then increase as the end of the alkyl chain comes closer to the aromatic ring.

A comparison of the I^* values on the dimethyl polysiloxanes, on UCON LB550X and on DB-wax shows the increasing polar character of the stationary phases. The values of I^* on DB-wax show the same decrease and then an increase as the chain length is increased. The contribution of the alkyl chain similarly varies the negative values showing that the effect is small compared to the contribution of the aromatic ring.

Several examples of the retention of isomers are evident, isopropylbenzene exhibiting a lower retention value than the *n*-alkyl homologue due to the more compact shape, diethylbenzene showing minimally lower values than *n*-alkylbenzene and cyclopropylbenzene and cyclohexylbenzene showing greater retention than the *n*-alkyl isomers due to the increased rigidity of the ring system.

Table II shows retention indices, together with dispersion and selectivity indices of several series of 1-(alkyl)$_m$(alkyl)$_n$benzenes where m varies from 1 to $(n - 1)$ while the value of $m + n$ remains constant.

Movement of a methylene group from the m or long alkyl chain to the short alkyl chain makes the molecule more symmetrical. The more symmetrical isomer exhibits the lower retention. The trend continues with all of the series and the isomer in each case where the two alkyl chains are closest in size has the lowest retention.

The selectivity indices on the polysiloxane station-

ary phase increase as the symmetry of the alkyl chains is reduced, the values showing the greater influence of the aromatic ring as the interference of the aliphatic structure is reduced. The effect is more apparent by subtraction of I^* for benzene from the I^* value of the compound where the polar interactions are reduced as the proximity of the alkyl groups are increased from the aromatic ring. With the DB-wax stationary phase the I^* values of the compounds are greatly enhanced while the values less the contribution doe to the aromatic ring are reduced, the interactions of the aromatic structure and the more polar phase overshadowing the effect of the alkyl substituents.

CONCLUSIONS

The retention of a larger range of alkyl chain lengths of *n*-alkylbenzenes than previously available have been examined. It is evident that while the I^* (selectivity index) values decrease with increased alkyl chain length they then increase as the polar character of the extremity of the chain increases due to its configuration and increasing proximity of the aromatic ring.

With 1-$(alkyl)_m(alkyl)_n$benzenes the selectivity indices increase as the symmetry of the alkyl chains is reduced the values showing the greater influence of the aromatic ring as the interference of the aliphatic structure is reduced. The I^* values show the greater influence of the aromatic ring with the stationary phase of increased polar character.

REFERENCES

1 M. B. Evans, J. K. Haken and T. Toth, *J. Chromatogr.*, 351 (1986) 155.
2 M. B. Evans and J. K. Haken, *J. Chromatogr.*, 471 (1989) 217.
3 W. Feng, *Shiyou Huagong*, 19 (1990) 484.
4 M. B. Evans and J. K. Haken, *J. Chromatogr.*, 462 (1989) 31.
5 J. K. Haken and R. J. Smith, *J. Chromatogr.*, 452 (1988) 31.
6 M. B. Evans and J. K. Haken, *J. Chromatogr.*, 468 (1989) 373.
7 C. T. Peng, R. L. Hau and D. Maltby, *J. Chromatogr.*, 589 (1992) 231.
8 H. Van den Dool and P. D. Kratz, *J. Chromatogr.*, 11 (1963) 463.
9 W. Engewald, I. Topalova, N. Pelsev and C. Dimitrov, *Chromatographia*, 23 (1987) 561.
10 C. Rehberg and C. H. Fisher, *Ind. Eng. Chem.*, 40 (1948) 1429.
11 E. H. Riddle, *Monomeric Acrylic Esters*, Reinhold, New York, 1954.

Journal of Chromatography, 623 (1992) 182–185
Elsevier Science Publishers B.V., Amsterdam

CHROM. 24 392

Short Communication

Gas chromatographic analysis of underivatized phenolic constituents from propolis using an electron-capture detector

R. Christov and V. Bankova

Institute of Organic Chemistry with Centre of Phytochemistry, Bulgarian Academy of Sciences, Acad. G. Bonchev str. bl. 9, 1113 Sofia (Bulgaria)

(First received February 17th, 1992; revised manuscript received June 2nd, 1992)

ABSTRACT

Underivatized phenolic constituents from propolis (flavonoid aglycones, phenolic acids and their esters) were analysed by capillary gas chromatography using an electron-capture detector. The analysis was possible because of the good electron-capture response of these compounds, which belong to the so-called "conjugated electrophores".

INTRODUCTION

Phenolic compounds are widespread in plants and they are important as active ingredients of many phytogenic preparations in cosmetics and medicine [1,2]. Phenolic compounds (flavonoid aglycones, phenolic acids and their esters) are the main components of propolis (bee glue) [3] and are thought to be responsible for its valuable biological activity [4]. Among the various methods used for the separation and analysis of complex mixtures of natural phenolics, such as propolis, capillary gas chromatography (GC) is of major importance due to its sensitivity and resolving power. It is common practice to prepare derivatives of phenolic compounds before GC analysis [methyl or trimethylsilyl (TMS) ethers] and to use flame ionization detection [5]. The derivatization is thought to be necessary to increase the volatility of the phenolic compounds, but it has some disadvantages, especially when flavonoids are to be analysed [5,6]. Some recent reports have shown that under the conditions of pyrolysis GC–mass spectrometry some flavonoid aglycones have been detected [7]. This is an indication that even the underivatized compounds of this type are volatile enough and transmit well through suitable GC columns at 300–350°C without thermal degradation. The main groups of propolis phenolics (flavonoid aglycones, phenolic acids and their esters) are also known to belong to the so-called "conjugated electrofores" which have a good electron-capture response [8] and in these compounds the electron-capture detector might be more sensitive than the flame ionization detector. This was confirmed by experiments to use electron capture for the detection of the TMS derivatives of phenolic

Correspondence to: Dr. R. Christov, Institute of Organic Chemistry with Centre of Phytochemistry, Bulgarian Academy of Sciences, Acad. G. Bonchev str. bl. 9, 1113 Sofia, Bulgaria.

0021-9673/92/$05.00

compounds. For this reason we tried to determine if underivatized phenolic compounds could be determined by capillary GC using an electron-capture detector.

EXPERIMENTAL

The flavonoids pinocembrin (**2**), tectochrysin (**3**) and galangin (**5**) were isolated from propolis as described by Bankova *et al.* [9]. The methodology of β-phenylethyl caffeate (**6**) synthesis has been described by Bankova [10]. Caffeic acid (**1**) was purchased from Merck and chrysin (**4**) from Roth. Propolis was collected in south Bulgaria near Plovdiv.

Extraction of propolis

Propolis (1 g) was grated after cooling and refluxed with 15 ml of methanol for 1 h. The hot extract was filtered, diluted with water and extracted successively with light petroleum (b.p. 40–60°C) (3 ×) and diethyl ether (3 ×). The ether extracts were combined and evaporated to dryness. This extract (1 mg) was dissolved in 100 μl of acetone, and 1–2 μl of this solution were injected into the gas chromatograph.

Trimethylsilylation

A 1 mg mass of the model mixture or of the ether extract of propolis was silylated with 50 μl of N,O-*bis*(trimethylsilyl)trifluoroacetamide at 65°C for 30 min; 1–2 μl of the solution was injected into the gas chromatograph.

Gas chromatography

GC analysis was carried out on a Perkin-Elmer 8700 instrument. The separation was accomplished on a 9 m × 0.25 mm I.D. SE-54 fused-silica capillary column with a film thickness of 0.25 μm. The linear velocity of the nitrogen carrier gas was 9 cm s^{-1} (split ratio 1:25). The temperature programme was as follows: 80–280°C, rate 20°C min^{-1}; 280–300°C, rate 2°C min^{-1}, with a 10-min hold at 300°C. The injector temperature was 320°C and the detector temperature was 350°C. At the end of the column the gas flow was split in a ratio of 1:1 using two 10 cm × 0.25 mm, 0.25 μm film thickness SE-54 capillaries, the first of them going into the flame ionization detector and the other into the electron-capture detector.

RESULTS AND DISCUSSION

Experiments were carried out to see if the TMS ethers of propolis phenolics have a significant electron-capture response. In these experiments a model mixture of representatives of the three main groups of propolis phenolics (caffeic acid, **1**; flavonoid aglycones pinocembrin, **2**; galangin, **5**; and the ester β-phenylethyl caffeate **6**) and propolis extract were used. At the end of the column both detectors were run simultaneously. It is shown that the electron-capture response was about one order of magnitude higher than the flame ionization response (Fig. 1). When the injector temperature was increased (280–320°C), higher responses were observed for both detectors because of the increasing vapour pressure of the compounds analysed. An increase in the detector temperature (320–350°C) resulted in a lower electron-capture response (15–40% for the different compounds). This is an indication that the electron-capture process in this instance occurs in a way which represents an undissociative attachment producing a stable negative molecular ion [8]. The high electron-capture response of the conjugated electrophores (silylated flavonoids and cinnamic acid derivatives) encouraged the analysis of the low-volatile underivatized compounds by capillary GC with electron-capture detection. The same column was used for the separation of derivatized and underivatized propolis phenolic components (caffeic acid, **1**; pinocembrin, **2**; tectochrysin, **3**; chrysin, **4**; galangin, **5**; and β-phenylethyl caffeate, **6**). A satisfactory resolution (not the optimum solution) of the underivatized compounds was achieved under the conditions used for the analysis of the TMS ethers, so these conditions were used for the comparison study (Fig. 2).

The injector temperature was 320°C; when it was increased to 350°C, only a slight increase in the relative areas of the peaks with the longest retention times (chrysin **4** and galangin **5**) was observed. The percentage of caffeic acid **1** (retention time 4.5 min) in these samples was low (less than 1%) [11] and was below the limit of detection. It is interesting to note that when underivatized propolis phenolic components were analysed using the two detection methods simultaneously, only the largest peaks pinocembrin and galangin, were satisfactorily detected by flame ionization detection at an acceptable signal-to-noise ratio.

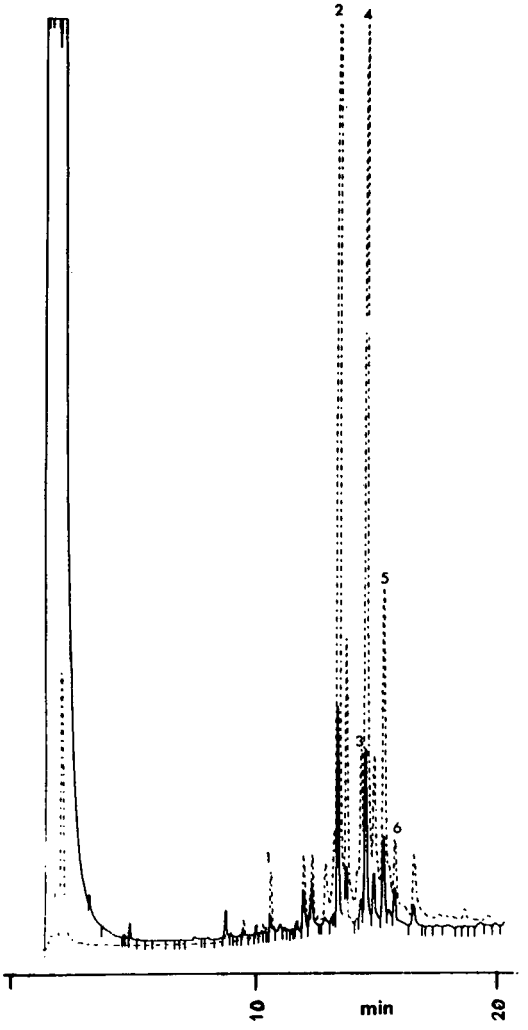

Fig. 1. Capillary gas chromatogram of TMS ethers of propolis phenolic constituents. For GC conditions, see under Experimental. Peaks: **1** = caffeic acid, **2** = pinocembrin, **3** = tectochrysin, **4** = chrysin, **5** = galangin, **6** = β-phenylethyl caffeate. (———) Flame ionization response; (----) electron-capture.

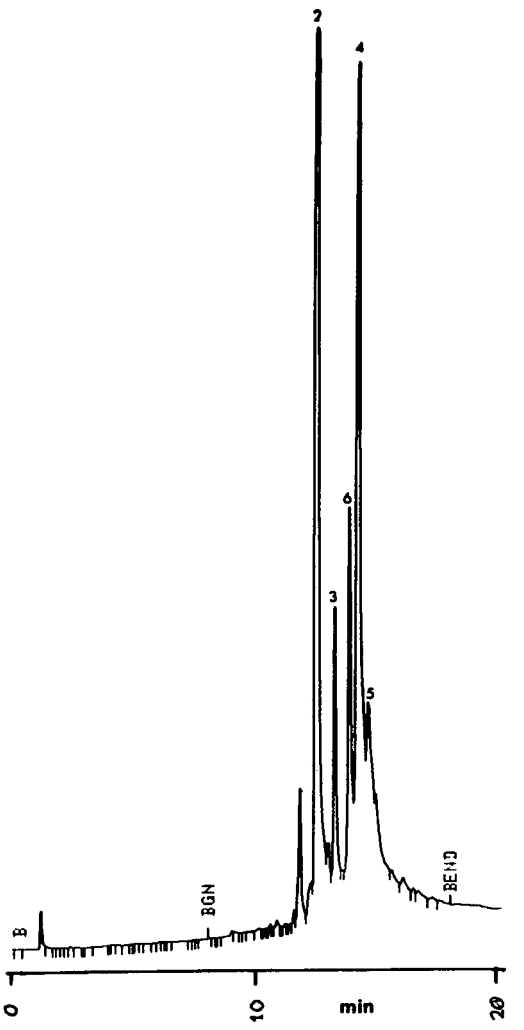

Fig. 2. Capillary gas chromatogram of underivatized propolis phenolic constituents using electron-capture detection. For GC conditions, see under Experimental. For peak identification, see Fig. 1.

To the best of our knowledge this is the first analysis of underivatized flavonoid aglycones by capillary GC. It was possible because of the good electron-capture response of these compounds. The method proposed allows the rapid qualitative analysis of the main biologically active components of propolis [12]. The good reproducibility of the peak areas is an indication that the method could also be used for the quantitative analysis of this valuable natural product.

ACKNOWLEDGEMENT

The authors are grateful to the National Foundation for Science (Contract No. X-45) for the partial support of this work.

REFERENCES

1 E. E. Conn, *The Biochemistry of Plants*, Vol. 7, Academic Press, New York, 1981, p. 425.

2 J. W. McClure, in J. Harborne, T. J. Mabry and H. Mabry (Editors), *The Flavonoids*, Chapmann & Hall, London, 1975, Ch. 18, p. 970.
3 P. Walker and E. Crane, *Apidologie*, 18 (1987) 327.
4 E. Ghisalberty, *Bee World*, 60 (1979) 59.
5 C. S. Creaser, M. R. Koupai-Abyazani and G. R. Stephenson, *J. Chromatogr.*, 478 (1989) 415.
6 W. Greenaway, T. Scaysbrook and F. R. Whatley, *Proc. R. Soc. London B* 232 (1987) 249.
7 H.-R. Schulten, N. Simmleit and R. Mueller, *Anal. Chem.*, 61 (1989) 221.
8 K. Peltonen, *LC · GC Int.*, 3 (1990) 52.
9 V. Bankova, S. Popov and N. Marekov, *J. Nat. Prod.*, 46 (1983) 471.
10 V. Bankova, *J. Nat. Prod.*, 52 (1990) 821.
11 V. Bankova, R. Christov, G. Stoev, S. Popov, *J. Chromatogr.*, in press.
12 V. Bankova, A. Kuyumgiev, A. Ignatova, Al. Dyulgerov, O. Pyreb, Z. Zamyansan and S. Popov, in R. Vlahov (Editor), *Proc. Int. Conf. Chem. Biotechnol. Biol. Active Nat. Prod., September 18–23, 1989, Varna*, Vol. 2, Bulgarian Academy of Sciences, Sofia, 1989, p. 239.

Journal of Chromatography, 623 (1992) 186–190
Elsevier Science Publishers B.V., Amsterdam

CHROM. 24 492

Short Communication

Analysis of legume oligosaccharides by high-resolution gas chromatography

Apostolos I. Karoutis and Robert T. Tyler

Food Processing Research Laboratory, Department of Applied Microbiology and Food Science, University of Saskatchewan, Saskatoon, Saskatchewan, S7N 0W0 (Canada)

George P. Slater

Plant Biotechnology Institute, National Research Council of Canada, 110 Gymnasium Place, Saskatoon, Saskatchewan, S7N 0W9 (Canada)

(First received February 27th, 1992; revised manuscript received July 3rd, 1992)

ABSTRACT

The suitability of high-resolution gas chromatography (HGRC) for the analysis of the raffinose family oligosaccharides (raffinose, stachyose, verbascose) was investigated. Aqueous methanol (80%) extracts of pea flour were dried and derivatized with either trimethylimidazole or N-methyl-bis(trifluoroacetamide). Separation of the sugar derivatives was achieved uitilizing a 10-m DB5-60W capillary column. The effects of carrier gas (He) flow-rate and split ratio on resolution and reproducibility were studied. HRGC analysis was characterized by excellent resolution and satisfactory reproducibility, and proved to be a rapid, sensitive method for quantitation of oligosaccharides in pea flours.

INTRODUCTION

A well known problem associated with the consumption of legume-based foods is their content of galactose-containing oligosaccharides (raffinose, stachyose, verbascose) at levels that may contribute to the development of flatulence [1]. These α-galactosides escape digestion and absorption in the small intestine due to the absence of α-galactosidase activity and are consequently metabolized by bacteria in the lower intestinal tract, resulting in the production of carbon dioxide and hydrogen.

A variety of chromatographic techniques have been employed for analysis of α-galactosides in legumes subsequent to an initial aqueous or alcoholic extraction and partial purification from non-carbohydrate material. Tanaka *et al.* [2] encountered considerable difficulties in the quantitation of α-galactosides by paper chromatography. The high-performance liquid chromatographic (HPLC) methodology employed to date suffers shortcomings related to peak resolution and detector sensitivity [3,4]. Anion-exchange chromatography at high pH, coupled with pulsed amperometric detection, overcomes the major shortcomings of conventional

Correspondence to: Dr. R. T. Tyler, Food Processing Research Laboratory, Department of Applied Microbiology and Food Science, University of Saskatchewan, Saskatoon, Saskatchewan, S7N 0W0, Canada.

0021-9673/92/$05.00

HPLC for the analysis of carbohydrates [5]. Its application to the analysis of legume oligosaccharides, however, has not yet been reported. Packed-column gas chromatography (GC) was used by Sosulski *et al.* [6] for the analysis of oligosaccharides in eleven legumes. Long retention times and poor reproducibility for larger oligosaccharides were major drawbacks of their methodology.

The aim of this work was to investigate the suitability of HRGC for rapid, quantitative determination of α-galactosides in pea flours.

EXPERIMENTAL

Chromatographic equipment

A Hewlett-Packard 5710A gas chromatograph was equipped with a 10-m DB5-60W (0.32 mm I.D., 0.25 μm film thickness) capillary column, a flame ionization detector (FID) using nitrogen as the make-up gas, and a Hewlett-Packard 3390A integrator. Helium was used as the carrier gas. The injector and detector temperatures were 250 and 300°C, respectively.

Standards

Sorbitol, sucrose, phenyl α-D-glucoside, raffinose and stachyose were purchased from Sigma (St. Louis, MO, USA).

Derivatization reagents

N-Methyl-bis(trifluoroacetamide) (MBTFA) and Tri-Sil Z reagents were purchased from Chromatographic Specialties (Brockville, Canada).

Trifluoroacetylation

Each sugar (0.1–5.0 mg) was dissolved in 0.25 ml pyridine (silylation grade, Chromatographic Specialties) in a reaction vial by shaking and heating at 70°C for 30 min. Derivatization was completed by adding 0.25 ml MBTFA and heating at the same temperature for 15 min. The same trifluoroacetylation procedure was applied to oligosaccharides extracted from pea flour (refer to *Extraction procedure*, below).

Silylation

Each sugar (0.1–5.0 mg) was dissolved in 0.50 ml Tri-Sil Z reagent in a reaction vial by shaking and heating at 70°C for 30 min. The same silylation procedure was applied to oligosaccharides extracted from pea flour (refer to *Extraction procedure*, below).

Pea flour

High protein pea flour (air-classified pea protein concentrate), containing approximately 55% protein, was supplied by Parrheim Foods (Saskatoon, Canada).

Extraction procedure

Extraction of α-galactosides from pea flour was carried out according to the procedure of Sosulski *et al.* [6] with modifications. Pea flour (2.0 g) was homogenized for 2 min in 30 ml 80% aqueous methanol. Samples were then centrifuged at 1000 *g* for 4 min. The supernatant was treated with saturated lead acetate solution (20 drops/5 ml) to precipitate soluble proteins, and clarified using a hydrophobic (0.22-μm) membrane filter (Acrodisc PTFE-Gelman, Montreal, Canada). A 2-ml volume of the filtrate was treated with 2 drops of saturated monopotassium phosphate to remove excess lead and filtered again. Finally, 1 ml of clear filtrate plus 1 ml of phenyl α-D-glucoside solution (1.0 mg/ml in 80% methanol) were evaporated to dryness in a reaction vial at 50°C under nitrogen. Refluxing of pea flour (2.0 g) for 1 h in 30 ml 80% aqueous methanol was an equally effective extraction procedure.

RESULTS AND DISCUSSION

Effect of carrier gas flow-rate on elution profile

As expected, the flow-rate of the carrier gas (He) had a pronounced effect on the elution profiles of the α-galactoside derivatives. Retention times decreased significantly with increasing flow-rates (Fig. 1). The excellent resolution obtained for trimethylsilyl (TMS) derivatives permitted the use of relatively high carrier flows, which markedly shortened analysis times.

MBTFA derivatives exhibited greater volatility than did the corresponding TMS derivatives, which led to considerably shorter retention times (Fig. 2). These findings were in agreement with results obtained earlier by Selosse and Reilly [7] for MBTFA derivatives of several trisaccharides, including raffinose. However, we observed poor resolution between the peaks corresponding to sucrose and

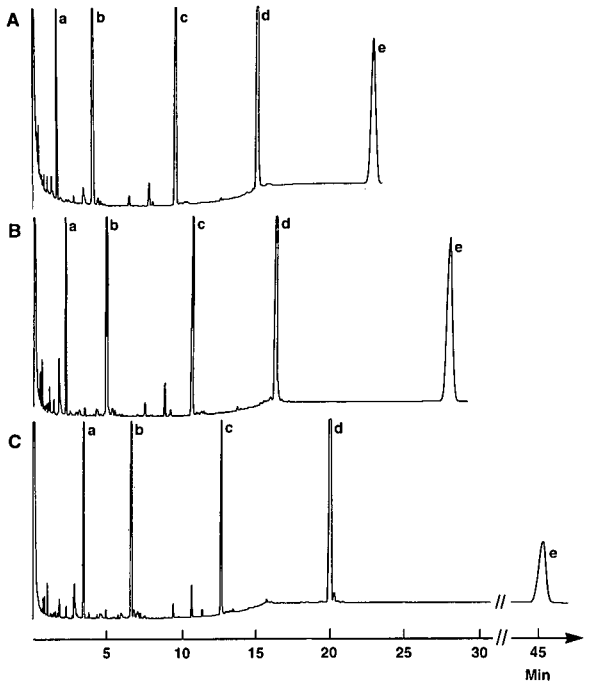

Fig. 1. The effect of carrier gas (He) flow-rate on the elution profiles of TMS derivatives of legume oligosaccharides extracted from air-classified pea protein concentrate. (A) 6.7 ml/min; (B) 3.7 ml/min; (C) 1.6 ml/min. Chromatographic conditions: split ratio 1:50; temperature programming: initial temperature, 188°C, temperature gradient, 8°C/min, final temperature, 316°C, hold time at final temperature, 8–32 min; column: DB5-60W (10 m × 0.32 mm I.D., 0.25 μm film thickness). Components identified: a = phenyl α-D-glucoside; b = sucrose; c = raffinose; d = stachyose; e = verbascose.

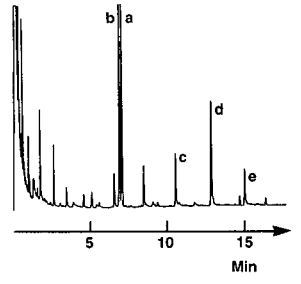

Fig. 2. HRGC analysis of MBTFA derivatives of oligosaccharides extracted from air-classified pea protein concentrate. Chromatographic conditions: carrier (He) flow, 2.7 ml/min; split ratio, 1:100; temperature programming: initial temperature, 80°C, temperature, gradient 8°C/min, final temperature, 250°C; column: DB5-60W (10 m × 0.32 mm I.D., 0.25 μm film thickness). Components identified: a = phenyl α-D-glucoside; b = sucrose; c = raffinose; d = stachyose; e = verbascose.

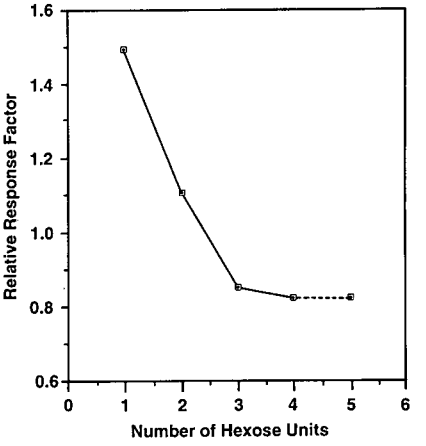

Fig. 3. Curve depicting relative response factors for sorbitol (1 hexose unit), sucrose (2 hexose units), raffinose (3 hexose units), and stachyose (4 hexose units). Phenyl α-D-glucoside was employed as internal standard. Dashed line indicates extrapolation required to obtain a response factor for verbascose (5 hexose units). Flow rate: 6.7 ml/min; split ratio: 1:50.

phenyl α-D-glucoside, the most suitable internal standard identified. At a carrier gas flow of 2.7 ml/min, the retention times for sucrose and phenyl α-D-glucoside were nearly identical at 7.0 and 7.2 min, respectively. Resolution was not improved at carrier gas flows lower than 2.7 ml/min (data not shown).

Quantitation of oligosaccharide TMS derivatives

The relationship between relative response factor (mass basis) and the number of hexose units is shown in Fig. 3 for sorbitol, sucrose, raffinose and stachyose TMS derivatives as determined at a flow-rate of 6.7 ml/min and a split ratio of 1:50. No standard was available for direct determination of a response factor for verbascose. However, extrapolation from the response factor curve indicated that it was very similar to that of stachyose. Quantitation of verbascose was based on this assumption. The marked decrease in relative response for larger oligosaccharides was attributed to discrimination against higher mass/less volatile derivatives in the injector of the chromatograph, and to on-column breakdown of derivatives, particularly at higher column temperatures (larger oligosaccharides). Injector discrimination was particularly evident at higher split ratios, as shown in Fig. 4, where the verbascose peak, in particular, became progressiv-

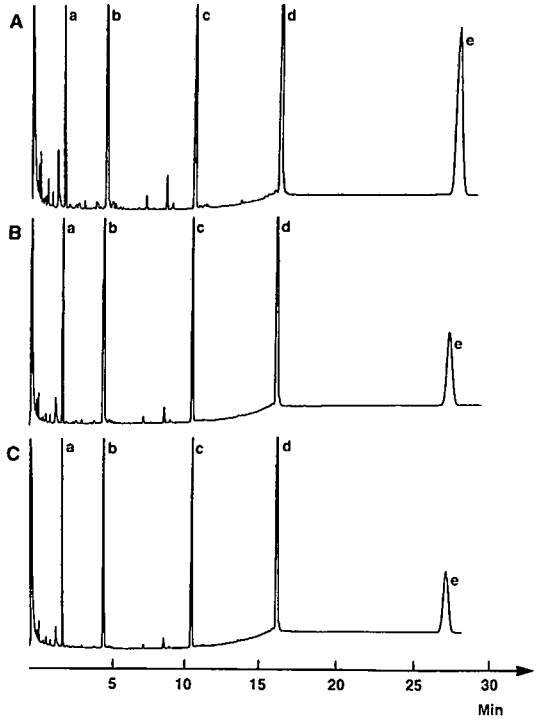

Fig. 4. The effect of split ratio on the elution profiles of TMS derivatives of legume oligosaccharides extracted from air-classified pea protein concentrate. (A) 1:50; (B) 1:100; (C) 1:150. Chromatographic conditions: carrier gas (He) flow-rate, 3.7 ml/min; temperature programming - initial temperature, 188°C, temperature gradient, 8°C/min, final temperature, 316°C, hold time at final temperature, 16 min; column: DB5-60W (10 m × 0.32 mm I.D., 0.25 μm film thickness). Components identified: a = phenyl α-D-glucoside; b = sucrose; c = raffinose; d = stachyose; e = verbascose.

ely smaller relative to other component peaks as the split ratio was increased from 1:50 to 1:150. Sosulski *et al.* [5] reported a similar, but essentially linear in their case, inverse relationship between relative response and mass using packed-column GC methodology.

Reproducibility of analyses

Although TMS derivatives generally gave satisfactory reproducibility at all carrier gas flow-rates (Table I), results were most reproducible at the highest flow-rate tested, 6.7 ml/min of He. Verbascose was an exception, reproducibility of analysis being poorest at 1.6 ml/min and best at 3.7 ml/min. Reproducibility improved (smaller coefficients of variation) with decreasing split ratio at all flow-rates tested (Table I) with the exception of raffinose at 1.6 ml/min and sucrose and stachyose at 3.7 ml/min.

Results using MBTFA as derivatizing agent were poorly reproducible, which we attributed to more severe and variable discrimination at the injector with the more volatile MBTFA derivatives. For example, the coefficients of variation for triplicate analyses of raffinose, stachyose and verbascose were 13, 16 and 25%, respectively, at 2.7 ml/min and a split ratio of 1:50. This was not the case in an earlier packed-column GC study [8] using MBTFA derivatives, where reproducibility for raffinose and stachyose was satisfactory.

TABLE I

THE EFFECT OF FLOW-RATE AND SPLIT RATIO ON REPRODUCIBILITY OF ANALYSIS OF α-GALACTOSIDE TMS DERIVATIVES

Flow-rate (ml/min)	Coefficient of variation (%)				Split ratio
	Sucrose	Raffinose	Stachyose	Verbascose	
1.6	2.4	5.8	4.2	10.2	1:50
	2.5	5.9	5.1	11.2	1:100
	2.7	5.7	6.2	11.6	1:150
3.7	2.5	2.2	0.4	2.2	1:50
	4.7	5.3	5.9	3.5	1:100
	4.6	6.1	4.9	7.6	1:150
6.7	1.4	0.8	0.3	5.2	1:50
	2.2	2.9	3.1	7.1	1:100
	2.8	3.1	4.5	8.3	1:150

CONCLUSIONS

The aim of the present study was to establish the efficacy of HRGC as a chromatographic technique for the analysis of legume oligosaccharides (raffinose, stachyose, verbascose). Research was focussed on the effect of analysis parameters such as carrier flow-rate, split ratio and the nature of the derivatizing agent on peak broadening and resolution, reproducibility, and analysis time.

TMS derivatives gave satisfactory results over a wide range of carrier gas (He) flow-rates (1.6–6.7 ml/min) with the fastest analysis (retention time of 23 min for verbascose, the largest oligosaccharide) and the least peak broadening at 6.7 ml/min. Resolution was excellent at all flow-rates and split ratios investigated. Reproducibility, in general, was satisfactory, with the best results at a flow-rate of 3.7 ml/min and a split ratio of 1:50 (coefficients of variation were 2.5% or less for all oligosaccharides). The more volatile MBTFA derivatives gave much lower elution temperatures and shorter analysis times than did TMS derivatives, but discrimination during splitting of the sample in the injector of the gas chromatograph caused serious reproducibility problems.

In summary, HRGC proved to be a rapid, sensitive method for quantitation of oligosaccharides in pea flour. Compared to packed-column GC, HRGC offered superior resolution and reproducibility, shorter analysis times and reduced peak broadening for larger oligosaccharides, verbascose in particular.

REFERENCES

1 J. J. Rackis, in A. Jeans and J. Hodge (Editors), *Physiological Effects of Food Carbohydrates* (*ACS Symposium Series*, No. 15), American Chemical Society, Washington, DC, 1975, p. 207.
2 M. Tanaka, D. Thananunkul, T.-C. Lee and C. O. Chichester, *J. Food Sci.*, 40 (1975) 1087.
3 I. M. Knudsen, *J. Sci. Food Agric.*, 37 (1986) 560.
4 B. Quemener, *J. Agric. Food Chem.*, 36 (1988) 754.
5 J. D. Olechno, S. R. Carter, W. T. Edwards and D. G. Gillen, *Am. Biotechnol. Lab.*, 5 (1987) 38.
6 F. W. Sosulski, L. Elkowicz and R. D. Reichert, *J. Food Sci.*, 47 (1982) 498.
7 E. J.-M. Selosse and P. J. Reilly, *J. Chromatogr.*, 328 (1985) 253.
8 P. Englmaier, *Carbohydr. Res.*, 144 (1985) 177.

Journal of Chromatography, 623 (1992) 191–195
Elsevier Science Publishers B.V., Amsterdam

CHROM. 24 456

Short Communication

Improved determination of brofaromine by capillary gas chromatography and by utilization of a multi-purpose injector

P. H. Degen, F. Risser and J. W. Lauber

Pharma Research and Development, Pharmaceuticals Division, Ciba-Geigy Ltd., Basle (Switzerland)

(First received January 31st, 1992; revised manuscript received June 30th, 1992)

ABSTRACT

A significantly improved method for the determination of the monoamine oxidase A inhibitor brofaromine hydrochloride and its major metabolite is described. A newly constructed multi-purpose injector for capillary column gas chromatography (cGC) was utilised. The injector can be used either in split/splitless or hot or cold quasi-on-column mode. For this purpose it was used in the hot on-column mode. The injector is equipped with a septum cooling device, allowing injection temperatures of up to 400°C without septum glueing. The utilization of cGC with the new highly thermally stable injector showed improvements over the standard GC procedure in terms of retention time stability and ease of operation.

INTRODUCTION

A procedure for the determination of brofaromine, a monoamine oxidase A inhibitor (MAOI), and its major metabolite, O-desmethylbrofaromine (Fig. 1), by packed-column gas chromatography (GC) was reported in a previous paper [1]. The method is based on liquid–liquid extraction followed by acylation with heptafluorobutyric anhydride (HFBA) and GC using an OV-17 column. Using packed columns, the chromatography of the major metabolite required time-consuming conditioning, to overcome adsorption losses, by repeated injections of O-desmethylbrofaromine. The utilization of capillary GC (cGC) columns in combination with automated quasi-on-column injection (injection into a precolumn or retention gap) was achieved by the use of a newly designed multi-purpose injector, which is based on the Grob injector [2].

The technique of hot on-column injections has been discussed before but has not often been utilized owing to a lack of adequate hardware [3,4]. The advantages of this injector are its flexibility in its use as a hot or cold quasi-on-column or as a split/splitless injector and especially its homogeneous temperature field over the entire injector. To avoid cold parts or spots at the splitter outlet and septum purge, these tubings are integrated within the heated block up to the exit valves. In addition, the dead volumes of these tubings are minimized. The problems arising from temperature gradients in the injector have been recognized and discussed in detail by Grob [2]. The temperatures of the top part

Correspondence to: Dr. P. H. Degen, Pharma Research and Development, Pharmaceuticals Division, Ciba-Geigy Ltd., Basle, Switzerland.

0021-9673/92/$05.00

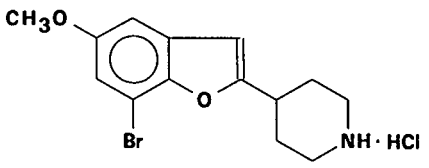

Brofaromine hydrochloride

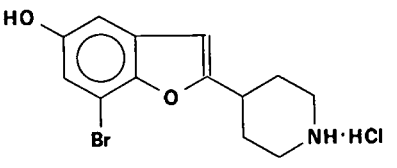

O-desmethyl brofaromine

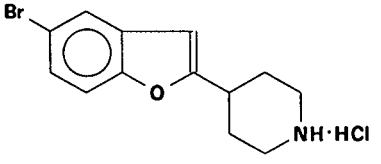

Internal standard

Fig. 1. Structures of brofaromine hydrochloride, O-desmethylbrofaromine hydrochloride and the internal standard.

of commercial injectors are kept relatively low in order to preserve the heat-sensitive septum. It was demonstrated that normalized peak areas of *n*-alkanes (C_{10}–C_{44}) showed the best stability when the top part of the injector was also actively heated. When injector temperatures above 250°C are to be used, an additional intensive septum cooling system is recommended to avoid septum glueing. The septum cooling system allows the utilization of injector temperatures as high as 400°C.

EXPERIMENTAL

Method

The extraction and derivatisation procedure was used as described previously [1]. Briefly, brofaromine [4-(7-bromo-5-methoxy-2-benzofuranyl)piperidine hydrochloride, $C_{14}H_{16}BrNO_2 \cdot HCl$, mol.wt. 346.65], its O-desmethyl metabolite [4-(7-bromo-5-hydroxy-2-benzofuranyl)piperidine hydrochloride, $C_{13}H_{14}BrNO_2 \cdot HCl$, mol.wt. 332.63] and the internal standard [4-(5-bromo-2-benzofuranyl)piperidine hydrochloride, $C_{13}H_{14}BrNO \cdot HCl$, mol.wt. 316.63] are extracted with diethyl ether–dichloromethane (4:1, v/v) at basic pH. After evaporation of the solvents, the compounds are acylated with HFBA and chromatographed.

Gas chromatographic instrumentation

The GC instrument used was a Carlo Erba MEGA Series Model 5360, equipped with a Model 91 Ciba-Geigy injector (Mechanical Workshop, Ciba-Geigy, Basle, Switzerland) and a A200S autosampler (Carlo Erba, Milan, Italy, for Europe and Leap Technology, Chapel Hill, NC, USA, for the USA). Data evaluation was performed with a Merck–Hitachi D-2500 MEGA integrator.

The Ciba-Geigy injector, tooled from stainless steel, can be operated either in the split/splitless or in the cold or hot quasi-on-column injection mode. All three injection techniques can be automated with the A200S autosampler. For application with brofaromine, the injector was used in the hot quasi-on-column mode with the splitter open, splitting ratio 1:20, during the entire analysis. Using hot on-column injection, the peak shape, the limit of detection and the quantitative reproducibility of the chromatograms were optimal.

Sectional views of the injector in the three modes are shown in Fig. 2. The diagrams show the possible

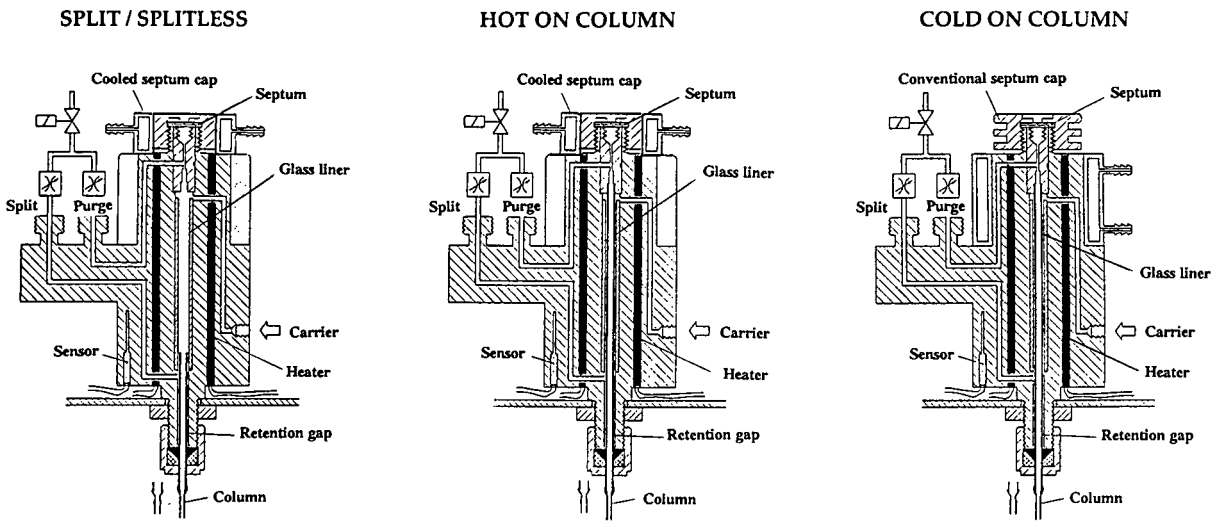

Fig. 2. Sectional views of the Ciba-Geigy Model 91 detector. Split/splitless mode and hot on-column mode: septum cooling device installed. Cold on-column mode: conventional septum cap installed.

different configurations of the injector, *e.g.*, if the injector is to be used for cold on-column, injections exclusively, no septum cooling cap would be necessary. For the split/splitless mode, the column ending is positioned just above the splitter outlet connection. For both other modes, the column ending is positioned at the very top of the injector below the septum purge exit.

Advantages of this injector over existing models are the temperature stability over the entire length of the injector, the placement of all gas lines within the uniformely heated injector body and its versatility. In addition, it can be fitted to most commercial gas chromatographs.

Column

GC analyses were performed with a 50 m × 0.3 mm I.D. glass capillary column [Duran-50 glass tubing obtained from Schott Ruhrglas, Bayreuth, Germany, drawn on a GCDM Model 03 instrument (Brechbühler, Schlieren, Switzerland)]. The capillaries were pretreated, coated and immobilized with SE-54, chemically bonded and cross-linked as described by Grob [5].

For autosampler injections an additional 18 cm × 0.5 mm I.D. glass tube was mounted at the start of the column. This was connected in front of the analytical column with a 2-cm length of fused silica (without polyimide) between the additional retention gap and the column, to prevent collapse during the connection process. The dimensions of the glass tubing allow the use of commercially available microsyringes (0.5 mm O.D. needle, *e.g.*, Hamilton 701N).

The column was used with 3-m retention gaps at both ends. With such columns, the direction of the gas flow is not critical, *i.e.*, the column may be installed either way. The loss of resolution due to the retention gap at the end of the column was insignificant for this application. The carrier gas was hydrogen with a precolumn pressure of 100 kPa.

Conditions

The injector temperature was 250°C and the detector temperature was 250°C. The column oven was heated using a temperature programme as follows: 120–240°C at 15°C/min, 240–290°C at 2.5°C/min, final temperature 290°C maintained for 6 min before a new cycle. The retention times of the derivatives under these conditions were as follows: O-desmethyl metabolite, 16.03 min; brofaromine, 18.05 min; and internal standard, 19.60 min.

RESULTS AND DISCUSSION

Calibration

Calibration graphs were prepared by analysis of plasma samples spiked with brofaromine hydrochloride and O-desmethylbrofaromine hydrochloride (metabolite). The peak-height ratios (brofaromine and metabolite/internal standard) were then plotted against original concentrations and analysed by quadratic least-squares regression analysis ($y = a + bx + cx^2$). The parameters obtained are given in Table I.

Chromatograms of blank matrix extracts and extracts of plasma samples spiked with brofaromine, metabolite and internal standard are given in Fig. 3.

TABLE I

CALIBRATION CURVES

Parameter[a]	Brofaromine	Metabolite
Range	14–588 pmol	15–302 pmol
a	0.0036	0.0065
b	0.0030	0.0040
c	−0.0000009	−0.0000002
R	0.9999	0.9997
S_y	0.0101	0.0092

[a] R = Correlation coefficient; S_y = estimated standard deviation.

Method validation

The method was validated as follows. Blank human plasma samples were spiked with brofaromine hydrochloride (14–588 nmol/l) and with O-desmethylbrofaromine hydrochloride (10–270 nmol/l) and analysed as described. The chromatograms were evaluated and the given − found results were subjected to a linear least-squares regression analysis ($y = a + bx$). The parameters obtained are given in Table II.

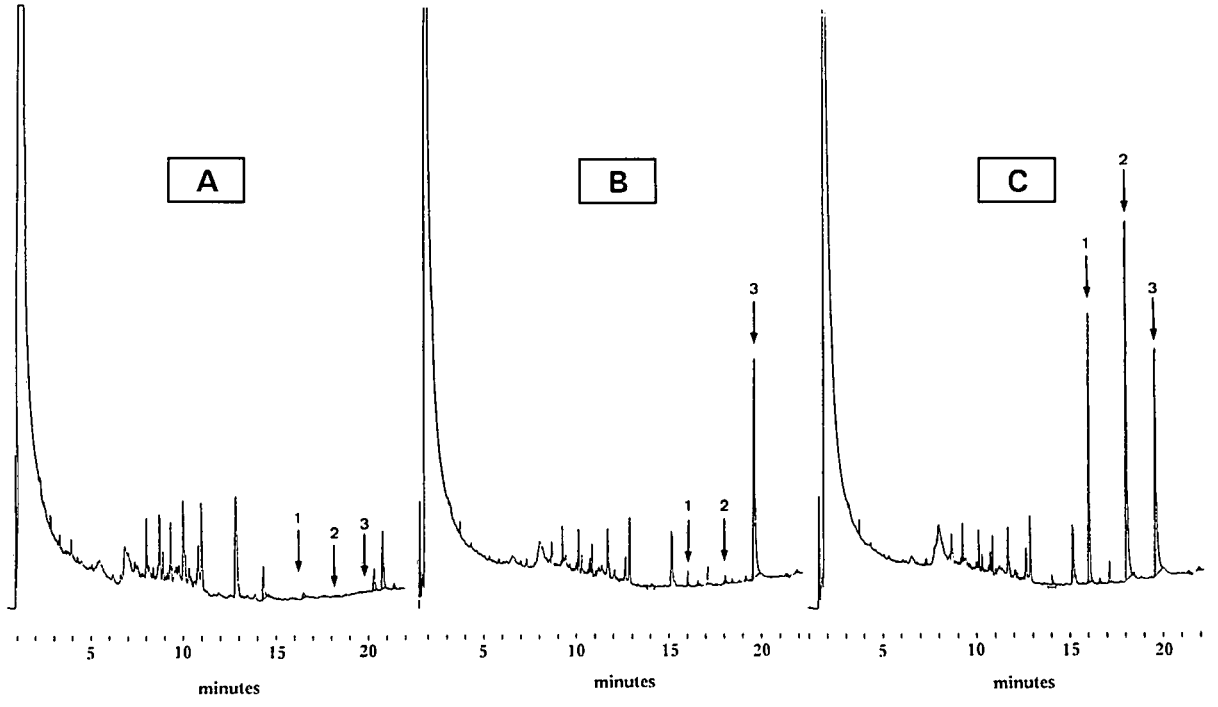

Fig. 3. Chromatograms of plasma extracts: (A) blank human plasma (1 ml); (B) human plasma (1 ml) spiked with brofaromine · HCl (14 nmol/l), O-desmethyl metabolite (15 nmol/l) and internal standard (1.26 μmol/l); (C) human plasma (1 ml) spiked with brofaromine · HCl (577 nmol/l), O-desmethyl metabolite (300 nmol/l) and internal standard (1.26 μmol/l). 1 = O-Desmethyl metabolite; 2 = brofaromine; 3 = internal standard.

TABLE II

METHOD VALIDATION

Parameter[a]	Brofaromine	Metabolite
Range	14–588 nmol/l	10–270 nmol/l
a	3.8088	−0.4094
b	1.0136	1.0261
R	0.9986	0.9953
S_y	10.3289	9.7682

[a] R = Correlation coefficient; S_y = estimated standard deviation.

Reproducibility of the retention times

In a pharmacokinetic study, extracts of 58 different plasma samples (varying concentrations over the entire range) were injected into the same column over a period of 3 weeks. The relative standard deviations were 0.05, 0.07 and 0.07% for O-desmethyl metabolite, brofaromine and the internal standard, respectively. This high reproducibility of $<0.1\%$ was probably achieved owing to the high temperature stability of the injector. With conventional split/splitless injectors the reproducibilities of retention times and the determinations were unsatisfactory.

CONCLUSIONS

The utilization of cGC and a newly constructed multi-purpose injector resulted in a dramatic improvement in the determination of brofaromine and its major metabolite in plasma. The injector has a high temperature stability, resulting in excellent reproducibility of the chromatograms. In addition, the injector may easily be used for other types of cGC injection techniques and can also be fitted to most commercial gas chromatographs.

ACKNOWLEDGEMENT

Thanks are due to Mr. H. P. Ruedisuehli for the skilful manufacture of the split/splitless, quasi-on-column injector.

REFERENCES

1 W. Schneider, B. Keller and P. H. Degen, *J. Chromatogr.*, 488 (1989) 275–282.
2 K. Grob, *Classical Split and Splitless Injection in Capillary GC*, Hüthig, Heidelberg, 1986.
3 J. V. Hinshaw, Jr., *J. Chromatogr. Sci.*, 25 (1987) 49–55.
4 W. Jennings and M. F. Mehzad, *J. Chromatogr. Sci.*, 24 (1986) 34–40.
5 K. Grob, *Making and Manipulating Capillary Columns for Gas Chromatography*, Hüthig, Heidelberg, 1986.

Journal of Chromatography, 623 (1992) 196–199
Elsevier Science Publishers B.V., Amsterdam

CHROM. 24 502

Short Communication

Determination of quaternary alkaloids from Coptidis Rhizoma by capillary electrophoresis

Ying-Mei Liu and Shuenn-Jyi Sheu

Department of Chemistry, National Taiwan Normal University, Taipei (Taiwan)

(First received May 15th, 1992; revised manuscript received July 14th, 1992)

ABSTRACT

A simple and rapid method for the simultaneous determination of eight quaternary alkaloids (coptisine, berberine, epiberberine, palmatine, columbamine, berberastine, jatrorrhizine and magnoflorine) in coptis rhizome by capillary electrophoresis was developed. A buffer solution composed of 85% 0.1 *M* sodium acetate solution and 15% methanol was found to be the most suitable electrolyte for this separation, whereby the levels of the eight quaternary alkaloids in the crude drug Coptidis Rhizoma could be easily determined.

INTRODUCTION

Coptidis Rhizoma (huang-lien) is a commonly used Chinese herbal drug indicated as a bitter-tasting gastric and intestinal regulative, and is known to contain seven protoberberinium salts (coptisine, berberine, epiberberine, palmatine, columbamine, berberastine and jatrorrhizine) and a quaternary aporphine salt(magnoflorine) (Fig. 1) as its major bioactive components [1–7].

Several methods have been reported for the determination of some of these eight quaternary alkaloids, including thin-layer chromatography [5, 8–12], micellar chromatography [13], electron microscopic analysis [14–16] and high-performance liquid chromatography (HPLC) [17–22]. However, none of these methods is entirely adequate because their accuracy, degree of separation or sensitivity is unsatisfactory and above all their resolution is limited to at the most six [20] (excluding columbamine and magnoflorine; the former was found to overlap with jatrorrhizine) of the eight quaternary alkaloids.

We describe here the development of a simple and rapid method for the simultaneous determination of these eight quaternary alkaloids in samples of crude Coptidis Rhizoma by capillary electrophoresis.

EXPERIMENTAL

Reagents and materials

Berberine chloride was purchased from Sigma (St. Louis, MO, USA), coptisine chloride from Nacalai (Kyoto, Japan) and palmatine chloride from Wako (Osaka, Japan). Sodium acetate was obtained from Osaka (Osaka, Japan) and benzyltriethylammonium chloride from Merck (Darmstadt, Germany). Epiberberine, columbamine, berberastine and jatrorrhizine were isolated from coptis rhizome [7,19]. Magnoflorine was isolated from

Correspondence to: Professor S.-J. Sheu, Department of Chemistry, National Taiwan Normal University, Taipei, Taiwan.

0021-9673/92/$05.00

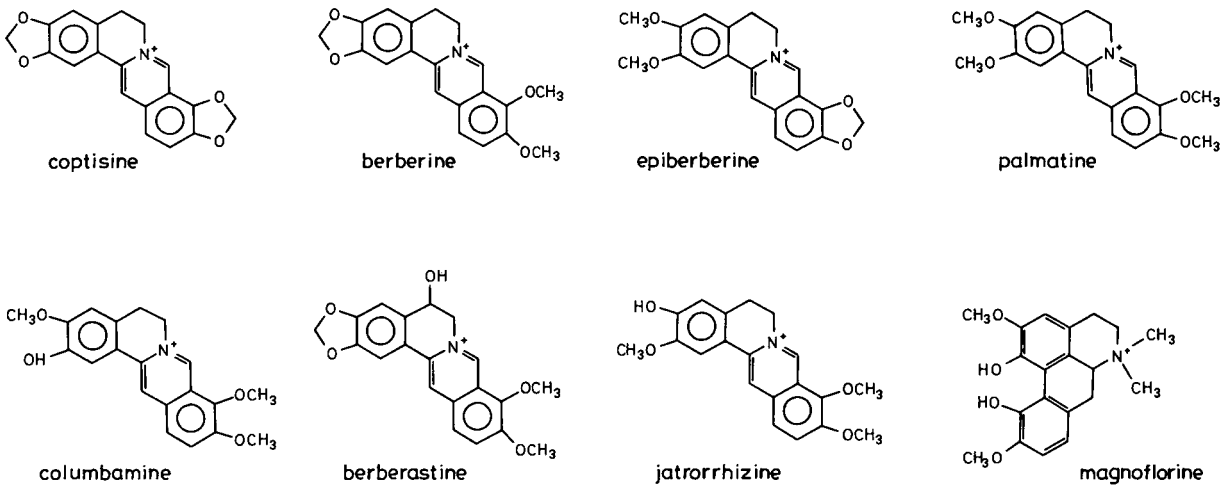

Fig. 1. The molecular structures of the eight alkaloids in Coptidis Rhizoma.

Phellodendri Cortex [23]. Coptidis Rhizoma was purchased from the Chinese herbal market in Taipei (Taiwan).

Preparation of Coptidis Rhizoma extracts

A 0.2-g sample of pulverized Coptidis Rhizoma was extracted with 50% ethanol (7 ml) by stirring at room temperature for 30 min, then centrifuged at 1500 *g* for 10 min. The extraction was repeated three times. The extracts were combined and filtered through a No. 1 filter-paper. After the addition of a 2.5-ml aliquot of internal standard solution (6 mg of benzyltriethylammonium chloride in 1 ml of water), the Coptidis Rhizoma extract was diluted to 25 ml with 50% ethanol. This solution was passed through a 0.45-μm filter and *ca.* 2.4 nl (8-s hydrostatic sampling) of the filtrate was injected into the capillary electrophoresis system directly.

Apparatus and conditions

All analysis were carried out on a Waters Quanta 4000 capillary electrophoresis system equipped with a UV detector set at 254 nm and a 100 cm × 100 μm I.D. uncoated capillary (Millipore, USA) with the detection window placed at 92.5 cm. The conditions were as follows: sampling time, 8 s hydrostatic; run time, 15 min; applied voltage, 25 kV (constant voltage, positive to negative polarity; electroosmotic flow, *ca.* 7.2 cm/min); temperature, 27.5–28.0°C. The electrolyte was a buffer solution consisting of 85% 0.1 *M* sodium acetate solution and 15% methanol. The electrolyte was filtered through a 0.45-μm filter before use.

RESULTS AND DISCUSSION

By eluting with a mixture of acetonitrile and a buffer solution that consisted of 15 ml of acetic acid, 3 g of sodium acetate, 1 g of sodium dodecylsulphate and 0.5 ml of diethylamine in 300 ml of water, we have developed an HPLC method for the separation of the eight quaternary alkaloids [24]. However, there are still some problems: the analysis time is too long, the composition of mobile phase is too complicated, and the retention times of peaks are unstable. Recently, capillary electrophoresis has been applied to the determination of the components of crude drugs [25,26] with good results. Hence, we tried to use it in our analysis.

The eight quaternary alkaloids of Coptidis Rhizoma do not differ much in their molecular masses, and each carries a single positive charge. So, it is necessary to find a counter-ion that can undergo different interactions with the positively charged nitrogen of the alkaloids and can also lead to an effective separation. We tested many negative ions and found that carboxylates gave the best results. At appropriate concentrations, sodium oxalate, sodium citrate and sodium acetate can each give good resolution. However, only sodium acetate can sepa-

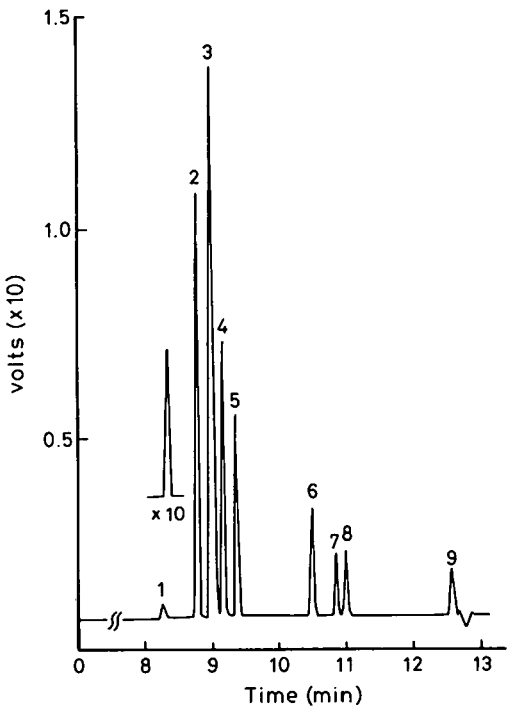

Fig. 2. Capillary electropherogram of a mixture of quaternary alkaloids usually present in Coptidis Rhizoma. Peaks: 1 = internal standard (benzyltriethylammonium chloride), 1.44 ng; 2 = coptisine, 0.56 ng; 3 = berberine, 1.10 ng; 4 = epiberberine, 0.36 ng; 5 = palmatine, 0.29 ng; 6 = columbamine, 0.26 ng; 7 = berberastine, 0.13 ng; 8 = jatrorrhizine, 0.07 ng; 9 = magnoflorine, 0.17 ng.

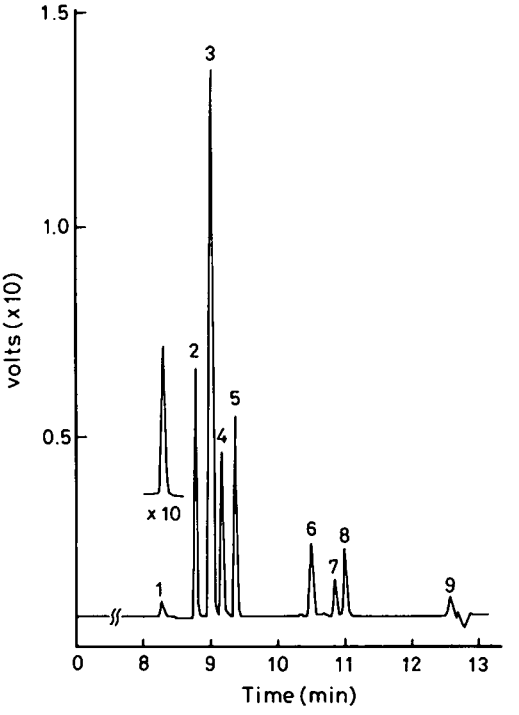

Fig. 3. Capillary electropherogram of the extract of a Coptidis Rhizoma sample. Peaks: 1 = internal standard, 1.44 ng; 2 = coptisine, 0.33 ng; 3 = berberine, 1.08 ng; 4 = epiberberine, 0.21 ng; 5 = palmatine, 0.27 ng; 6 = columbamine, 0.16 ng; 7 = berberastine, 0.09 ng; 8 = jatrorrhizine, 0.07 ng; 9 = magnoflorine, 0.07 ng.

rate the peak of magnoflorine from that of the solvent.

After a series of experiments, it was found that 0.1 *M* sodium acetate could separate all the alkaloids well, especially the coptisine, berberine, epiberberine and palmatine. Lower concentrations of acetate resulted in overlapping of these four components, and higher concentrations caused prolonged retention times and gave a high current. Addition of methanol to the buffer solution made the peaks sharper and produced a better separation. A concentration of 15% methanol was selected: smaller amounts had little effect, and higher amounts retarded the peaks.

An electrolyte containing 85% 0.1 *M* sodium acetate solution and 15% methanol was found to produce the best resolution. Fig. 2 is an electropherogram showing the separation of the eight authentic quaternary alkaloids with the following retention times: 8.3 min, benzyltriethylammonium chloride (internal standard); 8.8 min, coptisine; 9.0 min, berberine; 9.2 min, epiberberine; 9.4 min, palmatine; 10.5 min, columbamine; 10.8 min, berberastine; 11.0 min, jatrorrhizine; 12.6 min, magnoflorine. The measurement of all the constituents can be completed within 13 min. As the ethanol–water extract of Coptidis Rhizoma was injected directly and analysed, the results were as good as those obtained with pure chemical samples without interference, and the analysis could be completed within 13 min, as shown in Fig. 3.

Calibration graphs for quaternary alkaloids

Calibration graphs (peak-area ratio, y, *vs.* concentration, x, mg/ml) were constructed in the range 0.80–0.04 mg/ml for berberine, 0.25–0.02 mg/ml for

coptisine, epiberberine, and palmatine, and 0.15–0.01 mg/ml for columbamine, berberastine, jatrorrhizine and magnoflorine. The regression equations of these curves and their correlation coefficients were calculated as follows:

coptisine $y = 9.26x + 0.01$ ($r = 0.9999$);
berberine $y = 9.78x + 0.14$ ($r = 0.9997$);
epiberberine $y = 10.18x + 0.10$ ($r = 0.9996$);
palmatine $y = 9.81x + 0.09$ ($r = 0.9996$);
columbamine $y = 8.62x + 0.05$ ($r = 0.9991$);
berberastine $y = 6.24x + 0.00$ ($r = 0.9997$);
jatrorrhizine $y = 13.87x + 0.04$ ($r = 0.9994$);
magnoflorine $y = 5.53x + 0.01$ ($r = 0.9999$);

Determination of quaternary alkaloids in Coptidis Rhizoma

The coptis rhizome drug material was extracted at room temperature with water, with 50% methanol and with 50% ethanol. We found that 50% ethanol gave the best extraction yield, so the 50% ethanol extract of Coptidis Rhizoma was used as a test solution. When the test solution was analysed by capillary electrophoresis under the selected conditions, the electropherogram as shown in Fig. 3 was obtained. The peaks were identified by comparison with those obtained from authentic samples of the alkaloids. By substituting the area ratios of the individual peaks for y in the above equations, we obtained the contents of the individual quaternary alkaloids in the analysed Coptidis Rhizoma ($\pm$S.D., $n = 3$): coptisine, 1.95 $\pm$ 0.01%; berberine, 6.60 $\pm$ 0.02%; epiberberine, 0.96 $\pm$ 0.02%; palmatine, 1.57 $\pm$ 0.02%; columbamine, 0.78 $\pm$ 0.01%; berberastine, 0.61 $\pm$ 0.02%; jatrorrhizine, 0.51 $\pm$ 0.01%; magnoflorine, 0.55 $\pm$ 0.01%. Suitable amounts of the eight quaternary alkaloids were added to a sample of Coptidis Rhizoma of known alkaloidal content and the mixture was extracted and analysed using the proposed procedure. The recoveries of the alkaloids were 96.7–102.5% with relative standard deviations of 1.6–3.3%.

From the above results, it can be concluded that the method of simultaneous determination of the quaternary alkaloids in Coptidis Rhizoma by capillary electrophoresis as established in this study has the advantages that only a small amount of sample is required, the analysis time is short, and the electrolyte preparation is simple.

ACKNOWLEDGEMENT

Financial support from the National Science Council, Taiwan, is gratefully acknowledged.

REFERENCES

1 Y. Murayama and K. Shinozaki, *J. Pharm. Soc. Jpn.*, 46 (1926) 299.
2 Z. Kitazato, *J. Pharm. Soc. Jpn.*, 47 (1927) 315.
3 M. Tomita and S. Kura, *J. Pharm. Soc. Jpn.*, 76 (1956) 1425.
4 C. Tani and N. Takao, *Yakugaku Zasshi*, 77 (1957) 805.
5 G. Kurono, K. Ogura and Y. Sasaki, *Yakugaku Zasshi*, 85 (1965) 262.
6 M. P. Cava, T. A. Reed and J. L. Beal, *Lloydia*, 28 (1965) 73; *C.A.*, 63 (1965) 3226f.
7 A. Ikuta and H. Itokawa, *Shoyakugaku Zasshi*, 37 (1983) 195.
8 C. R. Chou, H. Y. Hsu and H. C. Chang, *T'ai-Wan Yao Hsueh Tsa Chih*, 22 (1971) 47.
9 T. Mura and T. Tominaga, *Shoyakugaku Zasshi*, 27 (1973) 135.
10 A. Ikuta, A. Kobayashi and H. Itakawa, *Shoyakugaku Zasshi*, 38 (1984) 279.
11 Y. Lu, Q. Xu and A. Shao, *Yaowu Fenxi Zazhi*, 5 (1985) 290; *C.A.*, 104 (1986) 39 829t.
12 F. Zang, X. Yang and G. Yang, *Yaowu Fenxi Zazhi*, 6 (1986) 100; *C.A.*, 105 (1986) 49 131u.
13 X. Qiu, C. Wu and B. Chen, *Yaoxue Xuebao*, 21 (1986) 458; *C.A.*, 105 (1986) 120 875x.
14 T. Namba, M. Mikage and T. Ushiyama, *Yakugaku Zasshi*, 102 (1982) 56.
15 T. Namba and M. Mikage, *Pharm. Tech. Jpn.*, 3 (1987) 227; *C.A.*, 106 (1987) 162 659f.
16 M. Mikage, T. Ushiyama and T. Namba, *Yakugaku Zasshi*, 107 (1987) 690.
17 O. Ishikawa, T. Hishimoto, T. Nakajima, O. Tanaka and H. Itokawa, *Yakugaku Zasshi*, 98 (1978) 976.
18 T. Misaki, K. Sagara, M. Ojima, S. Kakizawa, T. Oshima and H. Yoshizawa, *Chem. Pharm. Bull.*, 30 (1982) 354.
19 K. Yoneda, E. Yamagata, M. Miyaura, L. Hua and M. Mizuno, *Shoyakugaku Zasshi*, 41 (1987) 205.
20 K. Yoneda, E. Yamagata, L. Hua and M. Mizuno, *Shoyakugaku Zasshi*, 42 (1988) 116.
21 L. Zhao, X. Cai, S. Dong, S. Lin and D. An, *Zhongguo Yaoke Daxue Xuebao*, 20 (1989) 82; *C.A.*, 112 (1990) 125 306s.
22 G. Luo, Y. Wang; G. Zhou and Y. Yu, *J. Liq. Chromatogr.*, 13 (1990) 3825; *C.A.*, 114 (1991) 171 391e.
23 M. Tomita and J. Kunitomo, *Yakugaku Zasshi*, 78 (1958) 1444.
24 T. C. Wu and S. J. Sheu, unpublished data.
25 S. Honda, K. Suzuki, M. Kataoka, A. Makino and K. Kakehi, *J. Chromatogr.*, 515 (1990) 653.
26 Y. M. Liu and S. J. Sheu, *J. Chromatogr.*, 600 (1992) 370.

Journal of Chromatography, 623 (1992) 200–201
Elsevier Science Publishers B.V., Amsterdam

CHROM. 24 539

Book Review

Capillary electrophoresis—principles, practice and applications (*Journal of Chromatography Library*, Vol. 52), by S. F. Y. Li, Elsevier, Amsterdam, 1992, XXVI + 582 pp., price Dfl. 395, ISBN 0-444-89433-0.

Had Napoleon had the insight of Dr. Li, he might have won the Battle of Waterloo and I might have had to write this review in French! Certainly the members of the Electrophoresis Society (ES) at large were caught off guard by Dr. Li, and they have surely lost yet another battle. I must confess that I didn't know Dr. Li. When I received the galleys for a sneak preview, I went feverishly to consult the Gotha of the ES: from A to Z and back up from Z to A (just in case, I went up and down also through the letters of the Greek alphabet, from α to Ω, lest I had missed something) but Dr. Li was nowhere to be found. In a way I was relieved, since for at least 20 years I have been frequenting the ES fauna and have never crossed the war-path of Dr. Li. So, while the members of the ES were hacking each other to pieces over who should control the journal, who should be the president, and how many counsellors and treasurers and by-laws should be adopted, on the other side of the world Dr. Li was covertly collecting, cataloguing, labeling, ordering, laying the cornerstone (and all the other bricks) that resulted in this 'Summa Teologica' by the title: Capillary Electrophoresis: Principle, Practice and Applications, ex Oficina Elseviriana.

The book seems to be divided (grossò modò, as Napoleon would say: I keep being hunted by Heisenberg and his uncertainty principle!) into eight chapters, as follows: Recent advances and prospect for growth; Applications; Special systems and methods; Electrolyte systems; Column technology; Detection techniques; Sample injection methods; Introduction.

I am listing it from end to beginning, since the last chapter seems to be the freshest and is the most enjoyable to read: it quotes so many advances, new systems and so much progress that one should shoot for it directly before it ages. I suspect that Dr. Li was slow in delivering, and that the directors at Elsevier did to him what the director of La Scala did to Rossini: they locked him up in the attic of the theater and the poor composer had to write pages and pages of music even on the eve of the premiere. No sooner had the ink dried, the pages would be ejected from a small window and the orchestra would furiously try the last notes while the pages were gently floating down in the 'Golfo Mistico'. Poor Rossini must have been starving to death, so, when he took refuge in Paris, he made sure that outside the Opera there would be an army of cooks turning out what went down in history as Rossini's Turnedo (or Turnedo, as Napoleon would insist on pronouncing).

So, what about the book? I suspect that this will be 'the review that ends all reviews': anybody wanting to write a book on CZE after this would look like a fool. Everything seems to be there, any detection system you have ever dreamed of, any capillary coating, enough electrolyte systems to saturate your wits, and much, much more. I realize now why I was not familiar at all with Dr. Li: he must be a chromatographer who has transfused all the strength, knowledge and weight of chromatography into electrophoresis: so this is a delightful sonata for chromatography, with a power supply in the background. This cross-fertilization should certainly bridge the gap between the two techniques, which were married at the time of Tiselius, got divorced in due time and have reunited again.

Some minor criticism: I disliked the notion (p. 184) that polyacrylamide gels contain pores of average diameters from 0.6 to 4 μm, likely to separate proteins of molecular diameters from 1.6 to 8 μm! Now, who will dare bring this news to protein chemists and to polymer scientists? While talking

about polyacrylamides, a strange discovery is mentioned (p. 175) that they should be cross-linked with N,N′-diallyltartardiamide, a superb inhibitor of gel polymerization. Not to mention the other unique cross-linker, N,N′acryloyltris amino methane which, even if it existed, would surely degrade with zero-order kinetics.

These minor flaws do not subtract from the value of the book, which is by far the most thorough and comprehensive in the field yet to appear.

Milano (Italy) Pier Giorgio Righetti

Journal of Chromatography, 623 (1992) 202–204
Elsevier Science Publishers B.V., Amsterdam

CHROM. 24 497

Book Review

Element-specific chromatographic detection by atomic emission spectroscopy (*ACS Symposium Series*, No. 479), edited by P. C. Uden, American Chemical Society, Washington, DC, 1992, 350 pp., price US$ 79.95, ISBN 0-8412-2174-X.

Element-specific chromatographic detection by atomic emission spectroscopy is a multi-author volume developed from a symposium sponsored by the Division of Analytical Chemistry at the *199th National Meeting of the American Chemical Society* in Boston, MA, in 1990. In nineteen chapters, a broad range of information is provided, encompassing the moderately established technique of gas chromatography (GC)–atomic emission spectroscopic (AES) detection with commercial instrumentation utilizing a microwave helium discharge plasma and several less established techniques such as interfacing AES to liquid chromatography (LC) and supercritical fluid chromatography (SFC) and the utilization of unique excitation sources.

Chapter 1 provides a general overview of atomic spectral chromatographic detection. It summarizes the classes of atomic plasma emission spectrometers including the inductively coupled plasma (ICP), the direct current plasma jet, the microwave induced plasma (MIP) and the surface wave plasma. A very brief discussion of interfacing to GC, LC and SFC follows. An application and plasma–mass spectrometry section conclude the chapter.

Chapter 2 discusses the use of a helium microwave plasma for LC and SFC. The current status of LC with helium plasma atomic emission is summarized as follows: (1) common LC organic mobile phases cause spectral and excitation interferences; (2) lower-power plasmas are susceptible to extinguishment and reduction of emission intensity with the introduction of LC solvents; (3) higher-power plasmas are stable during the introduction of LC solvents but these plasmas cause increased complexity and intensity of the molecular background. The status of SFC is summarized as follows: (1) SFC mobile phases cause spectral interferences and decreased emission signals. Both parameters are dependent upon mobile phase flow-rate; (2) low-power plasma sources provide an adequate emission source for SFC–MIP; (3) the NIR spectral region seems superior to the UV–VIS spectral region in terms of background and emission characteristics.

Chapter 3 discusses quantitative elemental responses and empirical formula determination for hydrocarbons, chlorinated, brominated, and oxygenated species. Factors affecting accuracy and precision are discussed. The data indicates that the chemical structures of compounds may sometimes affect empirical formula determinations and the relative element response. Maximum errors in relative element responses were on the order of 10%. Elemental ratios were used to qualitatively identify freons.

Interferences affecting selectivity in GC–AES are discussed in Chapter 4. Chemical interferences are minimized by cooling of the discharge tube, by the introduction of post-column reagent gases, and by flow control of the make-up gas. Detection algorithms are discussed. Spectral snapshots collected during a chromatographic run can be used to confirm elemental determinations.

Chapter 5 discusses a new MIP torch design, the concentric dual flow torch. Advantages claimed over the conventional capillary quartz tube include a simplified background spectrum and improved plasma stability. Applications to the detection of alkyltin, selenium- and silicon-containing species after GC and SFC are demonstrated.

Chapter 6 reviews the developments of optical systems with respect to element selectivity in gas chromatography with plasma emission detection. The plasma emission detector based on oscillating interference filters is presented. With this system,

simultaneous background correction is achieved.

Twelve years of industrial experience with atomic emission detection at 3M Corporation are reviewed in Chapter 7. Examples include fluorine selective detection in human blood plasma, and derivatization tags with Cl, F and deuterium. Also discussed are direct pyrolysis experiments in the microwave plasma.

Analytical problem solving with simultaneous atomic emission and mass spectral detection is discussed in Chapter 8. The construction of a combined detector, using both a low-pressure and atmospheric-pressure splitter, and its operating characteristics are described. The system is utilized for qualitative and quantitative measurement of impurities in a bulk drug lot.

An element-specific detector based on a stabilized capacitive plasma (SCP) is described in Chapter 9. Radiofrequency at 27.12 MHz is coupled into a water-cooled fused-silica discharge tube by two annular electrodes. The radiofrequency power dissipated in the plasma is approximately 140 W. Examples are given for the selective detection of carbon, chlorine, bromine and sulfur at low pg/s detection limits.

An alternating current plasma for GC and high-performance LC is considered in Chapter 10. The detector produces a stable self-seeding discharge which does not extinguish itself with high solvent concentration. The instrument is demonstrated for the GC determination of organomercury, lead, and chlorine and the determination of organomercury by high-performance LC.

A helium surface wave plasma as an atomic emission detector for GC is introduced in Chapter 11. The plasma physical characteristics including excitation temperature, gas temperature and electron density are presented. Emission spectra of non-metals in the UV–visible range are presented and the affect of plasma operating conditions on atomic emission intensity reported. Application to the analysis of pesticides was discussed.

An overview of the design, analytical figures of merit, recent applications, and limitations of a helium discharge detector for element selective detection is presented in Chapter 12. Operational features, spectral characteristics, excitation temperatures and the mechanism of analyte excitation relative to the microwave induced plasma are discussed. Utilization of wavelengths in the near IR are evaluated for improved selectivity of elements traditionally detected in the UV.

The interfacing of ICP-AES to packed microcolumn supercritical fluid chromatography is discussed in Chapter 13. Performance is evaluated with 1.0 mm I.D. and 0.5 mm I.D. packed capillaries. The affects of the nebulizer gas and mobile phase flow-rate on peak height, dynamic range, and detection limits were studied. Polar modifiers and pressure programming is tested. SFC–ICP detection of metal acetylacetone complexes was studied.

The use of a helium high-efficiency microwave induced plasma as an element selective detector for packed column SFC is discussed in Chapter 14. The high CO_2 flow-rates experienced with packed column SFC did not affect the excitation temperature or the electron number density of the 150 W high-efficiency MIP. Minimum detectable quantities reported were 50 ng for S and Cl, 100 pg for P, 30 pg for Sn and 10 pg for Fe.

Chapter 15 discusses the speciation of trace levels of selenium using high-performance LC with UV and direct current plasma emission detection. A validated trace method of analysis is developed utilizing a reversed-phase ion pairing separation of ionic selenium species. Application to Se compounds in animal feed premixes is presented.

Chapter 16 discusses the analytical utility of an ICP–ion chromatographic system for the speciation and detection of transition metals. Species specific detection is demonstrated for Fe(II)/Fe(III) and Cr(III)/Cr(VI) systems.

A review of investigations concerning chromatographic detection by plasma mass spectrometry is presented in Chapter 17.

Chapter 18 presents element-specific detection of metallodrugs and their metabolites with high-performance LC–ICP-mass spectrometry. Examples of size-exclusion, reversed-phase and weak anion-exchange chromatography are given.

Chapter 19 introduces a fiber optic spectrochemical emission sensor as a detector for volatile chlorinated compounds. This radio frequency induced helium plasma demonstrated linearity from 0 to 500 ppm carbon tetrachloride and can also be used to monitor fluorine.

In general, *Element-specific chromatographic detection by atomic emission spectroscopy* is a well

written and thorough evaluation of the current status of interfacing chromatographic separations with AES. It provides a well rounded and even discussion of the use of several chromatographic techniques, interfaces and excitation sources. Numerous applications are included. One possible shortcoming is the lack of a chapter describing the use of AES for the qualitative identification of unknown species. I highly recommend the book to scientists involved in chromatography-AES, to industrialists interested in the utility of such systems, to detector aficionados, and to graduate students in their pursuit of truth.

Kingsport, TN (USA) Robert H. St. Louis

Journal of Chromatography, 623 (1992) 205–206
Elsevier Science Publishers B.V., Amsterdam

CHROM. 24 519

Book Review

The analysis of drugs of abuse, edited by T. A. Gough, Wiley, Chichester, New York, 1991, XVIII + 628 pp., price £ 90.00, ISBN 0-471-92267-6.

The analysis of drugs of abuse, edited by Terry A. Gough, is part of the *Separation Science Series* published by Wiley & Sons. The placement of this treatise in this series is questionable due to the large amount of material dealing with non-separation issues. The book is divided into two parts. The first part consisting of nine chapters describes analytical techniques, while the second part containing six chapters presents applications. Besides describing the analysis of drugs of forensic interest, the book deals with related issues such as the interface of the law and law enforcement personnel with a forensic laboratory, and the organization and management of a testing facility.

In the first chapter describing analytical techniques, J. Conrad Roberson describes the use of thin-layer chromatography (TLC) for the analysis of drugs of abuse. An excessive amount of time is spent describing principles and procedures which are much better treated in basic TLC texts. This is especially true since the material is not presented with the prospective of forensic drug analysis. The author makes a glaring error in describing the Van Deemter equation for liquid chromatography where the C_s and C_m terms are referred to as the concentrations of analyte in the stationary phase and mobile phase, respectively. In addition a term describing eddy diffusion and mobile phase mass transfer is deleted. The applications section presents a well organized compendium of TLC systems which is of value for the analysis of solid dosage forms and natural products such as opium, psilocybin and cannabis.

The next chapter, well written by Henk Huizer, describes the use of gas chromatography (GC) for the detection and quantitation of abused drugs. Unlike the previous chapter, theory is kept to a minimum. The principles and procedures that are discussed have direct relevance to drug analysis. Specific applications for various drug types are presented with the material most useful for analysts dealing with non-toxicological samples. Although the section on comparison of illicit drug samples is valuable, this subject matter warrants a chapter by itself. This is especially true since this subject matter is covered extensively in a later chapter.

In the third chapter Jan Piet Franke and Rokus A. de Zeeuw present an interesting discussion on the use of multiple techniques to increase discriminating power when screening for the identity of drugs. In the authors evaluation of analytical techniques only TLC, GC and UV are examined. Although I agree with the authors' assertion that high-performance liquid chromatography (HPLC) is lacking in reproducibility (long term and column-to-column), the use of a diode array UV detector in combination with a retention time window would be valuable for tentative drug identification, especially when dealing with mixtures. The use of this latter technique should provide better discrimination than UV alone. The subject matter in this chapter is especially useful for toxicologists.

Brian Caddy in the next chapter discusses the use of HPLC for the detection and quantitation of abused drugs. Although the principles and procedures presented are geared toward drug analysis, much of the material could have been significantly condensed. A fairly comprehensive application section follows with the material useful to both chemists analyzing bulk drugs and toxicological samples. There are several instances where statements are made that are not technically accurate, *i.e.* carbohydrates do not show UV absorption, and cannot be conveniently detected by electrochemical means.

The fifth chapter by Kenneth S. Webb presents an excellent blend of basic mass spectrometry and

applications. This chapter by far has the best balance between bulk drug and toxicological applications. It is curious that no mention is made of the mass selective detector, a relatively inexpensive bench-top quadrupole mass spectrometer, which is extensively used in forensic laboratories.

In the next chapter on applications of infrared spectroscopy, Terry Mills III and George J. Fontis present a unique and extremely effective approach for discussing procedures. Whether discussing sampling approaches, techniques combined with IR, or spectral stripping, the spectrum of cocaine is usually a focal point. The theory section is excessively detailed. The applications section does not contain literature references, but instead gives commercial sources for IR reference libraries.

Brian A. Dawson in the seventh chapter delivers a well written and concise chapter on the nuclear magnetic resonance (NMR) spectroscopy of abused drugs. Since there are a large number of books dealing with NMR very little theory is presented. A very useful discussion on the types of NMR experiments performed is given. In addition a comprehensive survey of the literature for various drug types is offered.

Kim Tan and Vincent Marks describe the use of immunoassay to detect drugs in body fluids. In the eight chapter there are excellent overviews of the principles of immunoassay, the production of antibodies, isotopic and non-isotopic traces, and practical considerations. However, there is a definite lack of specific applications.

A discussion on the examination of illicitly produced tablets and capsules is given by Peter J. Gomm and Rosemary J. Hughes in the ninth chapter. In the program discussed by the authors, evidence samples are compared with reference collection samples for identical physical characteristics such as color, shape, dimensions and toolmarks. Analysis is also made for ingredients contained in the exhibits. It is strange that no mention is made of the extensive work of the US Drug Enforcement Administration in the area of the examination of solid dosage forms (A. H. Tillson, *J. Forensic Sci.*, 19 (1974) 873 and E. S. Franzosa, *J. Forensic Sci.*, 30 (1985) 1194.

In the first chapter in the applications section Lorne Elias and Andre H. Lawrence describe the very timely subject of on-site sampling and detection of drug particulates. Due to the increasingly sophisticated techniques used by drug smugglers a need has arisen for instrumental methods to detect drugs of abuse at ports of entry. Bulk detection techniques such as X-ray imaging, γ backscattering and thermal neutron activation are described. In addition, air sampling techniques such as mass spectrometry, GC and ion mobility spectrometry are discussed.

The eleventh through fourteenth chapters discuss the operation, legal mandate, and relationship to other law enforcement personnel of various laboratories involved in forensic drug analysis. Manesh C. Dutt and Tong Kooi Lee discuss mass screening of urine for drugs of abuse. Brian Widdop and Richard Caldwell describe the operation of a hospital laboratory service for the detection of drugs of abuse. Keith R. Bedford discuss analysis for a forensic science service. Finally Terry A. Gough and Geoffrey F. Phillips outline scientific support for a customs service.

In the last chapter Terry A. Gough discusses the examination of drugs in smuggling offenses. The material covered could have been presented either in the chapters dealing with analytical techniques or in a separate chapter describing comparison analysis.

This book for the most part satisfies a great need for chemists involved in forensic drug analysis, *i.e.* a single source for the various analytical techniques required. In this vein, chapters on the use of color tests and microscopy for forensic drug analysis (other than for the examination of illicitly produced capsules and tablets) should have been included. The unevenness in quality of the chapters is to be expected in a volume involving multiple authors. The last five chapters could have easily been omitted, since they dilute the excellent material presented in the rest of the book. The subject matter dealing with forensic laboratories would be best covered in another book.

McLean, VA (USA) I. S. Lurie

Vol. 623, No. 1

Journal of Chromatography

NEWS SECTION

ANNOUNCEMENTS

7th INTERNATIONAL MEETING ON INSTRUMENTAL PLANAR CHROMATOGRAPHY, BRIGHTON, UK, MARCH 23–26, 1993

The scientific program will consist of invited plenary lectures given by leading workers in the field, supported by both oral papers and poster, while the latest developments in apparatus and technique will be featured in the accompanying exhibition.

Authors wishing to submit Abstracts should send their contribution (no more than one side of A4, typed with double spacing) to the address given below.

For further information contact: Executive Secretary, The Chromatographic Society, Suite 4, Clarendon Chambers, 32 Clarendon Street, Nottingham NG1 5JD, UK.

EURORESIDUE II, INTERNATIONAL CONFERENCE ON RESIDUES OF VETERINARY DRUGS IN FOOD, VELDHOVEN, NETHERLANDS, MAY 3–5, 1993

The aim of this symposium is to cover all aspects related to residues of veterinary drugs, with special emphasis on recent developments and applications of various analytical techniques. There are some aspects which should gain more attention than at the previous conference, such as the importance of cultivated fish, the possibilities of rapid tests and field tests, misuse of drugs, and other related topics. Trends will be reflected in the plenary lectures.

Key lectures will include:

- Present state and trends in using veterinary drugs;
- Toxicology and legislation: do they fit together?;
- Possibilities of LC–MS for drug residue analysis;
- Developments in screening methods for residues of veterinary drugs;
- Are reference materials and collaboratively tested methods necessary?;
- Problems with drug residues in farmed fish;
- Stability of veterinary drug residues; and,
- Residues of disinfectants and antiparasitic agents.

During the conference several workshops will be organized, which conference attendants are kindly invited to participate in.

A two-day course on veterinary drug residue analysis is planned after the Conference.

Anyone wishing to present an oral or poster presentation should send an Abstract not exceeding 200 words before November 16, 1992 to Professor A. Ruiter at the address given below. Contributors will be informed about acceptance before December 15, 1992. The deadline for full manuscripts is February 19, 1993. Papers will be included in the final programme only after payment of the registration fee.

The registration fee for participants is Dfl. 600.00 (includes tax); for students and postgraduate students under 30 years of age Dfl. 150.00.

For further information contact: Dr. N. Haagsma, Section of Food Chemistry, Department of Food of Animal Origin, Faculty of Veterinary Medicine, University of Utrecht, P.O. Box 80.175, 3508 TD Utrecht, Netherlands. Tel.: (+31-30) 535-365/535-367; Fax: (+31-30) 532-365.

15th INTERNATIONAL SYMPOSIUM ON CAPILLARY CHROMATOGRAPHY, RIVA DEL GARDA, ITALY, MAY 24–28, 1993

The scientific program of this symposium will feature the latest developments in:

Micro separation techniques:

- Capillary gas chromatography (CGC),
- Capillary GC–MS, GC–FTIR and GC–AES,
- Micro-HPLC,
- Supercritical fluid chromatography (SFC),
- Capillary zone electrophoresis (CZE),
- Micellar electrokinetic chromatography (MEKC).

New methods and applications in:

- Environmental analysis,
- Pharmaceutical analysis,
- Petroleum and petrochemicals,
- Foods and beverages,
- Biochemical separations,
- Organic chemicals,
- Drug testing,
- Flavors and fragrances,
- Proteins and peptides,
- Trace analysis,
- Sample preparation techniques; and,
- New columns and instrumentation.

The program will include review papers, invited papers, poster sessions, discussion sessions and workshop seminars.

Authors wishing to submit papers for the symposium must enter a 300-word abstract no later than December 15, 1992.

A limited number of scholarships will be awarded to students and young scientists. Application forms may be requested in writing to Professor Dr. P. Sandra.

Advanced registration fees accepted prior to April 25, 1993 are 300 ECU, on-site registration is 330 ECU and student registration fees are 150 ECU.

For further details contact: Professor Dr. P. Sandra, I.O.P.M.S., Kennedypark 20, B-8500 Kortrijk, Belgium. Tel.: (+32-56) 204-960; Fax: (+32-56) 204-859.

ICES–ELPHO '93, MEETING OF THE INTERNATIONAL COUNCIL OF ELECTROPHORESIS SOCIETIES, SANDEFJORD, NORWAY, JUNE 2–4, 1993

The emphasis of this meeting will be on techniques like capillary electrophoresis that is now moving towards the analysis of single cells, and on DNA electrophoresis which is basic to the exploration and practical use of modern genetics. The linkage between gene and protein by 2D-databases will be of central interest. Also relevant are all aspects of electrophoresis, including blotting techniques, image analyses and practical applications.

Lectures highlighted will be:

- Electrophoresis in biochemistry: present and future;
- Electrophoresis in space: why is it so important;
- What new developments can we expect in the design of the third generation capillary electrophoresis apparatus;
- Electrophoretic light scattering;
- Field inversion and pulsed-field gel electrophoresis in the analysis of yeast artificial chromosomes;
- DNA electrophoresis in forensic medicine;
- Two-dimensional gel protein databases: towards linking proteins and genome; and,
- History of electrophoretic methods – a mini-
- review.

Three workshops will be arranged at the same location on June 1, the day before the meeting:

- Capillary electrophoresis;
- Image analysis of electrophoretic patterns; and,
- Isoelectric focusing in agarose gels, titration and blotting.

The deadline for Abstracts is February 1, 1993.

The congress fee (not including lodging) is NOK 1500 (approximately US$ 240).

For further details contact: Professor Nils Olav Solum, Research Institute for Internal Medicine, Rikshopitalet, Pilestredet 32, N-0027 Oslo, Norway. Tel.: (+47-2) 868-226; Fax: (+47-2) 868-303.

INTERNATIONAL SYMPOSIUM ON ANALYSIS OF PEPTIDES, STOCKHOLM, SWEDEN, JUNE 2–4, 1993

A full announcement of this symposium has been published in an earlier issue of this journal (Vol. 603, Nos. 1&2). However, the date of the conference has been changed from May 24–26, 1993 to June 2–4, 1993.

For further information contact: Swedish Academy of Pharmaceutical Sciences, Symposium on "Analysis of Peptides", P.O. Box 1136, S-111 81 Stockholm, Sweden. Tel.: (+46-8) 245-085; Fax: (+46-8) 205-511.

XXVIII COLLOQUIUM SPECTROSCOPICUM INTERNATIONALE, YORK, UK, JUNE 29–JULY 4, 1993

This traditional biennial conference provides a forum for the international community of analytical spectroscopists to meet and exchange ideas. The scientific program will consist of plenary lectures and four parallel streams of contributed lectures (*e.g.* atomic, molecular and mass spectrometry, and surface analysis and characterisation) each session beginning with an invited lecture from a prominent scientist in the relevant field. Separate times will be made available for poster sessions.

Participants are invited to submit contributions for presentations in English, French or German (there will be no translation facilities) on the following topics:

Basic theory, techniques and instrumentation of:

- Atomic spectroscopy (emission, absorption, fluorescence);
- Computer applications and chemometrics;
- Electron spectroscopy;
- Gamma spectroscopy;
- Laser spectroscopy;
- Mass spectrometry (inorganic and organic);
- Methods of surface analysis and depth profiling;
- Molecular spectroscopy (UV, VIS, IR)
- Mössbauer Spectroscopy;
- Nuclear magnetic resonance spectrometry;
- Photoacoustic spectroscopy;
- Raman spectroscopy; and,
- X-ray spectroscopy.

Applications of spectroscopy in the analysis of:

- Biological samples;
- Environmental samples;
- Food and agricultural products;
- Geological materials;
- Industrial products; and,
- Metals and alloys.

The deadline for submission of Abstracts is January 31, 1993.

In connection with the XXVIII CSI, a number of symposia and workshops will be organised.

For further information contact: XXVIII Colloquium Spectroscopicum Internationale, Department of Chemistry (CSI Secretariat), Loughborough University of Technology, Loughborough, Leicestershire LE11 3TU, UK. Tel.: (+44-509) 222-575; Fax: (+44-509) 233-163; Telex: 34319.

9th INTERNATIONAL CONFERENCE ON FOURIER TRANSFORM SPECTROSCOPY, CALGARY, CANADA, AUGUST 23–27, 1993

The Scientific Program is open to any aspect of Fourier transform spectroscopy in the infrared, visible and ultraviolet regions. Topics will range from fundamental considerations of the methodology and its development, to current applications. It will include papers of primary interest to physicists, through papers mainly for chemists, to papers aimed at the industrial analyst.

Invited plenary lecturers will provide up-to-date coverage of specific topics and techniques of broad interest. Contributed papers will be presented in poster sessions to be scheduled throughout the week at times not conflicting with the lectures.

Experimental techniques both drive and support new developments in theory and application. The instrumentation exhibit is therefore an important aspect of the Fourier transform spectroscopy conferences in this series. Ample serviced exhibition space

will be available in close proximity to the lecture hall and poster space for optimal interaction between participants.

For further information contact: Conference Office, The University of Calgary, 2500 University Drive NW, Calgary, Alberta T2N 1N4, Canada. Tel.: (+1-403) 220-5051; Fax: (+1-403) 289-7287.

COURSES

ANALYTICAL CHEMISTRY SHORT COURSES, LOUGHBOROUGH, UK

The following short courses will be held later this year at the Department of Chemistry, University of Technology, Loughborough, UK:

- Separations for Biotechnology and Biochemistry; 9–13 November, 1992
- Statistics for Analytical Chemistry; 15–18 December, 1992
- Immunoassay; 17–18 December, 1992

For further details contact: Mrs. S. Maddison, Department of Chemistry, Loughborough University of Technology, Loughborough, Leics. LE11 3TU, UK. Tel.: (+44-509) 222-575; Fax: (+44-509) 233-163.

AWARDS

5th ANNUAL GOLAY AWARD

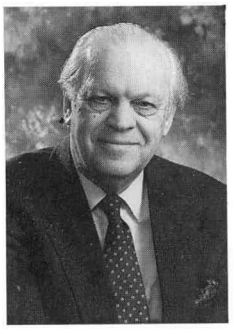

Dr. Leslie Ettre was presented with the fifth annual M.J.E. Golay Award in capillary chromatography at the Fourteenth International Symposium on Capillary Chromatography. An adjunct professor at Yale University's Department of Chemistry, Dr. Ettre retired in 1990 as senior scientist with the Perkin-Elmer Corporation after nearly 30 years of service.

Dr. Ettre worked with Marcel Golay during the late 1950s and early 1060s, and was deeply involved in the fundamental development and application of capillary gas chromatography (GC) columns, and GC instrumentation. He is the author, co-author or editor of over 200 publications, articles, and books on chromatography, and is an editor of the journal *Chromatographia*. His numerous contributions to the field of chromatography have been recognized with many national and international awards.

Sponsored by Perkin-Elmer, the Golay Award is presented annually to a scientist or scientists for significant contributions to the evolution of capillary chromatography. The Golay Award includes a medal, a scroll, and a financial endowment.

Nominations are now being accepted for the Sixth Annual Golay Award, to be presented at the Fifteenth International Symposium on Capillary Chromatography in May 1993, in Riva del Garda, Italy. All nominations should be sent to: Dr. Carel A. Cramers, Eindhoven University of Technology, Laboratory of Instrument Analysis, P.O. Box 513, 5600 MB Eindhoven, Netherlands. Tel.: (+31-40) 473-024; Fax: (+31-40) 453-762.

THE MARTIN AWARD

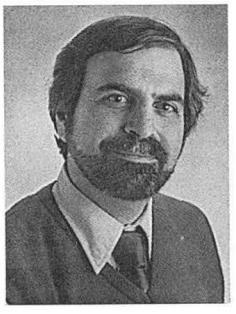

Professor Irving W. Wainer was presented with the Martin Award at HPLC '92, Baltimore, MD, USA. Irving William Wainer received his Bachelor of Science Degree from Wayne State University in Detroit, Michigan in 1965. In his undergraduate years, he majored in chemistry and received a National Science Foundation Undergraduate Fellowship to study with Carl R. Johnson. He also majored in American literature with an emphasis on Southern Gothic authors such as Carson McCullers.

Dr. Wainer completed his graduate work in synthetic organic chemistry at Cornell University and received his PhD in 1970. After post-doctoral studies at the Institute of Molecular Biology in the University of Oregon, he moved to the Department of Pharmacology at Thomas Jefferson University in Philadelphia.

In 1978, Dr. Wainer accepted a position at the Division of Drug Chemistry in the Food and Drug Administration. This was the beginning of his studies into the chromatographic separation of stereoisomers, a field which is still a major theme in his scientific work.

Between 1983–1984, Dr. Wainer took a sabbatical leave from the FDA and studied Molecular Pharmacology with Jean-Francois Cloix at INSERM U7 Hópital Necker in Paris, France. In 1985, he returned to the FDA and had the privilege of working for a year with Professor Göran Schill who brought with him the newly developed -acid glycoprotein chiral stationary phase (AGP–CSP) for HPLC, which had been invented by one of Göran's students, Jörgen Hermansson.

The time Dr. Wainer spent with Göran Schill was a key period in his scientific career. It not only led to a friendship and collaboration which lasted until Göran's untimely death in March 1992, but it also served to bring together three themes in Dr. Wainer's scientific training: chromatography, molecular biology and biochemical pharmacology. Out of this grew his work on the application of HPLC phases based upon immobilized biopolymers for the determination of substrates and inhibitors; a phase based upon human serum albumin, developed with Guy Felix, for the determination of ligand–protein interactions; a melanin-based column for screening compounds for binding to this biopolymer; and work into the development of a phase based upon immobilization of the calcium channel.

In 1986, Dr. Wainer took up a position as Director of Analytical Chemistry in the Pharmaceutical Division at St. Jude Children's Research Hospital in Memphis. Then in 1990, he accepted his present position as Professor and Director of the Pharmaceutical Division in the Department of Oncology at McGill University in Montreal. These steps reflect the third component of his research program, the effect of stereochemistry on pharmacokinetics and pharmacodynamics.

Dr. Wainer's scientific activities have resulted in the publication of over 200 papers, abstracts, reviews, chapters and 4 books. He is also the founding Editor-in-Chief of the journal *Chirality*.

While a number of people have played important roles in the development of his scientific life, the most important influence has been his wife, Pamela Zulli. Like many of his contemporaries, he was active in the Civil Rights and Equal Rights movements as well as the opposition of U.S. involvement in the Vietnam War. Part of these efforts resulted in the book Science and the Question of Human Equality, which was coedited by Margaret Collis and Theodore Bremmner and published by the American Association for the Advancement of Science in 1981. Dr. Wainer continues to contribute articles on the interaction of science and society to a variety of publications.

CALENDAR OF FORTHCOMING EVENTS

■ **Nov. 3–5, 1992**
Helsinki, Finland
KEMIA '92

Contact: Association of Finnish Chemical Societes, Eeva Kota-aho, Programme Secretary, Hietaniemenkatu 2, SF-00100 Helsinki Finland. Tel.: (358-0) 408-022; Fax: (+358-0) 408-780.

Nov. 4–6, 1992
Montreux, Switzerland
9th Montreux Symposium on Liquid Chromatography–Mass Spectrometry (LC–MS, SFC–MS, CZE–MS, MS–MS)

Contact: Marianne Frei, IAEAC Secretariat, P.O. Box 46, CH-4123 Allschwil, Switzerland. Tel.: (+41-61) 632789; Fax: (+41-61) 4820805.

Nov. 11, 1992
Loughborough, UK
European Radiochemistry

Contact: Dr. P. Warwick, Department of Chemistry, University of Technology, Loughborough, Leicestershire LE11 3TU, UK. Tel.: (+44-509) 263-171; Fax: (+44-509) 233-163.

Nov. 29–Dec. 2, 1992
Syndey, Australia
12th International Symposium on HPLC of Proteins, Peptides and Polynucleotides

Contact: 12 ISPPP Sectretariat, GPO Box 128, Sydney NSW 2001, Australia. Tel.: (+61-2) 262-2277; Fax: (+61-2) 262-2323.

Dec. 14–16, 1992
Budapest, Hungary
Budapest Chromatography Conference

Contact: Organizing Bureau, Agnes v. Rubányi, Intercongress, Dózsa György u. 84/a, H-1068 Budapest, Hungary. Tel.: (+36-1) 122-2203; Fax: (+36-1) 142-4118; Telex: 223955 ici pv.

Jan. 25–28, 1993
Orlando, FL, USA
5th International Symposium on High Performance Capillary Electrophoresis

Contact: Shirley E. Schlessinger, Symposium Manager, HPCE '93, Suite 1015, 400 E. Randolph Drive, Chicago, IL 60601, USA. Tel.: (+1-312) 527-2011.

March 8–12, 1993
Atlanta, GA, USA
PITTCON '93, 44th Pittsburgh Conference and Exposition on Analytical Chemistry and Applied Spectroscopy

Contact: Mrs. Alma Johnson, Program Secretary, Pittsburgh Conference, 300 Penn Center Blvd., Suite 332, Pittsburgh, PA 15235-5503, USA. Tel.: (+1-412) 825-3220.

■ **March 19, 1993**
Antwerp, Belgium
Symposium on Possibilities and Limitations of Chiral Separation Techniques

Contact: Royal Flemish Chemical Society (KVCV), Working Party on Chromatography, c/o Dr. R. Smits, BASF Antwerpen NV, Central Laboratory, Scheldelaan, B-2040 Antwerp, Belgium. Tel.: (+32-3) 568-2831; Fax: (+32-3) 568-3250; Telex: 31047 basant b.

■ **March 23–26, 1993**
Brighton, UK
7th International Meeting on Instrumental Planar Chromatography

Contact: Executive Secretary, The Chromatographic Society, Suite 4, Clarendon Chambers, 32 Clarendon Street, Nottingham NG1 5JD, UK.

April, 1993
Baltimore, MD, USA
4th International Symposium on Pharmaceutical and Biomedical Analysis

Contact: Shirley Schlessinger, Symposium Manager, Suite 1015, 400 E. Randoph Drive, Chicago, IL 60601, USA. Tel.: (+1-312) 527-2011.

April 4–7, 1993
Wrexham, UK
Ion-Ex '93

Contact: Ion-Ex '93, Conference Secretariat, Faculty of Science, The North East Wales Institute, Connah's Quay, Deeside, Clwyd, CH5 4BR, UK. Tel.: (+44-244) 831-531 ext. 245 or 276; Fax: (+44-244) 814-305.

■ **April 26–29, 1993**
Clearwater, FL, USA
18th International Technical Conference on Coal Utilization and Fuel Systems

Contact: Coal Utilization and Fuel Systems, Conference Organizing Committe, 1156 Fifteenth Street, NW, Suite 525, Washington, DC 20005, USA. Tel.: (+1-202) 296-1133; Fax: (+1-202) 223-3504.

■ **May 3–5, 1993**
Veldhoven, Netherlands
EURORESIDUE II-International Conference on Residues of Veterinary Drugs in Food

Contact: Dr. N. Haagsma, Section of Food Chemistry, Department of Food of Animal Origin, Faculty of Veterinary Medicine, University of Utrecht, P.O. Box 80.175, 3508 TD Utrecht, Netherlands. Tel.: (+31-30) 535-365/535-367; Fax: (+31-30) 532-365.

May 9–14, 1993
Hamburg, Germany
17th International Symposium on Column Liquid Chromatography

Contact: Gesellschaft Deutscher Chemiker, Abteilung Tagungen, P.O. Box 900440, Varrentrappstrasse 40-42, W-6000 Frankfurt am Main 90, Germany. Tel: (+49-69) 7917-360; Fax: (+49-69) 7917-475.

■ **May 24–28, 1993**
Riva del Garda, Italy
15th International Sympsium on Capillary Chromatography

Contact: Professor Dr. P. Sandra, I.O.P.M.S., Kennedypark 20, B-8500 Kortrijk, Belgium. Tel.: (+32-56) 204-960; Fax: (+32-56) 204-859.

May 25–27, 1993
Ghent, Belgium
5th International Symposium on Quantitative Luminescence Spectrometry in Biomedical Sciences

Contact: Dr. Willy R.G. Baeyens, Symposium Chairman, University of Ghent, Pharmaceutical Institute, Harelbekestraat 72, B-9000 Ghent, Belgium. Tel.: (+32-91) 218-951, ext. 246; Fax: (+32-91) 217-902.

■ **June 2–4, 1993**
Stockholm, Sweden
International Symposium on Analysis of Peptides

Contact: Swedish Academy of Pharmaceutical Sciences, Symposium on "Analysis of Peptides", P.O. Box 1136, S-111 81 Stockholm, Sweden. Tel.: (+46-8) 245-085; Fax: (+46-8) 205-511.

■ **June 2–4, 1993**
Sandefjord, Norway
ICES-ELPHO '93, Meeting of the International Council of Electrophoresis Societies

Contact: Professor Nils Olav Solum, Research Institute for Internal Medicine, Rikshopitalet, Pilestredet 32, N-0027 Oslo, Norway. Tel.: (+47-2) 868-226; Fax: (+47-2) 868-303.

June 14–16, 1993
Arlington, VA, USA
Prep '93, 10th International Symposium on Preparative Chromatography

Contact: Washington Chromatography Discussion Group, c/o Barr Enterprises, P.O. Box 279, Walkersville, MD 21793, USA. Tel.: (+1-301) 898-3772; Fax: (+1-301) 898-5596.

■ **June 29–July 4, 1993**
York, UK
XXVIII Colloquium Spectroscopicum Internationale

Contact: XXVIII Colloquium Spectroscopicum Internationale, Department of Chemistry (CSI Secretariat), Loughborough University of Technology, Loughborough, Leicestershire LE11 3TU, UK. Tel.: (+44-509) 222-575; Fax: (+44-509) 233-163; Telex: 34319.

July 26–29, 1993
Washington, DC, USA
107th Annual International Meeting and Exposition of the AOAC

Contact: Margaret Ridgell, AOAC, 2200 Wilson Blvd., Suite 400, Arlington, VA 22201-3301, USA. Tel.: (+1-703) 522-3032; Fax: (+1-703) 522-5468.

Aug. 23–27, 1993
Budapest, Hungary
9th Danube Symposium on Chromatography

Contact: Symposium Secretariat, Professor László Szepesy, Department of Chemical Technology, Technical University of Budapest, Budafoki út 8., H-1521 Budapest, Hungary. Tel.: (+36-1) 186-9000; Fax: (+36-1) 181-2755; Telex: 225931 muegy h.

■ **Aug. 23–27, 1993**
Calgary, Canada
9th International Conference on Fourier Transform Spectroscopy

Contact: Conference Office, The University of Calgary, 2500 University Drive NW, Calgary, Alberta T2N 1N4, Canada. Tel.: (+1-403) 220-5051; Fax: (+1-403) 289-7287.

Sept. 5–11, 1993
Edinburgh, UK
EUROANALYSIS VIII, 8th European Conference on Analytical Chemistry

Contact: Miss P.E. Hutchin-

son, Analytical Division, The Royal Society of Chemistry, Burlington House, Piccadilly, London W1V 0BN, UK. Tel.: (071) 4378656; Fax: (071) 734-1227; Telex: 268001.

Sept. 7–10, 1993
Verona, Italy
12th Internation Symposium on Biomedical Applications of Chromatography and Electrophoresis and 2nd International Symposium on the Applications of HPLC in Enzyme Chemistry

Contact: Dr. Franco Tagliaro, Istituto di Medicina Legale, Università di Verona, Policlinico, I-37134 Verona, Italy. Tel.: (+39-45) 807-4618/807-4246; Fax: (+39-45) 505-259.

Sept. 8–10, 1993
Prague, Czechoslovakia
4th Workshop on Chemistry and Fate of Modern Pesticides and Related Pollutants

Contact (for Eastern European countries): Dra. J. Hajslova, Department of Food Chemistry and Analysis, Institute of Chemical Technology, Suchbátarova 5, 166 28 Prague 6-Dejvice, Czechoslovakia. Fax: (+42-2) 311-4769. For all other countries, contact: IAEAC, M. Frei-Häusler, P.O. Box 46, CH-4123 Allschwil 2, Switzerland. Fax:(+41-61) 482-0805.

■ **Sept. 19–22, 1993**
Montréal, Canada
4th International Symposium on Chiral Discrimination

Contact: Chiral Secretariat, Conference Office, McGill University, West Tower, Suite 490, Montreal, Quebec H3A 1B9, Canada. Tel.: (+1-514) 398-3770; Fax: (+1-514) 398-4854.

■ **May 8–13, 1994**
Minneapolis, MN, USA
HPLC '94: 18th International Symposium on Column Liquid Chromatography

Contact: Janet E. Cunningham, Barr Enterprises, P.O. Box 279, Walkersville, MD 21793, USA. Tel.: (+1-301) 898-3772; Fax: (+1-301) 898-5596.

June 20–24, 1994
Bournemouth, UK
20th International Symposium on Chromatography

Contact: Executive Secretary, The Chromatographic Society, Nottingham Polytechnic, Burton Street, Nottingham, NG1 4BU, UK. Tel.: (+44-602) 500-596; Fax: (+44-602) 500-614.

■ Indicates new or amended entry.

Hyphenated Techniques in Supercritical Fluid Chromatography and Extraction

edited by **K. Jinno,** Toyohashi University of Technology, Toyohashi, Japan

Journal of Chromatography Library Volume 53

This is the first book to focus on the latest developments in hyphenated techniques using supercritical fluids. The advantages of SFC in hyphenation with various detection modes, such as, FTIR, MS, MPD and ICP and others are clearly featured throughout the book. Special attention is paid to coupling of SFE with GC or SFC.

In this edited volume, chapters are written by leading experts in the field. The book will be of interest to professionals in academia, as well as to those researchers working in an industrial environment, such as analytical instrumentation, pharmaceuticals, agriculture, food, petrochemicals and environmental.

Contents:

1992 x + 334 pages
Price: US $ 157.00/ Dfl. 275.00
ISBN 0-444-88794-6

ORDER INFORMATION
For USA and Canada
ELSEVIER SCIENCE PUBLISHERS
Judy Weislogel
P.O. Box 945
Madison Square Station,
New York, NY 10160-0757
Tel: (212) 989 5800
Fax: (212) 633 3880

In all other countries
ELSEVIER SCIENCE PUBLISHERS
P.O. Box 211
1000 AE Amsterdam
The Netherlands
Tel: (+31-20) 5803 753
Fax: (+31-20) 5803 705

US$ prices are valid only for the USA & Canada and are subject to exchange fluctuations; in all other countries the Dutch guilder price (Dfl.), is definitive. Books are sent postfree if prepaid.

ELSEVIER
SCIENCE PUBLISHERS

Announcement from the Publisher

ELSEVIER SCIENCE PUBLISHERS

prefers the submission of electronic manuscripts

Electronic manuscripts have the advantage that there is no need for the rekeying of text, thereby avoiding the possibility of introducing errors and resulting in reliable and fast delivery of proofs.

The preferred storage medium is a $5\frac{1}{4}$ or $3\frac{1}{2}$ inch disk in MS-DOS format, although other systems are welcome, e.g. Macintosh.

Your disk and (**exactly matching**) printed version (printout, hardcopy) should be submitted together to the accepting editor. In case of revision, the same procedure should be followed such that, on acceptance of the article, the file on disk and the printout are **identical**. Both will then be forwarded by the editor to Elsevier.

Please follow the general instructions on style/arrangement and, in particular, the reference style of this journal as given in 'Instructions to Authors'.

Please label the disk with your name, the software & hardware used and the name of the file to be processed.

Further information can be found under 'Instructions to Authors - Electronic manuscripts'.

Contact the Publisher for further information.

ELSEVIER SCIENCE PUBLISHERS B.V.
P.O. Box 330, 1000 AH Amsterdam
Netherlands
Fax: (+31-20) 5862-304

4/92

PUBLICATION SCHEDULE FOR 1993

Journal of Chromatography and *Journal of Chromatography, Biomedical Applications*

MONTH	O 1992	N 1992	D 1992
Journal of Chromatography	623/1 623/2 624	625/1 625/2	The publication schedule for further issues will be published later
Cumulative Indexes, Vols. 601–650			
Bibliography Section			
Biomedical Applications			

INFORMATION FOR AUTHORS

(Detailed *Instructions to Authors* were published in Vol. 609, pp. 437–443. A free reprint can be obtained by application to the publisher, Elsevier Science Publishers B.V., P.O. Box 330, 1000 AH Amsterdam, The Netherlands.)

Types of Contributions. The following types of papers are published in the *Journal of Chromatography* and the section on *Biomedical Applications:* Regular research papers (Full-length papers), Review articles, Short Communications and Discussions. Short Communications are usually descriptions of short investigations, or they can report minor technical improvements of previously published procedures; they reflect the same quality of research as Full-length papers, but should preferably not exceed five printed pages. Discussions (one or two pages) should explain, amplify, correct or otherwise comment substantively upon an article recently published in the journal. For Review articles, see inside front cover under Submission of Papers.

Submission. Every paper must be accompanied by a letter from the senior author, stating that he/she is submitting the paper for publication in the *Journal of Chromatography*.

Manuscripts. Manuscripts should be typed in **double spacing** on consecutively numbered pages of uniform size. The manuscript should be preceded by a sheet of manuscript paper carrying the title of the paper and the name and full postal address of the person to whom the proofs are to be sent. As a rule, papers should be divided into sections, headed by a caption (*e.g.*, Abstract, Introduction, Experimental, Results, Discussion, etc.). All illustrations, photographs, tables, etc., should be on separate sheets.

Abstract. All articles should have an abstract of 50–100 words which clearly and briefly indicates what is new, different and significant. No references should be given.

Introduction. Every paper must have a concise introduction mentioning what has been done before on the topic described, and stating clearly what is new in the paper now submitted.

Illustrations. The figures should be submitted in a form suitable for reproduction, drawn in Indian ink on drawing or tracing paper. Each illustration should have a legend, all the *legends* being typed (with double spacing) together on a *separate sheet*. If structures are given in the text, the original drawings should be supplied. Coloured illustrations are reproduced at the author's expense, the cost being determined by the number of pages and by the number of colours needed. The written permission of the author and publisher must be obtained for the use of any figure already published. Its source must be indicated in the legend.

References. References should be numbered in the order in which they are cited in the text, and listed in numerical sequence on a separate sheet at the end of the article. Please check a recent issue for the layout of the reference list. Abbreviations for the titles of journals should follow the system used by *Chemical Abstracts*. Articles not yet published should be given as "in press" (journal should be specified), "submitted for publication" (journal should be specified), "in preparation" or "personal communication".

Dispatch. Before sending the manuscript to the Editor please check that the envelope contains four copies of the paper complete with references, legends and figures. One of the sets of figures must be the originals suitable for direct reproduction. Please also ensure that permission to publish has been obtained from your institute.

Proofs. One set of proofs will be sent to the author to be carefully checked for printer's errors. Corrections must be restricted to instances in which the proof is at variance with the manuscript. "Extra corrections" will be inserted at the author's expense.

Reprints. Fifty reprints will be supplied free of charge. Additional reprints can be ordered by the authors. An order form containing price quotations will be sent to the authors together with the proofs of their article.

Reversed Phase CHIRAL HPLC Column

NEW CHIRALCEL® OD-R

Indapamide

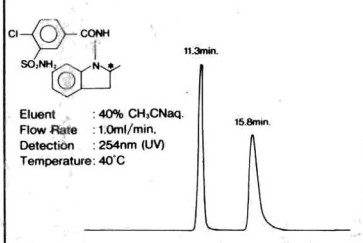

Eluent : 40% CH_3CNaq.
Flow Rate : 1.0ml/min.
Detection : 254nm (UV)
Temperature: 40°C

Verapamil

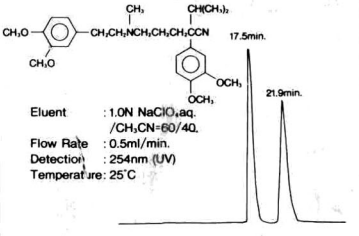

Eluent : 1.0N $NaClO_4$aq. /CH_3CN=60/40.
Flow Rate : 0.5ml/min.
Detection : 254nm (UV)
Temperature: 25°C

Hydroxyzine

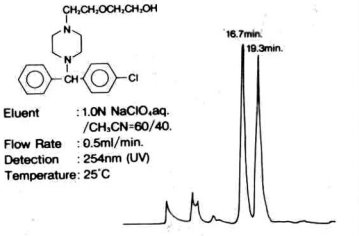

Eluent : 1.0N $NaClO_4$aq. /CH_3CN=60/40.
Flow Rate : 0.5ml/min.
Detection : 254nm (UV)
Temperature: 25°C

Propranolol

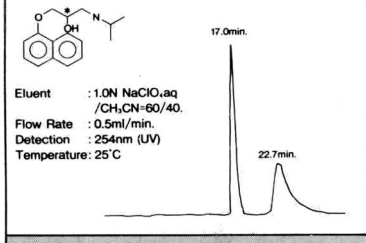

Eluent : 1.0N $NaClO_4$aq /CH_3CN=60/40.
Flow Rate : 0.5ml/min.
Detection : 254nm (UV)
Temperature: 25°C

Pindolol

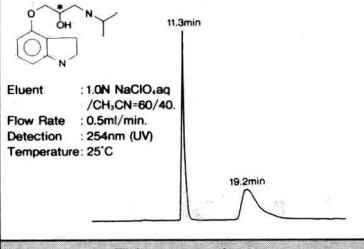

Eluent : 1.0N $NaClO_4$aq /CH_3CN=60/40.
Flow Rate : 0.5ml/min.
Detection : 254nm (UV)
Temperature: 25°C

1-Phenoxy-2-Propanol

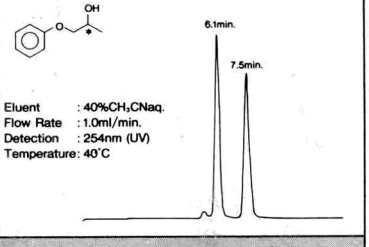

Eluent : 40%CH_3CNaq.
Flow Rate : 1.0ml/min.
Detection : 254nm (UV)
Temperature: 40°C

Alimemazine

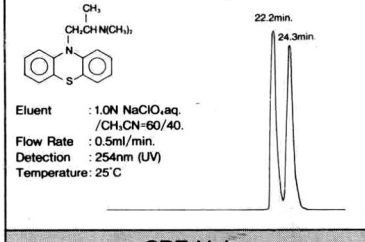

Eluent : 1.0N $NaClO_4$aq. /CH_3CN=60/40.
Flow Rate : 0.5ml/min.
Detection : 254nm (UV)
Temperature: 25°C

Trimepramine

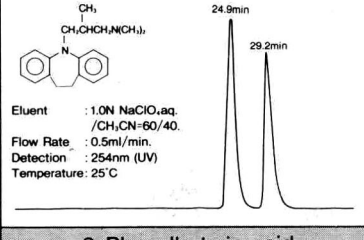

Eluent : 1.0N $NaClO_4$aq. /CH_3CN=60/40.
Flow Rate : 0.5ml/min.
Detection : 254nm (UV)
Temperature: 25°C

4-Pheny-2-butanol

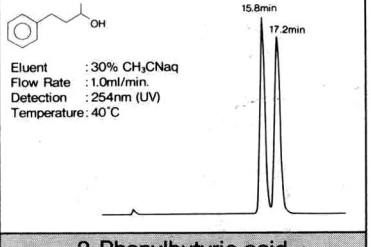

Eluent : 30% CH_3CNaq
Flow Rate : 1.0ml/min.
Detection : 254nm (UV)
Temperature: 40°C

CBZ-Val.

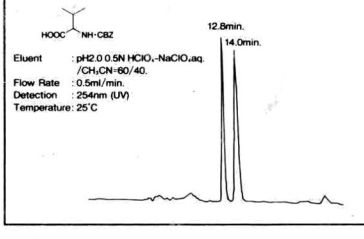

Eluent : pH2.0 0.5N $HClO_4$-$NaClO_4$aq. /CH_3CN=60/40.
Flow Rate : 0.5ml/min.
Detection : 254nm (UV)
Temperature: 25°C

3-Phenylbutyric acid

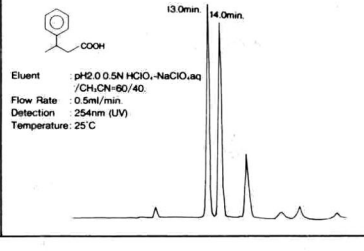

Eluent : pH2.0 0.5N $HClO_4$-$NaClO_4$aq /CH_3CN=60/40.
Flow Rate : 0.5ml/min.
Detection : 254nm (UV)
Temperature: 25°C

2-Phenylbutyric acid

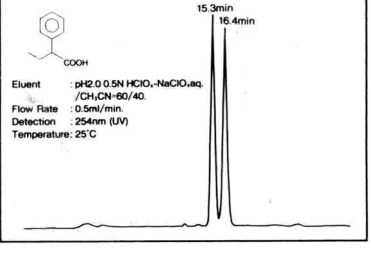

Eluent : pH2.0 0.5N $HClO_4$-$NaClO_4$aq. /CH_3CN=60/40.
Flow Rate : 0.5ml/min.
Detection : 254nm (UV)
Temperature: 25°C

For more information about CHIRALCEL OD-R column, please give us a call.

DAICEL CHEMICAL INDUSTRIES, LTD.
CHIRAL CHEMICALS DIVISION 8-1, Kasumigaseki 3-chome, Chiyoda-ku, Tokyo 100, JAPAN
Phone: +81-3-3507-3151 Facsimile: +81-3-3507-3193

AMERICA
CHIRAL TECHNOLOGIES, INC.
730 SPRINGDALE DRIVE
DRAWER I EXTON, PA 19341
Phone: 215-594-2100
Facsimile: 215-594-2325

EUROPE
DAICEL (EUROPA) GmbH
Ost Street 22
4000 Düsseldorf 1, Germany
Phone: +49-211-369848
Facsimile: +49-211-364429

ASIA/OCEANIA
DAICEL CHEMICAL (ASIA) PTE. LTD.
65 Chulia Street #40-07
OCBC Centre, Singapore 0104.
Phone: +65-5332511
Facsimile: +65-5326454